Acta Neurochir (2011) 153:1361–1366
DOI 10.1007/s00701-011-1063-9

HOW I DO IT

Clipping of MCA aneurysms: how I do it

Philippe Bijlenga · Vitor Mendes Pereira · Karl Schaller

Received: 3 May 2011 / Accepted: 24 May 2011 / Published online: 4 June 2011

Abstract
Introduction Aneurysms located at the middle cerebral artery bifurcation remain a clear neurosurgical indication. We detail here the steps necessary to enable safe surgery for Sylvian fissure aneurysms.
Methods An angiogram with 3D reconstruction is obtained and reviewed intraoperatively, just prior to the skin incision. During the exposure, the cistern is kept open by small cottonoids, thereby avoiding brain retraction. Continuous monitoring of MEPs along with ICG microscopic angio-fluorescence allows for detection of vascular compromise. Intraoperative angiography with 3D reconstruction allows for immediate correction of less than satisfactory surgical outcome.
Conclusions Careful planning of surgical strategy followed by a minimally invasive technique (with continuous neuro-monitoring) ensures safe surgery. The availability of intra-operative radiological guidance allows for optimal management.

Keywords Middle cerebral artery · Intracranial aneurysm · Clipping · Hybrid intervention · Neuro-monitoring · Indocyanine green angio-fluorescence · Per-operative angiography

Abbreviations

CSF	Cerebrospinal fluid
MCA	Middle cerebral artery
ICG	Indocyanine green
MEP	Motor evoked potential
DRA	Digital subtraction rotational angiography
3D-DRA	3D surface rendering reconstruction from DRA

Introduction

The field of vascular neurosurgery has undergone revolutionary developments that seek to improve patient care and outcomes. New treatment modalities and new devices continuously challenge the standard of care. The ISAT study showed that coiling of ruptured intracranial aneurysms is at least as effective and safe as microneurosurgical clipping performed within the first 72 h after ictus. As a result, most basilar tip and vertebral aneurysms are now coiled. On the other end of the spectrum, most middle cerebral artery (MCA) bifurcation aneurysms are still clipped and now secured within the first 24 h of ictus to reduce rebleeds [1, 4, 5]. As a result of increased opportunities and better quality cerebral imaging, more patients are being diagnosed with asymptomatic and unruptured intracranial aneurysms. The ISUIA study showed that some patients benefited more from conservative management, others from open surgery and finally, there were those who benefited from endovascular inter-

Electronic supplementary material The online version of this article (doi:10.1007/s00701-011-1063-9) contains supplementary material, which is available to authorized users.

P. Bijlenga (✉) · K. Schaller
Service de Neurochirurgie, Département de Neurosciences Cliniques, Hôpitaux Universitaire de Genève,
Faculté de médecine, Université de Genève,
Rue Gabrielle-Perret-Gentil 4,
1211 Geneva 14, Switzerland
e-mail: philippe.bijlenga@hcuge.ch

V. Mendes Pereira
Service de Neuroradiologie Diagnostique et Interventionelle,
Hôpitaux universitaire de Genève, Faculté de médecine,
Université de Genève,
Geneva, Switzerland

vention. The authors concluded that for aneurysms less than 7 mm in size located in the anterior circulation, there was a role for patient observation alone. However, no conclusion was drawn on a favored treatment modality should treatment be sought [8]. Recently, the advent of flow diverter stents has produced impressive results in the management of fusiform or side-wall saccular aneurysms, as well as ophthalmic aneurysms [3, 6]. Criteria to determine which patients and lesions are more appropriately treated by one method over the other remain ill-defined. Intuitively, patients with coagulopathy would clearly be better candidates for endovascular treatments while patients suffering vessel atherosclerosis with plaques, sub-occlusion or occlusion, are better candidates for surgery. Similarly, proximal lesions lying close to the circle of Willis are considered more accessible via the endoluminal route while lesions more superficial and distal in the vascular tree tend to be more amenable to a surgical approach. Aneurysm morphology is also important. A saccular shape with a small neck allows for high coil compaction with little risk of parent vessel occlusion. Aneurysms with large necks or those involving both parent arteries and branches are reconstructed using stents or clips [2]. Current efforts are devoted to better identifying such factors, establishing their relative importance and quantifying their impact on decision-making, with the end goal of improving safety and long-term efficacy of treatments (Table 1).

MCA aneurysms represent 25% of all intracranial aneurysms and more than 60% are incidental findings. Due to their position in the vascular tree and frequent incidence of large neck morphology, MCA aneurysms are mostly treated by microsurgical clipping [7]. We report advances introduced in our daily clinical practice to reduce peri-operative risks and offer an anatomical cure for such lesions affecting otherwise healthy patients with a median age between 55 and 60 years [8, 9].

Table 1 Information for patient and family for non-complex MCA bifurcation aneurysm clipping

1.	The operation is proposed if the risk of surgery is considered smaller than observation over a period of 5 years
2.	Less than 5% risk of stroke
3.	2% risk of infection that may require antibiotic treatment for weeks and sometimes removal of the bone flap that will be replaced by prosthesis
4.	1% risk of a hematoma that would require reoperation for evacuation
5.	Less than 1% epilepsy
6.	Overall: 5% risk of significant handicap for patients less than 50 years of age, 10% for patients over 50 years
7.	Overall: Less than 2% risk of death
8.	Minor chewing discomfort for 2 months
9.	Slight temporal muscle atrophy may be observed
10.	Pins from head clamp may induce some discomfort for 1 or 2 days
11.	Hematoma may be observed in the groin
12.	Possible black eye for 1 week

Operative technique (Table 2)

Preoperative imaging and angiography (Fig. 1)

Angiographic pre-operative images are studied by the treating team (comprising the senior and junior surgeons as well as the interventional neuroradiologist). The extent of sphenoid ridge to be removed is considered in relation to the superior orbital fissure. The anatomy of the circle of Willis is characterized with regards to the patency of left-to-right connections. This is to determine the optimal proximal clipping location in the event of precocious aneurysm rupture. Vascular and aneurismal anatomy to be anticipated during surgery is studied using 3D reconstructions. The segmented volumes are rotated to visualize projections as encountered during surgery. The aneurysm neck and orientation are measured and the clipping strategy is defined accordingly (Fig. 1). In case of a very wide or atherosclerotic aneurysm neck, bifurcation reconstruction may result in the occlusion of one or all branches. For those cases, a preventive bypass is discussed. Planning and operative technique of complex MCA aneurysms is out of the scope here. In order to prepare the pterional approach (see below), special attention is paid to the identification of pneumatized structures to be avoided during surgery. This extends from frontal sinuses to the anterior clinoid processes. The extent of Sylvian fissure opening is discussed and anatomical landmarks on MCA branches identified.

Table 2 Key points

1.	Examine and memorize the angio-architecture prior to skin incision
2.	Identify key reliable landmarks, such as bifurcations and curves of vessels
3.	Optimize dural opening in relation to the size of the bony exposure
4.	Assure venous epidural hemostasis by oxycellulose and temporary cottonoid application
5.	Avoid brain retraction, use small cottonoids to keep the Sylvian fissure open
6.	Prepare a clipping site prior to dissection of the aneurysm dome
7.	Puncture the aneurysm dome to assess complete exclusion
8.	Perform high-resolution angiographic imaging as soon as possible to assess surgical outcome

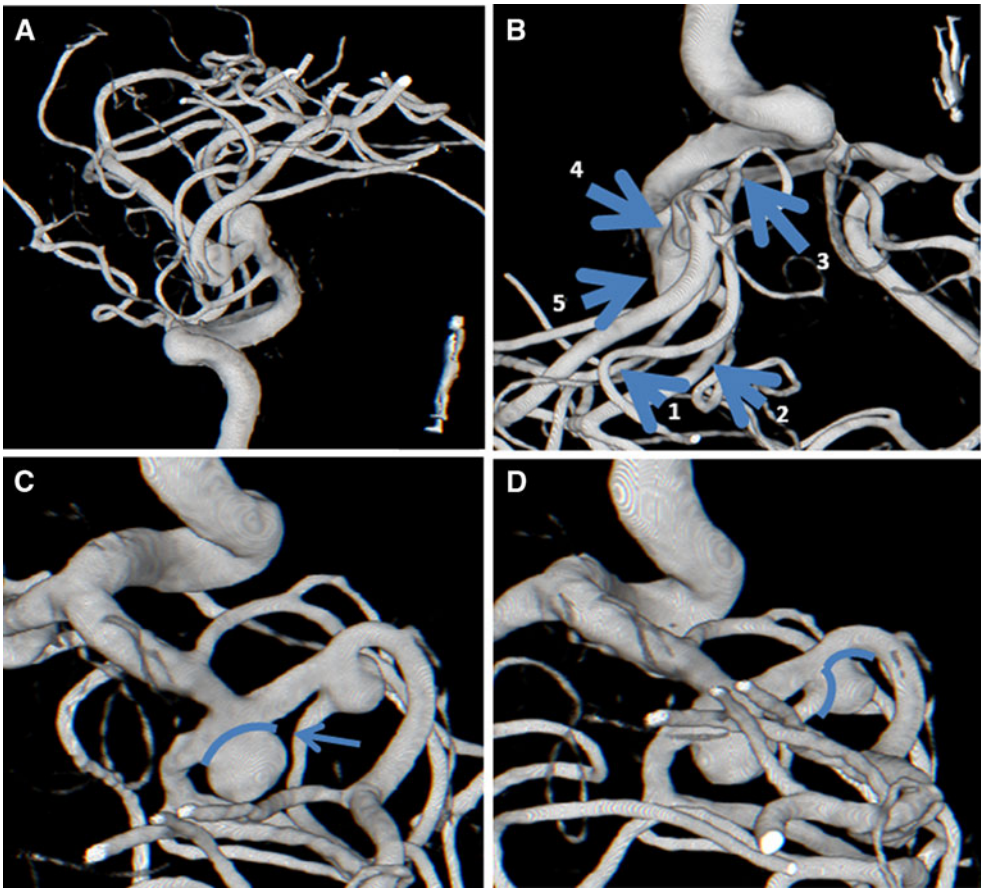

Fig. 1 Pre-operative 3D-DRA should be used to prepare intervention (**a**). The 3D volume is oriented to match with the surgical field (**b**). Landmarks are identified on vessels to aid surgical exploration. Examples include identifying the fissure opening point (B1) in order to establish the direction to the inferior trunk of M2 (B2). The bifurcation of the superior trunk is used as a proximity marker for a distal aneurysm (B3). The proximal control site is identified (B4) relative to the proximal aneurysm (B5). Clip shape and size is chosen for the proximal aneurysm that will be clipped first to avoid subsequent conflict when clipping the more superficial aneurysm (**c**). Clipping strategy is modeled for the second aneurysm (**d**)

Positioning of the patient and general settings (Fig. 2)

The patient lies supine in a ”Le Corbusier” lounge chair position. The shoulder on the operating side is elevated and the head is rotated 90° toward the opposite side. The head is fixed in a Mayfield head clamp using 3-pin fixation. Care is taken to keep the head above the level of the heart and to ensure both jugular veins remain patent. The groin is prepared for endovascular access. The anesthetist accesses the patient from the legs and left side of the body. The endovascular interventionist is positioned close to the right groin. The surgeon sits at the vertex.

We never use a lumbar drain. Patients receive antibiotics in the operating room approximately 20 min prior to the skin incision. Scalp electrodes are placed. Neurophysiological monitoring includes monitoring of motor evoked potential of the contra-lateral limbs.

Before draping, a ”time-out” (as per WHO guidelines) is performed in the presence of the anesthesiologist, interventionist, neurophysiologist, scrub nurse, and surgeons. The main stages of the procedure are reviewed and the instruments required for each stage are checked (emergency clips are chosen and prepared). Communication with all members of the team remains vital throughout the procedure.

Approach

A curved skin incision is carried-out beginning 1 cm anterior to the tragus at the level of the zygomatic arch and running behind the hairline, up to the midline. The pericranial flap is fashioned according to Yasargil’s description of interfascial dissection and reflected antero-inferiorly. The temporal muscle is detached from the bone sutures (starting from the orbito-zygomatic suture) and pterion, using a periosteal elevator. The upper insertion is sectioned using cutting monopolar. This technique allows preservation of the periosteum, thereby allowing for a better cosmetic outcome due to reduced risk of temporal muscle atrophy. The muscle is reflected posteroinferiorly [9].

A burr hole is performed over the thin temporal bone and dura is detached antero-superiorly. An oval-shaped craniotomy is carried out, with the longer diameter being aligned with the Sylvian fissure. An average-sized craniotomy is approximately 5 cm×4 cm wide. The anterior aspect of the craniotomy is drilled flush with the lateral wall of the orbit. Following elevation of the bone flap, the sphenoid ridge is removed using a Luer rongeur and drilled to achieve continuity with the lateral wall of the orbit. The meningo-orbital band is identified as the limit of bone removal. The bone flap is stored aside in normal saline for

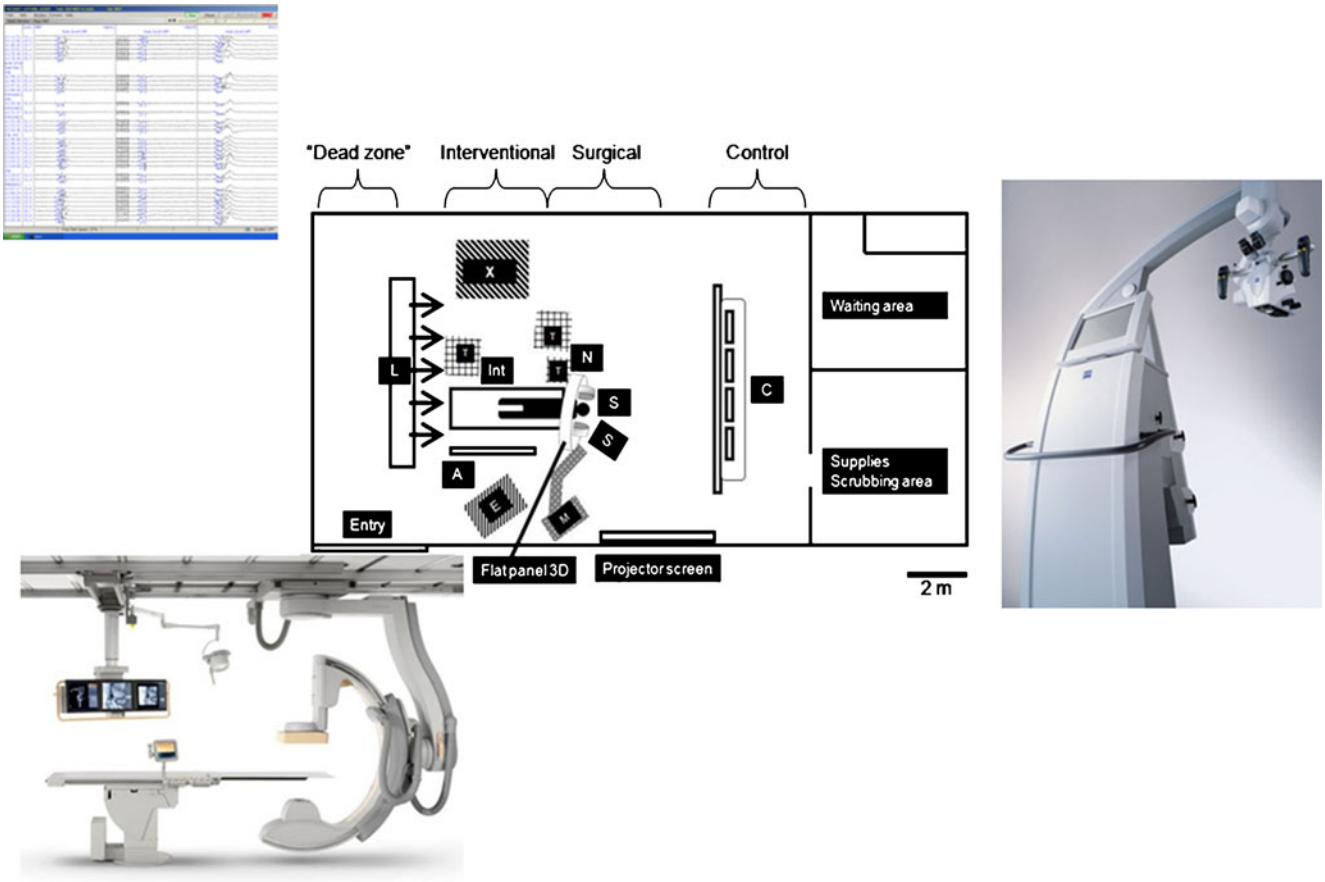

Fig. 2 Hybrid room configuration. The operating theatre is equipped with an Allura Xper FD20 (Philips Healthcare, Best, Netherlands). The head of the patient is fixed in a radiolucent Mayfield Infinity XR2 Scull Clamp (Integra Neuroscience Limited, Andover Hampshire, UK). During the procedure, MEPs are monitored by transcranial electric stimulation (Axon Eclipse, Axon Systems Inc, Hauppauge, NY) (*X*). Microsurgery is performed under a microscope using a OPMI® Pentero™ equipped with the INFRARED 800 option (*M*). The space is virtually divided into three regions. On the lower left of the patient is the anesthetic (*A*) corner with equipment (*E*). On the lower right is the interventional radiologist (*Int*) corner with instrument table (*T*). The surgical team (*S*) and scrub nurse (*N*) are located at the head of the patient. The operative field is protected by horizontal laminar flow (*L*). Control of equipment, image processing, and analysis is performed in the "control zone" (*C*). Images can be projected on a screen on the left side of the room or viewed on a Digital Lightbox© (BrainLab, Feldkirchen, Germany) on the right side

later reinsertion. Perfect hemostasis is now achieved, prior to moving on to the intradural stage.

The dura is opened in a "U"-shape against the orbital wall and reflected anteriorly. In young patients with no cerebral atrophy or in cases with a ruptured aneurysm and a swollen brain, we follow the orbital roof down to the olfactory nerve and then laterally to the optic nerve. CSF is drained from the pre-optic cistern. This maneuver allows an early exposure of the internal carotid artery for proximal control if needed. A small hole is created in the arachnoid of the Sylvian fissure approximately 4 cm posterior to the drilled sphenoid ridge. Normal saline is gently injected under pressure until distal reflux is observed. The hole is then enlarged and the Sylvian fissure is opened by sharp dissection (e.g., using a diamond knife) in the direction of the limen insula. If the patient suffers an intraparenchymal hematoma most but not all of it is removed to reduce mass effect but avoid rebleeding. The inferior trunk of M2 is identified and followed anteriorly towards the bifurcation. Very frequently, for proximal control, the M1 artery distal to the striate perforators, can be identified turning rostro-medially to the limen insula. Care is taken to gradually enlarge the arachnoids' opening on the surface of the Sylvian fissure when progressing deeper. It is easier to open the Sylvian fissure from the depth aiming superficially. Veins are preserved as much as possible by cutting arachnoids' adhesions both sides of the fissure allowing mobilization. If necessary, we favor sacrificing veins on the frontal side. The veins bridging to the sphenoparietal sinus are sometime wrapped with oxidized cellulose gaze. Once the distal M1 has been identified and the fissure opened sufficiently to avoid tension from retraction, cottonoids are used to keep the field open (thus

negating the need for self-retaining retractors). The aneurysm is usually partially exposed at this stage.

Aneurysm neck dissection and clipping

The next step is to identify the superior trunk of M2 and expose the neck of the aneurysm. Care is taken to ensure that the instruments used are wet. Arachnoid is cleared from the vessel and aneurysm wall using microsurgical dissectors and micro-scissors. Movements are tangential to vascular structures. Following exposure of all the M2 branches, M1 trunk, and the aneurysm neck, the clip strategy is assessed and an appropriate clip is chosen. When high-resolution angiographic intra-operative imaging is not available, flow or blood velocity measurements of the M1 trunk (proximal to the aneurysm) and all M2 branches (immediately distal to the aneurysm) are performed in order to assess for potential vascular compromise post-clipping. Depending on the size of the aneurysm or per-operative rupture, a temporary clip may be applied proximally to deflate the dome or reduce the bleeding. When proximal clipping is intended, the anesthesiologist is informed, who then increases the mean arterial blood pressure by 20%. MEPs are monitored.

Intra-operative quality control (Fig. 3)

When the aneurysm clip is placed on the neck, the proximal clip is removed and the aneurysm dome is completely exposed. The clipping is checked by puncturing the aneurysm dome with a 25-G needle. The aneurysm should deflate and the neck is then explored on both sides to exclude remnants or occlusion of neighboring small perforators. ICG angio-fluorescence imaging is performed to assess the patency of all vessels. If ICG is not available, patency is confirmed using micro Doppler. Papaverine 40 mg diluted in 10 ml of normal saline is applied to the Sylvian fissure. The operating field is protected by a wet compress and the head of the patient is positioned within a transparent draped. The interventional neuroradiologist performs a conventional angiogram as well as a 3D rotational angiogram. Images are compared to preoperative data to verify that all branches and perforators are patent.

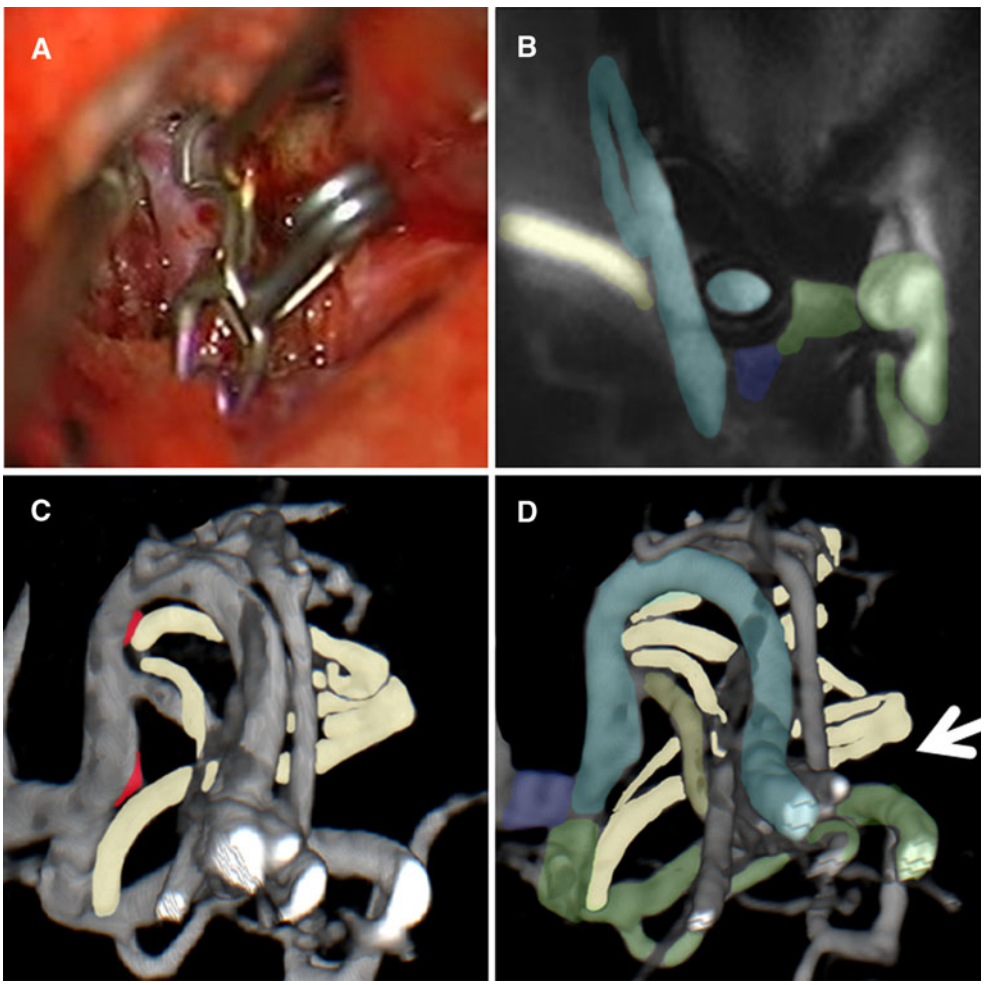

Fig. 3 The aneurysm clipping is checked visually (**a**). The aneurysm dome is punctured and flow in the different branches is assessed using indocyanine green angiofluorescence (**b**). The inferior M2 trunk (*green*), the anterior branch of the superior M2 artery (*light blue*), the posterior branch of the superior M2 artery (*yellow*) and the M1 trunk (*dark blue*) are recognized and the rate of fluorescence increase is checked for all branches. A rotational angiography is carried out and reconstructed to allow 3D surface rendering. Clipping is carefully inspected (**c**). In the example small remnants (*red*) are corrected with two mini clips before final control is achieved (**d**)

3D vessel morphology is reconstructed from the acquired DRA and checked from all angles to exclude micro residuals, dog ears, or stenosis. Clips are repositioned if considered necessary and reassessed by 3D-DRA as required.

Closure

At the end of surgery, watertight closure of the dura is undertaken. A Gelfoam® sterile compressed sponge is applied between the dura and the bone flap in the event of CSF leak. The bone flap is replaced and maintained with titanium plates and low profile screws. Replacement and suture of the temporal muscle is done using absorbable sutures. Subgaleal drainage is usually avoided. Skin closure is carried out in two layers.

Postoperative course and instructions from the surgeon

The patient is observed overnight in an intensive care unit. Low-molecular-weight heparin is started 6 h post-craniotomy to prevent thromboembolic complications. The patient is usually discharged after 5 days (at which stage sutures are removed). A post-operative check is performed after 6 weeks. Patients are followed-up with CT angiography at 1 year, 5 years, and every 5 years thereafter.

Potential future evolutions

Integration of virtual images updated by ultrasound and endoscopic tools may provide a visual environment that would allow performing the operation through a few burr holes reducing tissue retraction damage even further.

Conclusions

The morbidity of MCA aneurysm clipping can be reduced by careful planning, adoption of minimally invasive microsurgical techniques, and systematic continuous monitoring of MEPs. Intra-operative angiographic imaging allows timely correction of imperfections and allows for an optimal surgical result. Nevertheless, we still advocate long-term follow-up of these patients with CT angiography to reduce the risk of hemorrhage from newly formed lesions.

Conflicts of interest None.

References

1. Bakker NA, Metzemaekers JD, Groen RJ, Mooij JJ, Van Dijk JM (2010) International Subarachnoid Aneurysm Trial 2009: endovascular coiling of ruptured intracranial aneurysms has no significant advantage over neurosurgical clipping. Neurosurgery 66(5):961–962
2. Bendszus M, Chapot R (2007) Balloon-assisted coil embolization. Surgical clip application should be considered as a first treatment option in large and wide-necked aneurysms. J Neurosurg 106 (4):734–735
3. Lylyk P, Miranda C, Ceratto R, Ferrario A, Scrivano E, Luna HR, Berez AL, Tran Q, Nelson PK, Fiorella D (2009) Curative endovascular reconstruction of cerebral aneurysms with the pipeline embolization device: the Buenos Aires Experience. Neurosurgery 64(4):632–642
4. Molyneux AJ, Kerr RS, Birks J, Ramzi N, Yarnold J, Sneade M, Rischmiller J, ISAT Collaborators (2009) Risk of recurrent subarachnoid haemorrhage, death, or dependence and standardised mortality ratios after clipping or coiling of an intracranial aneurysm in the International Subarachnoid Aneurysm Trial (ISAT): long-term follow-up. Lancet Neurol 8(5):427–433
5. Molyneux AJ, Kerr RS, Yu LM, Clarke M, Sneade M, Yarnold JA, Sandercock P, International Subarachnoid Aneurysm Trial (ISAT) Collaborative Group (2005) International subarachnoid aneurysm trial (ISAT) of neurosurgical clipping versus endovascular coiling in 2143 patients with ruptured intracranial aneurysms: a randomised comparison of effects on survival, dependency, seizures, rebleeding, subgroups, and aneurysm occlusion. Lancet 366(9488):809–817
6. Nelson PK, Lylyk P, Szikora I, Wetzel SG, Wanke I, Fiorella D (2011) The pipeline embolization device for the intracranial treatment of aneurysms trial. AJNR Am J Neuroradiol 32(1):34–40
7. Regli L, Dehdashti AR, Uske A, de Tribolet N (2002) Endovascular coiling compared with surgical clipping for the treatment of unruptured middle cerebral artery aneurysms: an update. Acta Neurochir Suppl 82:41–46
8. Wiebers DO, Whisnant JP, Huston J 3rd, Meissner I, Brown RD Jr, Piepgras DG, Forbes GS, Thielen K, Nichols D, O'Fallon WM, Peacock J, Jaeger L, Kassell NF, Kongable-Beckman GL, Torner JC, International Study of Unruptured Intracranial Aneurysms Investigators (2003) Unruptured intracranial aneurysms: natural history, clinical outcome, and risks of surgical and endovascular treatment. Lancet 362(9378):103–110
9. Yasargil MG, Smith RD, Young PH, Teddy PJ, Roth P (1984) Microneursurgery, vol. 2. Georg Thieme Verlag, Stuttgart, p 385

Acta Neurochir (2011) 153:1367–1373
DOI 10.1007/s00701-011-1004-7

CLINICAL ARTICLE

Intra-operative MRI facilitates tumour resection during trans-sphenoidal surgery for pituitary adenomas

Jon Ramm-Pettersen · Jon Berg-Johnsen · Per Kristian Hol · Sumit Roy · Jens Bollerslev · Thomas Schreiner · Eirik Helseth

Received: 15 November 2010 / Accepted: 23 March 2011 / Published online: 27 April 2011

Abstract
Background During trans-sphenoidal microsurgical resection of pituitary adenomas, the extent of resection may be difficult to assess, especially when extensive suprasellar and parasellar growth has occurred. In this prospective study, we investigated whether intra-operative magnetic resonance imaging (iMRI) can facilitate tumour resection.
Methods Twenty patients with macroadenomas, (16 non-functioning, three growth-hormone secreting and one pharmaco-resistant prolactinoma) were selected for surgery in the iMRI. The mean tumour diameter was 27 mm (range 11–41). The mean parasellar grade, according to the Knosp classification, was 2.3. Pre-operative coronal and sagittal T1-weighted and T2-weighted images were obtained. The trans-sphenoidal tumour resection was performed at the edge of the tunnel of a Signa SP 0.5-Tesla MRI. The surgeon aimed at a radical tumour resection that was followed by a peri-operative MRI scan. When a residual tumour was visualised and deemed resectable, an extended resection was performed, followed by another MRI scan. This procedure was repeated until the imaging results were satisfactory. In all patients, we were able to obtain images to assess the extent of resection and to classify the resection as either total or subtotal.
Results After primary resection, eight out of 20 cases were classified as total resections. A second resection was performed in 11 of 12 cases classified as subtotal resections, and in four of these, total resection was achieved. A third resection was performed in three of the remaining seven cases with subtotal resections, but we did not achieve total resection in any of these cases. Therefore, the use of iMRI increased the number of patients with total resection from 8/20 (40%) to 12/20 (60%). The only observed complication was a transient spinal fluid leakage.
Conclusion Intra-operative MRI during trans-sphenoidal microsurgery is useful in selected patients for a safe and more complete resection.

Keywords Pituitary · Intra-operative MRI · Trans-sphenoidal · Surgery

This article is discussed in the editorial available at doi:10.1007/s00701-011-1005-6.

J. Ramm-Pettersen (✉) · J. Berg-Johnsen · E. Helseth
Department of Neurosurgery, Oslo University Hospital (OUS), 0027 Oslo, Norway
e-mail: jon.ramm-pettersen@oslo-universitetssykehus.no

J. Berg-Johnsen · E. Helseth
Faculty of Medicine, University of Oslo, Oslo, Norway

P. K. Hol · S. Roy
The Intervention Center, OUS, Oslo, Norway

J. Bollerslev · T. Schreiner
Section for Endocrinology, Clinic of Medicine, OUS, Oslo, Norway

Introduction

Approximately 95% of pituitary adenomas that require surgery can be approached through the trans-sphenoidal approach, whereas other tumours need a transcranial approach. The trans-sphenoidal approach is a minimally invasive, microsurgical approach that provides good access to the sella and the clivus; however, it has the limitation of no direct visualisation of the suprasellar and parasellar regions. After surgery for hormone-producing tumours, the hormonal activity levels act as a marker of the amount of remnant tumour. The remission rate for hormone-producing

macroadenomas ranges from 40% to 56% in large series [20], indicating that a large portion of patients harbour tumour remnants. In non-functioning tumours, the extent of removal of the tumour is more difficult to assess. Early post-operative magnetic resonance imaging (MRI) are difficult to interpret due to post-operative changes in the limited operative field [11]. Published series on non-functioning pituitary adenomas show that radical tumour removal is achieved in 28–70% of patients [2, 8, 11, 21], depending on tumour size and invasiveness. Therefore, there is clearly a need for better visualisation and tools to improve the removal of tumours during trans-sphenoidal surgery.

Various visualisation modalities have been implemented to increase the degree of resection in trans-sphenoidal surgery, but sagittal fluoroscopy has been the only standard imaging during surgery in most departments. This type of imaging shows the position of the speculum and the instruments in relation to the bony landmarks. The infusion of air from a cervical puncture gives additional information during the visualisation of the diaphragm of the sella and may facilitate the descendens of the suprasellar portion of the tumour [13]. The use of transcranial ultrasound-guided trans-sphenoidal surgery has been reported, but it has not yet gained widespread acceptance [17, 19]. The most promising new method to facilitate the resection of pituitary adenomas is the use of an endoscope [9]. One of the first applications of intra-operative MRI (iMRI) was its use during trans-sphenoidal surgery [18]. Nevertheless, there are few publications focusing solely on the results of MRI-guided trans-sphenoidal surgery in pituitary adenomas [3, 4, 6, 7, 12, 14, 16, 22].

Although the trans-sphenoidal approach is a minimally invasive, microsurgical approach, several complications are associated with this procedure. For example, injury to the carotid arteries is the most feared complication, and post-operative cerebrospinal fluid (CSF) leakage is the most frequent. The mortality rate of these patients is thought to be approximately 1%, severe morbidity is thought to occur in 3–4%, and lesser morbidity is observed in 4–5% of the patients [20].

The aim of the present study was to evaluate whether the use of iMRI improves tumour resection in trans-sphenoidal surgery for pituitary adenomas.

Methods and materials

Twenty patients with macroadenomas were selected for surgery with iMRI on the assumption that peri-operative imaging would be helpful during the procedure. Table 1 shows the patient characteristics. Of the 20 patients included in this study, five had been operated on previously using the trans-sphenoidal approach. Sixteen of the tumours were non-functioning adenomas, three secreted growth hormone, and one was a pharmaco-resistant prolactinoma. The maximum tumour diameter varied between 11 and 41 mm (mean 27 mm). The Knosp classification of parasellar extension was used [10]. Three tumours were classified as Knosp grade 0, one grade 1, seven grade 2, five grade 3 and four grade 4.

After anaesthesia was introduced (propofol and remi-phentanyl) and proper monitoring established, the operating table was docked to the Signa SP 0.5-Tesla MRI. Coronal and sagittal T1-weighted and T2-weighted images without gadolinium were obtained before the start of surgery. Surgery was performed with the patient in the supine position with the head slightly elevated at the edge of the MRI tunnel (Fig. 1). All instruments were MRI-compatible, and the nasal speculum was designed to produce minimal artefacts during imaging (Æsculap, Tuttlingen, Germany). An MRI-compatible microscope with a video camera was used, and the operative images were transferred to monitors located in the operating theatre and in the MRI control room (Møller-Wedel, Hamburg, Germany). The endonasal trans-septal approach was used for the primary surgery, and the direct endonasal approach was used for the re-operations. The surgery was performed in a similar manner as that performed in the ordinary operating theatre. When the surgeon decided that the surgery was complete, an MRI scan was performed with the speculum in place, and the resection cavity was filled with saline. Careful haemostasis was performed prior to imaging, and T1-weighted and T2-weighted images in the coronal and sagittal planes without contrast were obtained. Figure 2 shows examples of the pre-operative, peri-operative and post-operative images.

The iMRI scanning time was 3 min and 30 s per series performed. The pre-operative and intra-operative scans consisting of T1-coronal, T1-sagittal, T2-coronal and T2-sagittal, lasted approximately 14 min. After the completion of the surgery, we added T1-coronal and T1-sagittal series with contrast, so that the post-operative scan-time was 21 min. In addition to the time consumption of the scans, we needed approximately 3 min for transportation in and out of the scanner. Thus, in a typical case with one re-exploration, the use of iMRI added approximately 60 min of operating time.

If a surgically resectable tumour was observed in the peri-operative images, an extended resection was performed, followed by a new imaging sequence. If no further tumour was recognised, or if the remnant was deemed not to be surgically accessible, a final MRI scan with coronal and sagittal T1 images with gadolinium was performed as a post-operative control. When these images were evaluated as having no remnant tumour, the speculum was removed, the floor of the sella was closed with a dura substitute and

Table 1 Patient characteristics, tumour characteristics and result after resection

No.	Age (years)	Sex	Clinical visual +/−	Endocrine signs +/−	Previous surgery	Type of adenoma	Tumour diameter (mm)	Para-sellar extension (Knosp)	Primary resection	Second look	Third look	3 months after MRI
1	71	M	+	+	Yes	0-adenoma	40	4	Subtotal	Subtotal	Subtotal	Subtotal
2	53	M	+	+	No	0-adenoma	38	2	Subtotal	Subtotal	ND	Subtotal
3	59	F	-	+	No	Acromegaly	11	0	Subtotal	Total	ND	Total
4	23	M	+	-	No	0-adenoma	30	3	Subtotal	Subtotal	ND	Subtotal
5	44	F	-	+	No	Acromegaly	11	0	Total	ND	ND	Total
6	58	F	-	+	Yes	Acromegaly	30	4	Subtotal	Subtotal	Subtotal	Subtotal
7	57	M	+	-	Yes	0-adenoma	33	4	Subtotal	ND	ND	Subtotal
8	56	M	+	+	No	0-adenoma	30	3	Subtotal	Total	ND	Total
9	62	M	-	-	No	0-adenoma	19	3	Total	ND	ND	Total
10	73	M	+	+	No	0-adenoma	31	3	Total	ND	ND	Total
11	57	M	+	-	No	0-adenoma	38	2	Subtotal	Total	ND	Total
12	58	M	-	-	No	0-adenoma	17	2	Subtotal	ND	ND	Total
13	66	F	+	+	No	Prolactinoma	41	4	Subtotal	Subtotal	ND	Subtotal
14	32	M	+	-	No	0-adenoma	38	1	Total	ND	ND	Total
15	52	M	+	+	No	0-adenoma	32	2	Subtotal	Subtotal	Subtotal	Subtotal
16	48	M	+	-	Yes	0-adenoma	23	2	Subtotal	Subtotal	ND	Subtotal
17	49	F	+	-	No	0-adenoma	24	2	Total	ND	ND	Total
18	32	F	-	-	No	0-adenoma	12	0	Total	ND	ND	Total
19	61	F	+	+	No	0-adenoma	24	3	Total	ND	ND	Total
20	61	M	+	-	Yes	0-adenoma	20	2	Subtotal	Subtotal	ND	Total

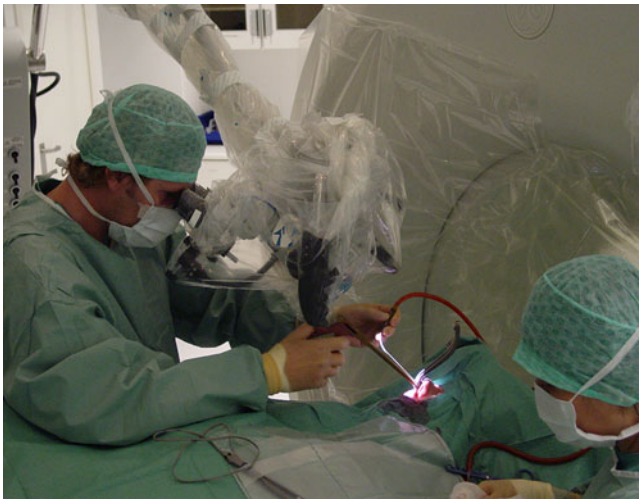

Fig. 1 The surgical set-up with the patient in the supine position. The patient's head was slightly elevated and rotated and was positioned just outside the MRI scanner. All the instruments were MRI-compatible, including the microscope. During imaging, the speculum was left in place, the resection cavity was filled with saline, and the patient was moved approximately 50 cm into the scanning position

bone from the midline or LactoSorb plates, and the sphenoid sinus was packed with gel foam.

All patients were seen for a 3-month follow-up at the Endocrinology Department. The evaluation included an assessment of post-operative pituitary function, an ophthalmologic examination, and a MRI scan. The pituitary function was assessed by tests for basal hormone values, 24-h urinary free cortisol and insulin tolerance. All MRI scans were evaluated by the two participating neuroradiologists. The coronal and sagittal T1, T2 and T1 with gadolinium scans that were performed after the completion of surgery were evaluated and graded as either showing tumour remnant or showing radical removal.

Results

In all patients, images were obtained that could be used to assess the extent of resection. No re-exploration was performed in nine of the 20 patients. One re-exploration was performed in eight patients, and two re-explorations were performed in three patients (Table 1). In all 11 patients where re-exploration was performed, the procedure resulted in the removal of additional tumour.

Extent of tumour resection

Using the MRI results from the 3-month follow-up as the outcome measurement regarding the extent of resection, 12 out of the 20 patients were free of tumour remnants (60%). In

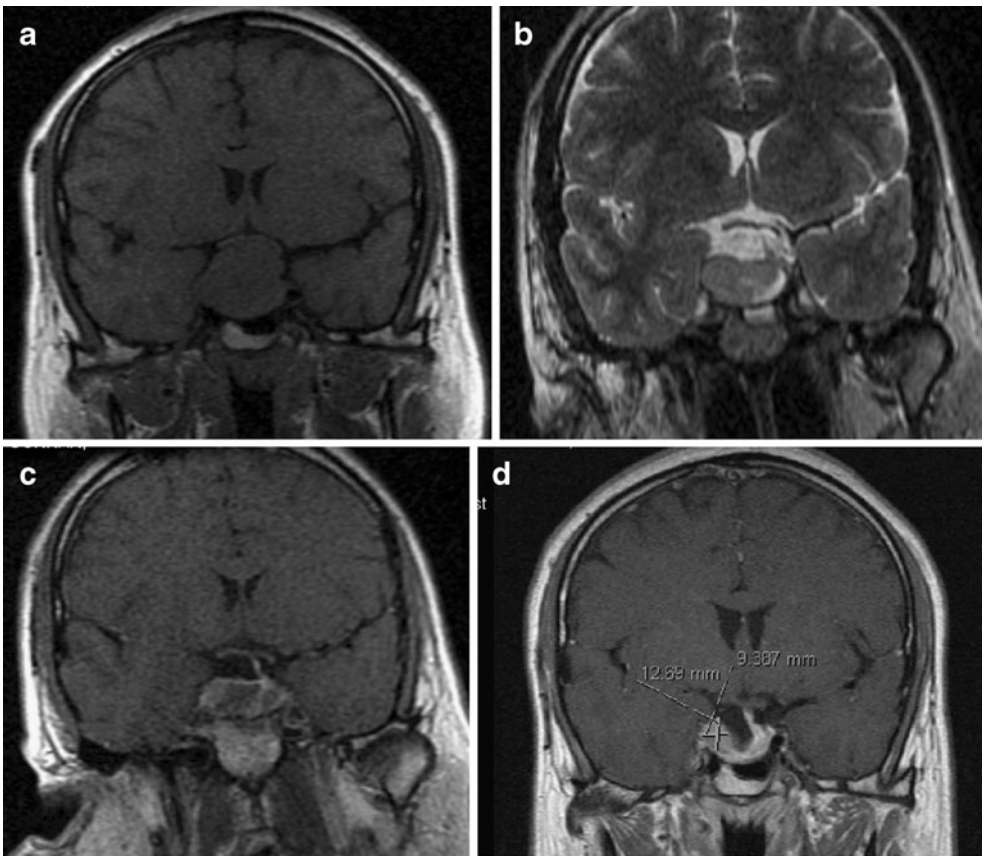

Fig. 2 MRI pictures from the surgery of patient 4, who had bilateral visual field deficits and was normopit pre-operative. At 3 months follow-up, the visual fields were normalised, and the patient was still normopit. **a** Pre-operative T1 without contrast in the Signa SP 0.5-Tesla scanner. **b** Intra-operative T2 after primary resection. **c** Intra-operative T1 with contrast enhancement after extended resection showing a suspect remnant in the right side of the sella. **d** Three months post-operative follow-up showing subtotal resection with a remnant in the right side of the sella

18 of the 20 patients, the extent of resection was similar when evaluated immediately post-operatively and at 3 months post-operatively. In two patients, a suspected remnant was observed in the post-operative scans, whereas at the 3-month follow-up, no tumour remnant was visible. Radical surgery was achieved in 12 patients: without re-exploration in eight, and with one re-exploration in the remaining four. We did not achieve radical surgery in any of the patients who underwent two re-explorations (Table 1). The mean tumour diameter in the group with total resection was 22 mm, compared with 33 mm in patients with tumour remnants. The mean Knosp grade in the patients with radical surgery was 1.75, and the mean grade was 3.13 in the group with tumour remnants. In all patients without parasellar extension (grade 0 or 1), we were able to extirpate the tumour. We achieved extirpation in 57% of the grade 2 patients, in 80% of the grade 3 patients, and in none of the grade 4 patients (Table 2).

In eight patients (40%), the tumour was removed completely without re-exploration. With radical surgery at 3 months follow-up as the goal of the treatment, we found that the risk of a false-positive result was 10% (two out of 20) and that there was no risk of a false-negative result.

Endocrinology

Pre-operatively, ten patients had normal pituitary hormonal activity, seven patients had deficits in one or more of the pituitary hormonal axes (including the patient with prolactinoma), and three patients had growth-hormone hypersecretion (pituitary acromegaly). Eight of the ten patients with normal pituitary function pre-operatively retained normal pituitary function after surgery. One patient developed a growth-hormone deficiency, and one patient developed growth hormone and ACTH deficiencies. Of the seven patients with pre-operative hormonal dysfunction, three had normalised pituitary hormonal secretion at 3 months follow-up, whereas four had persistent pituitary hormonal dysfunction. Two of the three patients with growth-hormone hypersecretion caused by a macroadenoma were cured after trans-sphenoidal surgery, and both of these patients had total resection on MRI evaluation. One patient with acromegaly and subtotal resection exhibited growth-hormone hypersecretion after surgery.

Table 2 Number of patients with no visible tumour on MRI at 3 months follow-up

Knosp grade	No. initial	No. with total resection	Percent total resection
0	3	3	100%
1	1	1	100%
2	7	4	57%
3	5	4	80%
4	4	0	0%

Ophthalmology

Fourteen of the patients in this study had visual field deficits prior to surgery. The visual field deficits improved in 12 of these patients after surgery (86%), and two of the patients had unchanged visual fields at 3 months follow-up. Five patients had reduced visual acuity before surgery, and all of the patients had improved visual acuity at 3 months follow-up.

Complications

No haematomas and no infections were encountered in these patients. One patient had a post-operative CSF leak that resolved after 4 days of treatment with lumbar drainage.

Discussion

Since iMRI was introduced more than 15 years ago, many scanners and surgical techniques have been developed [1]. Most of the scanner configurations that have been described require transportation of either the patient or the scanner, which is time-consuming, labour-intensive, and makes it difficult to maintain sterility and anaesthesia. The Signa SP/i 0.5-Tesla scanner that was used in this study was installed at our institution in 1996 and has been used mainly for biopsies and glioma surgeries. The ‘double-doughnut’ configuration of this scanner is designed to make it possible to operate inside the imaging field. The disadvantages of this scanner are its relatively low field strength of 0.5 Tesla and the requirement for non-magnetic instruments and microscopes. We have developed a system in which we operate just outside the MRI tunnel and slide the patient approximately 50 cm into the scanning position. We wanted to investigate the feasibility, safety and usefulness of this system during trans-sphenoidal surgery.

High-quality images were obtained in all patients, at the expected quality of the 0.5-Tesla field strength for the T1 and T2 sequences. Fahlbusch et al. [6] reported that the evaluation of the intra-operative images was obscured by an artefact in 13 of 44 patients (30%) due to metal debris from drilling or from blood in the cavity. We used a scissile to open the sella instead of a high-speed drill during surgery in the open MRI. The intra-operative imaging was performed without any closing of the sella and without any marker, like wax or cotton pledges, in the resection cavity. After thorough haemostasis, we filled the resection cavity and the speculum with isotonic saline. Remnant tumours and capsule membranes were visualised on T2 images as areas

of low signal intensity between the high signal intensity in the basal cisterns and the fluid-filled resection cavity.

We achieved primary radical surgery in 40% of the patients (eight out of 20), which correlates well with other published data reporting primary radical surgery in 27% [6] and 34% of patients [3]. Nevertheless, these figures cannot be compared directly because of the heterogeneity of the groups. In addition, we have shown that complete resection is more easily achieved in smaller tumours that have little to no parasellar extension.

The use of iMRI increased the percentage of patients that received radical surgery from 40% to 60%. The patients that were included in this study were selected on the assumption that intra-operative imaging would aid in complete resection during surgery, especially for the instances in which the tumours had a parasellar or supra-sellar extension, which predicted that parts of the tumour would not be directly visualised by the microscope in the operating field. If we had selected tumours that were located more in the centre of the sella, we would probably have achieved a higher percentage of patients with total resection; however, intra-operative imaging would have likely been less useful in these circumstances. When comparing the results from studies of trans-sphenoidal surgery, it is necessary to note the size of the tumours and the degree of parasellar extension.

Eight of ten patients exhibited normal pituitary hormonal activity after surgery (80%).

In the small subgroup of patients with growth-hormone–producing tumours (three patients), there was a 100% correlation between the intra-operative imaging results and the post-operative hormonal status. Two patients had no residual tumour, and they both exhibited a biochemical cure. The third patient, who had been operated on earlier and had a parasellar extension of the tumour (Knosp grade 4), had a tumour remnant on intra-operative imaging and showed growth-hormone hypersecretion at 3 months follow-up. Other publications have failed to show a similar correlation in acromegalic patients [7].

The design of this study was based on the presumption that the surgeon has performed as complete a resection of the tumour as possible before the iMRI scans are performed. Nevertheless, it is possible that the surgeon was more conservative during resection because an iMRI was available. The assumption that an iMRI leads to a more complete resection can thus be a self-fulfilling prophecy. The only way to avoid this bias is to design a study in which the tumours are randomised to either standard microsurgical trans-sphenoidal surgery or to trans-sphenoidal surgery with iMRI and to ensure that the groups are comparable in regard to tumour size and the degree of parasellar extension.

During treatment of hormone-producing tumours, it is important to strive for radicality in resection and to thereby cure the patient of a devastating disease. When treating non-producing tumours, however, a complete resection may not be as important. Striving for radicality in the resection increases the risk of complications during surgery, including post-operative CSF leakage, new endocrinologic deficits and haemorrhage. We reviewed the outcomes of pituitary surgeries in patients older than 70 years in our department and found that they had excellent outcomes on both mortality and performance scales, even though many of these patients had remnant tumours [15].

Traditionally, the usefulness of early MRI validation of trans-sphenoidal surgery has been questioned due to difficulty in interpreting the images. Precluding factors in this procedure can include the material used to close the sella, the haemostatic agents left in the cavity, and the difficulties in discerning blood from the tumour remnants and discerning the re-expanded pituitary gland from the tumour tissue [5]. Our experience with iMRI has taught us to use T1 with contrast enhancement and T2 as a post-operative control. At our institution, an early MRI control is performed within 48 h after all trans-sphenoidal procedures that are not performed in the iMRI. Learning from this objective evaluation of the extent of tumour resection immediately after surgery is extremely important, especially for less experienced surgeons.

Conclusion

Intra-operative MRI is a useful tool during trans-sphenoidal surgery for pituitary adenomas. Using this procedure, good results were achieved in regard to the extent of tumour resection and endocrinologic and visual outcomes, with a low complication rate. Learning from an objective evaluation of the extent of resection immediately after surgery is important, especially for less experienced surgeons, and may improve the results after trans-sphenoidal surgery.

Conflicts of interest None.

References

1. Albayrak B, Samdani AF, Black PM (2004) Intra-operative magnetic resonance imaging in neurosurgery. Acta Neurochir 146:543–557
2. Alameda C, Lucas T, Pineda E, Brito M, Uria JG, Magalon R, Estrada J, Barcelo B (2005) Experience in management of 51 non-

functioning pituitary adenomas: indications for post-operative radiotherapy. J Endocrinol Invest 28(1):18–22
3. Bohinski RJ, Warnick RE, Gaskill-Shiplev MF, Zuccarello M, van Loveren HR, Kormos DW, Tew JM Jr (2001) Intraoperative magnetic resonance imaging to determine the extent of resection of pituitary macroadenomas during transsphenoidal microsurgery. Neurosurgery 49(5):1133–1143
4. Darakchiev BJ, Tew JM Jr, Bohinski RJ, Warnick RE (2005) Adaptation of a standard low-field (0.3 T) system to the operating room: focus on pituitary adenomas. Neurosurg Clin N Am 16 (1):155–164
5. Dina TS, Feaster SH, Laws ER Jr, Davis DO (1993) MR of the pituitary gland postsurgery: serial MR studies following transsphenoidal resection. AJNR Am J Neuroradiol 14(3):763–769
6. Fahlbusch R, Ganslandt O, Buchfelder M, Schott W, Nimsky C (2001) Intraoperative magnetic resonance imaging during transsphenoidal surgery. J Neurosurg 95:381–390
7. Fahlbusch R, Keller B, Ganslandt O, Kreutzer J, Nimsky C (2005) Transsphenoidal surgery in acromegaly investigated by intraoperative high-field magnetic resonance imaging. Eur J Endocrinol 153(2):239–248
8. Greenman Y, Ouaknine G, Veshchev I (2003) Postoperative surveillance of clinically non-functioning pituitary macroadenomas: markers of tumour quiescence and regrowth. Clin Endocrinol 58(6):763–769
9. Kabil MS, Eby JB, Shahinian HK (2005) Fully endocopic endonasal vs. transseptal transsphenoidal pituitary surgery. Minim Invasive Neurosurg 48(6):348–354
10. Knosp E, Steiner E, Kitz K, Matula C (1993) Pituitary adenomas with invasion of the cavernous sinus space: a magnetic resonance imaging classification compared with surgical findings. Neurosurgery 33:610–618
11. Kremer P, Forsting M, Ranaei G, Wurster C, Hamer J, Sartor K, Kunze S (2002) Magnetic resonance imaging after Transsphenoidal Surgery of clinically non-functional pituitary macroadenomas and its impact on detecting residual adenoma. Acta Neurochir 144:433–443
12. Martin CH, Schwartz R, Jolesz F, Black PM (1999) Transsphenoidal resection of pituitary adenomas in an intraoperative MRI unit. Pituitary 2(2):155–162
13. Nesbakken R, Reinlie S, Eldevik OP (1984) Intraoperative gas cisternography and gas dissection in the operative treatment of pituitary tumors. A methodological description. Eur Surg Res 16 (Suppl 2):73–79
14. Pergolizzi RS Jr, Nabavi A, Schwartz RB, Hsu L, Wong TZ, Martin C, Black PM, Jolesz FA (2001) Intra-operative MR guidance during trans-sphenoidal pituitary resection: preliminary results. J Magn Reson Imaging 13(1):136–141
15. Rogne SG, Konglund A, Meling TR, Scheie D, Johannesen TB, Rønning P, Helseth E (2009) Intracranial tumor surgery in patients >70 years of age: is clinical practice worthwhile or futile? Acta Neurol Scand 120(5):288–294
16. Schwartz TH, Stieg PE, Anand VK (2006) Endoscopic transsphenoidal pituitary surgery with intraoperative magnetic resonance imaging. Neurosurgery 58(1 Suppl):ONS44–ONS51
17. Solheim O, Selbekk T, Løvstakken L, Tangen GA, Solberg OV, Johansen TF, Cappelen J, Unsgård G (2010) Intrasellar ultrasound in transsphenoidal surgery: a novel technique. Neurosurgery 66 (1):173–185
18. Steinmeier R, Fahlbusch R, Gansland O, Nimsky C, Buchfelder M, Kaus M, Heigl T, Lenz G, Kuth R, Huk W (1998) Intraoperative magnetic resonance imaging with the magnetom open scanner: concepts, neurosurgical indications, and procedures: a preliminary report. Neurosurgery 43(4):739–747
19. Suzuki R, Asai J, Nagashima G, Itokawa H, Chang CW, Noda M, Fujimoto M, Fujimoto T (2004) Transcranial echo-guided transsphenoidal surgical approach for the removal of large macroadenomas. J Neurosurg 100(1):68–72
20. Thapar K, Laws ER. (2004) Pituitary tumors: functioning and nonfunctioning. In: Youmans Neurological surgery, 5th edn. Saunders (Elsevier), Philadelphia, pp 1169-1206
21. Wischer-Rother M, Hoven S, Kristoff RA, Bliesener N, Stoffel-Wagner B (2004) Non-functioning pituitary adenomas: endocrinological and clinical outcome after transsphenoidal and transcranial surgery. Exp Clin Endocrinol Diabetes 112(6):323–327
22. Wu JS, Shou XF, Yao CJ, Wang YF, Zhuang DX, Mao Y, Li SQ, Zhou LF (2009) Transsphenoidal pituitary macroadenomas resection guided by PoleStar N20 low-field intraoperative magnetic resonance imaging: comparison with early postoperative high-field magnetic resonance imaging. Neurosurgery 65 (1):63–70

Acta Neurochir (2011) 153:1375–1376
DOI 10.1007/s00701-011-1005-6

EDITORIAL

The value of intra-operative MRI in trans-sphenoidal pituitary surgery

Michael Powell

Received: 22 March 2011 / Accepted: 23 March 2011 / Published online: 27 April 2011

Intra-operative MRI (iMRI) promises neurosurgeons a great deal, and far from being a research tool, as it was in the late 1990s, there are now a number of neurosurgical units throughout the world with this facility; more than 12 in Europe alone and many more in North America. It is finding many uses, perhaps most valuably in the resection of intrinsic brain tumours. At the time of commissioning of the iMRI in this author's unit in 2010, approximately 40% of the use of the machine was expected—like elsewhere in Europe—to be for the resection of pituitary adenomas.

It had always been a particularly attractive option for pituitary surgeons, as it offers us the possibility of finding out where, at the end of a trans-sphenoidal resection, residual tumour lies, long before the review MRI at some point after the end of the operative procedure. All those who manage these tumours on a regular basis, know that the early post-operative scan done in the following days can be disappointing and frustrating [2], and this reviewer had personally followed the advice given some 25 years ago by a world leader in the field to avoid doing this whenever possible—as it usually is, except when unforeseen post-operative events occur.

Many of us were strongly influenced by the papers from the University of Erlangen [4], where the fortunate conjunction of Siemens MRI scanning development occurred as well as being the then home of the unit of one of the most prolific pituitary neurosurgical units in Europe. As a consequence, we have seen a number of papers which set out the benefits in pituitary surgery. However, in practice when we had our own machines, not all of us were so convinced that the extra time (in my own unit more than doubling the operative time for a single scan) taken in obtaining an iMRI was, perhaps, as beneficial as the neurosurgeons in Erlangen had suggested. Most papers show that the completeness of resection rises by about 20%.

The disappointment stems from the knowledge that in awkwardly shaped tumours, most know where the residual tumour will lie, and have expected intra-operative difficulties in achieving complete resection. All the iMRI shows is just that, and that total tumour removal can remain frustratingly unachievable.

We have, of course, other options. A Seattle group [1] have reported the benefits of the quicker intra-operative CT scanner, and others have questioned whether endoscopy could do away with the need for iMRI at all [5].

There can be no doubt that 'complete' or very near complete resection of pituitary adenomas significantly reduces the chance of recurrence (unpublished data), so any method has at least theoretical major advantages. We have all to accept that the trans-sphenoidal route will not get tumour out of the cavernous sinus, except in exceptional circumstances, and the value of pursuing such a benign tumour into this surgically tricky area has long been debated. It is usually better to leave this area to radiation.

For the comparative novice, the secondary use of iMRI is as image guidance. As many have pointed out, experience reduces complications, and losing one's way in the approach to the pituitary fossa is the single most potent cause of these complications. However, the iMRI suites were not really a solution to these technical approach difficulties, because of the time penalty.

In this issue, Ramm-Pettersen et al. [3] propose the use of the low-field, mobile iMRI scanner. This is of interest as the number of units employing these devices is unknown, but far exceeds the vastly more expensive iMRI suite. It has always been thought that the image quality would be of lesser use, but perhaps this is not the case as the image quality is fine.

M. Powell (✉)
The National Hospital for Neurology and Neurosurgery,
Queen Square,
London WC1N 3BG UK
e-mail: michael.powell@uclh.nhs.uk

These authors conclude that it does not add significantly to the operation time—clearly a major advantage—and that it has significant advantages in low number units, with relative inexperience in the technique. Any such advantage may be worth a look for those in this position. No doubt we shall see.

Conflicts of interest None.

References

1. Eboli P, Shafa B, Mayberg M (2011) Intraoperative computed tomography registration and electromagnetic navigation for transsphenoidal pituitary surgery: Accuracy and time effectiveness. J Neurosurg 114:329–335
2. Kremer P, Forsting M, Ranaei G, Wuester C, Hamer J, Sartor K, Kunze (2002) Magnetic resonance Imaging after transsphenoidal surgery of clinically non functioning pituitary macroadenomas and it s impact on detecting residual adenoma. Acta Neurochir 144:433–443
3. Ramm-Pettersen J, Berg-Johnsen J, Hol PK, Roy S, Bollerslev J, Schreiner T, Helseth E (2011) Intraoperative MRI facilitates tumour resection during transsphenoidal surgery for pituitary adenomas. Acta Neurochir. doi:10.1007/s00701-011-1004-7
4. Steinmeier R, Fahlbusch R, Ganslandt O, Nimsky C, Buchfelder M, Kaus M, Heigl T, Lenz G, Kuth R, Huk W (1998) Intraopertaive magnetic resonance imaging with the magnetom open scanner: concepts, neurosurgical indications and procedures: a preliminary report. Neurosurgery 43:739–747
5. Theodosopoulos PV, Leach J, Kerr RG, Zimmer LA, Denny AM, Guthikonda B, Froelich S, Tew JM (2010) Maximising the extent of resection during transspenoidal surgery for pituitary adenoma: can endoscopy replace intraoperative magnetic resonance imaging? J Neurosurg 112:736–743

Acta Neurochir (2011) 153:1377–1390
DOI 10.1007/s00701-011-0973-x

CLINICAL ARTICLE

Benefit of 1.5-T intraoperative MR imaging in the surgical treatment of craniopharyngiomas

Bernd M. Hofmann · Christopher Nimsky · Rudolf Fahlbusch

Received: 16 August 2010 / Accepted: 10 February 2011 / Published online: 12 April 2011

Abstract
Background As low-field magnetic resonance imaging (MRI) has very limited significance for intraoperative control of total tumor removal (TTR), we examined the influence of 1.5-T MRI, incorporating higher resolution into the intraoperative strategy of craniopharyngioma surgery.
Methods Surgery with intraoperative imaging was performed in 25 selected patients in whom tumor resection was anticipated to be difficult according to pre-operative findings.
Results Intraoperative MRI confirmed the intended extent of tumor removal in 15 patients (14 TTRs, one intended incomplete removal, while a second procedure was scheduled due to complex shape). Misinterpretation was false positive or negative in one patient each. The extent of removal was not achieved as expected in eight patients (expectation: seven TTRs, one incomplete removal). In three patients, the expected TTR was achieved by resuming surgery. In another case, that goal was accomplished by performing an unscheduled second procedure. In total, by using intraoperative imaging, the rate of TTR was increased by 16% (four patients), leading to 80% in the entire series. Compared with the literature, the rate of new ophthalmologic and endocrine deficits is acceptable; the rate of other surgical complication is slightly higher but not directly caused by intraoperative imaging.
Conclusion Intraoperative 1.5-T MRI provides benefits because of good early prediction of TTR (sensitivity, positive predictive value: 93.8%; specificity, negative predictive value: 88.9%) and a low rate of false-positive results. Moreover, extended resection of remnants visualized is enabled and helps to increase the rate of TTR but does not exclude recurrence.

Keywords Craniopharyngioma · Reliability of intraoperative MRI · Outcome · Surgery · Total removal

B. M. Hofmann
Department of Neurosurgery, University of Halle/Saale, Halle, Germany

C. Nimsky
Department of Neurosurgery, Philipps-Universität, Marburg, Germany

R. Fahlbusch
International Neuroscience Institute, Hannover, Germany

B. M. Hofmann (✉)
Siemens AG Healthcare Sector, Allee am Röthelheimpark 3a, 91052 Erlangen, Germany
e-mail: Bernd.M.Hofmann@gmx.de

Introduction

Due to the benign behavior of craniopharyngiomas, two different treatment options are available, a more conservative, symptomatic treatment [4, 16] and a more radical one with the objective of total tumor removal. The latter comes along with an increased risk that important structures could be injured during surgery, resulting in increased complication and mortality rates [11, 30, 41, 49]. However, postoperative endocrine deficits, which occur most commonly [11, 23, 28, 30, 34, 49, 50, 52, 54, 58, 60, 63], can be treated adequately by modern substitution therapy, while total removal of tumor or capsule remnants [18] as suspected sources of regrowth can provide a higher rate of favorable results and long-term control [24, 57], as well as lower recurrence rates [25]. Contrarily, in case of a

conservative treatment, ongoing tumor regrowth from remnants is more difficult to treat than the initial tumor and may also cause severe neurological and endocrine deficits, resulting in a decreased rate of survival if untreated [7, 16, 34, 49, 56].

If more radical surgery with the intent of total tumor removal is preferred like in the study hospital [29], it is a prerequisite that every effort is made to localize tumor remnants as origins of possible regrowth intraoperatively. Otherwise, a higher risk of regrowth may be accompanied by higher morbidity caused by radical resection. Furthermore, in large intra- and suprasellar tumors requiring a two-step surgical procedure, intraoperative verification of the extent of removal is important in order not to leave tumor remnants behind which are not accessible during the second surgical procedure.

A review of the literature shows that, despite technical advances like endoscopy and neuronavigation, the overall surgical results [28, 31, 35, 40, 41, 49, 52, 55, 59, 60] remain unsatisfactory and no solutions for the above-mentioned problem have been found so far. In our opinion, even the use of an intraoperative low-field magnetic resonance imaging (MRI) was of limited benefit [43]. This was due to a high rate of recurrences and evidence for residual tumor found on imaging 3 months following surgery even if intraoperative 0.2-T MRI had indicated complete tumor removal. As we found cystic tumor configuration in follow-up imaging, it seems likely that regrowth originates from capsule remnants which may be easily missed in low-field MRI, while larger solid tumor remnants were easily demonstrated. Coming from that experience, it is obvious that visualizing and total removal of capsule remnants is the key in order to avoid further growth or radiation therapy. As those remnants may be hidden by scary tissue in repeated surgery, important neuronal structures (i.e., optic chiasm) or even the diaphragm, which is down-folded into the sellar floor in case of transsphenoidal surgery, we considered endoscopic surgery to be of limited benefit as well. With the availability of newly developed operating tables and faster MR sequences, however, the introduction of 1.5-T scanners into the operation room became possible and it was expected that the higher resolution provided by such scanners would lead to better image quality [42] and, as a consequence, to better surgical results by solving the above-mentioned issues. By now, this has already been proven in the surgery of pituitary adenomas [19, 44, 45].

The aim of this study is to evaluate the benefit of intraoperative resection control using high field MRI in craniopharyngioma surgery applied to patients suffering from a complex tumor extension. Special interest is paid to the correct interpretation and predictive value of intraoperative imaging compared with a "gold standard." The benefit and kind of modification, or resuming the surgical procedure (further resection of indicated tumorous tissue), or the strategy depending on findings of intraoperative imaging are demonstrated. Moreover, the rate of additional complete tumor removal and related complications is evaluated. To our knowledge, regarding craniopharyngioma surgery, this has not been reported in the literature until now.

Patients and methods

Patient population

After introduction of a 1.5-T MR scanner into the operating theatre in April 2002, a total of 32 patients suffering from a craniopharyngioma were treated at the study hospital until September 2005. A pilot study was initiated and the extent of resection was controlled in the selected 25 patients. Eighteen of these (ten males and eight females; male-to-female ratio: 1.25/1) underwent primary surgery, their mean age at the time of surgery was 30.9 years (3–57 years). Seven patients (five males, two females; male-to-female ratio: 2.5/1) underwent repeated surgery for recurrence or persistence, their mean age at the time of surgery was 25.8 years (10–49 years). All patients selected for inclusion into this study had tumors exhibiting a more complex shape and a proximity to important structures of the brain (pituitary stalk, hypothalamus, optic chiasm). These complex tumors were defined as tumors larger than 1 cm with an extension into more than one cranial fossa or into the ventricular system. Additional criteria included large cystic or calcified components. Furthermore, all patients who underwent repeated surgery were included in this study. Seven patients were excluded from the study as they were suffering from small, well circumscribed tumors (<2 cm) located within one cranial fossa. Three of them underwent transsphenoidal and four transcranial approaches. Previous radiation therapy was also an exclusion criterion.

All patients were referred to the study hospital due to the experience of the team in craniopharyngioma surgery and their results in treatment while intending total tumor removal. The treatment strategy was discussed with every patient and ethics committee approval as well as informed consent of patients or adequate family members were obtained preoperatively in all cases. The trial was conducted according to the Helsingbor Declaration of 1975.

Pre-, post-operative and follow up diagnostic workup, including neuroradiological, ophthalmologic and endocrine examinations, were performed prior to surgery, 1 week (except imaging) as well as 3 months following surgery and then every year.

Neuroradiological workup

In all patients, preoperative MRI was routinely used to determine the size and localization of the tumor. Furthermore, a computed tomography (CT) scan in thin layers was performed in most patients in order to detect calcification. Postoperative imaging was performed in order to document recurrence-free status or further tumor growth in case of a persisting tumor.

Ophthalmologic workup

During ophthalmologic workup (Department of Ophthalmology, University of Erlangen), a perimetry of the visual field was performed and the visual acuity as well as the eyeground were examined.

Endocrinological workup

All patients underwent sophisticated endocrinological workup. Routinely, a stimulation of the pituitary adrenal axis was performed by administering ACTH and determining the serum cortisol levels as well as the basal pituitary hormone levels. Furthermore, an insulin-induced hypoglycaemia was applied in patients without apparent clinical deficiencies and cortisol and growth hormone serum levels were measured. For assessment of the neurohypophyseal function, fluid intake and output prior to and following surgery, as well as the specific gravity of the urine, were determined. In case of normal findings, an additional water deprivation test was performed. The criteria for pituitary insufficiency are described elsewhere [17]. In case of a deficiency, replacement therapy was started immediately.

Surgical procedures

On the basis of our experience, patients suffering from hypothalamic deficits (hyperphagia, loss of diurnal rhythm or memory disturbances) were not subjected to open surgery until their condition improved [29]. The latter was achieved by draining cystic tumor components by way of stereotactic cyst aspiration or by placement of a cystoventricular shunt. A ventriculo-peritoneal shunt was inserted in case of a pre-existing hydrocephalus. Anti-oedematous treatment was initiated in case of an edema within the hypothalamic region. If no improvement could be achieved, radiotherapy was applied and the patients were not considered for this study.

Depending on the tumor size and localization, a transsphenoidal, a frontolateral, a transventricular, a subfrontal approach or a combination were performed. Prior to surgery, a decision was made as to whether total tumor removal could be achieved (23 cases) or if a two-step procedure is required (two cases). In the latter cases, the extent of removal targeted during the first surgical approach was defined preoperatively and compared with the extent of resection documented during intraoperative imaging.

Transsphenoidal surgery was performed in patients harboring an intra- and suprasellar subdiaphragmatic tumor arising from the pituitary fossa while suprasellar calcification was considered as a contraindication necessitating a transcranial approach [31]. The *frontolateral approach* was used in smaller and medium sized suprasellar craniopharyngiomas, as the short distance to the suprasellar region was considered to be an advantage. The *subfrontal interhemispheric midline approach*, providing a good overview over the tumor and the surrounding structures, was used in larger tumors developed into the third ventricle or the retrosellar area. The lamina terminalis was opened in case the tumor was developed retro- or subchiasmatically. A *transventricular approach* was used in large tumors which had developed into the third and the lateral ventricles. Details about the surgical strategy are presented elsewhere [18, 29]. All surgical procedures were performed by the senior author (R.F.).

Neuronavigation was used on a regular basis. Prior to intraoperative imaging, endoscopic exploration of the surgical field was performed.

Intra-operative imaging and impact on surgical procedure

A 1.5-T MRI scanner (Magnetom Sonata, Siemens, Erlangen, Germany) was used for intraoperative imaging. After the surgeon had the impression that tumor removal was complete or that the intended tumor volume had been resected, imaging was carried out by using the following sequences [45]. First, rapid MRI scans in 5-mm slices were performed in T_2 HASTE sequences (TR=1,000 ms, TE=89 ms, field of view=23×23 cm) without contrast enhancement. This sequence was chosen due to the short acquisition time in order to get a rapid overview over the surgical field and extent of tumor resection. The quality was sufficient to detect large remnants not necessitating meticulous image reading. Moreover, this was supported by the fact that large tumor remnants were causing a negative contrast after filling the surgical field with saline. If any remnant was found, imaging was stopped immediately and surgical procedure was continued. However, this technique was not suitable for detection of small capsule remnants, especially within the ventricular system. For that reason, the sequences described in the following were applied. Thin-layer MRI scans were performed in T_2-sequences (TR=4,000 ms, TE=97 ms, field of view=23×23 cm). These thin layer sequences of 0.6×0.4 mm provide the best in-plane spatial resolution. Additional T_1-sequences (TR=450 ms, TE=12 ms, field of view=27×27 cm) with and

without contrast enhancement were applied if complete resection was confirmed on the T_2 images. The latter is important since repeated application of contrast medium would lead to a nonspecific contrast enhancement at the resection margin. All sequences were performed in coronal and sagittal planes. Scanning time, which included both planes, was 25 s for T_2 HASTE, 6 min for T_2 and 5 min for T_1 sequences. If the full protocol was applied, scanning took no longer than 30 min, including preparation.

If the impression of a total tumor removal was confirmed or the intended extent of tumor removal had been achieved, the wound was closed. Otherwise, a repeated inspection of the surgical field and, if possible, further tumor removal took place.

Endpoints and reliability

Surgery was considered to be successful if either intraoperative imaging was indicating no tumor remnants or if the intended extent of removal was documented like defined prior to surgery. In that case, intraoperative imaging was indicating a *positive result* in the sense of this trial. Furthermore, intraoperative imaging was considered to be beneficial if any relevant changes in surgical strategy were drawn from its findings, like resuming surgical procedure in case of indicated tumor remnants (contingency table: *negative result*).

Determining the diagnostic reliability was considered as the *primary endpoint*. For that reason, sensitivity, specificity, positive predictive value (PPV) and negative predictive value (NPV) were calculated by comparing the results of intraoperative imaging with a "gold standard," i.e., images obtained 3 months following surgery. Accordingly, a positive surgical result was achieved in case intraoperative MRI indicated total tumor removal or the intended extent of removal and this finding was confirmed in the first follow-up images. An indicated tumor remnant (negative result) had to be confirmed by resection of tumorous tissue during ongoing surgery. In the case of a false-negative result, neither a tumor remnant was found during repeated inspection of the surgical field nor during follow-up imaging.

Furthermore, as another *primary endpoint*, the rate of additional complete tumor removal was calculated. In that case, a tumor remnant had to be indicated during intraoperative imaging and to be confirmed and removed during ongoing surgical procedure. Total removal had to be confirmed in first follow-up imaging, moreover.

Table 1 Detailed results of and consequences drawn from intraoperative imaging (according to surgical procedure)

Patient	Approach	Result intraoperative MRI	Surgical consequence	Classification
1	Subfrontal	Capsule remnant misinterpreted as blood clot	No consequence → regrowth	Misinterpretation of imaging
2	Subfrontal	Intrasellar remnant	Transsphenoidal surgery	Modification of approach → complete resection during 2nd procedure
3	Tsphen	Suspicious remnant	Further inspection: no remnant found → remission	Misinterpretation of imaging
4	Tsphen	Small remnant	Further resection → complete (2nd MRI)	Resume surgery
5	Tsphen	Small remnant	Further resection → judged as complete (no MRI) → regrowth	Resume surgery misinterpretation during surgical re-inspection
6	Subfrontal	Tumor remnant; intended extent of removal not achieved	Decompression of brainstem → intended removal confirmed by 2nd MRI	Resume surgery
7	Tventr	Tumor remnant like expected	CSF passage free → subfrontal surgery	Confirmation of intend. resection = goal achieved
8	Recurrent tsphen	Capsule at optic chiasm	No consequence: out of range	Resume surgery ↔ not possible
9	Recurrent tsphen	Capsule in cavernous sinus	Further inspection: misinterpreted as scar → regrowth	Resume surgery Misinterpretation during surgical reinspection
10	Recurrent tsphen, see case report	Large tumor remnant	Further resection → total removal (2nd MRI)	Resume surgery
11	Recurrent subfrontal	Capsule remnant	Further resection → total removal (2nd MRI)	Resume surgery
12-25	5 tsphen, 1 frontolat, 5 subfrontal, 2 recur. transphen., 1 recurrent subfrontal	Total removal	Wound closure → Total removal confirmed during FU imaging	Complete removal

frontolat frontolateral, *tsphen* transsphenoidal, *tventr* transventricular, *CSF* cerebrospinal fluid

Table 2 Classification of the interpretation of imaging according to the consequences drawn from it and its contribution to success of surgery

Interpretation of imaging & consequence	Number of patients	Classification of interpretation
Confirmation of total removal & wound closure (pat. 12 – 25)	14 (56%)	Correct positive
Confirmation of intended resection & total removal during 2nd step procedure (pat. 7)	1 (4%)	
Misinterpretation of imaging:	(Total: n=2)	
tumor remnant not identified in imaging (pat 1)	1 (4%)	False positive
suspicion of remnant in imaging; not confirmed during surgery (pat. 3)	1 (4%)	False negative
Resume surgery:	(Total: n=7)	
not possible due to surgical condition (pat. 8)	1 (4%)	Correct negative
leading to incomplete removal due to intra-operative misinterpretation, (pat. 5, 9)	2 (8%)	
leading to complete removal (pat. 4, 10, 11)[a]	3 (12%)	
to achieve intended resection (pat. 6)[a]	1 (4%)	
Modification of approach (subsequent procedure) & total removal (pat. 2)[a]	1 (4%)	

pat. patient

[a] Intraoperative imaging had an impact on the outcome of surgery by indicating incomplete extent of intended tumor removal, resulting in repeated inspection of the surgical field and further tumor resection, or performance of an additional surgical procedure

In order to facilitate both analysis, consequences drawn from intraoperative imaging were classified as follows: confirmation of the intended total tumor removal or extent of resection, misinterpretation of imaging, modification of the surgical approach necessitating a second surgical procedure, resume surgery with further tumor resection (Tables 1 and 2). Furthermore, misinterpretations during further tumor resection are pointed out.

The *secondary endpoint* of this study was the rate of surgical complications.

Histological workup

Neurohistological workup was performed by the Department of Neuropathology, University Erlangen-Nuremberg to confirm the diagnosis of a craniopharyngioma in all patients.

Results

Primary endpoint: diagnostic reliability of intraoperative MRI in indicating the targeted extent of tumor removal

Image quality allowed an adequate assessment of tumor or capsule remnants in all cases. Examples of characteristic findings during intraoperative imaging are shown in Figs. 1, 2, and 3. A detailed overview about findings in all patients, consequences drawn from it and results of surgery are given in Table 1. A classification of the interpretation of intraoperative imaging, the consequences drawn from it and its contribution to the success of surgery is given in Table 2 and Fig. 4.

Achievement of surgical objectives indicated correctly by intraoperative MRI

In 15 out of 25 patients (60%), the expected extent of tumor removal was documented by intraoperative MRI (correct positive result). In 14 of these patients (56.0%), total removal was achieved as expected. In another case (case 7), the tumor could not be removed totally via the transventricular route but the intended extent of tumor removal was achieved.

False-positive or -negative results

Misinterpretation of imaging occurred in two cases. In one patient (pat. 1), a tumor remnant was considered to be a blood clot and the surgical procedure was finished (false positive), while in another patient (pat. 3) the suspicion of a

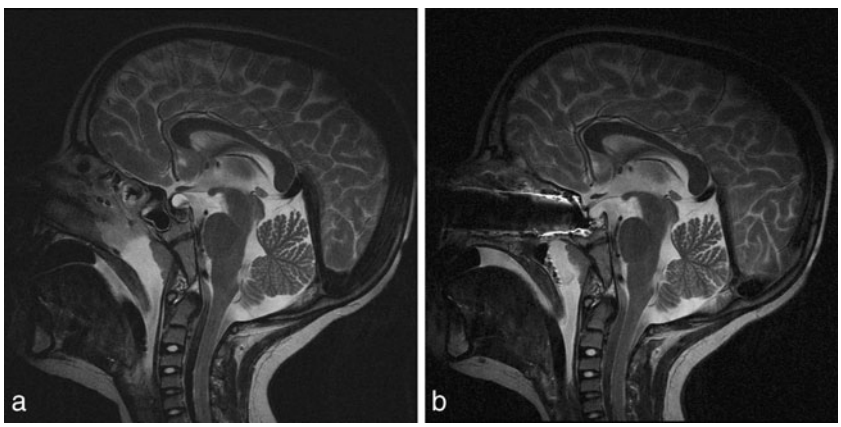

Fig. 1 Intraoperative imaging (T_2) indicating total tumor removal following transsphenoidal surgery in a 10-year-old female. **a** Preoperative imaging. **b** Intraoperative imaging indicating complete removal

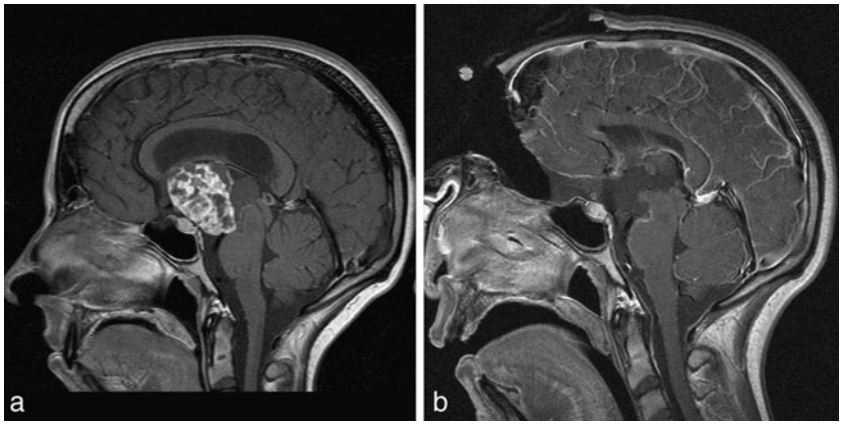

Fig. 2 Intraoperative imaging (T_1, contrast enhanced) indicating total tumor removal following transcranial surgery in a 25-year-old female. **a** Preoperative imaging. **b** Intraoperative imaging indicating complete removal

tumor remnant was not verified during ongoing surgery (false negative) without evidence for any tumor growth, so far. In the latter patient, re-exploration did not result in any additional morbidity.

Correct negative results and consequences drawn from

Intraoperative imaging was considered to be beneficial in eight patients (32%).

In one of those patients (pat. 6), the intended extent of incomplete removal was not achieved when first imaging took place. By resuming the surgical procedure, that target was met, however. Due to the comorbidity of the patient, a scheduled second surgical procedure had to be cancelled later.

In the other seven cases (28%), surgery had to be resumed due to tumor remnants indicated correctly but not expected prior to imaging. Unexpected capsule remnants were found in three of those cases, small tumor remnants in two, as well as a medium tumor remnant in one and a large tumor remnant in another. The characteristics of those seven patients were as follows. In one patient (pat. 8), who underwent repeated transsphenoidal surgery, a capsule remnant was found at the optic chiasm which was not accessible for the surgeon during repeated exploration. As

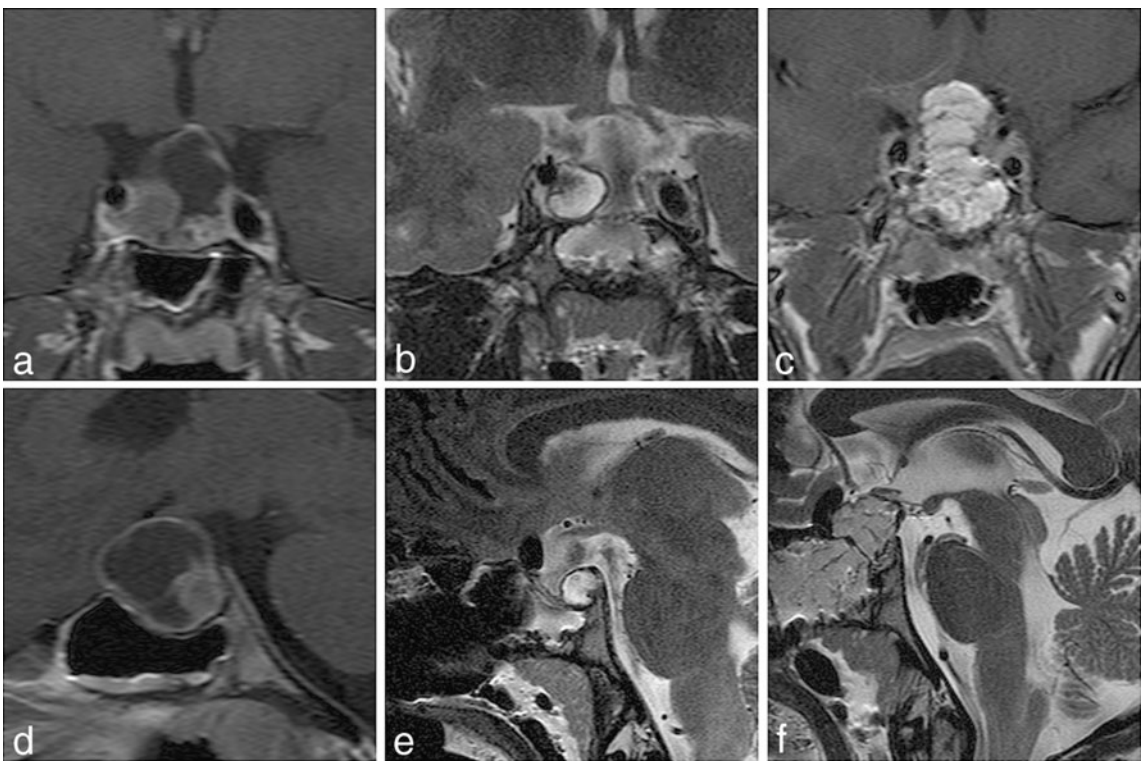

Fig. 3 Imaging during recurrent transsphenoidal surgery for a cystic intra- and suprasellar developed craniopharyngioma in a 17-year-old female. **a**, **d** Prior to operation. **b**, **e** First intraoperative imaging: a solid tumor remnant was localized right intrasellar leading to further resection. **c**, **f** Second intraoperative imaging: the tumor was removed totally and fat was packed to seal the sella

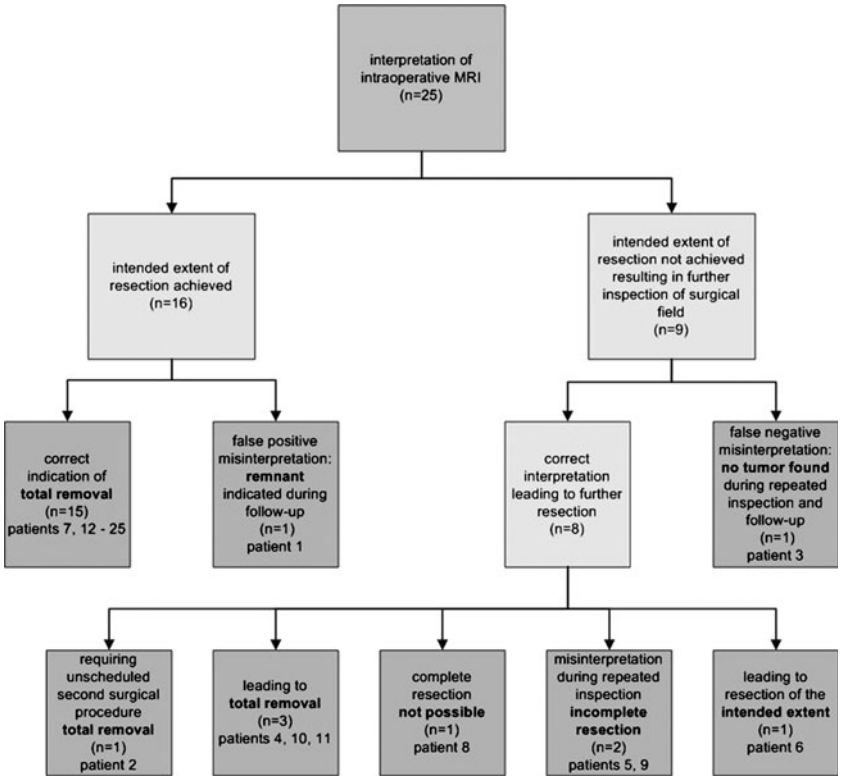

Fig. 4 Reliability of interpretation of intraoperative MRI and consequences drawn from it with regard to surgical results

this patient had a higher risk for anesthesia, transcranial surgery was abandoned. In two of the patients (pat. 5, 9) with ongoing surgery, total tumor removal was not achieved because of intraoperative misinterpretation by the surgeon and omission of repeated intraoperative imaging. This was because the surgeon had the wrong impression of total tumor removal in one case, while in the other case the tumor remnant was covered by scar tissue and not found during repeated inspection of the surgical field. An additional total tumor removal was possible in three patients (pat. 4, 10, 11) following repeated inspection. In the last of those seven patients (pat. 2), the surgical strategy had to be changed due to the results of intraoperative imaging. An indicated intrasellar tumor part could not be reached during transcranial surgery but was removed during a subsequent transsphenoidal procedure.

Determination of diagnostic reliability

The diagnostic reliability (Table 3) of intraoperative MRI was evaluated by comparing with the "gold standard" and, if indicated, the intraoperative findings together with the findings from intraoperative imaging (Tables 1 and 2).

Correct interpretation was done in 92% of the cases, misinterpretation occurred in two patients—one false-positive and one false-negative result. Specificity and NPV were 88.9%, sensitivity and PPV were 93.8%.

Primary endpoint: additional tumor removal as a consequence from intraoperative MRI

Benefit of intraoperative MRI

Intraoperative imaging had an impact on the surgical results in five cases (20%) (as indicated in Table 2). In three of them, the goal of total tumor removal was achieved during the same surgical procedure increasing the rate of total tumor removal by 12%. In another patient, this was achieved during a subsequent surgical procedure. In summary, the rate of total removal was increased by 16%. In the remaining case, intraoperative imaging indicated that the intended extent of removal was not achieved and further resection was required to achieve that goal.

As described before, in another two patients a tumor remnant was correctly indicated during intraoperative imaging. During surgical reinspection, however, those findings were misinterpreted and residual parts left behind. Unfortunately, another intraoperative imaging procedure increasing the probability for discovery of these remnants and supporting total tumor removal was not performed.

Additional total tumor removal depended on the approach applied

The rates of additional total tumor removal between primary transsphenoidal (1/8, 12.5%) and transcranial (1/10, 10.0%)

Table 3 Reliability of intraoperative 1.5-T imaging regarding estimated extent of tumor removal and continuation of surgical procedure

Intraoperative imaging	"Gold standard"[a]		
	Intended extent achieved	Intended extent not achieved	
Intended extent achieved (% of patients)	15 (60%) procedure finished correctly	1 (4%) procedure finished incorrectly	PPV: 15/16=93.8%
Intended extent not achieved (% of patients)	1 (4%) procedure resumed incorrectly	8 (32%) procedure resumed correctly	NPV: 8/9=88.9%
	Sensitivity: 15/16=93.8%	Specificity: 8/9=88.9%	

[a] As defined in "Patients and methods"

approaches as well as transsphenoidal (2/13, 15.4%) and transcranial (2/12, 16.7%) approaches in general are comparable (Table 4). While intraoperative imaging contributed to additional total tumor removal in 11.1% (2/18) of the patients following primary surgery, it was helpful in 28.6% (2/7) of the cases during repeated surgery, indicating a greater benefit of intraoperative MRI during repeated surgery.

Overall surgical results achieved in this series

In this series, total tumor removal was possible in 80.0% (20/25) of the patients.

Open surgery, following the initial diagnosis of a craniopharyngioma, was performed in 18 patients and total tumor removal was achieved in 83.3% of them (Table 5). Following a transsphenoidal approach, total tumor removal was achieved in seven out of eight patients (85.7%) without a subsequent recurrence, while the same was true for eight out of ten patients who underwent primary transcranial surgery.

Seven patients with a recurrent craniopharyngioma or a tumor regrowth were included in this study and total tumor removal was achieved in 71.4% of them while a recurrence was observed in 20.0% (Table 6). In this group, total tumor removal was achieved in three out of five patients (60.0%) who underwent transsphenoidal surgery and in the two patients who underwent a subfrontal interhemispheric approach. Unfortunately, one true recurrence was observed in former cases.

Table 4 Additional gross total tumor resection depending from approach

	Transsphenoidal surgery (13/25)	Transcranial surgery (12/25)	Total (n=25)
Primary surgery (18/25)	12.5% (1/8)	10% (1/10)	11.1% (2/18)
Repeated surgery (7/25)	20% (1/5)	50% (1/2)	28.6% (2/7)
Total (n=25)	15.4% (2/13)	16.7% (2/12)	

Secondary endpoint: surgical complications

Ophthalmologic results

The rate of new ophthalmologic deficits was two out of 25 (8.0%). In both patients, pre-existing ophthalmologic deficits deteriorated following transcranial surgery (2/12, 16.7%). In one of them, operated on via an interhemispheric subfrontal approach, visual acuity deteriorated from 0.2 and 0.3 to 0.1 for both eyes. In this patient, a supra- and retrosellar, partly solid tumor, measuring 37 mm in diameter, was removed completely. The other patient, who was first operated on by way of a subfrontal interhemispheric and then by a transsphenoidal approach, experienced a deterioration of vision and visual fields for both eyes. During surgery, an intra- and suprasellar, partly solid tumor measuring 35 mm in diameter was removed completely. No new deficits were found following repeated surgery.

Endocrine results

In the whole series, the rate of new endocrine deficits was 44% (11/25).

The degree of new postoperative endocrine deficits depends on their pre-existence. Prior to repeated surgery, all patients suffered from a panhypopituitarism, while in all patients who underwent primary surgery, at least partial pituitary function was preserved prior to surgery. Among the patients operated on by way of a transsphenoidal route, four out of eight (50%)—and following transcranial surgery, seven out of ten (70%)—experienced a deterioration. In total, 61.1% of the patients (11/18) who underwent primary surgery had one or more new postoperative endocrine deficits.

Surgical complications

In this series, three complications (12.0%) were observed. One patient developed sinusitis following a two-step transcranial/transsphenoidal approach. In one patient, operated on by way of a transsphenoidal approach, meningitis developed, and in another one, a CSF fistula was found.

Table 5 Surgical results following primary craniopharyngioma surgery with intraoperative MRI

	Total patients		Complete removal		Capsule remnants		(Intended) incomplete		Recurrence	
	n	%	*n*	%	*n*	%	*n*	%	*n*	%
Tsphen	7	38.9	6	85.7	1	14.3				
& aspiration	1	5.6	1	100						
Total tsphen	8	44.5	7	87.5	1	12.5%			0	
frontolat										
& aspiration	1	5.6	1	100						
Total frontolat	1	5.6	1	100						
Subfrontal	4	22.2	3	75.5			1	25.0		
& aspiration	3	16.7	2	66.7	1	33.3				
- & tsphen	1	5.6	1	100						
- & tventr	1	5.6	1	100						
Total subfrontal	9	50.0	7	77.8						
Tcran total	10	55.6	8	80.0	1	10.0%	1	10.0%	0	
Total series	18		15	83.3	2	11.1	1	5.6	0	

aspiration stereotactic cyst aspiration, *frontolat* frontolateral, *tsphen* transsphenoidal, *tventr* transventricular, *tcran* transcranial

One patient operated on by way of a subfrontal interhemispheric approach was in a confused mental state following surgery and left the hospital dressed inappropriately. A subsequent pneumonia led to a lethal sepsis (mortality rate: 1/25, 4.0%). No complication occurred in the patients with a false-negative interpretation of intraoperative MRI.

Discussion

In an earlier study [43] we found that intraoperative imaging using a 0.2-T MR scanner is of limited benefit during surgery of craniopharyngiomas. One reason was that the low spatial resolution did not allow an adequate visualization of smaller capsule remnants, especially those located within or in the vicinity of the cavernous sinus. Coming from that experience, the goal of this study was to examine whether the use of a 1.5-T MR scanner is of greater value. For that reason, analysis of sensitivity, specificity, PPV and NPV was performed as well as an analysis of the rate of additional total tumor removal and complications.

Value of intraoperative imaging and resulting consequences

The reliability of a 1.5-T scanner used for intraoperative imaging was found to be adequate as the rate of correct interpretation (92%), sensitivity and PPV were high (93.8%), while the specificity and NPV were satisfactory (88.9%) (Table 3). The main objectives of the intraoperative MRI were fulfilled, as the high sensitivity and PPV as well as the low rate of false positive results are indicators that this tool is useful for the confirmation of total tumor removal without leaving remnants behind unintentionally. High specificity and NPV assure that the rate of unnecessary re-exploration, affected with a higher risk for complications, remains low. As no complications were clearly attributed to longer duration of surgery attributed to intraoperative imaging, the latter figures indicating the number of re-explorations were also acceptable.

Table 6 Surgical results following repeated craniopharyngioma surgery with intraoperative MR-imaging

	Total patients		Complete removal		Capsule remnants		(Intended) incomplete		Recurrence	
	n	%	*n*	%	*n*	%	*n*	%	*n*	%
Tsphen.	5	71.4	3	60.0	2	40.0			1	33.3
Subfrontal	2	28.6	2	100						
Total series	7		5	71.4	2	28.6			1	20.0

Tsphen transsphenoidal

The discovery rate of unexpected tumor remnants (28%) in intraoperative imaging is lower than in cases of adenomectomy [45]. If surgical procedures are continued in that case, the additional rate of total tumor removal (16%) is comparable with the one achieved in cases of acromegaly (11%) [19] but lower than in nonfunctioning macroadenomas (24%) [45]. In this series, the results are expected to be better if a second intraoperative MRI would have been carried out in two patients following repeated inspection of the surgical field. In general, a randomized prospective trial including less complex cases and a higher number of patients may lead to even higher sensitivity and PPV as well as more evidence based results.

Relevance of intraoperative imaging for surgeons

Discovering large remnants by using intraoperative imaging, leading to further resection, is rare if surgery is performed by experienced surgeons with the intent of total tumor removal. However, intraoperative MRI provides advantages for the experienced group of surgeons as well as it is helpful in detecting small capsule remnants which may remain in place especially during recurrent surgery. Several reasons for leaving tumor remnants in place were identified. First of all, in transsphenoidal surgery the anatomy provides a limited overview and down-folding of the diaphragm following tumor resection may cover suprasellar remnants. Capsule remnants are difficult to differentiate from thickened arachnoid belonging to the basal cisterns. In recurrence surgery, scars may cover some tiny tumor remnants as well. The same is true for significant anatomical structures in transcranial surgery or if the tumor is spreading into the ventricular system or along the skull base. In all cases, the images have to be reviewed carefully and care has to be taken that tumor remnants detected during intraoperative imaging are found in situ and removed. During resumed surgery, repeated imaging has to take place in every case, even if the surgeon has the impression of total tumor removal. Using an endoscope is not helpful as remnants covered by the above-mentioned structures may not be visible. However, endoscopy provides an immediate and rough overview over the degree of resection. Therefore, imaging should only be started if no remnant is found during endoscopy.

In large, complex tumors requiring a two-stage strategy, intraoperative imaging provides information for optimizing the extent of tumor removal in respect to sparing eloquent areas and it documents a free CSF passage. In addition to the facts discussed above, it is important in those cases to remove all parts of the tumor which are accessible only by this operative approach.

Finally, one has to admit that some remnants may still not be as accessible during surgery even if identified on MRI. In those cases, the patient should not be harmed by hazardous manoeuvres.

For inexperienced neurosurgeons, the answer to all the above-mentioned questions becomes most important for surgical success. Moreover, one gains an immediate impression about a good surgical result without a period of uncertainty until imaging is performed during first follow-up examination.

Beneficial effects on the rate of total tumor removal

By indicating tumor remnants, the rate of total removal in this series of complex cases following primary surgery was increased above the ones reported in most of the literature [8, 14, 15, 53, 57]. It is comparable with two series [48, 58], while only two series reported better results (91% [4] and 92% [49]). Following transsphenoidal surgery, the resection rate found in this series (87.5%) is better than reported in most papers [1, 18, 31, 38–41, 63], while only one author [11] has reported better results (90%). Following transcranial surgery, only two authors have reported better results (83% [41], 90% [27]), while in most of the series [6, 18, 23, 34, 52, 55] the results were worse than in this series (80%). The only resection rate (45%) cited in the literature [14] regarding recurrent surgery is lower than the one reported here (71.4%), indicating that intraoperative imaging is especially helpful in those cases.

Noninferiority of surgery with the use of intraoperative imaging

Besides proving the benefit of intraoperative imaging regarding the rate of total tumor removal, one has to demonstrate that it is not associated with a higher rate of complications.

As we accept panhypopituitarism as a consequence of aggressive tumor resection in order to achieve complete removal, deterioration of *endocrine function* is common. Our results are comparable with those reported in the literature [11, 12, 23, 37, 48, 52, 58, 59] and there is no difference to a larger series of patients operated by the same strategy published by the authors [29]. For that reason, deterioration is not associated with intraoperative imaging but, if at all, with the more radical surgical strategy.

The same is true for *ophthalmologic complications*. Even if the rate of *ophthalmologic deterioration* (16.7%) following transcranial surgery is in the centre of the span reported in the literature [11, 12, 14, 41, 58, 59] (0% [48, 49, 52, 60] to 32% [27]) the results could be attributed to the more radical strategy of surgery and the complexity of the cases and not to the prolongation of the surgical procedure caused by intraoperative imaging.

It remains open whether the deterioration of the mental state of one patient was due to the longer duration of the surgical procedure because of intraoperative imaging. As the tumor was compromising the fornices, this event might have occurred during surgery even without resection control as well. The *mortality rate* in this series is comparable with the majority of the literature [13, 15, 34, 40, 49, 58, 59, 62], while even higher rates [6, 55] but also no mortality at all [1, 11, 52], are reported.

The *morbidity rate* (12%) reported in the series is high in the scale of the rates reported in the literature [8, 59], ranging from 5.7% in transsphenoidal [18] surgery to 12.8 or 14.3% in transcranial [18, 41] surgery. Only two authors [23, 39] have reported worse rates. However, we see no contraindication for using intraoperative imaging in craniopharyngioma surgery as the complications were of minor severity and as it is highly probable that they would have also occurred without using intraoperative imaging. If at all, they occurred due to a more aggressive surgical strategy and the complexity of the cases.

Generally speaking, indication of tumor remnants in intraoperative MRI may cause the surgeon, even unintentionally, to undertake more risky maneuvers in order to remove the tumor and therefore induce an increased number of complications, such as reported in glioma surgery using low field MRI [46]. This should be kept in mind while using this innovative technology.

Compared with the results in performing endoscopic removal of craniopharyngiomas, the rate of total removal reported in this series is superior. Following endoscopic approaches, the rate of total removal varies between 18.2% and 75% [9, 10, 22, 32, 33]. While the authors' results in transsphenoidal surgery are comparable with one series [20], their results in transcranial surgery are even better. The same is true for the rates of new endocrine deficits or other surgical complications. Endoscopic surgery is affected with a high rate of hypopituitarism (57.1–67% new cases) and complication rates vary between 12% and 35.7% [9, 32, 33].

Use of neuronavigation and cost-effectiveness of intraoperative MRI

Applying solely neuronavigation in craniopharyngioma surgery is not sufficient from the authors' point of view but it appears to be helpful for exact localization and rapid accession of the tumor. Furthermore, by enabling intraoperative orientation, faster preparation as well as resection becomes possible. Resolution of preoperative imaging and precision of registration may limit the benefit, especially in critical decisions. During an ongoing surgical procedure, brainshift may become an issue and neuronavigation may no longer be helpful in indicating tiny capsule remnants or differentiation between tumor remnants and important neuronal structures. Furthermore, tumor remnants which are hidden by a down-folded diaphragm may not be visualized and therefore missed.

Intraoperative MRI is balancing the negative effects of brainshift, especially in indicating the extent of removal, and may, as a result, help to avoid additional radiation therapy as well as repeated surgical procedures in case of larger tumor remnants. However, it is an expensive tool requiring additional dedicated surgical equipment. Advantages and disadvantages of both entities are given in Table 7. In summary, intraoperative MRI and neuronavigation will complement one another and should not be considered as mutually independent devices in craniopharyngioma surgery.

Determining the cost-effectiveness of intraoperative imaging is difficult due to different reimbursement systems and costs for construction and equipment all over the world. Furthermore, no detailed scientific data are available regarding the latter. From one author's (B.M.H.) experience, and according to the literature, typical facility breakdown costs for rebuilding a surgical theatre are about US $1.13 million for HVAC, plumbing, cabinet and storage, costs for space (800 square feed), medical gasses, demolition and miscellaneous construction. For general equipment and integration, another US $375,000 have to be estimated [21]. Summarizing those figures, the total cost will be US $1.51 million for construction and general equipment. However, costs for reconstruction depend on the size of the operating room (OR) and whether this is built from the scratch or integrated into an existing environment. In Germany, an equivalent of 1.4 million euros has to be estimated. In order to provide an insight, the German DRG system was used for further calculations.

Regarding costs for an MR scanner and dedicated surgical table, about 1.4 million euros have to be estimated depending on the software configuration as well as another 100,000 euros for RF shielding, depending on the size of the OR.

Additional costs for each surgical procedure have to be calculated, as well. One minute for anesthesia is about 2.85 euros [36], i.e., one scanning procedure lasting 30 min causes costs of an additional 85.50 euros. Assuming that in seven out of 25 surgical procedures a second scanning procedure is necessary, an average of 110 euros has to be calculated for additional anesthesia. Furthermore, 500 euros have to be added for disposable surgical material [61], resulting in additional costs of about 600 euros per surgical procedure performed using intraoperative MRI.

The subsequent profitability analysis is based on the assumption that an average of 200 surgical procedures including all types of surgical procedures (i.e., pituitary, glioma, epilepsy and others) will be carried out per year and

Table 7 Advantages and disadvantages of neuronavigation and intraoperative MRI

Intraoperative MRI		Neuronavigation	
Pro	Con	Pro	Con
Indication: tumor, epilepsy surgery, stereotaxy		Indication: tumor, epilepsy surgery, stereotaxy	
Elimination of brainshift			Efficacy limited by brainshift
			Accuracy depending on resolution of imaging & precision during registration
Indication of small capsule remnants			Limited benefit in indicating small capsule remnants
Indication of hidden tumor remnants			Hidden tumor remnants not indicated
Further surgical resection in case of incomplete removal is enabled			Incomplete resection indicated in epilepsy surgery, only
Repeated scanning possible	Prolonging surgical procedure Expensive	Easy and rapid access to tumor & easy intraoperative orientation enabled due to predefined endpoint & trajectory	
	Dedicated non magnetic surgical instruments required		
	Contraindicated in patients with pacemaker, implants, etc.		

the scanner will be used for 10 years. This number of procedures was almost achieved in the study hospital within the first year after implementation of the scanner [44]. Based on those figures, the pro rata cost for construction would be 700 euros and pro rata costs for the scanner would be 750 euros per case. If costs for surgical equipment and anesthesia are added, a total of 2,050 euros would be due for each surgical procedure. Unfortunately, no reimbursement is available for using intraoperative MRI today, but is requested meanwhile.

Administering the German DRG system, 9,045 euros would be reimbursed for surgical treatment in a noncomplicated case. In case of delayed radiation therapy, another 4,550 euros would be reimbursed. Assuming an average annual incidence of 1.5 cases per million inhabitants [2, 5], 122 patients suffer from a newly diagnosed craniopharyngioma in Germany each year. As a result from this trial, in four out of 25 cases, radiation therapy could be avoided by performing intraoperative imaging. Based on those figures, radiation therapy could be avoided in a total of 20 patients per year, resulting in savings for insurance companies of 91,000 euros. If those savings would be used for additional reimbursement (750 euros per surgical case), from a hospital's point of view, at least costs for disposable material and 10% of the pro rata costs regarding OR facilities would be covered. By using an actively shielded scanner, performing higher numbers of surgical procedures using the intraoperative setting described here and by applying sophisticated models for using the scanner for routine imaging as well, e.g., by using a sliding gantry [47], or using the scanner for longer than 10 years, this ratio could be improved further. In the end, however, the welfare of the patient should prevail over economic considerations. Anyway, it will become one task for neurosurgical societies in the near future to take care for appropriate agreements regarding reimbursement. This is supported by the fact that individual contracts between payers and several German hospitals regarding reimbursement of intraoperative imaging have been made meanwhile, especially in glioma surgery, which are covering the above-mentioned expenses. This is due to the fact that intraoperative imaging in glioma surgery was proven to be beneficial, as it was helpful in order to increase the extent of resection and the rate of gross total removal, resulting in an improvement of patient survival [3, 26, 51].

Conclusions

Not only inexperienced surgeons benefit from intraoperative MRI, because tumor remnants hidden by relevant anatomical structures or scars can be visualized in a considerable percentage of cases, especially in recurrent surgery. This is not the case when using endoscopy only. In this series of anatomically complex craniopharyngiomas, intraoperative MRI revealed relevant findings in two-fifths of the cases and led to additional total tumor removal in a significant number, while only a low number of false-positive and -negative findings was experienced. The methodology is useful especially for smaller tumor and capsule remnants, as only in one recurrent case a large tumor remnant was left behind unintentionally. For that reason, however, meticulous interpretation of intraoperative imaging and an exact evaluation of suspicious findings during surgery are essential. The same is true for repeated intraoperative imaging in case of resumed tumor resection.

Another advantage of using intraoperative imaging is the fact that one can gain immediate information as to whether total tumor removal will be possible or not.

Acknowledgements We wish to thank Prof. Blümcke and Dr. Buslei, Department of Neuropathology, University of Erlangen-Nuremberg for histopathological workup, Prof. Huk and Prof. Dörfler, Department of Neuroradiology, University of Erlangen-Nuremberg for providing MRI scans as well as the Department of Ophthalmology and the technicians of the Neuroendocrine Laboratory and the Intraoperative Imaging Suite. Furthermore, we are indebted to Mr. F. Bittner for providing the illustrations and Prof. M Klinger for revising the manuscript.

R.F. changed to the International Neuroscience Institute, Hanover in 2005, C.N. to the University of Marburg in 2008.

Financial disclosure One author (B.M.H.) is an employee of Siemens AG Healthcare Sector since September 2006 but has not received any financial support to conduct this study.

Conflicts of interest None.

References

1. Abe T, Luedecke DK (1999) Transnasal surgery for infradiaphragmatic craniopharyngiomas in pediatric patients. Neurosurgery 44:957–966
2. Adamson TE, Wiestler OD, Kleihues P, Yasargil MG (1990) Correlation of clinical and pathological features in surgically treated craniopharyngiomas. J Neurosurg 73:12–17
3. Ahmadi R, Dictus C, Hartmann C, Zürn O, Edler L, Hartmann M, Combs S, Herold-Mende C, Wirtz CR, Unterberg A (2009) Long-term outcome and survival of surgically treated supratentorial low-grade glioma in adult patients. Acta Neurochir 151:1359–1365
4. Baskin DF, Wilson CB (1986) Surgical management of craniopharyngiomas. J Neurosurg 65:22–27
5. Blair V, Birch JM (1994) Patterns and temporal trends in the incidence of malignant disease in children: II. Solid tumors of childhood. Eur J Cancer 30A:1498–1511
6. Bülow B, Attewell R, Hagmar L, Malmström P, Nordström CH, Erfurth EM (1998) Postoperative prognosis in craniopharyngioma with respect to cariovascular mortality, survival, and tumor recurrence. J Clin Endocrinol Metab 83:3897–3904
7. Cabezudo JM, Vaquerro J, Areitio E, Martinez R, de Sola RG, Bravo G (1981) Craniopharyngiomas: a critical approach to treatment. J Neurosurg 55:371–375
8. Caldarelli M, Massimi L, Tamburrini G, Cappa M, DiRocco C (2005) Long-term results of the surgical treatment of craniopharyngioma: the experienxce at the Policlinico Gemelli, Catholic University, Rome. Childs Nerv Syst 21:747–757
9. Campbell PG, McGettigan B, Luginbuhl A, Yadla S, Rosen M, Evans JJ (2010) Endocrinological and ophthalmological consequences of an initial endonasal endoscopic approach for resection of craniopharyngiomas. Neurosurg Focus 28:E8
10. Cavallo LM, Prevedello DM, Solari D, Gardner PA, Esposito F, Snyderman CH, Carrau RL, Kassam AB, Cappabianca P (2009) Extended endoscopic endonasal transsphenoidal approach for residual or recurrent craniopharyngiomas. J Neurosurg 111:578–589
11. Chakrabarti I, Amar AP, Couldwell W, Weiss MH (2005) Long-term neurological, visual, and endocrine outcomes following transnasal resection of craniopharyngioma. J Neurosurg 102:650–657
12. Chen C, Okera S, Davies PE, Selva D, Crompton JL (2003) Craniopharyngioma: a review of long-term visual outcome. Clin Experiment Ophthalmol 31:220–228
13. Chen JCT, Amar AP, Choi SH, Singer P, Couldwell WT, Weiss MH (2003) Transsphenoidal microsurgical treatment of Cushing disease: postoperative assessment of surgical efficacy by application of an overnight low-dose dexamethasone suppression test. J Neurosurg 98:967–973
14. Dhellemmes P, Vinchon M (2006) Radical resection for craniopharyngiomas in children: surgical technique and clinical results. J Pediatr Endocrinol Metab 19(Suppl 1):329–335
15. Di Rocco C, Caldarelli M, Tamburrini G, Massimi L (2006) Surgical management of craniopharyngiomas—experience with a pediatric series. J Pediatr Endocrinol Metab 19(Suppl 1):335–366
16. Duff JM, Meyer FB, Ilstrup DM, Laws ER Jr, Schleck CD, Scheithauer BW (2000) Long-term outcomes for surgically resected craniopharyngiomas. Neurosurgery 46:291–305
17. Fahlbusch R, Buchfelder M (2000) Tests of endocrine function for neurosurgical patients. In: Crockard A, Hayward R, Hoff JT (eds) Neurosurgery. The scientific basic of clinical practice, vol 2. Blackwell, Boston, pp 936–945
18. Fahlbusch R, Honegger J, Paulus W, Huk WJ, Buchfelder M (1999) Surgical treatment of craniopharyngiomas: experience with 168 patients. J Neurosurg 90:237–250
19. Fahlbusch R, von Keller B, Ganslandt O, Kreutzer J, Nimsky C (2005) Transsphenoidal surgery in acromegaly investigated by intraoperative highfield magnetic resonance imaging. Eur J Endocrinol 153:239–248
20. Fatemi N, Dusick JR, dePaiva Neto MA, Malkasian D, Kelly DF (2009) Endonasal versus supraorbital keyhole removal of craniopharyngiomas and tuberculum sellae meningiomas. Neurosurgery 64:269–284
21. Ford A (2010) Technology insights: The hybrid operating room. HCIC teleconference. The Advisory Board
22. Gardner PA, Kassam AB, Snyderman CH, Carrau RL, Mintz AH, Grahovac S, Stefko S (2008) Outcomes following endoscopic, expanded endonasal resection of suprasellar craniopharyngiomas: a case series. J Neurosurg 109:6–16
23. Gonc EN, Yordam N, Ozon A, Alikasifoglu A, Kandemir N (2004) Endocrinological outcome of different treatment options in children with craniopharyngioma: a retrospective analysis of 66 cases. Pediatr Neurosurg 40:112–119
24. Gupta DK, Ojha BK, Sarkar C, Mahapatra AK, Mehta VS (2006) Recurrence in craniopharyngiomas: analysis of clinical and histological features. J Clin Neurosci 13:438–442
25. Gupta DK, Ojha BK, Sarkar C, Mahapatra AK, Sharma BS, Mehta VS (2006) Recurrence in pediatric craniopharyngiomas: analysis of clinical and histological features. Childs Nerv Syst 22:50–55
26. Hatiboglu MA, Weinberg JS, Suki D, Rao G, Parbhu SS, Shah K, Jackson E, Sawaya R (2009) Impact of intraoperative high-field magnetic resonance imaging guidance on glioma surgery: a prospective volumetric analysis. Neurosurgery 64:1073–1081
27. Hoffmann HJ (1994) Surgical management of craniopharyngioma. Pediatr Neurosurg 21(Suppl 1):44–49
28. Hoffmann HJ, De Silva M, Humphreys RP, Drake JM, Smith ML, Blaser SI (1992) Aggressive surgical management of craniopharyngiomas in children. J Neurosurg 76:47–52
29. Hofmann BM, Höllig A, Strauss C, Buslei R, Buchfelder M, Fahlbusch R (2011) Results after treatment of craniopharyngiomas: further experiences with 73 patients since 1997. In review
30. Honegger J, Buchfelder M, Fahlbusch R (1999) Surgical treatment of craniopharyngiomas: endocrinological results. J Neurosurg 90:251–257
31. Honegger J, Buchfelder M, Fahlbusch R, Däubler B, Dörr HG (1992) Transsphenoidal microsurgery for craniopharyngioma. Surg Neurol 37:189–196

32. Jane JA Jr, Kiehna E, Payne SC, Early SV, Laws ER Jr (2010) Early outcome of endoscopic transsphenoidal surgery for adult craniopharyngiomas. Neurosurg Focus 28:E9
33. Jane JA Jr, Prevedello DM, Alden TD, Laws ER Jr (2010) The transsphenoidal resection of pediatric craniopharyngiomas: a case series. J Neurosurg Pediatr 5:49–60
34. Karavitaki N, Brufani C, Warner JT, Adams CBT, Richards P, Ansorge O, Shine B, Turner HE, Wass JAH (2005) Craniopharyngiomas in children and adults: systematic analysis of 121 cases with long-term follow-up. Clin Endocrinol 62:397–409
35. König A, Luedecke DK, Herrmann HD (1986) Transnasal surgery in the treatment of craniopharyngiomas. Acta Neurochir 83:1–7
36. Kraemer MW (2008) Kosten-Nutzen- und Kosten-Effektivitäts-Analyse der anästhesiologischen Prozesse im Anästhesiemodul des Klinischen Behandlungspfades "Laparoskopische radikale Prostatektomie" anhand eines Vergleiches zweier unterschiedlicher Allgemeinanästhesieverfahren. Department of Anesthesiology. Medizinischen Fakultät der Charité—Universitätsmedizin Berlin Berlin
37. Larijani B, Bastanhagh MH, Pajouhi M, Kargar Shadab F, Vasigh A, Aghakhani S (2004) Presentation and outcome of 93 cases of craniopharyngioma. Eur J Cancer Care 13:11–15
38. Laws ER Jr (1980) Transsphenoidal microsurgery in the management of craniopharyngioma. J Neurosurg 52:661–666
39. Laws ER Jr (1994) Transsphenoidal removal of craniopharyngioma. Pediatr Neurosurg 21:57–63
40. Maira G, Anile C, Albanese A, Cabezas D, Pardi F, Vignati A (2004) The role of transsphenoidal surgery in the treatment of craniopharyngiomas. J Neurosurg 100:445–451
41. Maira G, Anile C, Rossi GF, Colosimo C (1995) Surgical treatment of craniopharyngiomas: an evaluation of the transsphenoidal and pterional approaches. Neurosurgery 36:715–724
42. Nimsky C, Ganslandt O, Fahlbusch R (2005) Comparing 0.2tesla with 1.5tesla intraoperative magnetic resonance imaging analysis of setup, workflow and efficiency. Acad Radiol 12: 1065–1079
43. Nimsky C, Ganslandt O, Hofmann B, Fahlbusch R (2003) Limited benefit of intraoperative low-field magnetic resonance imaging in craniopharyngioma surgery. Neurosurgery 53:72–80
44. Nimsky C, Ganslandt O, von Keller B, Romstöck J, Fahlbusch R (2004) Intraoperative high-field-strength MR imaging: implementation and experience in 200 patients. Radiology 233:67–78
45. Nimsky C, von Keller B, Ganslandt O, Fahlbusch R (2006) Intraoperative high-field magnetic imaging in transsphenoidal surgery of hormonally inactive pituitary macroadenomas. Neurosurgery 59:105–114
46. Oh DS, Black PM (2005) A low-field intraoperative MRI system for glioma surgery: is it worthwhile? Neurosurg Clin N Am 16:135–141
47. Pamir MN, Özduman K, Dincer A, Yildiz E, Peker S, Özek MM (2010) First intraoperative shared-resource, ultrahigh-field 3-tesla magnetic resonance imaging systm and its application in low-grade glioma resection. J Neurosurg 112:57–69
48. Pereira AM, Schmid EM, Schutte PJ, Voormolen JHC, Biermasz NR, van Thiel SW, Corssmitt EPM, Smit JWA, Roelfsema F, Romijn JA (2005) High prevalence of long-term cardiovascular, neurological and psychosocial morbidity after treatment for craniopharyngioma. Clin Endocrinol 62:197–204
49. Poretti A, Grotzer MA, Ribi K, Schonle E, Boltshauser E (2004) Outcome of craniopharyngioma in children: long-term complications and quality of life. Dev Med Child Neurol 46:220–229
50. Sanford RA (1994) Craniopharyngioma: Results of survey of the American Society of Pediatric Neurosurgery. Pediatr Neurosurg 21(Suppl 1):39–43
51. Senft C, Franz K, Blasel S, Osvald A, Rathert J, Seifert V, Gasser T (2010) Influence of iMRI-guidance on the extent of resection and survival of patients with glioblastoma multiforme. Technol Cancer Res Treat 9:339–346
52. Shirane R, Su CC, Kusaka Y, Jokura H, Yoshimoto T (2002) Surgical outcomes in 31 patients with craniopharyngiomas extending outside the suprasellar cistern: an evaluation of the frontobasal interhemispheric approach. J Neurosurg 96:704–712
53. Sosa IJ, Krieger MD, McComb JG (2005) Craniopharyngiomas of the childhood: the CHLA experience. Childs Nerv Syst 21:785–789
54. Stahnke N, Grubel G, Lagenstein I, Willig RP (1984) Long-term follow-up of children with craniopharyngioma. Eur J Pediatr 142:179–185
55. Steno J, Malácek M, Bízik I (2004) Tumor-third ventricular relationships in supradiaphragmatic craniopharyngiomas: correlation of morphological, magnetic resonance imaging, and operative findings. Neurosurgery 54:1051–1060
56. Sung D, Chang C, Harisiadis L, Carmel P (1981) Treatment results of craniopharyngiomas. Cancer 47:847–852
57. Tomita T, Bowman RM (2005) Craniopharyngiomas in children: surgical experience at Children's Memorial Hospital. Childs Nerv Syst 21:729–746
58. Van Effenterre R, Boch A-L (2002) Craniopharyngioma in adults and children: a study of 122 surgical cases. J Neurosurg 97:3–11
59. Villani RM, Tomei G, Bello L, Sganzerla E, Ambrosi B, Re T, Barilari MG (1997) Long-term results of treatment for craniopharyngioma in children. Childs Nerv Syst 13:397–405
60. Weiner HL, Wisoff JH, Rosenberg ME, Kupersmith MJ, Cohen H, Zagzag D, Shiminski-Maher T, Flamm ES, Epstein FJ, Miller DC (1994) Craniopharyngiomas: a clinicopathological analysis of factors predictive of recurrence and functional outcome. Neurosurgery 35:1001–1011
61. Winkler O (2010) Intraoperative Bildgebung durch CT, MRT und dreidimensionale Bildgebung. DIMDI OPS Vorschlag. http://www.dimdi.de/dynamic/de/klassi/downloadcenter/ops/vorschlaege/vorschlaege2011/008-intra-operative-bildgebung.pdf. Accessed 4 Oct 2010
62. Xu X, Shigemori M (1998) Microsurgical management of craniopharyngiomas: outcomes in 56 patients. Kurume Med J 45:53–57
63. Zhou ZQ, Shi XE (2004) Changes of hypothalamus-pituitary hormones in patients after total removal of craniopharyngiomas. Chin Med J 117:357–360

Comment

This manuscript confirms the utility of intraoperative MRI to improve the accuracy of tumor resection in craniopharyngioma surgery. Based upon our experience of endoscopic endonasal management of these lesions, it could be argued that the endoscopic exploration could be sufficient to detect any remnant. However, if it is true in most of the cases, it has to be considered that craniopharyngiomas with bigger and bigger sizes and asymmetric pattern of growth are operated on via this latter route. In these conditions, where an increased risk of leaving remnants could be feared, the intraoperative MRI could be really useful. Though, if on the one hand the use of neuronavigation systems helps in defining a tailored approach to the lesion, on the other the use of intraoperative MRI provides relevant, more detailed information concerning the lesion removal while the surgical procedure is still going on. Each surgical procedure represents a different challenge that is not worth performing twice in the same way. Therefore, in such a delicate field, we think that the authors' experience contributes and favours the adoption of such a tool to improve the efficacy and the safety of the surgical approaches to craniopharyngiomas.

Paolo Cappabianca
Napoli, Italy

Acta Neurochir (2011) 153:1391–1399
DOI 10.1007/s00701-011-0959-8

CLINICAL ARTICLE

Results of endoscopic transsphenoidal pituitary surgery in 40 patients with a growth hormone-secreting macroadenoma

Margreet Albertina E. M. Wagenmakers · Romana T. Netea-Maier · Erik J. van Lindert · Gerlach F. F. M. Pieters · André J. A. Grotenhuis · Ad R. M. M. Hermus

Received: 18 October 2010 / Accepted: 28 January 2011 / Published online: 24 February 2011

Abstract
Objective Transsphenoidal pituitary surgery (TS) is the primary treatment of choice for patients with acromegaly. Macroadenomas (>1 cm) are more difficult to resect than microadenomas (remission rate ± 50% compared to ± 90%). Besides the conventional microscopic TS, the more recently introduced endoscopic technique is nowadays frequently used. However, no large series reporting on its results have yet been published. We evaluated the outcome of endoscopic TS in 40 patients with a growth hormone (GH)-secreting macroadenoma treated in our hospital between 1998 and 2007.
Methods Medical records were retrospectively reviewed. Remission was defined as disappearance of clinical symptoms of acromegaly, normal serum insulin-like growth factor-1 levels (≤2 SD) and serum GH levels suppressed to <2 mU/l after an oral glucose tolerance test within the first 4 months after TS.
Results In four patients TS aimed at debulking of the tumour. In the remaining 36 patients, remission was achieved in 20 patients. In the first 5 years remission was achieved in 6 out of 18 patients (33%) compared to 14 out of 22 patients (63%) in the following 5 years (p=0.06). Thirteen patients had a mild perioperative complication. Before TS 15 patients received hormonal substitution therapy compared to 12 patients (33%) after TS.
Conclusion Endoscopic TS is a good primary therapeutic option for patients with a GH-secreting macroadenoma, resulting in a remission rate of up to 63% in experienced hands. This technique can potentially improve the outcome of TS in these patients.

Keywords Pituitary · Acromegaly · Endoscopy · Macroadenoma · Transsphenoidal surgery

Funding No specific grants from any funding agency in the public, commercial, or not-for-profit sector were received for this research.

Previous presentations Portions of this work were presented as an oral presentation at the Klinische endocrinologie dagen, Maarssen, The Netherlands, January 2009; at the Fifth Congress of the International Federation of Neuroendoscopy, Athens, Greece, May 2009; and in poster form at the 92nd annual meeting of the Endocrine Society, Washington DC, June 2009.

M. A. E. M. Wagenmakers (✉) · R. T. Netea-Maier · G. F. F. M. Pieters · A. R. M. M. Hermus
Pituitary Centre Nijmegen, Department of Endocrinology, Radboud University Nijmegen Medical Centre, Geert Grooteplein 10, 6525 GA, Nijmegen, The Netherlands
e-mail: m.wagenmakers@endo.umcn.nl

E. J. van Lindert · A. J. A. Grotenhuis
Pituitary Centre Nijmegen, Department of Neurosurgery, Radboud University Nijmegen Medical Centre, Reinier Post Laan 4, 6525 GC, Nijmegen, The Netherlands

Introduction

Untreated acromegaly causes significant morbidity, and is associated with a two- to threefold increase in mortality. When acromegaly is treated successfully and "safe" growth hormone (GH) and insulin growth factor-1 (IGF-1) values are achieved, the mortality rate normalises [32]. Therefore, appropriate treatment of acromegaly is crucial. However, symptoms and signs of acromegaly develop insidiously, and there is often a delay in diagnosis for up to 10 years. Therefore, approximately 70% of GH-secreting adenomas are ≥1 cm (macroadenomas) at the time acromegaly is diagnosed [32].

According to experts, transsphenoidal pituitary surgery (TS) is the treatment of choice for acromegaly [28, 31], potentially rapidly restoring normal physiology by a single intervention. Macroadenomas, however, are difficult to remove by TS, especially when invasive. This may explain the relatively low remission rate of about 50% reported after TS in macroadenomas, whereas remission rates up to 90% are achieved by TS in microadenomas (<1 cm) [34]. Since more recently developed medical therapies achieve good results in controlling acromegaly, some authors have recommended medical therapy as a primary treatment option instead of TS for patients with a GH-secreting macroadenoma that does not cause mass effects [13, 25].

Nowadays, the endoscopic technique of TS is increasingly used by many neurosurgeons instead of the conventional microscopic technique. This technique, offering a panoramic wide angle view with increased illumination, was first developed in the 1990s. Different angles can be used, making it possible to effectively reach supra- and parasellar portions of the lesion and work around the corner [10, 14]. Due to these advantages, it has been suggested that the endoscopic technique may be preferable to the conventional technique, especially in patients with invasive macroadenomas [14, 28, 39]. However, due to the recent introduction of this technique, no large series reporting on the results of endoscopic TS in acromegaly have yet been published.

To gain insight in the role of endoscopic TS as a primary treatment option for patients with GH-secreting macroadenomas, we evaluated the results of endoscopic TS in 40 consecutive patients with a GH-secreting macroadenoma treated in our hospital between 1998 and 2007.

Patients and methods

Patients

Between 1998 and 2007, 40 patients with acromegaly and a macroadenoma on a preoperative magnetic resonance imaging (MRI) scan underwent endoscopic TS in our centre. The medical records of these patients (19 males and 21 females, Table 1) were retrospectively reviewed. Age at time of TS was 47.4±11.4 (mean±SD) years and BMI was 29.0±4.9 kg/m^2. We collected data on preoperative as well as early postoperative evaluation, complications that occurred during TS or in the early postoperative period, and data on the follow-up of these patients.

Preoperative evaluation and perioperative treatment

The initial diagnosis of acromegaly was based on clinical grounds and biochemical tests, including assessment of serum GH levels (basal and after oral administration of glucose) and serum IGF-1 levels. Furthermore, the thyrotropic, gonadotropic and pituitary-adrenal axes were assessed, as well as the prolactin blood level. Preoperative pituitary imaging by MRI was performed in all patients.

Long-acting somatostatin analogues (SA) were given preoperatively in 34 patients for a median period of 7 months (range 1–28), 1 patient received 10 mg/4 weeks, 20 patients received 20 mg/4 weeks and 13 patients received 30 mg/4 weeks.

One hour before surgery, administration of glucocorticoids (prednisolone, 25 mg i.v. every 8 h) was started. Two days after surgery glucocorticoid administration was changed from i.v. to oral, and the dose was tapered rapidly.

Surgical technique

The endoscopic technique of TS was introduced in our hospital in 1994 and first used for acromegaly in 1998. From 1998 onward practically all TSs (n=365) were performed endoscopically. The surgeries were exclusively performed by two neurosurgeons. The technique is very similar to the technique that Jho et al. and Cappabianca et al. have described previously [7, 8, 21, 22]. However, a binostril transsphenoidal approach to the sella turcica was used, during which the endoscope was handheld.

For the endoscopic transnasal TS, 0º and 30° rigid endoscopes with a lens diameter of 4 mm with a separate shaft were used, which allow easy and comfortable holding, while offering a suction-irrigation-system for cleaning the lens (Karl Storz GmbH, Tuttlingen, Germany). The instruments used are principally the same as used with the microsurgical technique. Because an adenoma was visible on preoperative MRI, a selective adenomectomy was performed in all patients.

Postoperative evaluation

A complication of TS was defined as any event occurring during or after TS that required treatment. As intraoperative cerebrospinal fluid (CSF) leakage is inherent to the surgical procedure and is closed during TS with a fat graft, it was not regarded as a complication, whereas postoperative CSF leakage was considered a complication.

On the 7th day postoperatively, at least 48 h after the last dose of glucocorticoids, early biochemical evaluation was carried out by measuring the serum concentrations of IGF-1, fasting cortisol, adrenocorticotropic hormone (ACTH), thyrotropin (TSH), free thyroxine (FT4), gonadotropines (LH and FSH), testosterone, estradiol and prolactin.

Patients were re-evaluated every 2 to 4 weeks during the first 3 months after surgery. Serum GH and IGF-1

levels were measured at each visit. Four months after surgery a new MRI of the pituitary was performed to check for tumour remnants. An oral glucose tolerance test (OGTT; 100 g of glucose [36]) was performed if the IGF-1 level had normalised or was marginally elevated. Thereafter patients who were in remission were evaluated at least once a year or earlier in case of clinical suspicion of a relapse.

Criteria for remission and relapse

Remission was defined as disappearance of clinical symptoms of active GH hypersecretion with in addition normal serum IGF-1 levels (≤mean+2 standard deviations for age) and suppression of serum GH levels to <2 mU/l during OGTT within the first 4 months after surgery [19, 20].

Relapse was defined as development of clinical signs of active GH hypersecretion with elevated serum IGF-1 levels (>mean+2 standard deviations for age) and serum GH levels ≥2 mU/l during OGTT [19, 20].

Imaging

All preoperative and postoperative MRI scans were evaluated by the same neurosurgeon to prevent bias. Maximal diameter of the adenoma was defined as the largest distance that could be measured in any direction of the adenoma. Invasion was defined as suspected growth of the adenoma beyond the sella into the cavernous sinus or the sphenoid sinus.

Analysis of factors influencing outcome and statistics

Data were analysed using SPSS 16.0. Characteristics of patients operated on in the first and second 5 years were compared using unpaired T-test and Pearson's chi-square test. The influence of various factors on the chance to achieve remission by TS was analysed by binary logistic regression. The factors analysed were: date of operation (as a surrogate measure for experience of the neurosurgeons), age, gender, the level of preoperative IGF-1 and GH, the diameter of the adenoma on preoperative MRI, evidence of invasion on the preoperative MRI, occurrence of perioperative complications and the need for hormonal substitution therapy after TS. The influence of dichotomous variables (gender, substitution therapy before TS, evidence of invasion on the preoperative MRI, TS in the first or second 5 years, occurrence of perioperative complications and the need for hormonal substitution therapy after TS) on the chance of remission were also analysed using Pearson's chi-square test. Statistical significance was defined as p=<0.05 (two-sided).

Results

Remission rates after TS

The results of endoscopic TS in the 40 patients with a GH-secreting macroadenoma are shown in Fig. 1. The individual data per patient are presented in Table 1. Histological investigation of the removed tissue showed evidence of a GH-producing adenoma in all cases. The overall remission rate in our series is 50%. However, four patients (patients 21, 30, 33 and 34, Table 1) had an invasive adenoma of more than 30 mm in diameter and suffered from local mass effects. The intention of the TS in these patients was to debulk the adenoma, as it was appreciated that cure could not be achieved by TS. In the remaining 36 patients, in whom the intent was cure, remission was achieved in 20 patients. In this group the remission percentage thus was 56%. Median follow-up was 56 months (range 6–126). Recently, two patients (patients 12 and 35) developed a mild relapse. Patient 12 is now being treated with octreotide, while the relapse of patient 35 was very mild and no treatment had yet been initiated.

The date of TS significantly influenced the chance of remission after TS. If a patient was operated on at a later date, the chance of achieving remission after TS was higher (p=0.04). If the results of TS during the first 5-year interval after the introduction of the endoscopic technique are compared with the second 5-year interval, remission was achieved in 6 out of 18 patients (33%) during the first 5 years, whereas in the next 5 years, 14 of 22 patients (63%) were in remission after TS (p=0.06). However, the four patients who only underwent debulking were all operated on in the last 5 years. If these patients are excluded, the remission rate achieved in the last 5 years is 77%, which is significantly better than the remission rate over the first 5 years (p=0.01). Table 2 shows that baseline characteristics of patients operated on during the first 5 years do not significantly differ with baseline characteristics of patients operated on during the last 5 years, except for preoperative IGF-1 levels, which were significantly higher in the second group. This does not change if the four patients who underwent debulking are excluded.

There were no statistically significant differences between the patients who underwent successful or unsuccessful TS with respect to age, gender, occurrence of perioperative complications, preoperative IGF-1 levels or need for hormonal substitution therapy after TS. There was a trend that if the diameter of the adenoma was larger, the chance to achieve remission was smaller (p=0.06 in all patients); however if the four patients who underwent only debulking were excluded, this trend was no longer present (p=0.56). Eight of 19 patients (42%) with evidence of invasion on preoperative MRI, and 12 of 21 patients (57%) without

Table 1 Results of endoscopic transsphenoidal pituitary surgery in patients with acromegaly (1998–2007)

Patient number, gender, age (years)	Preoperative octreo-tide	MRI (mm)	Invasion on preoperative MRI	Year of TS	Postoperative IGF-1		Postoperative oGTT	TS result	Additional therapy	Last IGF-1		Follow-up (months)
					nmol/l	SD				nmol/l	SD	
1. f, 52	Y	20	Sc r	1998	50.3	>2	-	F	RT+cab	19.0	1	127
2. m, 43	N	25	-	1999	24.0	1	38	F	Octr	32.8	>2	38
3. f, 27	N	18	Sc r	2000	92.7	>2	9	F	GK	10.6	-2	109
4. m, 40	Y	10	-	2000	23.1	1	<2	R	-	12.9	-1	106
5. f, 24	Y	17	-	2000	77.0	>2	-	F	Octr+cab	41.0	>2	78
6. f, 59	Y	20	Ssphen,sc l	2001	64.5	>2	-	F	TS, RT+peg	15.6	0	76
7. f, 54	N	11	Sc l	2001	62.8	>2	-	F	RT+octr	23.5	1	73
8. m, 39	N	14	-	2001	73.6	>2	-	F	RT+octr, cab	28.1	2	68
9. m, 49	Y	43	Ssphen, sc l+r	2001	60.5	>2	-	F	TS+octr, cab	21.6	1	91
10. f, 50	Y	12	-	2001	10.2	-2	<2	R	-	15.4	0	74
11. f, 49	Y	13	-	2001	38.4	>2	-	F	Octr	14.0	0	91
12. m, 37	Y	20	-	2001	28.3	1	<2	R	Octr	15.6	0	87[a]
13. m, 44	Y	10	Sc r	2001	83.6	>2	-	F	GK+octr, peg	27.9	2	86
14. f, 34	Y	16	-	2002	10.5	-2	<2	R	-	11.4	-2	70
15. f, 55	Y	18	-	2002	30.9	>2	3	F	Octr	9.8	-2	86
16. f, 56	Y	11	Sc r	2002	12.7	-1	<2	R	-	13.6	0	79
17. m, 56	Y	14	-	2002	16.8	0	<2	R	-	15.2	0	77
18. m, 64	Y	12	-	2002	18.0	1	2	F	Octr	18.3	1	57
19. f, 66	Y	16	Ssphen, sc r	2003	27.1	2	<2	R	-	25.0	2	65
20. f, 45	Y	30	Sc l	2003	24.7	1	<2	R	-	29.0	2	48
21. m, 35	Y	39	Ssphen	2003	66.3	>2	-	F	Octr	14.1	-1	69
22. f, 56	Y	15	Sc r	2003	15.3	0	<2	R	-	16.5	0	47
23. f, 41	Y	15	-	2003	28.0	1	<2	R	-	22.7	1	66
24. m, 54	Y	13	-	2004	19.8	1	<2	R	-	16.6	0	44
25. f, 43	Y	11	-	2004	29.5	2	<2	R	-	22.8	1	43
26. m, 48	N	12	-	2005	35.8	>2	-	F	Octr	23.6	1	31
27. f, 29	Y	10	Sc l	2005	25.6	1	<2	R	-	23.5	1	37
28. f, 51	Y	13	-	2005	11.7	-1	<2	R	-	15.6	0	49
29. m, 64	Y	14	Sc r	2005	30.0	>2	-	F	Cab	21.4	1	36
30. m, 68	Y	30	Sc l+r, ssphen	2005	31.5	>2	-	F	Octr	16.8	1	30
31. m, 46	Y	21	-	2005	43.1	>2	<2	F	-	36.2	>2	32
32. m, 45	N	15	-	2005	46.0	>2	<2	F	-	31.3	>2	38
33. m, 35	Y	42	Sc l+r	2005	163.8	>2	595	F	RT+octr, cab	56.9	>2	33
34. f, 28	Y	45	Sc l+r	2006	98.7	>2	-	F	RT+octr	33.3	>2	15
35. f, 67	Y	11	-	2006	21.5	1	<2	R	-	27.4	>2	31[a]
36. m, 40	Y	21	Sc r	2007	22.9	0	<2	R	-	21.3	1	14
37. m, 62	Y	20	-	2007	18.4	1	<2	R	-	18.4	1	6
38. f, 41	Y	24	Sc re	2007	31.7	2	<2	R	-	12.0	-1	15
39. f, 46	Y	18	-	2007	16.2	0	<2	R	-	21.3	1	8
40. m, 54	Y	27	Sc r	2007	26.6	2	<2	R	-	26.6	2	6

f: female; m: male; preoperative octreotide Y: treated with octreotide before surgery; preoperative octreotide N: not treated with octreotide before surgery; MRI: magnetic resonance imaging results given as maximal diameter of the visualised tumour in mm; sc r: cavernous sinus right; sc l: cavernous sinus left; ssphen: shenoid sinus; ssphen: sphenoid sinus; TS: transsphenoidal surgery; IGF-1 nmol/l: value of insulin-like growth factor-1; IGF-1 SD: standard deviation of insulin-like growth factor-1 compared to normal values in people of the same age and sex; oGTT: minimal value of growth hormone achieved during the postoperative oral glucose tolerance test; GTT -: no oral glucose tolerance test performed after surgery; TS result R: remission; TS result F: failure; RT: conventional radiotherapy; octr: octreotide; cab: cabergoline; GK: gamma knife radiosurgery; peg: pegvisomant; [a]: relapse at last follow-up

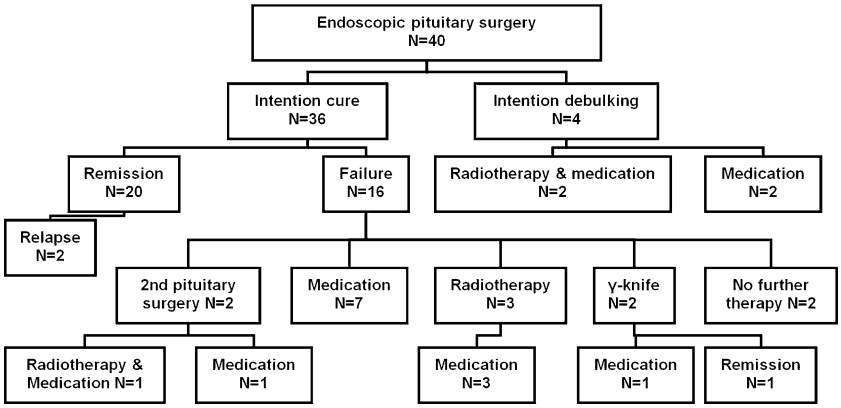

Fig. 1 Results of endoscopic pituitary surgery in patients with a growth hormone secreting macroadenoma (1998–2007)

invasion achieved remission after TS (p=0.34). If the four patients in whom the intention of the TS was to debulk the adenoma were not taken into account, the remission rate in patients with suspected invasion was 53%, indicating that in this study invasion did not significantly influence the chance to achieve remission (p=0.82).

Additional treatment and benefits of TS in patients with persistent acromegaly after TS

Although remission was not achieved via TS in 20 patients, the maximal diameter of the adenoma was reduced from a median of 18 mm (range 10–45) on the preoperative MRI to a median of 7 mm (range 0–35) on the MRI performed 4 months after surgery. The adenoma was reduced in size in all patients, and in six patients no residual adenoma was visible on the postoperative MRI. In three patients (patients 11, 15 and 18), normal IGF-1 levels could be achieved with a dose of octreotide that was the same or even lower than the dose prescribed before the operation and that had been insufficient to suppress IGF-1 to normal levels before TS.

Figure 1 shows how the 20 patients with persisting acromegaly after TS were treated. A second TS was attempted in two patients but failed to result in cure. Of the eight patients receiving additional conventional radiotherapy, none is presently in remission and all are still receiving medical treatment to control the acromegaly. Radiosurgery (γ-knife) was performed in two patients and resulted in remission in one of them. Of the remaining patients not cured by the TS, all patients except patient 32 and 33 were exclusively treated with medication. Patient 32 and 33 did not receive any further treatment. In patient 32 the IGF-1 level was only slightly elevated with no symptoms of active acromegaly, GH was suppressed to <2 mU/l after OGTT, and the mean GH values are below 6.5 mU/l. Patient 33 refused to be tested or treated further after TS because the symptoms of acromegaly had disappeared.

Complications of TS and influence of TS on deficiencies of pituitary hormones

Only mild complications occurred in our series. Fourteen patients developed a very mild transient diabetes insipidus (DI) for a maximum of 2 to 3 days. This was not regarded as a complication. Only one patient (patient 33) had a more severe transient DI. Five patients, of whom two had had mild transient DI early after the operation, were treated with fluid restriction when they developed a mild hyponatremia

Table 2 Comparison of baseline characteristics of the patients operated on during the first 5 years and the patients operated on during the second 5 years

	First 5 years (n=18)	Second 5 years (n=22)	Significance
Gender (% male)	8 (44%)	11 (50%)	p=0.76
Age (years)	46.2 (±11.0)	48.4 (±11.9)	p=0.56
BMI (kg/m^2)	29.8 (±4.4)	26.6 (±5.3)	p=0.32
Preoperative medication	13 (72%)	20 (91%)	p=0.12
Adenoma diameter (cm)	16.9 (±7.8)	20.9 (10.4)	p=0.18
Invasion on preoperative MRI	7 (39%)	12 (54%)	p=0.32
Preoperative IGF-1 value (nmol/l)	93.3 (±23.5)	116.6 (±36.9)	p=0.03

Data are expressed as means and standard deviations in case of continuous variables and as exact numbers and percentages in case of nominal or ordinal variables. BMI: Body mass index; IGF-1: insulin-like growth factor-1; MRI: magnetic resonance imaging

Table 3 Influence of transsphenoidal surgery on substitution therapy in 40 patients with acromegaly caused by a macroadenoma

TS: transsphenoidal surgery, GH: growth hormone.

	Levothyroxine substitution	Androgen substitution	Glucocorticoid substitution	GH substitution	Desmopressin substitution	Total
Discontinued after TS	5	5	1			11
Started after TS	4	2	2	1	1	10
Continued after TS	4	3	3			10

because of inappropriate ADH secretion. Four patients had mild epistaxis, controlled with nasal tampons. Three patients had cerebrospinal fluid (CSF) leakage postoperatively. They were treated successfully with an external lumbar drain.

Fifteen patients (38%) already received substitution therapy for deficiency of one or more hormones before TS. After TS 33% of all patients receive long-term hormonal substitution. Twenty percent of the patients receive substitution with levothyroxine, 12.5% receive androgens, 12.5% receive glucocorticoids, 2.5% receive GH therapy and 2.5% receive desmopressin (Table 3).

Discussion

In this study we report on the results of endoscopic TS in 40 consecutive patients with acromegaly and a pituitary macroadenoma on preoperative MRI, operated on in our hospital between 1998 and 2007. Although some results of endoscopic TS in small numbers of patients with acromegaly have been mentioned in large series of patients with different pituitary tumours [6, 11, 26, 42], no series focussing on the results of endoscopic TS in patients with acromegaly have yet been published. All previous published series on results of TS in patients with GH-secreting macroadenomas used the conventional technique of TS.

Remission rates after conventional TS reported in these larger series of patients with GH-secreting macroadenomas (including giant macroadenoma) vary widely, from 15 to 71% (Table 4) [1, 2, 4, 15, 18, 23, 29, 34, 40, 41, 43, 45]. The overall remission rate of 50% in this study is in concordance with these results. However, not all series have used the same criteria to describe remission. The studies that used the criteria for remission formulated by Giustina et al. in 2000 [19, 20], as we did in our series, reported remission rates in patients with macroadenomas of maximally 50%. Therefore, the remission rate of 50% reported in our series is comparable to the best previously published remission rates achieved in patients operated on by the conventional microscopic method of TS.

However, the remission rate of 63% (or 77% if the patients who underwent debulking are excluded) we achieved in the last 5 years, compared to a remission rate of 33% in the first 5 years, is very promising for the future. The characteristics of patients operated on in the first 5 years and second 5 years were comparable (Table 2). The only significant difference was that the patients operated upon in the second 5 years had a significantly higher IGF-1 level. Therefore, we believe that the higher remission rate achieved in the last 5 years is not biased by patients on whom it was easier to operate. So, it is more likely that the large difference between the remission rate achieved in the

Table 4 Review of the criteria to define remission of acromegaly and remission percentages in macroadenomas reported in the most recently published series (1997–2005)

Author	N	Criteria of remission	Remission %
van Lindert et al. [45]	40	GH <2 ng/ml after OGTT, IGF1 N	55
Abosch et al. [2]	254	Basal GH <5 ng/ml	71
Swearingen et al. [41]	129	GH <2 ng/ml after OGTT or IGF1 N or basal GH <2.5 ng/ml	48
Gittoes et al. [18]	45	GH <2 mU/l after OGTT or basal GH <5 mU/l	51
Laws et al. [29]	51	GH ≤1 ng/ml after OGTT or IGF1 N or basal GH ≤2.5 ng/ml	51
Kaltsas et al. [23]	50	Basal GH <2.5 ng/ml, IGF1 N	26
Abe and Ludecke [1]	126	Basal GH <2.5 ng/ml, IGF1 N	68
Shimon et al. [40]	44	GH <2 ng/ml basal or after OGTT, IGF1 N	64
Beauregard et al. [4]	77	GH ≤1 ng/ml after OGTT or IGF1 N or basal GH ≤2.5 ng/ml	49
Trepp et al. [43]	64	GH <1 ng/ml after OGTT or IGF1 N or basal GH <2.5 ng/ml	39
Erturk et al. [15]	19	GH ≤2 ng/ml basal or after OGTT	15
Nomikos et al. [34]	364	GH <1 ng/ml after OGTT or IGF1 N or GH <2.5 ng/ml	50

N: number of patients included; GH: growth hormone; OGTT: oral glucose tolerance test; IGF1: insulin-like growth factor type 1

first 5 years and the second 5 years after introduction of the endoscopic technique of TS can be explained by the increasing experience of the two neurosurgeons who performed all endoscopic TSs in our hospital. Strong evidence exists that success rates of microscopic TS critically depend on the skills and experience of the neurosurgeon [3, 15, 18]. Our data indicate that this is no different for endoscopic TS. This argues in favour of concentrating endoscopic TS for acromegaly in a limited number of experienced centres.

Previously published series on conventional microscopic TS in patients with acromegaly and a macroadenoma found that the chance of remission after TS could be predicted by the suspected invasiveness of the macroadenoma on the preoperative MRI scan [2, 4, 18]. However, in this study, although we observed a non-significant trend towards a lower chance of successful TS if tumour invasion was suspected, remission was still achieved in 42% of patients with suspected invasion. This may be explained by the fact that the endoscopic technique enables the use of different angles to operate, making it possible to reach suprasellar and parasellar portions of the lesion effectively [10, 14]. If this is the case, the endoscopic technique might be preferable in case of invasive macroadenomas.

Due to the good results that have been achieved by medical therapy in patients with acromegaly and the relatively low remission rates after TS for patients with a GH-secreting macroadenoma, some authors have recommended medical therapy as a primary treatment option instead of TS for patients with a GH-secreting macroadenoma not causing mass effects [13, 25, 39]. Nowadays long-acting somastatin analogues (SA) have the potential to normalise IGF-1 levels in two thirds of patients, additionally controlling tumour size [17]. The more recently developed GH receptor antagonist pegvisomant can normalise IGF-1 in up to 97% of patients [44]. Furthermore, studies on combination therapies with SA and pegvisomant or SA and dopamine agonists have shown that combination therapy may be successful when monotherapy has failed [16, 33, 38]. Although medical treatment can result in long-term remission, it cannot cure acromegaly. Moreover, pegvisomant, which is effective by preventing GH action in the target tissues (organs), lacks a direct effect on the tumour to control long-term tumour growth. This might limit its use as primary therapy for patients with macroadenomas until more long-term data on safety are available. Last but not least, lifelong use of expensive medication is required with the risk of serious side effects.

Studies have shown that surgical debulking can improve control of acromegaly by SA [12, 24, 35]. So even if a patient cannot be cured by TS, TS should still be considered, especially if acromegaly cannot be controlled by SA before TS. In this study TS reduced the size of the adenoma in all patients who were not cured by TS and improved the response to SA treatment in at least five of these patients. Unfortunately, a preoperative IGF-1 value during SA therapy was not available in all patients, so possibly more patients benefited from the TS to control their acromegaly.

Preoperative treatment with SA has been associated with improved results of TS, especially in macroadenomas [1, 5, 9, 30]. This could possibly be explained by adenoma shrinkage or a change in the consistency of the adenoma [9]. However, most published studies have limitations. They are retrospective, have poor remission rates or small numbers of patients. Furthermore, other studies have not confirmed this positive effect [27, 37]. A negative effect of preoperative treatment with SA on the outcome of TS results, however, has never been found. Therefore, and because pretreatment with SA improves metabolic control, we prescribed preoperative therapy with octreotide in all but six patients. Of these six patients, none achieved remission after TS. However, because of the small number of patients who did not receive preoperative treatment and the retrospective character of this study, it was not possible to evaluate whether preoperative treatment had an effect on the results of TS.

Thirteen patients in our study had a perioperative complication. All complications were mild, and no serious complications occurred. This is in concordance with the incidence of complications associated with TS via the microscopic technique [1, 2, 4, 15, 18, 23, 29, 34, 40, 41, 43, 45]. However, the endoscopic technique is probably more comfortable for the patients as the nose septum is almost left intact and usually no nasal packing is required after surgery. Besides the four patients with mild epistaxis, no rhinologic/local complications occurred, which seems to be less than those reported with the conventional technique. However, most patients that are operated upon via the microscopic technique do not need nasal packaging, but receive it because of a longstanding surgical habit.

In this series the number of hormonal deficiencies caused by TS was equal to the number of deficiencies cured by TS. All patients had a macroadenoma, which frequently causes a hormonal deficiency by itself before surgery. If the adenoma is selectively removed, normal pituitary function can potentially be restored [45]. Therefore, in macroadenomas, the fear of creating new hormonal deficiencies should probably not be a reason to restrain from TS.

Conclusion

Endoscopic TS is a treatment that should be considered as a primary therapeutic option for patients with a GH-secreting macroadenoma. In this series of patients operated on by

experienced surgeons, it resulted in a remission rate of at least 50%, with only mild complications. The relatively high remission rate of 63% (or 77% excluding the patients who underwent primary debulking) we achieved in the last 5 years indicates that operation results can improve further if experience is gained. Because the endoscopic technique enables the surgeon to use different angles, this technique can potentially improve the outcome of TS in macroadenomas, especially in patients with invasive macroadenomas. However, a randomised clinical trial comparing endoscopic and conventional TS in patients with a GH-secreting macroadenoma is needed to determine the exact pros and cons of both techniques.

Conflicts of interest None.

References

1. Abe T, Ludecke DK (2001) Effects of preoperative octreotide treatment on different subtypes of 90 GH-secreting pituitary adenomas and outcome in one surgical centre. Eur J Endocrinol 145:137–145
2. Abosch A, Tyrrell JB, Lamborn KR, Hannegan LT, Applebury CB, Wilson CB (1998) Transsphenoidal microsurgery for growth hormone-secreting pituitary adenomas: initial outcome and long-term results. J Clin Endocrinol Metab 83:3411–3418
3. Bates PR, Carson MN, Trainer PJ, Wass JA (2008) Wide variation in surgical outcomes for acromegaly in the UK. Clin Endocrinol (Oxf) 68:136–142
4. Beauregard C, Truong U, Hardy J, Serri O (2003) Long-term outcome and mortality after transsphenoidal adenomectomy for acromegaly. Clin Endocrinol (Oxf) 58:86–91
5. Beckers A (2008) Does preoperative somatostatin analog treatment improve surgical cure rates in acromegaly? A new look at an old question. J Clin Endocrinol Metab 93:2975–2977
6. Cappabianca P, Alfieri A, Colao A, Ferone D, Lombardi G, de Divitiis E (1999) Endoscopic endonasal transsphenoidal approach: an additional reason in support of surgery in the management of pituitary lesions. Skull Base Surg 9:109–117
7. Cappabianca P, Alfieri A, de Divitiis E (1998) Endoscopic endonasal transsphenoidal approach to the sella: towards functional endoscopic pituitary surgery (FEPS). Minim Invasive Neurosurg 41:66–73
8. Cappabianca P, Alfieri A, Thermes S, Buonamassa S, de Divitiis E (1999) Instruments for endoscopic endonasal transsphenoidal surgery. Neurosurgery 45:392–395
9. Carlsen SM, Lund-Johansen M, Schreiner T, Aanderud S, Johannesen O, Cooper SJ, JG HJK, Fougner SL, Bollerslev J (2008) Preoperative octreotide treatment in newly diagnosed acromegalic patients with macroadenomas increases cure short-term postoperative rates: a prospective, randomized trial. J Clin Endocrinol Metab 93:2984–2990
10. Ceylan S, Koc K, Anik I (2010) Endoscopic endonasal transsphenoidal approach for pituitary adenomas invading the cavernous sinus. J Neurosurg 112:99–107
11. Charalampaki P, Reisch R, Ayad A, Conrad J, Welschehold S, Perneczky WC (2007) Endoscopic endonasal pituitary surgery: surgical and outcome analysis of 50 cases. J Clin Neurosci 14:410–415
12. Colao A, Attanasio R, Pivonello R, Cappabianca P, Cavallo LM, Lasio Lodrini A, Lombardi G, Cozzi R (2006) Partial surgical removal of growth hormone-secreting pituitary tumors enhances the response to somatostatin analogs in acromegaly. J Clin Endocrinol Metab 91:85–92
13. Danoff A, Kleinberg D (2003) Somatostatin analogs as primary medical therapy for acromegaly. Endocr 20:291–297
14. de Divitiis E, Cappabianca P, Cavallo LM (2002) Endoscopic transsphenoidal approach: adaptability of the procedure to different sellar lesions. Neurosurgery 51:699–705
15. Erturk E, Tuncel E, Kiyici S, Ersoy C, Duran C, Imamoglu S (2005) Outcome of surgery for acromegaly performed by different surgeons: importance of surgical experience. Pituitary 8:93–97
16. Feenstra J, de Herder WW, ten Have SM, van den Beld AW, Feelders RA, Janssen JA, van der Lely AJ (2005) Combined therapy with somatostatin analogues and weekly pegvisomant in active acromegaly. Lancet 365:1644–1646
17. Freda PU, Katznelson L, van der Lely AJ, Reyes CM, Zhao S, Rabinowitz D (2005) Long-acting somatostatin analog therapy of acromegaly: a meta-analysis. J Clin Endocrinol Metab 90:4465–4473
18. Gittoes NJ, Sheppard MC, Johnson AP, Stewart PM (1999) Outcome of surgery for acromegaly—the experience of a dedicated pituitary surgeon. QJM 92:741–745
19. Giustina A, Barkan A, Casanueva FF, Cavagnini F, Frohman L, Ho K, Veldhuis J, Wass J, Von Werder K, Melmed S (2000) Criteria for cure of acromegaly: a consensus statement. J Clin Endocrinol Metab 85:526–529
20. Giustina A, Chanson P, Bronstein MD, Klibanski A, Lamberts S, Casanueva FF, Trainer P, Ghigo E, Ho K, Melmed S (2010) A consensus on criteria for cure of acromegaly. J Clin Endocrinol Metab 95:3141–148
21. Jho HD, Alfieri A (2000) Endoscopic transsphenoidal pituitary surgery: various surgical techniques and recommended steps for procedural transition. Br J Neurosurg 14:432–440
22. Jho HD, Carrau RL (1997) Endoscopic endonasal transsphenoidal surgery: experience with 50 patients. J Neurosurg 87:44–51
23. Kaltsas GA, Isidori AM, Florakis D, Trainer PJ, Camacho-Hubner C, Afshar F, Sabin I, Jenkins JP, Chew SL, Monson JP, Besser GM, Grossman AB (2001) Predictors of the outcome of surgical treatment in acromegaly and the value of the mean growth hormone day curve in assessing postoperative disease activity. J Clin Endocrinol Metab 86:1645–1652
24. Karavitaki N, Turner HE, Adams CB, Cudlip S, Byrne JV, Fazal-Sanderson V, Rowlers S, Trainer PJ, Wass JA (2008) Surgical debulking of pituitary macroadenomas causing acromegaly improves control by lanreotide. Clin Endocrinol (Oxf) 68:970–975
25. Katznelson L (2006) Drug insight: primary medical therapy of acromegaly. Nat Clin Pract Endocrinol Metab 2:109–117
26. Koc K, Anik I, Ozdamar D, Cabuk B, Keskin G, Ceylan S (2006) The learning curve in endoscopic pituitary surgery and our experience. Neurosurg Rev 29:298–305
27. Kristof RA, Stoffel-Wagner B, Klingmüller D, Schramm J (1999) Does octreotide treatment improve the surgical results of macroadenomas in acromegaly? A randomized study. Acta Neurochir (Wien) 141:399–405
28. Laws ER (2008) Surgery for acromegaly: evolution of the techniques and outcomes. Rev Endocr Metab Disord 9:67–70
29. Laws ER, Vance ML, Thapar K (2000) Pituitary surgery for the management of acromegaly. Horm Res 53(Suppl 3):71–75
30. Mao Z, Zhu Y, Tang H, Wang D, Zhou J, He D, Lan H, Luo B, Wang H (2010) Preoperative lanreotide treatment in acromegalic

patients with macroadenomas increases short-term postoperative cure rates: a prospective, randomised trial. Eur J Endocrinol 162:661–666
31. Melmed S (2006) Medical progress: acromegaly. N Engl J Med 355(2558–2573):14–12
32. Melmed S (2009) Acromegaly pathogenesis and treatment. J Clin Invest 119:3189–3202
33. Neggers SJ, van Aken MO, Janssen JA, Feelders RA, de Herder WW, van der Lely AJ (2007) Long-term efficacy and safety of combined treatment of somatostatin analogs and pegvisomant in acromegaly. J Clin Endocrinol Metab 92:4598–4601
34. Nomikos P, Buchfelder M, Fahlbusch R (2005) The outcome of surgery in 668 patients with acromegaly using current criteria of biochemical 'cure'. Eur J Endocrinol 152:379–387
35. Petrossians P, Borges-Martins L, Espinoza C, Daly A, Betea D, Valdes-Socin H, Stevenaert A, Chanson P, Beckers A (2005) Gross total resection or debulking of pituitary adenomas improves hormonal control of acromegaly by somatostatin analogs. Eur J Endocrinol 152:61–66
36. Pieters GF, Smals AG, Kloppenborg PW (1980) Defective suppression of growth hormone after oral glucose loading in adolescence. J Clin Endocrinol Metab 51:265–270
37. Plöckinger U, Quabbe HJ (2005) Presurgical octreotide treatment in acromegaly: no improvement of final growth hormone (GH) concentration and pituitary function
38. Selvarajah D, Webster J, Ross R, Newell-Price J (2005) Effectiveness of adding dopamine agonist therapy to long-acting somatostatin analogues in the management of acromegaly. Eur J Endocrinol 152:569–574
39. Sheppard MC (2003) Primary medical therapy for acromegaly. Clin Endocrinol (Oxf) 58:387–399
40. Shimon I, Cohen ZR, Ram Z, Hadani M (2001) Transsphenoidal surgery for acromegaly: endocrinological follow-up of 98 patients. Neurosurgery 48:1239–1243
41. Swearingen B, Barker FG, Katznelson L, Biller BM, Grinspoon S, Klibanski A, Moayeri N, Black PM, Zervas NT (1998) Long-term mortality after transsphenoidal surgery and adjunctive therapy for acromegaly. J Clin Endocrinol Metab 83:3419–3426
42. Tabaee A, Anand VK, Barron Y, Hiltzik DH, Brown SM, Kacker A, Mazumdar M, Schwartz TH (2009) Endoscopic pituitary surgery: a systematic review and meta-analysis. J Neurosurg 111:545–554
43. Trepp R, Stettler C, Zwahlen M, Seiler R, Diem P, Christ ER (2005) Treatment outcomes and mortality of 94 patients with acromegaly. Acta Neurochir (Wien) 147:243–251
44. Van der Lely AJ, Hutson RK, Trainer PJ, Besser GM, Barkan AL, Katznelson L, Klibanski A, Herman-Bonert V, Melmed S, Vance ML, Freda PU, Stewart PM, Friend KE, Clemmons DR, Johannsson G, Stavrou S, Cook DM, Phillips LS, Strasburger CJ, Hackett S, Zib KA, Davis RJ, Scarlett JA, Thorner MO (2001) Long-term treatment of acromegaly with pegvisomant, a growth hormone receptor antagonist. Lancet 358:1754–1759
45. Van Lindert EJ, Hey O, Boecher-Schwarz H, Perneczky A (1997) Treatment results of acromegaly as analyzed by different criteria. Acta Neurochir (Wien) 139:905–912

Acta Neurochir (2011) 153:1401–1408
DOI 10.1007/s00701-011-1029-y

CLINICAL ARTICLE

Combined simultaneous transcranial and transsphenoidal resection of large-to-giant pituitary adenomas

Gilberto Ka Kit Leung · Hing Yu Law · Kwun Ngai Hung · Yiu Wah Fan · Wai Man Lui

Received: 30 January 2011 / Accepted: 8 April 2011 / Published online: 30 April 2011

Abstract
Background While large-to-giant pituitary adenomas (PAs) may be safely removed by experienced surgeons through a single route, the procedure is technically challenging. We present the outcome of a simultaneous combined transcranial and transsphenoidal approach and discuss its applications.
Methods A retrospective review was conducted on 12 consecutive patients. Surgical complications, visual and endocrinological functions, and tumour control were reviewed.
Results There were four men and eight women, with a mean age of 47.6 years. All but one patient had non-functioning PAs. The mean tumour height was 4.1 cm (range: 2.3–5.5). The predominant presenting symptoms were visual field loss in eight patients, headache in three patients and mental confusion in one patient. There was no operative mortality. Post-operative cerebrospinal fluid leakage occurred in one patient. Five of the eight patients who presented with visual field loss achieved full recovery, and three had partial improvement. Two patients developed permanent diabetes insipidus after surgery. Panhypopituitarism occurred in one patient. Gross total removal (GTR) was achieved in five, and subtotal removal (STR) in seven patients. Seven patients received post-operative external irradiation. All patients who had GTR remained tumour-free and all those with STR had stable diseases after a mean follow-up period of 53.1 months (range: 14.1–92.1).
Conclusion The simultaneous 'above and below' approach is a safe and effective surgical strategy for large-to-giant PAs, particularly when expertise in endoscopic transsphenoidal surgery is unavailable. Its use, however, should be limited to a carefully selected group of patients, and tailored to individual user's expertise and experience.

Keywords Pituitary adenoma · Transsphenoidal · Craniotomy · Surgical approach · Complications

G. K. K. Leung (✉) · H. Y. Law · K. N. Hung · Y. W. Fan · W. M. Lui
Division of Neurosurgery, Department of Surgery,
Li Ka Shing Faculty of Medicine, The University of Hong Kong,
Queen Mary Hospital,
102 Pokfulam Road,
Hong Kong SAR, China
e-mail: gilberto@hkucc.hku.hk

Introduction

Surgery for large-to-giant pituitary adenomas (PAs) is technically challenging. Although the transsphenoidal approach has been widely adopted as a safe and effective method for the removal of the majority of PAs, large lesions may still present with considerable difficulties [1, 5, 8, 12, 13, 35]. Some of the large PAs may have a fibrous consistency or an 'hour-glass' configuration, rendering complete removal through the transsphenoidal route alone difficult and hazardous. With incomplete removal, a residual suprasellar tumour mass may be complicated by haemorrhages at the early post-operative period, resulting in acute hydrocephalus or optic nerve compression. The transcranial approach is effective for the removal of a suprasellar tumour mass but provides only limited visualization of the intrasellar region. Since some of the large PAs may be highly vascular, a direct transcranial attack may be associated with significant bleeding within the intradural space. Previous studies have reported high operative mortality and morbidity rates using the transsphenoidal or the transcranial approach alone [9, 14, 31, 32].

Several alternative approaches have been described, including the extended endoscopic transsphenoidal approach

[4, 17], the staged transsphenoidal approach [1], the staged transcranial-transsphenoidal approach [2], the combined endoscopic transsphenoidal transventricular approach [10, 24, 25], and the simultaneous combined transcranial and transsphenoidal approach [2, 7, 19]. The latter, in particular, has the advantage of achieving radical tumour removal in a single setting of general anaesthesia. We report our experiences with this simultaneous 'above and below' technique, and discuss its advantages and limitations.

Materials and method

A retrospective study was conducted on 12 consecutive patients who underwent simultaneous combined microscopic transsphenoidal and transcranial surgery for the removal of PAs between January 2000 and December 2008. The diagnosis of PA was made on magnetic resonance imaging (MRI) and confirmed histologically. All giant PAs (>4 cm in height) were approached with this technique during the study period. For large PAs (>2 cm and <4 cm in height), this approach was used when there was significant lateral suprasellar or third ventricular tumour extension, and/or an hourglass configuration.

The anatomical classification of PA described by Wilson et al. [34] was adopted. The relationship of the PA to the sella and sphenoidal sinus was graded as I (normal sella), II (enlarged sella), III (localized sellar perforation), IV (diffuse sellar destruction), and V [cerebrospinal fluid (CSF) or blood-borne spread]. Extrasellar extension was staged as 0 (none), A (occupying cistern), B (third ventricular obliteration), C (grossly displaced third ventricle), D (intracranial parasellar extension), and E (extradural parasellar extension).

Patients' pre-operative and post-operative (6-month) visual and endocrinological functions, and surgical complications were reviewed. The first follow-up MRI was performed three months after surgery. Gross total removal (GTR) and subtotal removal (STR) were defined as the absence or presence of contrast-enhancing lesions on the first post-operative MRI, respectively. Thereafter, MRI was performed 12-monthly for patients with GTR, and 6-monthly for those with STR. Tumour control and the patients' Karnofsky Performance Score (KPS) were assessed upon the latest follow-up.

Surgical technique

The tumour was approached both transcranially and transsphenoidally under a single setting of general anaesthesia. Prophylactic broad spectrum antibiotics (ceftriaxone and metronidazole) were given on induction and continued for 3 days post-operatively. Each of the transsphenoidal and transcranial phases had its own surgeon, scrub nurse, operating microscope and set of instruments. The transsphenoidal surgeon stood on the right side of the patient while the transcranial surgeon was seated at the head end. The two operative fields were separate by a vertical drape to minimize contamination.

The transcranial approach was conducted through the anterior interhemispheric route (ten patients) or the subfrontal route (two patients). The patient's head was positioned using a Mayfield clamp in the neutral position for the former, or turned to the side for the latter. The transsphenoidal phase was performed using either the sublabial transseptal route (ten patients) or the transnasal route (two patients).

After the initial opening, two operating microscopes were brought into position (Fig. 1). The tumour was exposed on the cranial side, but every effort was made to avoid breaching the tumour capsule in order to minimize the amount of bleeding within the subarachnoid space. The cranial surgeon's role was to deliver the tumour down towards the sphenoidal sinus, to dissect the tumour capsule from adjacent intradural structures, and to protect the latter against the transsphenoidal surgeon's manipulations, which may at times extend well up rostrally. The tumour capsule was opened on the transsphenoidal side, followed by tumour debulking with suction and curettage. In all of our cases, the intrasellar and intradural tumour bulks were removed completely. Figure 2 illustrates tumours that were removed using this technique.

The subsequent skull base defect was repaired with abdominal fat graft. Again, the cranial surgeon served to prevent against over-enthusiastic packing by the transsphenoidal surgeon. The rest of wound closure was performed in the standard manner. A subgaleal suction

Fig. 1 The setting in the operating room, with two microscopes positioned to allow the simultaneous participation of the transcranial and transsphenoidal surgeons

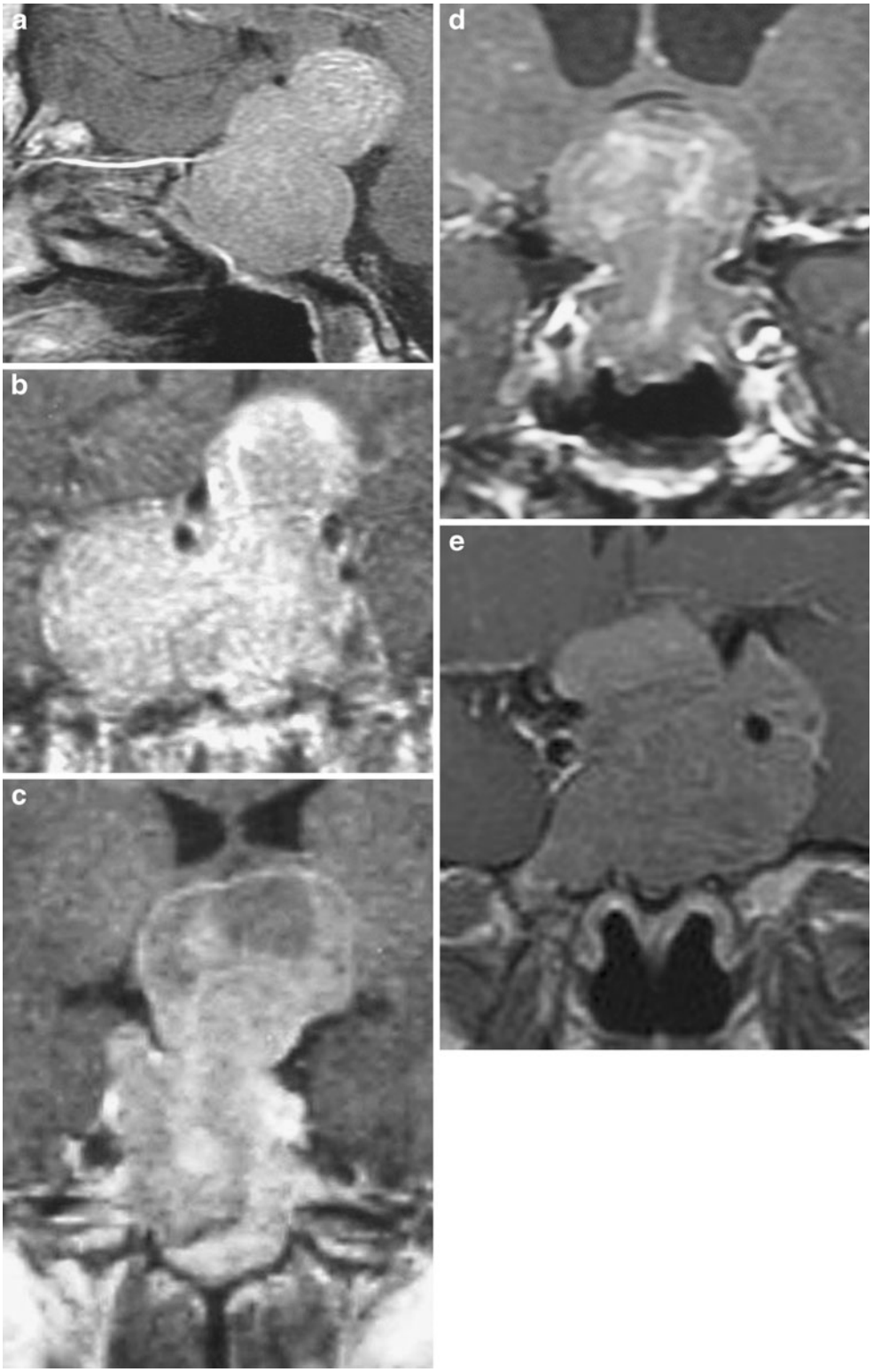

Fig. 2 Pre-operative contrasted T1-weighted MRI studies illustrating tumours which were removed using the combined technique. The patient numbers correspond to those in Table 1. **a** Patient 4, **b** patient 5, **c** patient 9, **d** patient 11, **e** patient 12

drain was inserted on the cranial side, and the nasal passages were packed for one to two days. No lumbar drain was used. All patients received post-operative care in the intensive care unit. Except for those patients who had previous irradiation therapy, all were offered post-operative fractionated external irradiation as adjuvant treatment.

Results

Patient characteristics

There were four (33.3%) men and eight (67.7%) women, with a mean age of 47.6 years (range: 32–79) (Table 1).

Table 1 Patient characteristics and operative procedures

Patient no.	Sex/age (years)/	Symptoms	Tumor size (cm)[a]	Tumor grade[b]	Cranial approach	Transsphenoidal approach	Extent of removal	Operation time (mins)
1	F/54	BTH	3.0×3.2×4.5	III C	AIH	Sublabial	GTR	420
2	F/45	HA	2.9×2.5×4.4	III E	Subfrontal	Sublabial	STR	360
3	M/41	HA	2.8×2.3×2.3	III D	Subfrontal	Sublabial	GTR	400
4	M/62	BTH	3.0×4.1×5.2	III D	AIH	Sublabial	GTR	380
5	F/62	Acromegalic features, BTH	3.3×2.6.3.6	III E	AIH	Sublabial	STR	460
6	M/47	HA	3.0×3.5×5.5	IIIE	AIH	Sublabial	STR	370
7	F/32	BTH	3.0×3.7×3.1	III E	AIH	Transnasal	STR	380
8	F/65	BTH	3.2×2.2×2.9	III E	AIH	Sublabial	STR	350
9	F/58	BTH	3.3×2.2×5.0	IV C	AIH	Sublabial	GTR	450
10	F/52	BTH	3.6×4.4×4.6	IV E	AIH	Sublabial	STR	210
11	M/79	Confusion	2.0×1.8.×2.8	III C	AIH	Transnasal	GTR	300
12	F/34	BTH	3.7×3.6×5.3	IV E	AIH	Sublabial	STR	360

AIH anterior interhemispheric, *BTH* bitemporal hemianopia, *GTR* gross total removal, *HA* headache, *RT* external radiotherapy, *STR* subtotal removal

[a] Width × length × height

[b] Modified Hardy's grading staging

Eleven patients had non-functioning PAs and one had a growth-hormone-secreting tumour. The mean tumour height was 4.1 cm (range: 2.3–5.5). Nine were grade III tumours and three were grade IV tumours. The numbers of stage C, D and E tumours were three, two and seven, respectively. Three cases were recurrent tumours with previous transsphenoidal surgery and radiotherapy performed. The predominant presenting symptoms were visual field loss in eight, headache in three, and mental confusion in one patients.

Operative procedures and complications

The transcranial approach was anterior interhemispheric in ten patients and subfrontal in two patients (Table 2). The transsphenoidal approach was sublabial transseptal in ten patients and transnasal in two patients. The mean operation time was 370 min (range: 210–460).

There was no operative mortality. One patient died 28 months after surgery due to an unrelated cause. One patient (8.3%) had post-operative CSF leakage, which was successfully treated with lumbar drainage. One patient (8.3%) developed deep vein thrombosis without pulmonary complication, and was successfully managed with an inferior vena caval filter and anticoagulation. No patient suffered from meningitis, hydrocephalus or new onset of cranial nerve palsy.

Of all eight patients who presented with visual field loss, five (62.5%) achieved full visual field recovery, and three (37.5%) had partial improvement. None experienced worsening of vision. All four patients who presented with headache and confusion had symptomatic improvement after surgery. Four patients developed diabetes insipidus (DI) after surgery—two were transient (16.7%) and two permanent (16.7%). Panhypopituitarism occurred in one patient. Three other patients had new onset of isolated anterior pituitary deficiencies. All patients had KPS of 70 or above upon the last follow-up.

Tumour control

Based on the first post-operative MRI, GTR was achieved in five (41.7%, all stage C or D lesions), and STR in seven patients (58.3%, all stage E lesions). Three patients received previous external radiotherapy and were not offered further irradiation. Of the remaining nine patients, seven received post-operative fractionated external irradiation and two declined it. The mean follow-up period was 53.1 months (range: 14.1–92.1). Upon the last follow-up, all five patients who had GTR remained tumour-free, whilst all patients with STR had stable residual diseases. The one patient with acromegaly had STR and continued to receive bromocriptine for biochemical control.

Discussion

Large and giant PAs are difficult to remove safely. The operative mortality rates have been reported to be as high as 25% for transcranial resection and 14% for transsphenoidal resections [31]. Advancement in neurosurgical techniques has led to an improvement in outcome. Sinha et al. [28]

Table 2 Patients' post-operative outcome

Patient no.	Visual function	New permanent hormonal deficit	Surgical complication	Post-op RT	Tumour status	KPS	FU duration (months)	Remarks
1	Normal	DI, ↓ACTH	None	Yes	Tumour-free	90	109	None
2	Normal	None	None	No	Stable residue	90	104	Recurrence after previous transsphenoidal removal and RT
3	Normal	None	None	No	Tumour-free	90	105	Recurrence after previous transsphenoidal removal and RT
4	Normal	DI	None	Yes	Tumour-free	80	28	Died 28 months later from unrelated cause
5	Residual left HeAn	Panhypopituitarism	None	Yes	Stable residue	90	93	Biochemical remission with bromocriptine
6	Normal	None	CSF leakage	Yes	Stable residue	90	65	None
7	Normal	None	None	No	Stable residue	100	63	Patient refused RT
8	Improved BTH	None	None	No	Stable residue	80	55	Recurrence after previous transsphenoidal removal and RT
9	Normal	↓TSH	Deep vein thrombosis	Yes	Tumour-free	100	54	Deep vein thrombosis treated with caval filter.
10	Residual left HeAn	↓ACTH	None	Yes	Stable residue	100	24	None
11	Normal	None	None	No	Tumour-free	70	24	Patient refused RT
12	Normal	None	None	Yes	Stable residue	100	26	None

ACTH adrenocorticotropic hormone, *BTH* bitemporal hemianopia, *CSF* cerebrospinal fluid, *DI* diabetes insipidus, *FU* follow-up since surgery, *HeAn* hemianopia, *KPS* Karnofsky Performance Score, *RT* external radiotherapy, *TSH* thyrotropic stimulating hormone

reported the surgical outcomes of 250 patients with giant PAs. Near-total (>90%) tumour removal was achieved in 74% and improvement of vision in 53% of patients. The mortality and morbidity rates were 4.4% and 14%, respectively. Xue-Fei et al. [35] treated 54 patients with large PAs using a variety of surgical approaches and achieved complete tumour removal in 21% of cases. The peri-operative mortality rate was 7.9%. In another series of 111 patients, Mortini et al. [21] reported a mortality rate of 2.7%. The incidences of 'major' complications (e.g. cranial nerves, hypothalamic and vascular injuries, CSF leakages and tumour haemorrhages), and 'minor' complications (e.g. endocrinological) were 18% and 26%, respectively. Using the same categorization, the incidences of 'major' and 'minor' complications in our present series were comparable at 8.3% and 25%, respectively. The extent of removal in our series, however, was comparatively lower, which was probably due to our conservative approach towards tumours within the cavernous sinuses.

The transsphenoidal approach is the treatment of choice for the majority of PAs. But for tumours that arise in or extend into the suprasellar region, transsphenoidal surgery is generally contraindicated when there is a normal-sized sella turcica, normal pituitary function, or adherence of the tumour to major intracranial structures [6, 12, 14, 18]. A tumour that is fibrous in consistency or has an hour-glass configuration may also be difficult to remove completely with a single transsphenoidal procedure [20]. Lumbar subarachnoid saline or air injection may be used to facilitate the descent of the suprasellar tumour bulk into the sella, but the method is effective only in a subgroup of patients [29, 37]. In a prospective study, Honegger et al. [11] demonstrated that the vertical intracranial extension, and an irregular or multilobular configuration, were significant and independent predictors for incomplete resection. To address this, the two-staged transsphenoidal approach has been advocated, in which, after the removal of the intrasellar tumour component, the suprasellar residual tumour was given time to descend and then removed by a second-stage transsphenoidal procedure [1, 26, 31]. The disadvantages of this approach include the need for two operations and the potential risks of tumour swelling and haemorrhages after the first-stage surgery.

The introduction of endoscopic transsphenoidal surgery has revolutionized the treatment of sellar tumours [4]. It has been shown to be safe and effective, and is now an arguably standard therapy for the majority of PAs. But despite the vastly improved illumination and visualization provided by

the use of endoscopes, a giant or invasive PA is amenable to a single-stage removal by a limited number of experts only [30]. Wang et al. [33] reported an 80% total resection rate in a series of 64 patients without mortality or tumour recurrence. Similarly, Sanai et al. [27] reported a GTR rate of close to 50%, with no incidence of CSF leakage, new panhypopituitarism or worsening of vision. Nakao et al. [23] treated 43 patients using the endoscopic endonasal approach and an intracapsular resection technique. Gross total removal was achieved in close to 50% of cases and there was no major complication. While the indications for endoscopic pituitary surgery are expanding, its use and limits for the treatment of huge PAs are yet to be defined. The extended endoscopic transsphenoidal approach, in particular, is a technically demanding technique. It requires specialized and advanced training, and may not be readily acquired by surgeons without the necessary case volume [4].

For many, the transcranial approach continues to play a role in the management of PAs inaccessible from the transsphenoidal route alone [36]. When compared with the transsphenoidal approach, there is a trend towards greater visual improvement, but the benefit may be offset by a greater risk of post-operative pituitary dysfunction [22]. The disadvantages of the transcranial approach include the amount of brain retraction required and the limited visualization of the intrasellar area [15]. In our experience, a transcranial resection of vascular tumours may also be associated with significant bleeding within the intradural space. This may further obscure the surgical view, and potentially increase the risks of brain swelling and hydrocephalus. One of the advantages of our simultaneous combined approach is that tumour bleeding would occur predominantly on the transsphenoidal side. The transcranial surgeon only serves to deliver the tumour bulk towards the sella, and to protect the intradural structures.

Loyo et al. [19] first described the combined supra-sellar and infra-sellar approach in 1984 for the resection of very large PAs, and advocated it as superior to either the transsphenoidal or the intracranial approach alone. Case reports on the use of the 'above and below' approach for a large craniopharyngioma [16], and a PA with lateral ventricle extension have been described [10]. To our knowledge, there are two reported case series on the combined approach for large-to-giant PAs. Alleyne et al. [2] reported a GTR rate of 40% in a cohort of ten patients. More than half of those who presented with pre-operative visual field loss experienced complete recovery. Permanent DI occurred in 20% of patients. In D'Ambrosio et al.'s series [7], GTR was achieved in six out of 11 patients (55%). Seven patients (64%) experienced visual improvement post-operatively and no major complication occurred. Panhypopituitarism was observed in four and persistent DI in two patients. The authors of these two series focused mainly on early operative outcomes but not tumour control. Our present study yielded similar early outcomes. In addition, we were also able to demonstrate satisfactory medium-term tumour control. Admittedly, the use of up-front fractionated external irradiation, instead of radio-surgery, in our series warrants careful scrutiny in view of the former's potential side-effects. This is a limitation of our treatment paradigm that needs to be improved.

Conceptually, we consider this technique to be a posterior extension of that of craniofacial resection for anterior skull base tumours, in that lesions which occupy two adjoining skull base compartments are best approached simultaneously from both compartments for maximal tumour removal and safety [15]. Although pathologically very different, these two disease groups may exhibit similar morphological features, such as close adherence to intracranial structures, irregular configurations and extensive skull base destruction. Technically, we favour the anterior inter-hemispheric route for the transcranial phase because it provides a better view of the parasellar region bilaterally. The subfrontal or pterional route, on the other hand, requires some head-turning, which may potentially disorientate the transsphenoidal surgeon.

One of the main goals of surgery for huge PAs is optic nerve/chiasm decompression, for which the combined approach appears to be a safe and effective method. The main advantages of our technique include the need for only one procedure, the protection offered by the transcranial surgeon, and the avoidance of complications potentially caused by any residual suprasellar tumour bulk. The main disadvantages include the involvement of two operative fields, the doubling of staff and instruments required, the long operating time, and the potential complications of a craniotomy. The need for two operating microscopes, however, may be obviated by the use of endoscopes for the transsphenoidal phase of the procedure. More recently, an alternative 'above and below' approach has been described by several authorities for the treatment of PAs with significant third ventricular extensions. It uses a simultaneous endoscopic transsphenoidal-transventricular technique and therefore obviates the need for a craniotomy [10, 24, 25].

In terms of tumour control, stage C (grossly displaced third ventricle) and D (intracranial parasellar extension) are potentially amenable to total removal with our technique; stage E (extradural parasellar extension) lesions may require a more extensive extradural approach. However, being a retrospective case series, this report may suffer from case selection bias, suboptimal data collection, and the lack of a control cohort for outcome analysis. The optimal treatment of large-to-giant PAs is likely to require a more tailored approach, based on individual patients' conditions and the surgeons' experiences and abilities. A multi-

modality management strategy should be adopted to take full advantages of the benefits provided by surgery and radiotherapy [8]. The use of intra-operative MRI may also significantly improve resection rate and safety [3]. Our combined approach represents only one of the many surgical strategies that can be used in dealing with these challenging PAs, particularly when expertise in endoscopic surgery is unavailable.

Conclusion

Large and giant PAs are challenging lesions. Although many experienced surgeons would be able to remove these tumours endoscopically through the transsphenoidal route alone, the necessary expertise is not easy to acquire. The present study demonstrates that the simultaneous transcranial transsphenoidal approach is a safe and feasible alternative. It requires teamwork and more readily available technical skills from the transcranial and transsphenoidal surgeons. Its use, however, should be limited to a carefully selected group of patients, and tailored to individual users' expertise and experiences.

Acknowledgements We thank Miss Gloria K.B. Ng and Mr. Gary Lee for their assistance in preparing this manuscript.

Conflicts of interest None.

References

1. Abe T, Iwata T, Kawamura N, Izumiyama H, Ikeda H, Matsumoto K (1997) Staged transsphenoidal surgery for fibrous nonfunctioning pituitary adenomas with suprasellar extension. Neurol Med Chir (Tokyo) 37:830–835; discussion 835–837
2. Alleyne CH Jr, Barrow DL, Oyesiku NM (2002) Combined transsphenoidal and pterional craniotomy approach to giant pituitary tumors. Surg Neurol 57:380–390; discussion 390
3. Baumann F, Schmid C, Bernays RL (2010) Intraoperative magnetic resonance imaging-guided transsphenoidal surgery for giant pituitary adenomas. Neurosurg Rev 33:83–90
4. Cappabianca P, Cavallo LM, Esposito F, De Divitiis O, Messina A, De Divitiis E (2008) Extended endoscopic endonasal approach to the midline skull base: the evolving role of transsphenoidal surgery. Adv Tech Stand Neurosurg 33:151–199
5. Chacko G, Chacko AG, Lombardero M, Mani S, Seshadri MS, Kovacs K, Scheithauer BW (2009) Clinicopathologic correlates of giant pituitary adenomas. J Clin Neurosci 16:660–665
6. Couldwell WT (2004) Transsphenoidal and transcranial surgery for pituitary adenomas. J Neurooncol 69:237–256
7. D'Ambrosio AL, Syed ON, Grobelny BT, Freda PU, Wardlaw S, Bruce JN (2009) Simultaneous above and below approach to giant pituitary adenomas: surgical strategies and long-term follow-up. Pituitary 12:217–225
8. de Paiva Neto MA, Vandergrift A, Fatemi N, Gorgulho AA, Desalles AA, Cohan P, Wang C, Swerdloff R, Kelly DF (2010) Endonasal transsphenoidal surgery and multimodality treatment for giant pituitary adenomas. Clin Endocrinol (Oxf) 72:512–519
9. Goel A, Nadkarni T, Muzumdar D, Desai K, Phalke U, Sharma P (2004) Giant pituitary tumors: a study based on surgical treatment of 118 cases. Surg Neurol 61:436–445; discussion 445–436
10. Greenfield JP, Leng LZ, Chaudhry U, Brown S, Anand VK, Souweidane MM, Schwartz TH (2008) Combined simultaneous endoscopic transsphenoidal and endoscopic transventricular resection of a giant pituitary macroadenoma. Minim Invasive Neurosurg 51:306–309
11. Honegger J, Ernemann U, Psaras T, Will B (2007) Objective criteria for successful transsphenoidal removal of suprasellar nonfunctioning pituitary adenomas. A prospective study. Acta Neurochir (Wien) 149:21–29; discussion 29
12. Jane JA Jr, Laws ER Jr (2001) The surgical management of pituitary adenomas in a series of 3,093 patients. J Am Coll Surg 193:651–659
13. Jane JA Jr, Han J, Prevedello DM, Jagannathan J, Dumont AS, Laws ER Jr (2005) Perspectives on endoscopic transsphenoidal surgery. Neurosurg Focus 19:E2
14. Jeffreys RV (1989) The surgical treatment of large pituitary adenomas. Br J Neurosurg 3:147–152
15. Kabil MS, Jarrahy R, Shahinian HK (2005) The application of craniofacial techniques and intracranial endoscopy to pituitary surgery. J Craniofac Surg 16:812–818
16. Kobayashi S, Takemae T, Sugita K (1984) Combined transsphenoidal and transoral approach for clivus chordoma. No Shinkei Geka 12:1339–1346
17. Laufer I, Anand VK, Schwartz TH (2007) Endoscopic, endonasal extended transsphenoidal, transplanum transtuberculum approach for resection of suprasellar lesions. J Neurosurg 106:400–406
18. Liu JK, Das K, Weiss MH, Laws ER Jr, Couldwell WT (2001) The history and evolution of transsphenoidal surgery. J Neurosurg 95:1083–1096
19. Loyo M, Kleriga E, Mateos H, de Leo R, Delgado A (1984) Combined supra-infrasellar approach for large pituitary tumors. Neurosurgery 14:485–488
20. Mohr G, Hardy J, Comtois R, Beauregard H (1990) Surgical management of giant pituitary adenomas. Can J Neurol Sci 17:62–66
21. Mortini P, Barzaghi R, Losa M, Boari N, Giovanelli M (2007) Surgical treatment of giant pituitary adenomas: strategies and results in a series of 95 consecutive patients. Neurosurgery 60:993–1002; discussion 1003–1004
22. Musleh W, Sonabend AM, Lesniak MS (2006) Role of craniotomy in the management of pituitary adenomas and sellar/parasellar tumors. Expert Rev Anticancer Ther 6(Suppl 9):S79–S83
23. Nakao N, Itakura T (2011) Surgical outcome of the endoscopic endonasal approach for non-functioning giant pituitary adenoma. J Clin Neurosci 18:71–75
24. Ojha BK, Husain M, Rastogi M, Chandra A, Chugh A, Husain N (2009) Combined trans-sphenoidal and simultaneous transventricular-endoscopic decompression of a giant pituitary adenoma: case report. Acta Neurochir (Wien) 151:843–847; discussion 847
25. Romano A, Chibbaro S, Marsella M, Oretti G, Spiriev T, Iaccarino C, Servadei F (2010) Combined endoscopic transsphenoidal-transventricular approach for resection of a giant pituitary macroadenoma. World Neurosurg 74:161–164
26. Saito K, Kuwayama A, Yamamoto N, Sugita K (1995) The transsphenoidal removal of nonfunctioning pituitary adenomas with

suprasellar extensions: the open sella method and intentionally staged operation. Neurosurgery 36:668–675; discussion 675–666
27. Sanai N, Quinones-Hinojosa A, Narvid J, Kunwar S (2008) Safety and efficacy of the direct endonasal transsphenoidal approach for challenging sellar tumors. J Neurooncol 87:317–325
28. Sinha S, Sharma BS (2010) Giant pituitary adenomas—an enigma revisited. Microsurgical treatment strategies and outcome in a series of 250 patients. Br J Neurosurg 24:31–39
29. Spaziante R, de Divitiis E (1989) Forced subarachnoid air in transsphenoidal excision of pituitary tumors (pumping technique). J Neurosurg 71:864–867
30. Tabaee A, Anand VK, Barron Y, Hiltzik DH, Brown SM, Kacker A, Mazumdar M, Schwartz TH (2009) Endoscopic pituitary surgery: a systematic review and meta-analysis. J Neurosurg 111:545–554
31. Takakura K, Teramoto A (1996) Management of huge pituitary adenomas. Acta Neurochir Suppl 65:13–15
32. van Lindert EJ, Grotenhuis JA, Meijer E (1991) Results of follow-up after removal of non-functioning pituitary adenomas by transcranial surgery. Br J Neurosurg 5:129–133
33. Wang RZ, Yin J, Su CB, Ren ZY, Yao Y, Tao W (2006) Extended transsphenoidal operation for giant and invasive pituitary adenomas. Zhonghua Wai Ke Za Zhi 44:1548–1550
34. Wilson CB (1984) A decade of pituitary microsurgery. The Herbert Olivecrona lecture. J Neurosurg 61:814–833
35. Xue-Fei S, Yong-Fei W, Shi-Qi L, Jing-Song W, Yao Z, Ying M, Liang-Fu Z (2008) Microsurgical treatment for giant and irregular pituitary adenomas in a series of 54 consecutive patients. Br J Neurosurg 22:636–648
36. Youssef AS, Agazzi S, van Loveren HR (2005) Transcranial surgery for pituitary adenomas. Neurosurgery 57:168–175; discussion 168–175
37. Zhang X, Fei Z, Zhang J, Fu L, Zhang Z, Liu W, Chen Y (1999) Management of nonfunctioning pituitary adenomas with suprasellar extensions by transsphenoidal microsurgery. Surg Neurol 52:380–385

Comment

In managing a huge and multilobed tumour, the surgeon accepts that the now generally adopted transsphenoidal approach is going to run the risk of leaving benign tumour in the suprasellar space and, of course, invading the cavernous sinus and that residual will cause problems with swelling and haemorrhage in a few. The question is how to manage them.

I can accept the occasional need to link cranial and transsphenoidal surgery, but my problem is why there is a need to do them both together, exactly at the same time. Why not do the transsphenoidal and go on, if absolutely necessary, at the same sitting. The transsphenoidal is so quick, and all I could see is the cranial part getting in the way.

Michael Powell
London, UK

Acta Neurochir (2011) 153:1409–1416
DOI 10.1007/s00701-011-1044-z

CLINICAL ARTICLE

Long-term clinical and radiological outcomes following stand-alone PLIF surgery using expandable cylindrical threaded cages in patients with degenerative lumbar spine disease

Jin Hoon Park · Sung Woo Roh

Received: 25 January 2011 / Accepted: 27 April 2011 / Published online: 15 May 2011

Abstract
Purpose Although posterior lumbar interbody fusion (PLIF) using stand-alone cages was a popular arthrodesis method, the effectiveness of using such cages has been questioned. We assessed retrospectively the long-term clinical and radiological outcomes of PLIF surgery using stand-alone cages for the treatment of degenerative lumbar spine disease, the incidences of pseudoarthrosis, and its risk factors.
Methods Between May 2000 and May 2005, we performed surgery on 211 patients with degenerative lumbar disease. Among those patients, 180 were clinically and radiologically followed for more than 60 months. All 180 patients underwent postoperative follow-up X-rays, including a dynamic view after 3, 6, 12, 24, and 60 months, and computed tomography (CT) after 24 months. The clinical outcomes were analyzed using the mean numeric rating scale (NRS), Oswestry Disability Index (ODI), and Odom's criteria. The factors affecting the clinical success and non-fusion were also analyzed.
Results The mean NRS scores for the back and leg were 7.1 and 6.9 preoperatively, and 3.0 and 2.7 at 60 months postoperatively, respectively. The ODI decreased from 29.5 preoperatively to 14.1 at 60 months postoperatively. The clinical success rate was only 74.4% in the Odom's criteria, and the significant factor affecting the clinical success was radiological fusion. The radiological fusion assessment at 24 months postoperatively indicated success at 167 levels (85.2%) and failure at 29 levels (14.8%). Disc height changed from 10.25 mm preoperatively to 15.02 mm immediately postoperatively, and gradually decreased to 12.28 mm for 60 months after surgery. The gradual decrease was statistically significant ($p<0.001$). The segmental angle changed from 13.59° preoperatively to 12.85° immediately postoperatively, and to 12.76° 60 months after surgery. There was no statistically significant change of the segmental angle during any time ($p>0.05$).
Conclusion The use of PLIF with stand-alone threaded cages in degenerative lumbar disease patients resulted in a long-term clinical success rate of 74.4%. Although the radiological fusion rate was 85.2%, continuous reduction of disc height and poor alignment preservation were observed. We conclude, therefore, that PLIF using only stand-alone cages is a poor surgical option for achieving good alignment and disc height restoration in patients with degenerative lumbar disease.

Keywords Posterior lumbar interbody fusion · PLIF · Expandable threaded cages · Pseudoarthrosis · Risk factor · Stand-alone

J. H. Park · S. W. Roh
Department of Neurological surgery, Asan Medical Center, University of Ulsan, College of Medicine, Seoul, Korea

S. W. Roh (✉)
Department of Neurosurgery, Asan Medical Center, 388–1 Pungnap-2dong, Songpa-gu, Seoul 138–736, Korea
e-mail: swroh@amc.seoul.kr

Introduction

Posterior lumbar interbody fusion (PLIF) using stand-alone, cylindrical, threaded cages was a popular arthrodesis method for the surgical treatment of degenerative lumbar spine diseases [1, 8, 12–14, 16, 18]. However, the effectiveness of such cages has been questioned, with some investigators claiming that supplementary posterior fixation is required in order to produce better long-term clinical

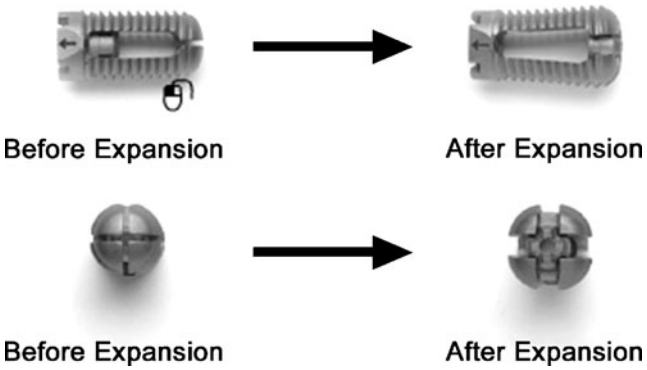

Fig. 1 Threaded expandable cages

results [2, 5, 15, 17, 19]. Therefore, the use of stand-alone cages has sharply declined during the past few years.

Our study examined the long-term clinical and radiological outcomes following the use of PLIF with stand-alone, expandable, threaded cages for patients with degenerative lumbar spine diseases. We assessed the relationship between the clinical and radiological outcomes, and analyzed the factors affecting the occurrence of pseudoarthrosis.

Materials and methods

Surgery was performed at our medical center between May 2000 and May 2005 by a single surgeon on 211 patients with degenerative lumbar disease. Of those patients, 180 (85 male and 95 female) were clinically and radiologically followed for more than 60 months. The other 31 patients were excluded as they were lost during follow-up. The mean follow-up period was 94 months, and the minimum period was 60 months. All study patients had symptoms of radiculopathy which was unresponsive to a minimum of 3 months of conservative treatment. The inclusion criteria included a grade 1 degenerative spondylolisthesis (n=47, 26.1%), degenerative stenosis with instability (n=52, 28.9%), recurrent disc herniation (n=69, 38.3%) and others (n=12, 6.7%), including discogenic back pain, huge disc herniation, and foraminal stenosis. The exclusion criteria were previous fusion at the involved level(s), systemic infection, metabolic bone disease, circulatory problems, symptomatic cardiac disease, malignancy, and isthmic spondylolisthesis.

The Tyche cage (Kyungwon Medical, Korea) which we used is made so it can expand and anchor with a thread between the endplates. The difference between the anterior and posterior height gives the cage a 7°, angulated, lordotic shape (Fig. 1).

We performed subtotal laminectory or bilateral partial hemi-laminectomy at the involved level(s) and attempted to preserve the facet capsule in all patients. After identifying the correct surgical level(s), discectomy was performed in the usual manner. After bone chips, which were obtained by laminectomy or iliac harvest, were inserted into the disc space, two cages with proper size were then inserted and expanded under fluoroscopic guidance. After remaining bone chips were filled into the cages, then we identified complete packing of the bone chips with a direct visualization and impaction during a thecal sac retraction. On postoperative day 2, patients were allowed to stand without assistance. They were advised to maintain lumbosacral orthosis for 2 months postoperatively.

Patient medical records were reviewed up to 60 months postoperatively, with additional information obtained via telephone interviews conducted by persons not associated with the present study. All patients underwent follow-up X-

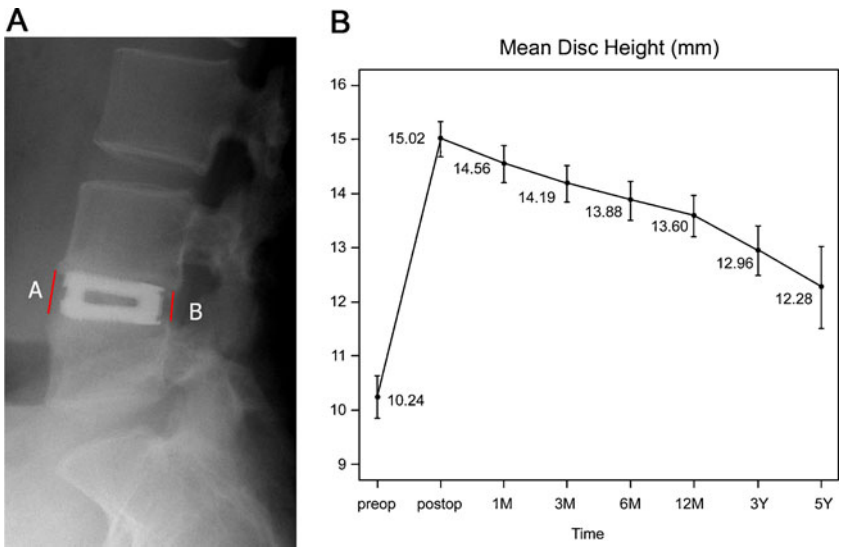

Fig. 2 **a** Lumbar spine lateral view. The intervertebral disc height is calculated by dividing the sum of anterior and posterior intervertebral disc heights by 2 (a+b/2). **b** Disc height changed from 10.25 mm preoperatively to 15.02 mm immediately post-operatively, and gradually de-creased to 12.28 mm at 60 months following surgery

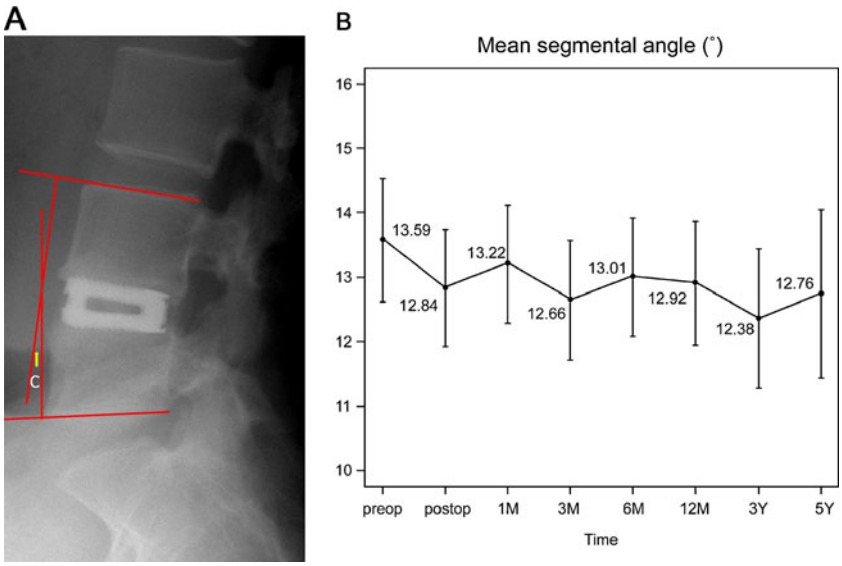

Fig. 3 **a** Lumbar spine lateral view. The angle between the superior and inferior endplates of the adjacent vertebrae is the degree of segmental angle (*C*). **b** The segmental angle changed from 13.59 mm preoperatively to 12.85 mm immediately postoperatively, and to 12.76 mm at 60 months following surgery

rays, including a dynamic view, at 3, 6, 12, and 24 months, and a last follow-up at more than 60 months postoperatively, and a computed tomography (CT) scan at 24 months postoperatively.

Clinical outcomes were analyzed using the mean numeric rating scale (NRS), Oswestry Disability Index (ODI), and Odom's criteria. Changes in the disc height, defined as the average of the anterior and posterior height on plain radiographs, were assessed (Fig. 2a). Changes in the segmental angle between the superior and inferior endplate of adjacent vertebrae, as seen on plain radiographs, was assessed (Fig. 3a). All measurements were performed preoperatively and postoperatively. Interbody fusion was also assessed using dynamic X-rays and CT scan. The fusion criteria included stability on the dynamic view (angular difference <3°), absence of a halo, and formation of a contiguous, bony bridge. We determined that the fusion occurred only in those cases that satisfied all of the criteria.

The factors affecting the clinical outcomes and non-fusion were also analyzed using univariate and multivariate logistic regression. Linear mixed models and Wilcoxon signed rank tests were used for statistical analysis. A p value<0.05 was considered to indicate statistical significance.

Results

The mean NRS scores for the back and leg were 7.1 and 6.9 preoperatively, and 3.0 and 2.7 at 60 months postoperatively, respectively. These decreases were found to be statistically significant. The ODI decreased from 29.5 preoperatively to 14.1 at 60 months postoperatively. Outcomes according to Odom's criteria were excellent in 27 (15.0%) cases, good in 107 (59.4%) cases, fair in 33 (18.3%) cases and poor in 13 cases (7.2%). Therefore, the clinical success rate was 74.4% (the sum of the excellent and good outcomes) (Table 1).

The total number of surgical levels involved was 196, including 169 at one level, 12 at two levels, and one at three levels. Radiological fusion assessment at 24 months postoperatively indicated success at 167 levels (85.2%) and failure at 29 levels (14.8%). Disc height changed from 10.25 mm preoperatively to 15.02 mm immediately

Table 1 Clinical outcomes for PLIF patients

	Preoperative	Postoperative 60 months	p value
NRS for back pain	6.9±3.72	3.0±1.43	<0.001
NRS for leg pain	7.1±2.49	2.7±1.77	<0.001
ODI	29.5±5.12	14.1±1.51	<0.001
Outcomes based on Odom's criteria			
Excellent		27 (15.0 %)	
Good		107 (59.4%)	
Fair		33 (18.3%)	
Poor		13 (7.2 %)	

NRS numeric rating scale, *ODI* Oswestry Disability Index

Table 2 The results of univariate logistic regression analysis to identify factors associated with clinical outcomes

Factor	Character	The number of cases in which clinical success or failure occurred Success (n=134) : failure (n=46)	Odds ratio	p value
Age	≥60 years	89 : 31 cases	1.04	0. 871
	<60 years	45 : 15 cases		
Gender	Male	64 : 21 cases	0.92	0.794
	Female	70 : 25 cases		
Type of laminectomy	STL	71 : 27 cases	1.26	0.535
	Bi. PHL	63 : 19 cases		
Bone graft	Local bone	91 : 34 cases	1.34	0.541
	Iliac bone	43 : 12 cases		
Number of surgery levels	≥2	10 : 3 cases	0.87	0.355
	1	124 : 43 cases		
Smoking	Smoker	20 : 10 cases	1.58	0.832
	Non-smoker	114 : 36 cases		
Chronic alcoholism	Yes	9 : 1 cases	0.31	0.797
	No	125 : 45 cases		
Osteoporosis (T-score ≤−2.5)	Yes	20 : 5 cases	0.70	0.973
	No	114 : 41 cases		
Type 2 DM	Yes	12 : 8 cases	2.14	0.707
	No	122 : 38 cases		
Physical labor in daily activity	Yes	38 : 7 cases	0.45	0.607
	No	96 : 39 cases		
Body mass index (BMI)	BMI≥27 kg/m^2	50 : 12 cases	0.59	0.941
	BMI<27 kg/m^2	84 : 34 cases		
Diagnosis	Recurrent HNP	55 : 14 cases	0.76	0.860
	Spondylolisthesis	33 : 14 ases	1.27	
	Stenosis	37 : 15 cases	1.22	
	Others	9 : 3 cases		
Pain duration	≥6 months	85 : 31 cases	1.19	0.540
	<6 months	49 : 15 cases		
Radiological fusion	Yes	120 : 36 cases	0.42	0.039
	No	14 : 10 cases		

Clinical success excellent or good status in Odom's criteria, *Clinical failure* fair or poor status in Odom's criteria, *STL* subtotal laminectomy, *Bi. PHL* bilateral partial hemi-laminectomy, *Chronic alcoholism* >40 g alcohol/day, *Type 2 DM* diagnosed with type 2 diabetes mellitus

postoperatively and gradually decreased to 12.28 mm for 60 months after surgery. This gradual decrease was statistically significant (p<0.001) (Fig. 2b). The segmental angle changed from 13.59° preoperatively to 12.85° immediately postoperatively and to 12.76° 60 months after surgery. There was no statistically significant change of the segmental angle during any time (p>0.05) (Fig. 3b).

We assessed whether the clinical outcome was associated with any of the following factors : age; gender; type of laminectomy; kind of bone graft; surgical level; smoking history; chronic alcoholism; osteoporosis; type 2 diabetes mellitus (DM); physical activity; body mass index (BMI); preoperative diagnosis; length of pain duration; radiological fusion success. Among these factors, only the radiological fusion success showed only a significant, clinically favorable outcome on the univariate logistic regression test (p= 0.039) (Table 2).

Clinical success according to Odom's criteria was achieved in 120 (76.9%) fusion patients (n=156) and in 14 (58.3%) non-fusion patients (n=24). This difference of clinical success between the two groups, i.e., fusion and non-fusion patients, was statistically significant according

Table 3 The results of multivariate logistic regression analysis to identify factors associated with clinical outcomes

Factor	Character	The number of cases in which clinical success or failure occurred Success (n=134) : failure (n=46)	Rate of success (%)	p value
Radiological fusion	Yes	120 : 36 cases	76.9	0.047
	No	14 : 10 cases	58.3	

Table 4 The results of univariate logistic regression analysis to identify factors associated with non-fusion

Factor	Character	The number of levels at which fusion or non-fusion occurred Fusion (n=167) : non-fusion (n=29)	Odds ratio	p value
Age	≥60 years <60 years	74 : 11 levels 93 : 18 levels	0.77	0.180
Gender	Male Female	82 : 12 levels 85 : 17 levels	0.73	0.174
Type of laminectomy	STL Bi. PHL	93 : 20 levels 74 : 9 levels	1.77	0.160
Bone graft	Local bone Iliac bone	114 : 24 levels 53 : 5 levels	2.23	0.140
Number of surgery levels	≥2 1	18 : 9 levels 149 : 20 levels	3.73	0.002
Smoking	Smoker Non-smoker	26 : 5 levels 141 : 24 levels	1.13	0.696
Chronic alcoholism	Yes No	11 : 2 levels 156 : 27 levels	1.05	0.724
Osteoporosis (T-score ≤−2.5)	Yes No	30 : 6 levels 137 : 23 levels	1.19	0.190
Type 2 DM	Yes No	19 : 10 levels 148 : 19 levels	4.10	0.007
Physical labor in daily activity	Yes No	48 : 13 levels 119 : 16 levels	2.01	0.092
Body mass index (BMI)	BMI ≥27 kg/m^2 BMI <27 kg/m^2	65 : 12 levels 101 : 17 levels	1.10	0.326

to the multivariate logistic regression test (p=0.047) (Table 3).

We then examined whether the radiological fusion was associated with any of the following factors: age; gender; type of laminectomy; kind of bone graft; surgical level; smoking history; chronic alcoholism; osteoporosis; type 2 DM; physical activity; BMI. We found that surgery at multiple levels and having type 2 DM were both associated with fusion failure (p=0.008 and 0.027) (Tables 4 and 5).

Surgery-related complications occurred in 11 (6.1%) patients and consisted of symptomatic, junctional degeneration (five patients), infection (three patients), dura tear (two patients), and postoperative hematoma (one patient). In addition, post-operative paresthesia of the leg occurred in 20 patients, with a maximum duration of 6 days.

Figures 4 and 5 show the patients approved for radiological fusion and non-fusion according to our fusion criteria.

Table 5 The results of multivariate logistic regression analysis to identify factors associated with non-fusion

Factor	Character	Odds ratio	p value
Number of surgery levels	≥2 1	3.74	0.008
Type 2 DM	Yes No	3.23	0.027

Discussion

Although several previous reports have advocated the use of stand-alone cages for PLIF [1, 8, 12–14, 18], the opposite opinion does have common sense regarding the efficacy and stability of that approach compared with PLIF with pedicle screws [2, 5, 15, 17, 19]. Our study examined the long-term clinical and radiological outcomes of a large series following PLIF using stand-alone cages.

Although there was an overall improvement in pain and the ODI, our clinical success rate was only 74.4%. This rate compares poorly with rates reported in other studies advocating the use of stand-alone cages and indicates that a significant proportion of our patients had prolonged or recurrent discomfort.

The present study's radiological fusion success rate was 85.2%. Other studies assessing interbody implants without pedicle fixation have reported fusion rates of between 83% and 100% [6, 9, 10]. A review of the literature indicates that a large discrepancy exists between radiological success rates, as manifested by radiological fusion, and clinical success rates. Many studies question the ability of the current techniques to accurately diagnose pseudarthrosis, thereby suggesting that previously reported fusion rates might be incorrect and too high [3, 7]. So, we checked all of our patients' CT scans and dynamic X-rays and determined that radiological fusion was successful only in

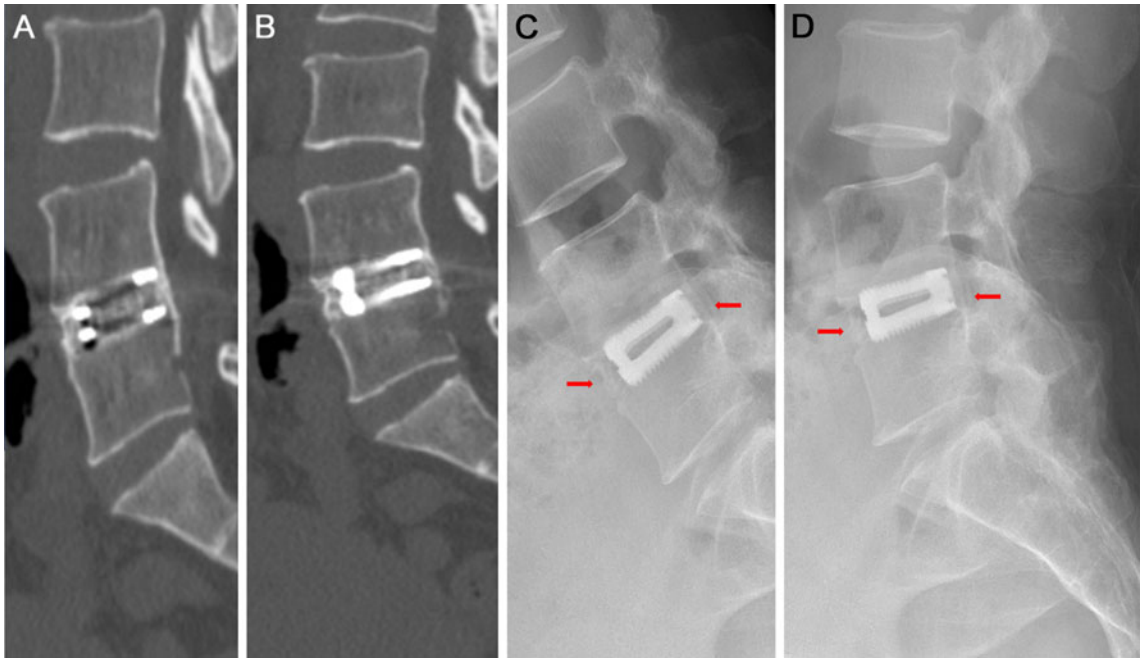

Fig. 4 **a**, **b** The CT image of the patient approved fusion. Bone bridge indicating fusion is seen around cage. **c**, **d** Dynamic X-ray lateral views, i.e., flexion and extension views, of the same patient. Bone bridge is also seen (*red arrows*). Motion is not observed on these two images

those cases that satisfied all of the provided fusion criteria so as to reduce any potential bias. We then found that more sucessful clinical outcomes were only possible with radiologically fused vertebrae. This result showed that the attempt to make a complete fusion after decompression is necessary. In order to elevate the fusion rate, adding pedicle screws to our surgical procedure may be an option. We also believe that the use of pedicle screws can also offer better clinical outcomes than stand-alone PLIF surgery.

The present study sought to identify factors associated with non-fusion. In our analysis, a number of factors revealed that multiple levels of surgery and type 2 DM were risk factors for non-fusion. Previous studies of PLIF surgery using threaded, stand-alone cages reported that the

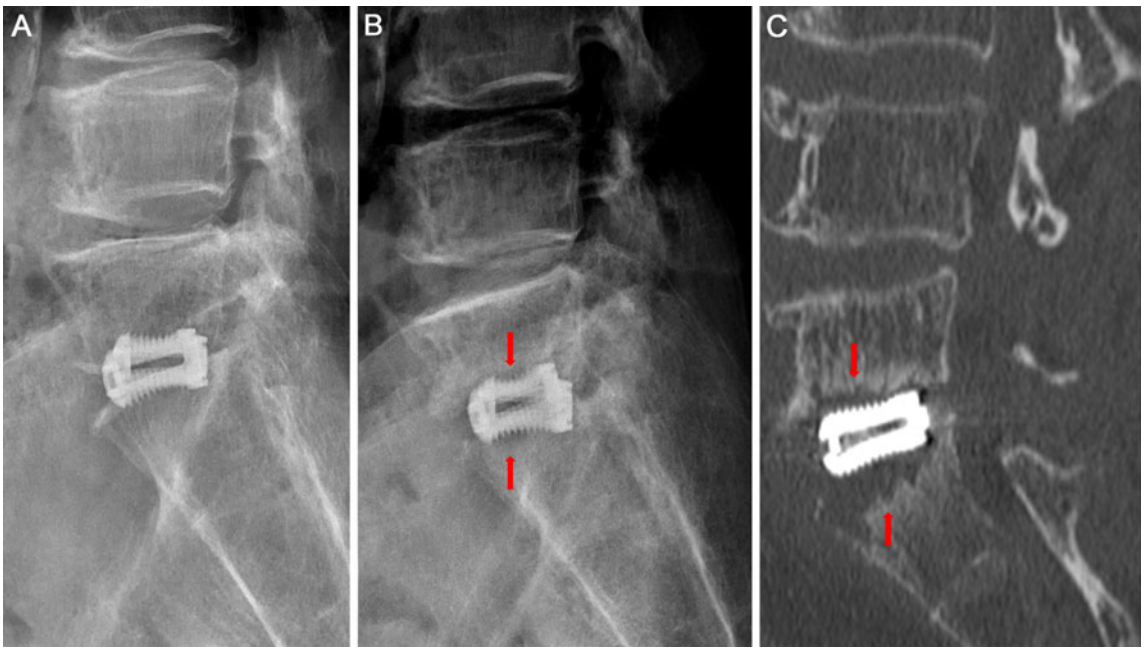

Fig. 5 **a**, **b** X-ray lateral views, i.e., postoperative 12 and 24 months, of the patient who approved non-fusion. Halo is seen around cage (*red arrows*). **c** The 24-month postoperative CT image of the same patient. Endplate erosion is seen (*red arrows*)

risk factors for pseudoarthrosis included the failure to achieve adequate distraction, Type 2 DM, use of local bone chips rather than the iliac bone chips, cage insertion at too lateral position, a large amount of facet resection, a small cage, a small amount of bone graft, and a small amount of disc excision [3, 4, 6, 14]. Although we attempted to preserve the facets in all patients, even those with canal stenosis, we believe that this is sometimes a virtually impossible task or one that should not even be attempted. In fact, with severe stenosis it may be better to sacrifice the facets for interbody fusion and to add pedicle screws rather than to procure a space and insertion of the spacer at a cost of too much root and thecal sac retraction. We also believe that a considerable amount of facet might have been unintentionally sacrificed in our cases, with the iatrogenic instability thus possibly causing poor radiological fusion.

The use of stand-alone cages for a lumbar fusion surgery was reported to be unsuccessful in preserving or re-establishing segmental lordosis [11]. In contrast, others reported that the segmental angle increased at postoperative 24 months and that disc height increased immediately postoperatively and then decreased [8]. Our study found that the postoperative segmental angle did not preserve the preoperative segmental angle and the disc height increased immediately postoperatively and then gradually decreased, thus indicating cage subsidence. We also believe that this stand-alone PLIF surgery is less effective for restoring better sagittal alignment, which can only be obtained by adequate compression of the posterior column and distraction of the vertebral plates using pedicle screws. In addition, continuous loss of disc height is another problem with the stand-alone cage, and it can be solved with the addition of pedicle screws.

Considering the poor clinical and radiological results which were derived from our study with a long-term followed large series, we concluded that PLIF using stand-alone cages is a poor surgical option for patients with degenerative lumbar disease, including grade I spondylolisthesis, stenosis with instability, and recurrent disc herniation. The combined use of pedicle screws with cages may be a solution for these problems and will guarantee a better radiological fusion rate, which should then offer a more successful clinical outcome.

In particular, in patients with the known risk factor for pseudoarthrosis, this surgery should be avoided.

Conclusion

The use of PLIF with stand-alone threaded cages in degenerative lumbar disease patients resulted in a long-term clinical success rate of 74.4%. Although the radiological fusion rate was 85.2%, the continuous reduction of disc height and poor alignment preservation were observed. The clinical outcome was significantly associated with radiological fusion. Our study showed that PLIF using only stand-alone cages is a poor surgical option for creating good alignment and height restoration in patients with degenerative lumbar disease. In particular, in patients with known risk factors for pseudoarthrosis, such as type 2 DM, multi-level surgery, etc., PLIF surgery using stand-alone cages should be avoided.

Conflicts of interest None.

References

1. Bagby GW (1988) Arthrodesis by the distraction-compression method using a stainless steel implant. Orthopedics 11:931–934
2. Brantigan JW, Steffee AD (1993) A carbon fiber implant to aid interbody lumbar fusion. Two-year clinical results in the first 26 patients. Spine Phila Pa 1976 18:2106–2107
3. Cassinelli EH, Wallach C, Hanscom B, Vogt M, Kang JD (2006) Prospective clinical outcomes of revision fusion surgery in patients with pseudarthrosis after posterior lumbar interbody fusions using stand-alone metallic cages. Spine J 6:428–434
4. Chen L, Yang H, Tang T (2005) Cage migration in spondylolisthesis treated with posterior lumbar interbody fusion using BAK cages. Spine Phila Pa 1976 30:2171–2175
5. Flynn JC, Hoque MA (1979) Anterior fusion of the lumbar spine. End-result study with long-term follow-up. J Bone Joint Surg Am 61:1143–1150
6. Fuji T, Oda T, Kato Y, Fujita S, Tanaka M (2003) Posterior lumbar interbody fusion using titanium cylindrical threaded cages: is optimal interbody fusion possible without other instrumentation? J Orthop Sci 8:142–147
7. Kant AP, Daum WJ, Dean SM, Uchida T (1995) Evaluation of lumbar spine fusion. Plain radiographs versus direct surgical exploration and observation. Spine Phila Pa 1976 20:2313–2317
8. Kim JW, Park HC, Yoon SH, Oh SH, Roh SW, Rim DC, Kim TS (2007) A multi-center clinical study of posterior lumbar interbody fusion with the expandable stand-alone cage (Tyche(R) cage) for degenerative lumbar spinal disorders. J Korean Neurosurg Soc 42:251–257
9. Kim KH, Park JY, Chin DK (2009) Fusion criteria for posterior lumbar interbody fusion with intervertebral cages: the significance of traction spur. J Korean Neurosurg Soc 46:328–332
10. Kim Y (2001) Prediction of mechanical behaviors at interfaces between bone and two interbody cages of lumbar spine segments. Spine Phila Pa 1976 26:1437–1442
11. Klemme WR, Owens BD, Dhawan A, Zeidman S, Polly DW (2001) Lumbar sagittal contour after posterior interbody fusion: threaded devices alone versus vertical cages plus posterior instrumentation. Spine Phila Pa 1976 26:534–537
12. Kuslich SD, Danielson G, Dowdle JD, Sherman J, Fredrickson B, Yuan H, Griffith SL (2000) Four-year follow-up results of lumbar spine arthrodesis using the Bagby and Kuslich lumbar fusion cage. Spine Phila Pa 1976 25:2656–2662
13. Matge G, Leclercq TA (2000) Rationale for interbody fusion with threaded titanium cages at cervical and lumbar levels. Results on 357 cases. Acta Neurochir Wien 142:425–434
14. McAfee PC (1999) Interbody fusion cages in reconstructive operations on the spine. J Bone Joint Surg Am 81:859–880

15. Newman MH, Grinstead GL (1992) Anterior lumbar interbody fusion for internal disc disruption. Spine Phila Pa 1976 17:831–833
16. Onesti ST, Ashkenazi E (1998) The Ray Threaded Fusion Cage for posterior lumbar interbody fusion. Neurosurgery 42:200–205
17. Oxland TR, Lund T (2000) Biomechanics of stand-alone cages and cages in combination with posterior fixation: a literature review. Eur Spine J 9(Suppl 1):S95–S101
18. Ray CD (1997) Threaded titanium cages for lumbar interbody fusions. Spine Phila Pa 1976 22:667–680
19. Stauffer RN, Coventry MB (1972) Anterior interbody lumbar spine fusion. Analysis of Mayo Clinic series. J Bone Joint Surg Am 54:756–768

Comment

This article serves a point. It tells us that the use of stand-alone PLIFs for the treatment of lumbar DDD is not the current recommended strategy. The conclusions are somewhat outdated, as I think that this is nowadays a common assumption. As stated by the authors, one of the limitations of this technique is that it is less effective in restoring sagital lordosis than if one adds up pedicular screws. Lordosis can, in fact, be better obtained at the cost of both the distraction of the vertebral plates and compression of the screws.

The authors say that they were able to preserve the facets even in cases with important canal stenosis. In my experience, this is at times a virtually impossible task or one that should not even be pursued when attempting an intersomatic fusion. In fact, with severe stenosis it may be better to sacrifice the facets (with PLIFs) or just one (with TLIF) than to procure space and the insertion of the spacer at the cost of too much root and the cal sac retraction. In the text the authors seem to acknowledge this reality, but they do not add any comments as to how to deal with the iatrogenic instability it creates.

This is of more relevance given the fact that this is a PLIF stand-alone procedure which poorly addresses the issue of instability resulting from facet failure.

This being a personal single surgeon series, one would really need a similar, even if shorter, series of patients treated for the same problem with the intersomatic/pedicle screw technique to compare results with.

Manuel Cunha e Sá
Almada, Portugal

Acta Neurochir (2011) 153:1417–1425
DOI 10.1007/s00701-011-1039-9

CLINICAL ARTICLE

Accuracy of freehand fluoroscopy-guided placement of C1 lateral mass and C2 isthmic screws in atlanto-axial instability

Enrico Tessitore · Andrea Bartoli · Karl Schaller · Michael Payer

Received: 23 March 2011 / Accepted: 19 April 2011 / Published online: 21 May 2011

Abstract
Background The C1 lateral mass and C2 isthmic stabilization, as introduced by Goel and Laheri and by Harms and Melcher, is a well-known fixation technique. We present the clinical and radiographic results with freehand fluoroscopy guided C1 lateral mass and C2 isthmic fixation in a consecutive series of 28 patients, evaluating the accuracy of screw placement.
Methods Twenty-eight consecutive patients suffering from post-traumatic and other C1-C2 instability were operated on between 2001 and 2010. Indications for surgery were: trauma (n=21 cases), os odontoideum (n=1), cranio-verterbal malformation (n=1), and arthritis (n=3) and idiopathic instability (n=2). C1 lateral mass and C2 isthmic screws were placed according to the usual anatomical landmarks with lateral fluoroscopy guidance. All patients underwent a postoperative CT scan. The extent of cortical lateral or medial breach was determined and classified as follows: no breach (grade A), 0–2 mm (grade B), 2–4 mm (grade C), 4–6 mm (grade D), more than 6 mm (grade E). Grade A and B screws were considered well positioned.
Results A total of 56 C1 lateral mass and 55 C2 isthmic screws were placed. Accuracy of screw placement was as follows: 107 grade A (96.4%), four grade B (3.6%), and no grade C, D or E. Clinical and radiological follow-up showed improvement in symptoms (mainly pain) and stability of the implants at the end of the follow-up.
Conclusions Freehand fluoroscopy-guided insertion of C1 lateral mass and C2 isthmic screws can be safely and effectively performed.

Keywords C1-C2 instability · C1-C2 internal fixation · Computer-assisted spinal surgery · Screw placement

E. Tessitore (✉) · A. Bartoli · K. Schaller · M. Payer
Department of Neurosurgery, Geneva University Medical Center,
Faculty of Medecine, University of Geneva,
6, Rue Perret-Gentil,
1211 Geneva, Switzerland
e-mail: enrico.tessitore@hcuge.ch

M. Payer
Hirslanden Clinic,
Zurich, Switzerland

Introduction

C1-C2 instability may result from trauma, tumor, infection, arthritis, and malformations, and it frequently requires surgical fixation. Different techniques have been described in the literature to achieve C1-C2 stabilization. Magerl introduced transarticular C1-C2 fixation, coupled to posterior wiring and bone grafting. This is considered biomechanically the strongest technique with fusion rates approaching 100% [4, 20]. Nevertheless, it is associated with a risk of vertebral artery (VA) damage. In order to reduce this risk and to achieve equivalent stability, first Goel and Laheri [5], and then Harms and Melcher [6], introduced a technique in which C1 lateral mass and C2 isthmic/pedicle screws are used [10, 12, 15].

A residual risk remains for any technique in C1-C2 fixation, due to the proximity of the screw trajectory and the VA, the spinal cord, the internal carotid artery, and the hypoglossal nerve. Even if the risk of neurological deficit from VA injury has been calculated to be 0.2% per patient and 0.1% per screw, the consequence of VA injury can lead to brain infarction, massive bleeding and even death [32].

Consequently, different intraoperative image-guided systems have been developed to reduce the risk for malpositioning of the screws [7–9], allowing the surgeon to achieve

a solid fixation in a safe way. Navigation and robotic systems are now available in the majority of spine centers, where so-called "computer assisted surgery" (CAS) is performed. Potential advantages of CAS are well known: the ability to plan a preoperative surgical strategy, the possibility to simulate surgery by advance, the safety of the procedure, and, when associated with minimally invasive techniques, less length of hospitalization time for patients, less postoperative pain and smaller complication rates. Nevertheless, CAS is apt to inaccuracy as well, which might be particularly relevant in such a delicate and mobile region as the cranio-cervical junction [27]. Adequate preoperative imaging and deep knowledge of anatomical structures and landmarks are thought be sufficient to perform surgical fixations in this region.

We therefore analyzed our experience with C1 lateral mass and C2 isthmic screw fixation in 28 patients to define placement precision relying on traditional anatomical landmarks and intraoperative lateral fluoroscopy.

Materials and methods

Twenty-eight consecutive patients, ten male and 18 female, with a mean age of 59.8 years have been operated on for C1-C2 instability or painful osteoarthritis in the Department of Neurosurgery between 2001 and 2010. Twelve of these patients were included in a previous report with a short follow-up, and under different viewpoints [19]. C1-C2 instability was caused by: trauma in 21 cases (75%), malformation in one (3.5%), os odontoideum in one (3.5%). Three patients (10.7%) suffered from painful osteoarthritis and two patients (7.1%) had idiopathic C1-C2 instability. Among the 21 trauma cases, the indications for surgery were: highly unstable fractures (n=9, 42.8%), failure of conservative treatment with hard collar (n=7, 33.4%), pseudoarthrosis after anterior screw placement for odontoid fractures (n=4, 19.1%), and old non-healed odontoid fracture (n=1, 4.7%) (Table 1).

Preoperative symptoms were: pain (in all), and cervical myelopathy (in two). Neck pain was classified according to the visual analogue score (VAS). The mean preoperative VAS for cervical pain was 4.9 (Table 1). All patients had a preoperative bone computed tomography (CT) with angiographs and cranio-cervical magnetic resonance imaging (MRI). The CT scan allowed for studying the bony anatomy of the region and the course of the vertebral artery. Measurements of C1 lateral mass and C2 isthmus were performed on preoperative CT axial and sagittal views to calculate the maximum space available for the screws. The size of the screws used during the surgery was recorded on the operative chart.

Postoperative thin-cut CT was performed 1–3 days post surgery. The accuracy of the screws was evaluated according to the Gertzbein and Robbins grading [3]: grade A (perfectly into the pedicle), grade B (0–2 mm of cortical breach), grade C (2–4 mm), grade D (4–6 mm), and grade E (more than 6 mm). Grade A and B screws were considered well positioned.

Mean follow up was 10 months, ranging from 2 to 48 months (Table 1).

Surgical technique

The surgical technique used by authors has been already described in details in a previous paper [19].

Briefly, the patient is placed in the prone position with the head in a Mayfield head-holder in a "military tuck" position in order to facilitate the access to C1-C2 region. Manual reduction under fluoroscopic lateral view is attempted prior to surgery. A midline skin incision is performed from the occiput to the C3 spinous process. After opening of the fascia and subperiosteal dissection of cervical posterior muscles, anatomical bony landmarks are identified: C1 posterior arch with posterior tubercle, C2 posterior arch with posterior bifid spinous process, C2-C3 articular rim, medial border of the C2 isthmus.

The C1 lateral mass entry point is identified just below the posterior arch by pushing caudally the C2 nerve root with a hook. Hemostatic sponge or gel is used to control the venous plexus bleeding. The medial and lateral borders of the lateral mass of C1 are identified and palpated. The entry point is in the midway, and an electric drill 2.7 mm is used for a pilot hole. The sagittal cranio-caudal direction is determined by pointing to the C1 anterior tubercle on lateral C-arm view. Around 10° of convergence are needed. The screw path is completed, till the anterior cortex is gently pierced. The usual length of the C1 screw is 30–34 mm, necessary to allow rod placement posteriorly.

The entry point for C2 isthmic screw is about 2–3 mm above the C2-C3 articulation and 2–3 mm lateral from its center. The sagittal cranio-caudal direction is determined under direct fluoroscopic view, aiming at the C1 anterior tubercle until the tip of the screw reaches the posterior border of C2 vertebral body. Usually, the VA is projected anterior to this line, so by staying posterior to it, less risk for VA damage is expected. The trajectory is quite steep in order to have the longest purchase into the isthmus. At that point, if needed, pulling the spinous process in a cranial direction with a clamp allows for a steep sufficiently trajectory. The trajectory is convergent, aiming towards the medial wall of the C2 isthmus. The usual length of the C2 isthmic screw is 14–20 mm. Then, the head of the screws are connected with rods (here: Vertex System, Medtronic, Memphis, TN, USA). A monocortical bone graft from the posterior iliac crest is put between C1 and C2

Table 1 Case series

Sex	Age	Indication	Preop neck pain (VAS)	C1 screws MC/BC	C1 screws GR Grade	C2 screws GR Grade	Neck pain at F-UP	Stability at F-UP
F	65	Pseudoarthrosis type III odontoid fracture	7	One BC, one MC	A-A	A-A	2	Yes
M	48	Pseudoarthrosis type II odontoid fracture	6	Both BC	A-A	A-A	4	Yes
F	75	Pseudoarthrosis type II odontoid fracture	8	Both BC	A-A	A-A	1	Yes
M	64	C1C2 instability with malformation	6	Both BC	A-A	A-B	3	Yes
F	72	C1C2 osteoarthritis	8	Both BC	A-A	A-B	2	Yes
M	77	Pseudoarthrosis after odontoid screwing	5	Both BC	A-A	A-A	0	Yes
M	78	Pseudoarthrosis after odontoid screwing	5	Both BC	A-A	A-A	5	Yes
F	23	Complex C2 fracture	0	Both BC	A-A	A-A	0	Yes
F	62	Complex C2 fracture	7	Both BC	A-A	A-A	3	Yes
F	27	Pseudoarthrosis of C2 fracture	0	Both BC	A-A	A-A	1	Yes
F	38	Unstable Jefferson fracture	7	Both BC	A-A	A-A	4	Yes
F	49	Complex C2 fracture	7	Both BC	A-A	A-A	0	Yes
F	85	Pseudoarthrosis after odontoid screwing	0	Both BC	A-A	A-A	0	Yes
F	75	Pseudoarthrosis after odontoid screwing	5	Both BC	A-A	A-B	0	Yes
F	40	Unstable type III odontoid fracture	4	Both BC	A-A	A-A	0	Yes
F	50	Unstable type III odontoid fracture	7	One MC, one BC	A-A	A-A	4	Yes
M	60	Unstable type II odontoid fracture	4	Both BC	A-A	A-A	1	Yes
F	75	Pseudoarthrosis type II odontoid fracture	0	One MC, one BC	A-A	Translaminar-A	0	Yes
F	82	Pseudoarthrosis type II odontoid fracture	4	Both BC	A-A	A-A	1	Yes
M	23	Pseudoarthrosis type II odontoid fracture	3	Both MC	A-A	A-A	0	Yes
F	34	Os odontoideum	4	Both BC	A-A	A-A	0	Yes
M	59	Pseudoarthrosis type II odontoid fracture	5	One BC, one MC	A-A	A-A	2	Yes
M	51	Complex C2 fracture	6	Both MC	A-A	A-A	1	Yes
M	68	Unstable Jefferson fracture+type II odontoid fracture	4	Both B	A-A	A-A	0	Yes
M	60	Idiopathic C1C2 instability	7	Both BC	A-A	A-B	1	Yes
F	75	C1C2 osteoarthritis	8	Both BC	A-A	A-A	4	Yes
F	78	C1C2 osteoarthritis	8	Both BC	A-A	A-A	6	Yes
F	82	Idiopathic C1C2 instability with stenosis	4	Both BC	A-A	A-A	2	Yes

M male, *F* female, *VAS* visual analogue score, *MC* monocortical, *BC* bicortical, *GR* Gertzbein and Robbins, *F-UP* follow-up

posterior arches according to Gallie technique, modified by Sonntag. The different layers are closed on a suction drainage. Patients are mobilized from the first postoperative day on in a soft collar.

Results

Examples of screw fixations are shown in Figs. 1, 2, 3, and 4.

Fifty-six C1 lateral mass screws were inserted: 25 screws were 34 mm long (44.6%), 22 (39.3%) screws were 32 mm, and nine screws (16.1%) were 30 mm. Fifty-five C2 isthmic screws were implanted: 19 screws were 14 mm long (34.5%), 15 screws were 16 mm long (27.3%), 12 screws were 18 mm long (22%), seven screws were 20 mm long (12.7%), and two screws were 12 mm long (3.6%). In one case, a 26-mm C2 laminar screw had been inserted because of an iatrogenic fracture of the lateral part of the isthmus.

Twenty-eight postoperative CT scans were analyzed. All 56 C1 lateral mass screws (100%) were grade A according to the Gertzbein and Robbins grading. C1 lateral mass screws breaching the anterior cortex were not considered to be malpositioned, because this is part of the surgical technique. Eight out of 56 C1 screws (14.3%) were monocortical. Four C2 isthmic screws resulted to be grade B (7.2%), while the remaining 51 were considered grade A (92.8%) and one screw was translaminar because of an iatrogenic isthmic fracture. Considering grade A+B as ideal

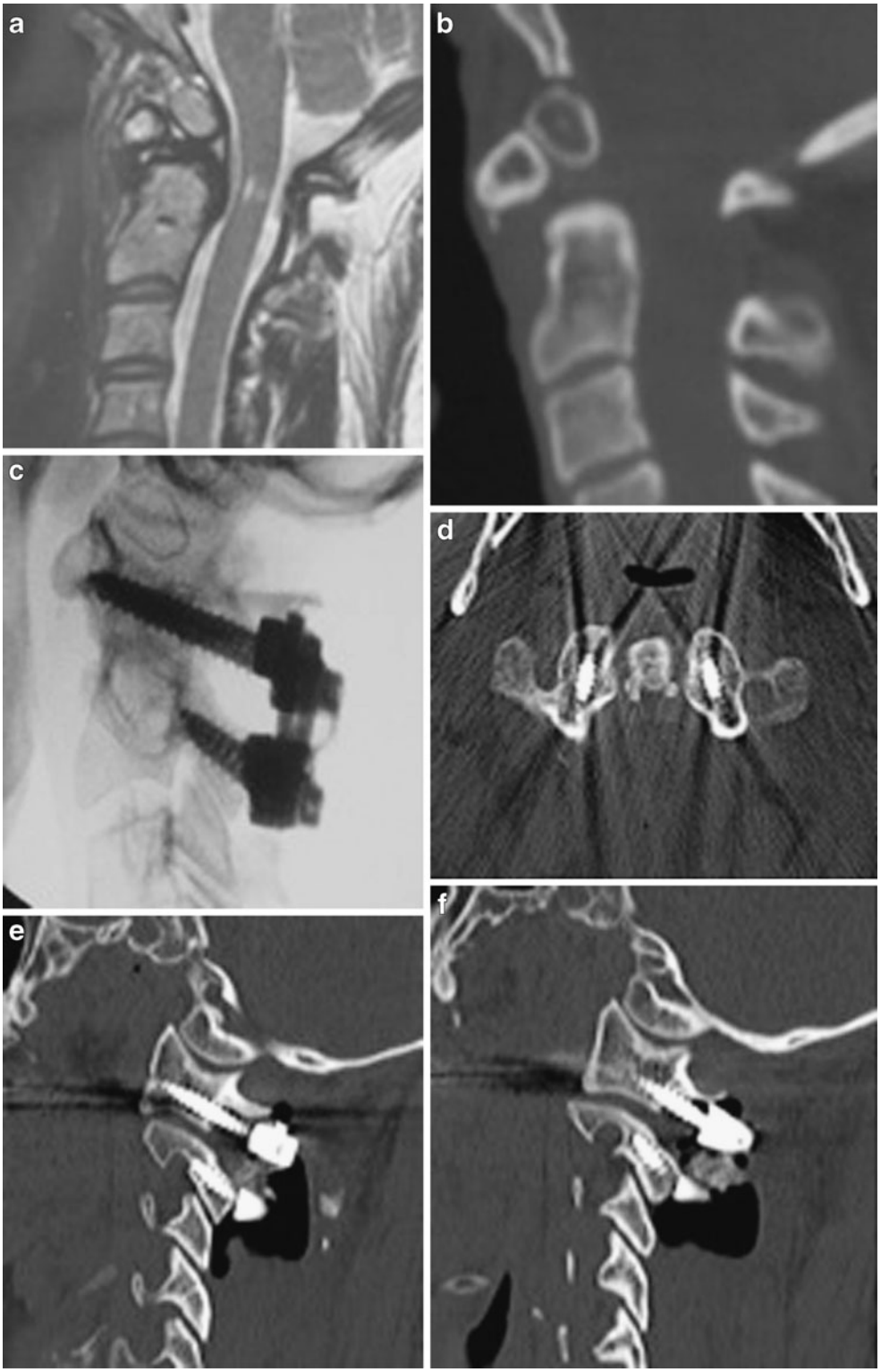

Fig. 1 Os odontoideum. **a** MR image showing an os odontoideum with a high cervical spinal cord hypersignal. **b** CT scan showing an os odontoideum non-fused to the clivus. **c** Postoperative lateral X-ray showing a C1-C2 posterior fixation. **d** Postoperative axial CT scan showing well-positioned C1 LM screws. **e**. Postoperative sagittal CT scan showing right C1 LM and C2 isthmic screws. **f** Postoperative sagittal CT scan showing left C1 LM and C2 isthmic screws

positioning, all screws had showed to be well positioned (Table 1).

Mean operating time was 152.9 min (ranging from 90 to 225 min). Mean blood loss was 477 ml (ranging from 150 to 800 ml). At the end of the follow-up the postoperative mean VAS score for cervical pain was 1.6. At the end of the follow-up, all 28 patients (100%) showed stability on dynamic X-rays and a solid fusion was obtained (Table 1).

Complications occurred in six patients (21.4%). A greater occipital nerve neuralgia was evident in three cases (10.7%). The pain was treated with specific drugs with complete recovery at the end of the follow-up in all cases.

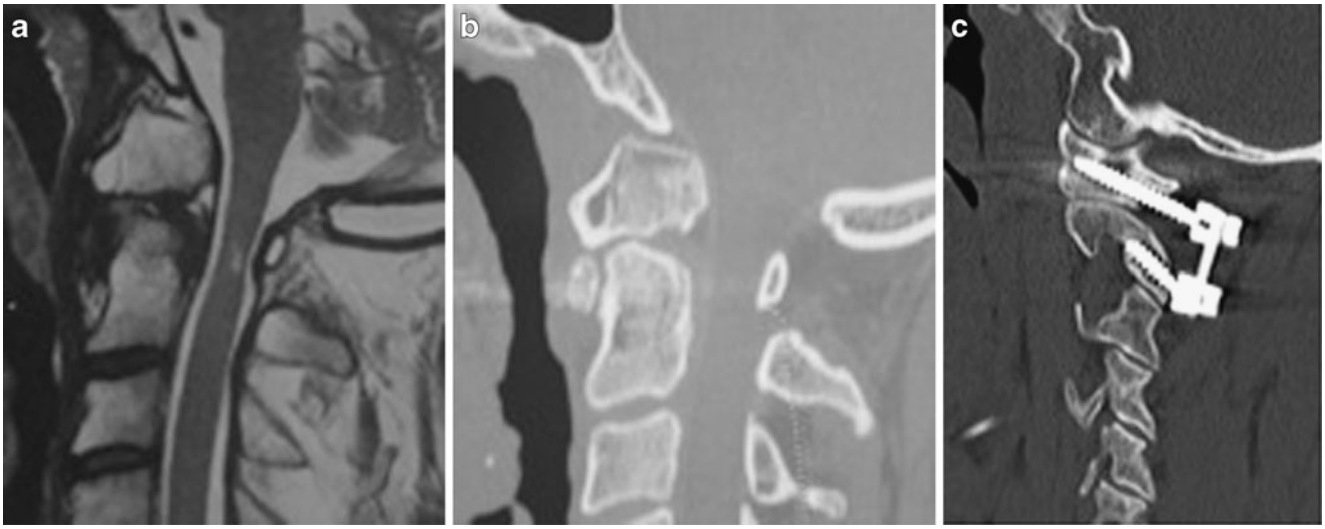

Fig. 2 Old non-healed type II odontoid fracture. **a** MR image showing an old non-healed type II odontoid fracture with fusion between the anterior C1 arch and the bony fragment. **b** CT scan showing an old non-healed fracture. **c** Postoperative CT scan showing C1 LM and C2 isthmic screws on the right side. The first one is unicortical

This relatively high incidence of transitory neuralgia is maybe related to a conflict between the screw and the C2 nerve root at the entry site. In up to 25% of cases some of the C1 lamina may need to be removed to achieve an adequate entry site. Alternatively, pre-ganglionic division of the C2 nerve root can be utilized to gain access to the entry site [5, 30].

Furthermore, we had a superficial wound infection in one case (3.5%), which has been successfully treated with intravenous antibiotics. One patient (3.5%) had pain at the iliac harvested site for several weeks with spontaneous regression. A posterior progressive intestinal herniation through the iliac scar was seen in one case (3.5%), which required surgical repair.

Discussion

Techniques of C1-C2 fixation

Atlanto-axial instability can be related to a variety of pathologies: trauma, tumors, infections, arthritis, and congential malformations. It might be associated with pain or neurological compromise, and if misdiagnosed or mistreated it may lead to catastrophic neurological consequences.

C1-C2 fixation and stabilization can be achieved with different techniques. Magerl and Freeman [12] first introduced in 1987 the so-called transarticular procedure, in which atlanto-axial stability is obtained by a bilateral placement of transarticular screws. This technique has biomechanical advantages in term of stiffness and stability, but it presents also some limitations: first, the two articular processes must be well aligned and the pre-existing degree of luxation needs to be reduced; then, it can be performed only if the VA is not "in the way" of the trajectory of the screw [4]. Furthermore, VA anatomical variants occur in up to 20% of patients, thus resulting in a potential conflict between the screw and the medially located VA [17]. It has been calculated that in the transarticular technique there is a risk of VA damage of 2% per screw [32].

First Goel and Laheri in 1994 [5] and then Harms and Melcher in 2001 [6] introduced a different technique in which C1 lateral mass and C2 pedicle/isthmic screws are connected, respectively, with plates or rods. In literature, it is still unclear which of the two techniques is biomechanically the stiffest. Anyway, the Goel-Harms procedure can be performed even if the C1-C2 luxation is not completely reduced. Furthermore, the risk for damaging the VA is clearly reduced. We prefer the latter technique, and have already published our own results with this technique in a consecutive series of 12 patients [19].

Unicortical or bicortical C1 lateral mass screw?

The need for unicortical or bicortical fixation in C1 lateral mass remains a point of debate. A unicortical purchase has been advocated in literature, in order to reduce the risk of injury to the ICA and the hypoglossal nerve, which both lie directly in front of the lateral mass [11]. We prefer a bicortical purchase for biomechanical reasons. The perforation of the anterior cortex cannot be seen during the operation, but it can be felt with a pedicle feeler during the drilling procedure as a loss of resistance. Thereafter in this series, 87.4% of C1 screws were found to be bicortical on the postoperative CT.

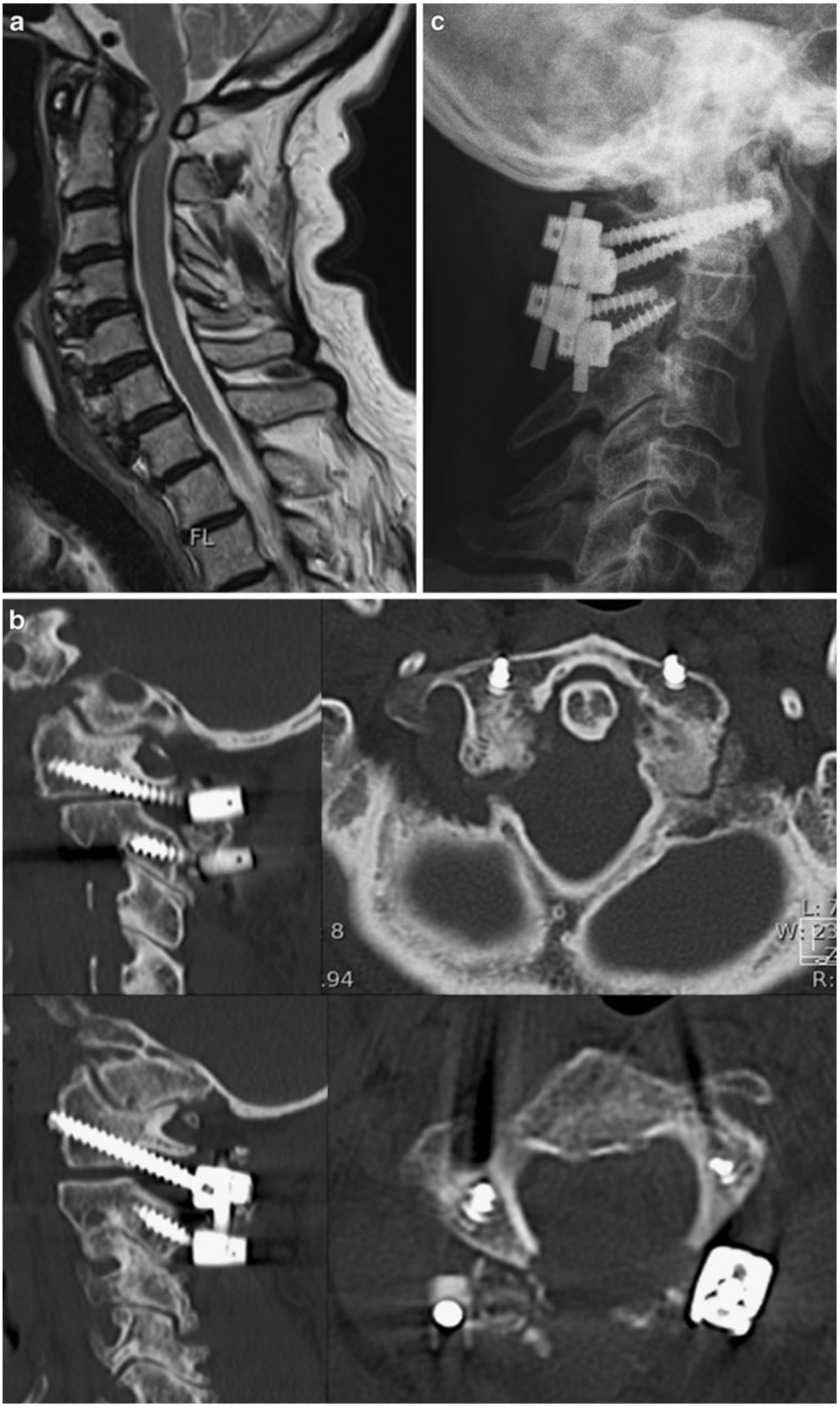

Fig. 3 Idiopathic C1-C2 instability. **a** MR image showing a spinal cord compression at C1/2 due to retrodental pannus of unknown origin; a diffuse idiopathic skeletal hyperostosis (DISH) is evident in the lower C spine. **b** Postoperative CT confirms correct screw positions in C1 and C2 on sagittal CT reconstruction and axial cuts after C1-C2 fixation and C2 laminectomy. **c** Lateral and anteroposterior (AP) radiographs after 6 months

Eck et al. [2] presented a biomechanical study of pullout strength of unicortical versus bicortical C1 lateral mass screws performed on 15 cadaveric cervical spine specimens. The mean pullout strengths of the unicortical screws and

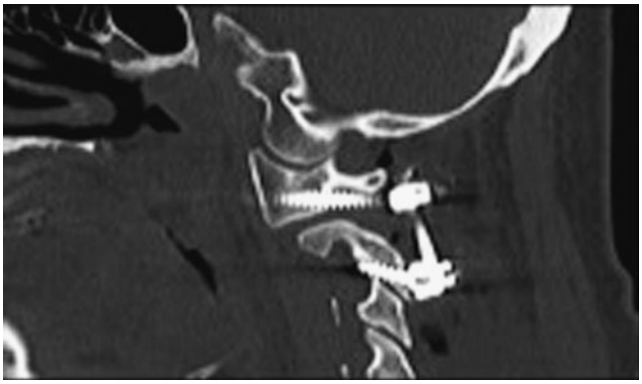

Fig. 4 Example of C2 GR grade B screw. A C2 isthmic screw is breaching the anterior cortex by 2 mm

bicortical screws were 588 N (range, 212–1,234 N) and 807 N (range, 163–1,460 N), respectively (P=0.008). They concluded that bicortical C1 lateral mass screws were significantly stronger than unicortical ones.

Navigation systems for C1-C2 screw placement

Navigation systems for the reduction of the risk for vessel and spinal cord injuries had gained popularity in spinal surgery. Thanks to technologically developed "online" camera-tracking of a patient's spinal anatomy with calibrated instruments, based on preoperative or intraoperative CT or three-dimensional (3D) rotational radiographic imaging, implant positioning has been described as safe and efficient in many reports, including the CCJ [14]. While image-guided surgery is a logical effort to improve safety and precision, several imprecisions are unavoidable in such a highly mobile region as the craniocervical junction (CCJ). Thus, even with perfect data transformation, navigation accuracy is reduced by several factors:

1. Calibration errors: they have been shown in 3D fluoroscopy-based systems, for example, to account for approximately 1 mm accuracy in a phantom model [25].

2. Bending of instruments: in a cadaver model, navigation inaccuracy was around 2.5 mm due to bending of instruments and or reference during manipulation [26]; in practice, occasional blocking of the camera field of view or inadvertently touching/hitting references can cause additional loss of precision [27].

3. Non-rigid connection between the reference base and the actual surgical site: concerning specifically CCJ, attaching a reference frame in this region is problematic; therefore, the reference frame is often attached to the head, creating potentially important motion between the actual surgical site at C1 or C2 and the frame [27].

Due to these navigation inaccuracies, most surgeons verify their drilling and screw positioning and lengths by conventional intraoperative fluoroscopy and do not show complete faith in image guidance [18]. So far, there is not a single report where the surgeon trusted the image-guidance more than intraoperative fluoroscopic or anatomic verification. It remains unclear whether the computer-assisted surgery leads to a lower incidence of screw replacement and a lower incidence of screw-placement-related complications [22, 28].

On the other hand, Mueller et al. [13] state that the use of spinal navigation in C2 pedicle screw insertions is justified by the high rate of misplaced screws, despite the fact that no neurovascular injury occurred. They reported on the technique of transpedicular C2 screw fixation without spinal navigation. The accuracy was assessed on postoperative CT scans according to Gertzbein and Robbins (GRGr) (see above). A total of 47 C2 pedicle screws in 27 patients were performed. An association between intraoperative direct visualization and fluoroscopy was used. The postoperative CT findings showed in 55.3% GRGr 1, in 27.7% GRGr 2, in 10.6% GRGr 3, and in 6.3% GRGr 4 pedicle screw insertion accuracy. Screw malpositioning (i.e., GRGr 3 and 4) was observed mainly with thin (<5 mm) pedicle diameters. If a GRGr 4 screw placement occurred, angiography was performed to exclude VA damage.

Freehand C1-C2 screw placement

Nevertheless, this paper shows that C1 lateral mass and C2 isthmic screws may be safely inserted without any navigation assistance.

Liu et al. [11] reported on a series of 46 C1 lateral mass screws inserted in 24 consecutive patients. All C1 lateral mass screws were inserted unicortically using a microscope-assisted freehand technique. No vertebral artery injury or cerebral spinal fluid leakage during the screw insertion was observed and all the C1 screws were considered to be well positioned. They stated that C1 lateral mass screws can be inserted without fluoroscopy with microscope assistance, and they considered the intraoperative fluoroscopy time consuming, cumbersome, and dangerous as it exposes both the patient and surgical team to radiation. Simsek et al. [23] demonstrated that unicortical C1 lateral mass screws could be placed safely and rapidly without fluoroscopy guidance in 17 consecutive patients. No screw malpositions or neurovascular complications related to screw insertion were observed. They concluded that C1 lateral mass screws might be used in upper cervical spine without intraoperative fluoroscopy guidance and the use of the spinal navigation systems. In our series, all 56 C1 screws were well positioned. We personally think that fluoroscopy is a useful tool and that the total amount of radiation can be limited to few shots per procedure. It is mainly useful to decide the depth of C1 bicortical lateral mass screw in relationship to the anterior

atlas tubercle and the sagittal direction of the C2 isthmic screws in relationship to the VA groove.

Ondra et al. [16] showed that an open technique combined with lateral C-arm guidance provides rapid and safe placement of C2 pedicle screws in a retrospective review of 150 C2 pedicle screw. As we normally do, they exposed the C2 isthmic and they palpated it with a dissector to provide coronal orientation while a lateral C-arm radiograph was obtained for sagittal orientation. A total of 71 patients had bilateral screws placed and eight patients had unilateral screws placed. In this series, eight non-critical and one critical (then revised) screw misplacement occurred.

Wang et al. [31] made a retrospective radiographic study of the technique for C1 lateral mass screw (C1LMS) and C2 pedicle screw (C2PS) fixation on 319 patients with atlanto-axial instability. They used a freehand fluoroscopy-guided technique. CT angiography or magnetic resonance angiography were performed after surgery in cases with malpositioned screws to assess potential VA injury. In 95.5% of C1LMS fixations and of C2PS fixations, the screws were found to be in a "good" position, which meant a screw respecting the outer borders of C1 lateral mass and C2 isthmic in axial, sagittal and coronal cuts. Even if six cases presented with misplaced screws, no vascular problem was noted. Thus, they stated that the technique for C1LMS and C2PS fixation appears to be safe and effective for achieving posterior C1-C2 fixation.

Sciubba et al. [21] made a prospective follow-up of 55 consecutive patients who underwent C2 instrumented fusion. The cortical breaches were classified upon the percentage of screw diameter beyond the cortical edge. One hundred consecutive screws were placed. They had 15% total breaches. The magnitude of the breach was classified as I (<25%) in ten cases (66.7% of breaches), II (26-50%) in three cases (20% of breaches), III (51-75%) in one case (6.7%), and IV (76-100%) in one case (6.7%). They concluded that when the isthmic interarticularis/pedicle is assessed preoperatively with CT scan and found to be suitable for screw placement, freehand placement of screws in the C-2 pedicle could be done safely and effectively without the use of intraoperative fluoroscopy or navigation. But we argue that their 15% of total breaches is too high and not acceptable in a delicate region as C1-C2.

Stulik et al. [24] evaluated the accuracy of C1 lateral mass and C2 pedicle freehand screw placement in their series of 28 consecutive patients operated on for atlanto-axial fixation. All 56 C1 screws were well positioned and all but one were bicortical, while three of the 56 C2 screws were malpositioned (5.4%). Chen et al. [1] presented their technique for C1-C2 fixation. In their series of 11 cases, only one C2PS violated the medial wall of the pedicle without any clinical consequence. Inthe series of Vilela et al. [29], any cortical violation of C1LM was detected in the postoperative CT scans of their 11 patients (21 LM screws).

Conclusion

Knowledge of anatomical landmarks is mandatory for performing safe C1-C2 internal fixation procedures. In experienced hands, the accuracy of the freehand fluoroscopy-guided Harms-Goel technique is high. Navigation-assisted screw placement systems might reduce the rate of misplaced screws in selected cases.

Conflict of interest None.

References

1. Chen JF, Wu CT, Lee SC, Lee ST (2005) Posterior atlantoaxial transpedicular screw and plate fixation. Technical note. J Neurosurg Spine 2(3):386–392
2. Eck JC, Walker MP, Currier BL, Chen Q, Yaszemski MJ, An KN (2007) Biomechanical comparison of unicortical versus bicortical C1 lateral mass screw fixation. J Spinal Disord Tech 20(7):505–508
3. Gertzbein SD, Robbins SE (1990) Accuracy of pedicular screw placement in vivo. Spine 15(1):11–14
4. Gluf WM, Schmidt MH, Apfelbaum RI (2005) Atlantoaxial transarticular screw fixation: a review of surgical indications, fusion rate, complications, and lessons learned in 191 adult patients. J Neurosurg Spine 2(2):155–163
5. Goel A, Laheri V (1994) Plate and screw fixation for atlanto-axial subluxation. Acta Neurochir (Wein) 129(1–2):47–53
6. Harms J, Melcher RP (2001) Posterior C1-C2 fusion with polyaxial screw and rod fixation. Spine 26(22):2467–2471
7. Kamimura M, Ebara S, Itoh H, Tateiwa Y, Kinoshita T, Takaoka K (2000) Cervical pedicle screw insertion: assessment of safety and accuracy with computer-assisted image guidance. J Spinal Disord 13:275
8. Kosmopoulos V, Schizas C (2007) Pedicle screw placement accuracy: a meta-analysis. Spine 32:E111–E120
9. Kotani Y, Abumi K, Ito M, Minami A (2003) Improved accuracy of computer-assisted cervical pedicle screw insertion. J Neurosurg 99(3 Suppl):257–263
10. Kuroki H, Rengachary SS, Goel VK, Holekamp SA, Pitkänen V, Ebraheim NA (2005) Biomechanical comparison of two stabilization techniques of the atlantoaxial joints: transarticular screw fixation versus screw and rod fixation. Neurosurgery 56(1 Suppl):151–159
11. Liu G, Buchowski JM, Shen H, Yeom JS, Riew KD (2008) The feasibility of microscope-assisted "free-hand" C1 lateral mass screw insertion without fluoroscopy. Spine 33(9):1042–1049
12. Magerl F, Seeman PS (1987) Stable posterior fusion of the atlas and axis by transarticular screw fixation. In: Kehr P, Weidner A (eds) Cervical spine. Springer, Wien, pp 322–327
13. Mueller CA, Roesseler L, Podlogar M, Kovacs A, Kristof RA (2010) Accuracy and complications of transpedicular C2 screw placement without the use of spinal navigation. Eur Spine J 19 (5):809–814

14. Nottmeier EW, Foy AB (2008) Placement of C2 laminar screws using three-dimensional fluoroscopy-based image guidance. Eur Spine J 17(4):610–615
15. Oda I, Abumi K, Sell LC, Haggerty CJ, Cunningham BW, McAfee PC (1999) Biomechanical evaluation of five different occipito-atlanto-axial fixation techniques. Spine 24:2377–2382
16. Ondra SL, Marzouk S, Ganju A, Morrison T, Koski T (2006) Safety and efficacy of C2 pedicle screws placed with anatomic and lateral C-arm guidance. Spine 31(9):E263–E267
17. Paramore CG, Dickman CA, Sonntag VK (1996) The anatomical suitability of the C1-2 complex for transarticular screw fixation. J Neurosurg 85:221–224
18. Parker SL, McGirt MJ, Farber SH, Amin AG, Rick AM, Suk I, Bydon A, Sciubba DM, Wolinsky JP, Gokaslan ZL, Witham TF (2011) Accuracy of free-hand pedicle screws in the thoracic and lumbar spine: analysis of 6816 consecutive series. Neurosurgery 68(1):170–178
19. Payer M, Luzi M, Tessitore E (2009) Posterior atlanto-axial fixation with polyaxial C1 lateral mass screws and C2 isthmic screw. Acta Neurochir (Wein) 151(3):223–229
20. Richter M, Schmidt R, Claes L, Puhl W, Wilke HJ (2002) Posterior atlantoaxial fixation: biomechanical in vitro comparison of six different techniques. Spine 27(16):1724–1732
21. Sciubba DM, Noggle JC, Vellimana AK, Alosh H, McGirt MJ, Gokaslan ZL, Wolinsky JP (2009) (2009) Radiographic and clinical evaluation of free-hand placement of C-2 pedicle screws. Clinical article. J Neurosurg Spine 11(1):15–22
22. Seller K, Wild A, Urselmann L, Krauspe R (2005) Prospective screw misplacement analysis after conventional and navigated pedicle screw implantation. Biomed Tech 50(9):287–292
23. Simsek S, Yigitkanli K, Seckin H, Akyol C, Belen D, Bavbek M (2009) Freehand C1 lateral mass screw fixation technique: our experience. Surg Neurol 72(6):676–681
24. Stulik J, Vyskocil T, Sebesta P, Kryl J (2007) Atlantoaxial fixation using the polyaxial screw-rod system. Eur Spine J 16(4):479–484
25. van de Kraats EB, van Walsum T, Kendrick L, Noordhoek NJ, Niessen WJ (2006) Accuracy evaluation of direct navigation with an isocentric 3D rotational X-ray system. Med Image Anal 10(2):113–124
26. van de Kraats EB, van Walsum T, Verlaan JJ, Voormolen MH, Mali WP, Niessen WJ (2006) Three-dimensional rotational X-ray navigation for needle guidance in percutaneous vertebroplasty: an accuracy study. Spine 31(12):1359–1364
27. Verlaan JJ (2008) Placement of C2 laminar screws using three-dimensional fluoroscopy-based image guidance by Eric W. Nottmeier and Andrew B. Foy. Eur Spine J 17(4):616–617
28. Verma R, Krishan S, Haendlmayer K, Mohsen N (2010) A functional outcome of computer-assisted spinal pedicle screw placement: a systematic review and meta-analysis of 23 studies including 5,992 pedicle screws. Eur Spine J 19(3):370–375
29. Vilela MD, Jermani C, Braga BP (2006) C1 lateral mass screws for posterior segmental stabilization of the upper cervical spine and a new method of three-point rigid fixation of the C1-C2 complex. Arq Neuropsiquiatr 64(3B):762–767
30. Wang MY, Samudrala S (2004) Cadaveric morphometric analysis for atlantal lateral mass screw placement. Neurosurgery 54 (6):1436–1440
31. Wang S, Wang C, Wood KB, Yan M, Zhou H (2011) Radiographic evaluation of the technique for C1 lateral mass and C2 pedicle screw fixation in three hundred nineteen cases spine. Spine (Phila Pa 1976)36(1):3-8
32. Wright NM, Lauryssen C (1998) Vertebral artery injury in C1-2 transarticular screw fixation: results of a survey of the AANS/CNS section on disorders of the spine and peripheral nerves. American Association of Neurological Surgeons/Congress of Neurological Surgeons. J Neurosurg 88:634–640

Comment

The authors present a series of 28 patients treated with C1-2 fusion using C1 lateral mass C2 isthmus screws placed with a freehand technique based on anatomical landmarks. There were no significant screw-related complications and screw placement was accurate based on postoperative CT in the vast majority of screws, with results comparable with series using computer-aided navigation. While this is only a retrospective case series, it emphasizes the fact that well-trained surgeons do not require the use of expensive adjuncts to perform procedures. A thorough knowledge of patient anatomy and adequate training allow for the safe performance of these procedures.

Daniel Resnick
Wisconsin, USA

Acta Neurochir (2011) 153:1427–1434
DOI 10.1007/s00701-011-1043-0

CLINICAL ARTICLE

Microsurgical fenestration of perineural cysts to the thecal sac at the level of the distal dural sleeve

Axel Neulen · Sven R. Kantelhardt · Sara M. Pilgram-Pastor · Imke Metz · Veit Rohde · Alf Giese

Received: 23 February 2011 / Accepted: 26 April 2011 / Published online: 12 May 2011

Abstract
Background Surgery for symptomatic sacral perineural cysts remains an issue of discussion. Assuming micro-communications between the cyst and thecal sac resulting in a valve mechanism and trapping of CSF as a pathomechanism, microsurgical fenestration from the cyst to the thecal sac was performed to achieve free CSF communication.
Methods In 13 consecutive patients (10 female, 3 male), MRI revealed sacral perineural cysts and excluded other pathologies. Micro-communication between the thecal sac and the cysts was shown by delayed contrast filling of the cysts on postmyelographic CT. Surgical fenestration achieved free CSF communication between the thecal sac and cysts in all patients. The patient histories, follow-up examinations and self-assessment scales were analyzed. Symptoms at initial presentation included lumbosacral pain, pseudoradicular symptoms, genital pain and urinary dysfunction. Mean follow-up was 10.7±6.6 months.
Findings Besides one CSF fistula, no surgical complications were observed. Five patients did not improve after surgery; in four of these cases multiple cysts were found, but small and promptly filling cysts remained untreated. Seven patients reported lasting benefit following surgery; three of these had single cysts, and all had cysts >1 cm. One patient initially benefited from cyst fenestration but experienced recurrent pain within 2 months postoperatively. Re-myelography revealed delayed contrast filling of the recurrent cyst; however, surgical revision did not lead to an improvement despite successful fenestration and collapse of the cyst revealed by postoperative imaging.
Conclusions Microsurgical fenestration of sacral perineural cysts to the thecal sac is a surgical approach that has shown success in the treatment of lumbosacral pain, pseudoradicular symptoms, genital pain and urinary dysfunction associated with sacral perineural cysts. Our analysis, however, shows that mainly patients with singular large cysts benefit from this treatment.

Keywords Sacral perineural cyst · Tarlov cyst · Meningeal cyst · Meningeal diverticulum · Sacral radiculopathy

Parts of this study were presented at the 61st Annual Meeting of the German Society of Neurosurgery (DGNC) in 2010.

A. Neulen · S. R. Kantelhardt · S. M. Pilgram-Pastor · V. Rohde · A. Giese
Department of Neurosurgery, Center of Neurological Medicine, University of Göttingen, Göttingen, Germany

S. M. Pilgram-Pastor
Department of Neuroradiology, Center of Neurological Medicine, University of Göttingen, Göttingen, Germany

I. Metz
Department of Neuropathology, Center of Neurological Medicine, University of Göttingen, Göttingen, Germany

A. Neulen (✉) · S. R. Kantelhardt · A. Giese
Department of Neurosurgery, Johannes Gutenberg University of Mainz, Langenbeckstrasse 1, 55131 Mainz, Germany
e-mail: axel.neulen@gmx.de

Introduction

Sacral perineural cysts (Tarlov cysts) are cysts of the sacral nerve roots. They rarely become symptomatic, but have been associated with lumbar and sacral pain, pseudoradicular and radicular symptoms, and bowel and bladder dysfunction [1–5, 7, 10, 11]. Perineural cysts, most of

which were asymptomatic, showed a prevalence of 1.5% to 4.6% in radiological studies [6, 9]. Their etiology remains unclear (reviewed in [5]). Micro-communications at the distal dural sleeve of the nerve root functioning as a valve that allows CSF influx while restricting CSF efflux is thought to be one possible underlying pathomechanism of perineural cyst growth [8]. Cyst expansion may eventually lead to irritation or compression of the affected or adjacent nerve roots, and erosion of surrounding bone with consecutive irritation of periostal pain fibers.

Cystic lesions of the sacral region can be diagnosed by CT or MRI. The presence of a communication between the cyst and thecal sac differentiates perineural cysts from other cystic lesions [8]. These micro-communications can be demonstrated by myelography and postmyelographic CT. Delayed contrast filling of the cystic lesion indicates the presence of micro-communications and hence a possible valve mechanism [1, 2, 7, 8, 11].

Surgical management of sacral perineural cysts remains a matter of discussion. Numerous strategies have been proposed, including cyst fenestration, cyst imbrication, cyst resection, neck ligation and percutaneous aspiration [1–5, 7, 10, 11]. Based on the supposed pathomechanism, we used a microsurgical approach for symptomatic sacral perineural cysts that establishes a free communication between the thecal sac and the perineural cyst. In this study we report our experience with 13 patients who underwent surgery for sacral perineural cysts between June 2008 and October 2010.

Patients and methods

Patients

The study was approved by the ethics committee of the medical faculty of the University of Göttingen, protocol no. 23/7/09. Patients who presented with lumbosacral pain, pseudoradicular and radicular symptoms, genital pain or urinary dysfunction were examined by MRI and routine neurological examination. If cystic lesions of the sacral region were diagnosed, other reasons for patients' symptoms were excluded. If conservative treatment failed to relieve symptoms, myelography with early and delayed postmyelographic CT was performed.

The early postmyelographic plain x-rays and CT scans were obtained directly after contrast application; late postmyelographic CT was done 3–4 h after contrast application. Delayed filling of cysts becomes apparent as lack or partial contrast filling of the cyst in the early postmyelographic CT and increased contrast filling in the late postmyelographic CT, which can be verified by an increase in Hounsfield units (Fig. 1). Patients with promptly

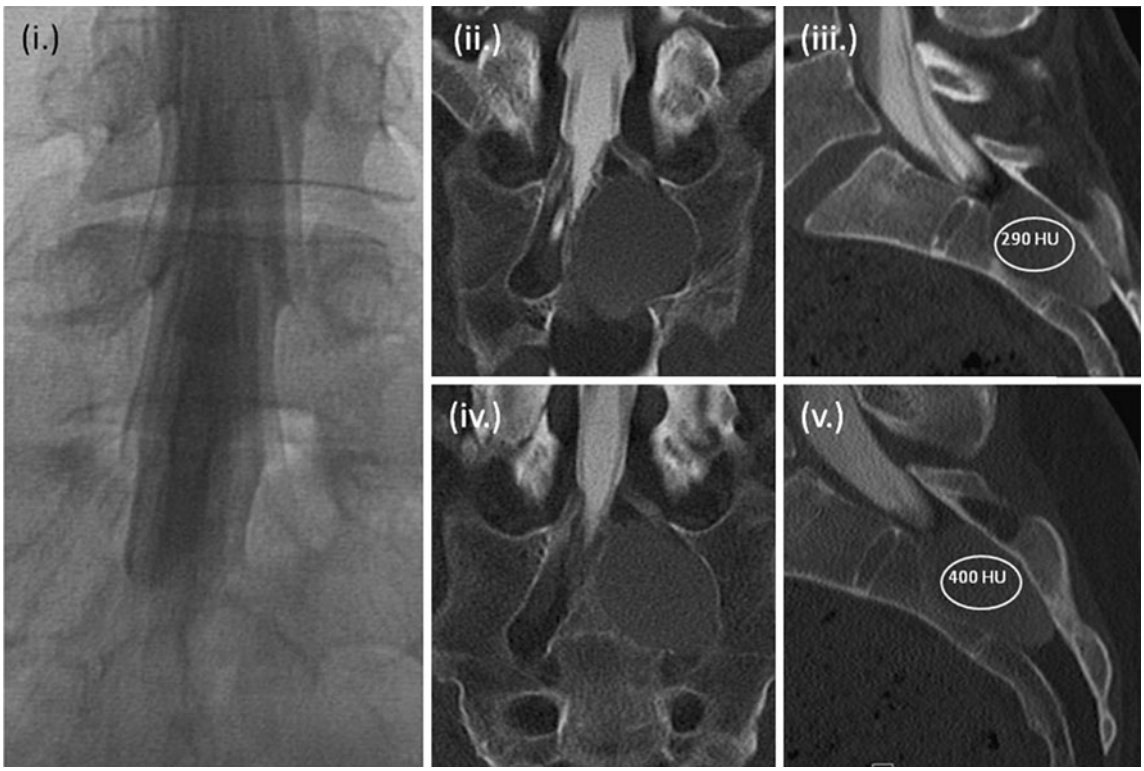

Fig. 1 Imaging findings. Anteroposterior myelography (i), coronal (ii, iv) and sagittal (iii, v) postmyelographic CT reformations demonstrated a delayed contrast filling of the cysts in all patients considered for surgery (ii and iii: early postmyelographic CT; iv and v: late postmyelographic CT). Numbers indicate a ROI analysis for Hounsfield units (HU)

contrast enhancing lesions in myelography and early postmyelographic CT were not scheduled for surgery, while delayed contrast filling indicated the presence of micro-communications and a possible valve mechanism. In these patients surgery was considered. Ten patients had two or more cysts; in seven of these only the largest cysts thought to be responsible for the patient's symptoms were treated, while small and promptly filling cysts were not operated on.

Microsurgical technique

Patients were operated on in the prone position under general anesthesia. A 4-cm skin incision was placed directly over the lesion (usually between L5 to S3). The sacrum was exposed, and unroofing of the sacral canal and dorsal aspects of the neuroforamen exposed the cyst. The thecal sac was exposed at the level of S1. Care was taken to preserve the integrity of the cyst wall, and dissection of the cyst from surrounding structures was limited to what was essential to expose the neck of the cyst and identify the dural sleeve of the involved nerve root (Fig. 2, i–ii). The dura of the thecal sac was opened, and CSF was drained; during CSF drainage the cyst remained filled in all cases (Fig. 2, iii), proving a restricted CSF communication suggestive of the proposed valve mechanism. The course of the involved nerve root into the dural sleeve was identified, and the dural incision was extended into the dural sleeve of the nerve root under direct microscopic visualization of the nerve (Fig. 2, iv–vi). The dural incision was continued distally and the nerve was followed into the cyst, which led to collapse of the cyst. Typically the nerve root thinned at the entry into the cyst and became part of the ventral and medio-dorsal cyst wall (Fig. 2, vii). At the termination of the dural sleeve, fibrous arachnoidal tissue was typically found to be circular and adherent to the nerve root, obstructing the neck of the cyst. The fibrous tissue was resected, the nerve root was entirely freed, and a communication through the fibrous barrier between the cyst and thecal sac was established (Fig. 2, vii). A biopsy was taken from translucent parts of the cyst wall where possible. The cyst wall was mobilized, and plication of the cyst was performed. The dural incision and the cyst wall were closed using 6.0 non-resorbable sutures; if indicated, duraplasty was performed at the neck of the dural sleeve of the nerve root. At the end of surgery free macrocommunication between the cyst and thecal sac was established in all cases (Fig. 2, viii). After dura closure lumbar drains were not required. Patient mobilization started on postoperative day 1.

Neurological outcome and pain assessment

A retrospective analysis of the patients' history was performed by review of the patient charts. Additional information was gathered from self-assessment scales and telephone interviews. Assessment included (1) preoperative symptoms, (2) number, size and location of cysts, and (3) improvement of symptoms. Symptoms were summarized in the following categories: (1) lumbosacral pain, (2) pain radiating into the buttocks, (3) pain radiating into the legs, (4) genital pain, (5) bowel/bladder dysfunction, and (6) pain radiating into the groin and abdomen.

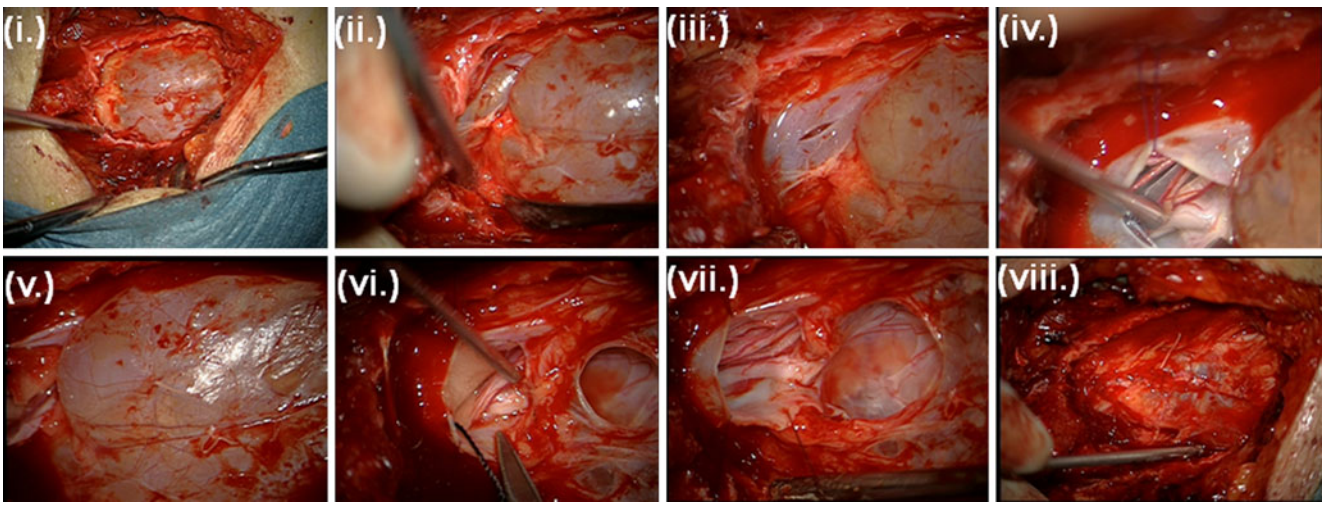

Fig. 2 Surgical approach. A sacral laminectomy was performed (i), and the thecal sac and the cyst were exposed (ii). The thecal sac was opened (iii), and the nerve was followed intradurally through the dural sleeve of the nerve root into the cyst (iv). Because of a valve mechanism the cysts did not collapse even though the thecal sac was opened (v). Fibrous arachnoidal tissue obstructing the neck of the cyst was resected, establishing a communication between the cyst and the thecal sac (vi, vii). The dura was then closed with watertight sutures. Where feasible, plication of the cyst was performed (viii)

Histopathological examination

Specimens were fixed in 4% paraformaldehyde and embedded in paraffin; 4-μm-thick slices were stained with hematoxylin and eosin (HE), elastica van Gieson stain and periodic acid-Schiff stain (PAS). Immunohistochemical staining for neurofilaments was performed with a biotin-avidin technique. Anti-NF antibody was used as primary antibody (anti-NF200, Sigma-Aldrich, USA).

Results

Epidemiology and clinical characteristics

Between June 2008 and October 2010, a total of 1,873 operations were performed for various spinal disorders. Thirteen patients during this period were treated for symptomatic perineural cysts and were included in this study. Mean age at surgery was 60±9.8 years. Ten patients were female and three male. Symptoms had been present for 8.7±11.5 years (6 months to 30 years). Postoperative mean follow-up was 10.7±6.6 months (2.5 to 20 months). All perineural cysts originated from the nerve roots S1, S2 or S3. Lumbosacral pain was the most frequent symptom (10 of 13), followed by pain radiating into the buttocks (8 of 13), legs (7 of 13), groin and abdomen (4 of 13), genital pain (3 of 13) and bowel/bladder dysfunction (3 of 13). Figure 3 gives an overview of symptoms. No patient had a history of trauma or infection.

Clinical course

Five patients did not improve, while eight patients significantly benefited from surgery. Mostly, patients were discharged from the hospital on postoperative day 10 (5 to 14 days). One patient had to be treated with a lumbar drain for 7 days because of CSF fistula. No other complications were observed. One of the patients who initially improved experienced recurrent pain after 2 months. Re-myelography and postmyelographic CT again showed delayed postmyelographic contrast filling of a recurrent cyst; however, the patient did not benefit from reoperation, despite successful refenestration and duraplasty resulting in complete collapse and disappearance of the cyst demonstrated by postoperative imaging.

Analysis of outcome

All five patients who did not improve after surgery had multiple cysts, and in four of these patients one or several small or promptly filling cysts remained untreated; in two of the patients who did not improve, the operated cysts were smaller than 1 cm in diameter.

Of the eight patients who benefited from surgery, three had single cysts (among these was the patient with recurrent symptoms and reoperation). Two patients had two cysts with delayed contrast filling of similar size each. In both patients both cysts were treated. Three patients had multiple cysts, and only large and delayed filling cysts were operated on. In all patients who improved, the operated cysts were >1 cm in diameter (1.2 cm to 3 cm).

Of eight patients who answered to a questioner whether surgery was successful, four responded with “no” and four with “yes.” Of those who responded with “no,” three had two cysts and only the larger cyst had been operated on. The remaining patient was the one with a single cyst who suffered a relapse of pain after an initial pain-free period. Of the four patients who responded with “yes,” two had been treated for single cysts, and two others had two cysts and both cysts had been operated on.

Improvement related to the different symptoms was analyzed. The best improvement was documented for pain radiating into the legs and buttocks, genital pain and lumbosacral pain while improvement of bowel/bladder dysfunction and pain radiating into the groin and abdomen was observed less frequently (Fig. 4).

Histological results

HE staining showed the cyst wall with membranous tissue (Fig. 5, i). Similar to other studies, nerve fibers embedded into connective tissue were detected (Fig. 5, ii, Elastica van Gieson stain for connective tissue and Fig. 5, iii, anti-NF staining for nerve fibers). There was no evidence of inflammation.

Discussion

This report summarizes the experience from 13 patients who underwent surgical treatment for sacral perineural cysts in a single neurosurgical department between 2008 and 2010. The epidemiological characteristics of the patients in our study are similar to those reported in other series [2, 5]. This is one of the largest series reported so far; to our knowledge, only one larger series of 15 patients has been presented previously [2]. However, in the latter study an approach based on cyst resection was used.

The etiology of sacral perineural cysts remains unclear [5]. However, there is general acceptance that enlargement of the cysts is caused by pulsatile and hydrodynamic forces of CSF entering the cyst combined with a valve mechanism that only allows influx of CSF [1, 2, 5, 7, 8,

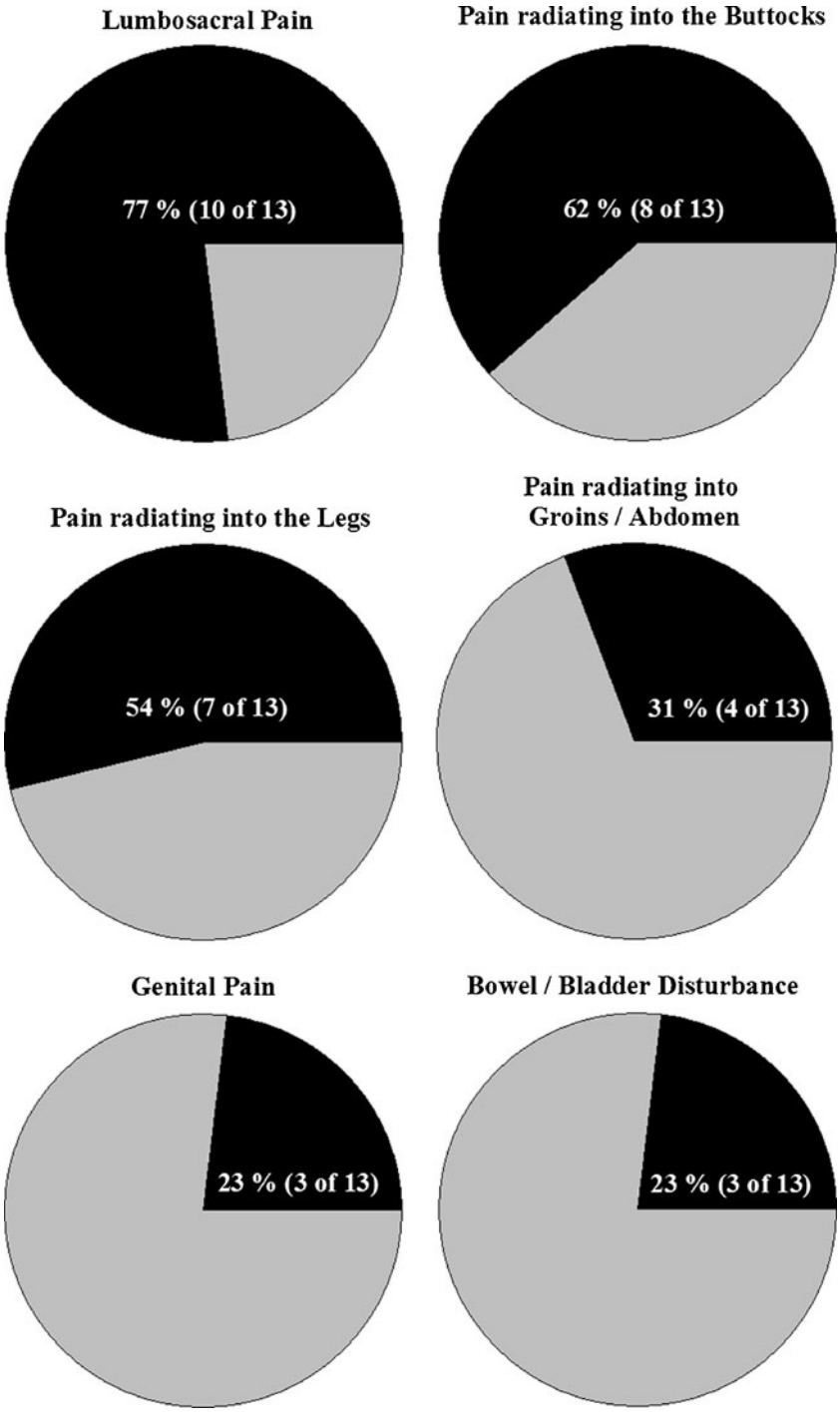

Fig. 3 Patient characteristics—relative frequency of different symptoms prior to surgery. Symptoms were categorized as lumbosacral pain, pain radiating into the buttocks, legs, groin and abdomen, genital pain and bowel/bladder dysfunction

10, 11]. Similar to other studies [1, 2, 7, 11], the diagnosis of a cystic lesion of the sacral area was followed by myelography with early and late postmyelographic CT. This invasive imaging modality allows diagnosis of communications between the cyst and thecal sac, which is suspected to function as a valve. Delayed filling after intrathecal contrast application is therefore typical; this phenomenon was demonstrated by the delayed increase in Hounsfield units within the cyst compared to the thecal sac (Fig. 1) and was the main criteria for patient selection. The valve mechanism was further confirmed by our intraoperative findings. All cysts did not collapse after incision of the thecal sac and CSF drainage, but remained filled until the cyst itself was opened (Fig. 2, iii–v).

The symptoms associated with perineural cysts can be attributed to (1) radicular involvement, i.e., sacral ischialgia and bowel/bladder dysfunction. Radicular symptoms may either result from compression of neighboring nerve roots

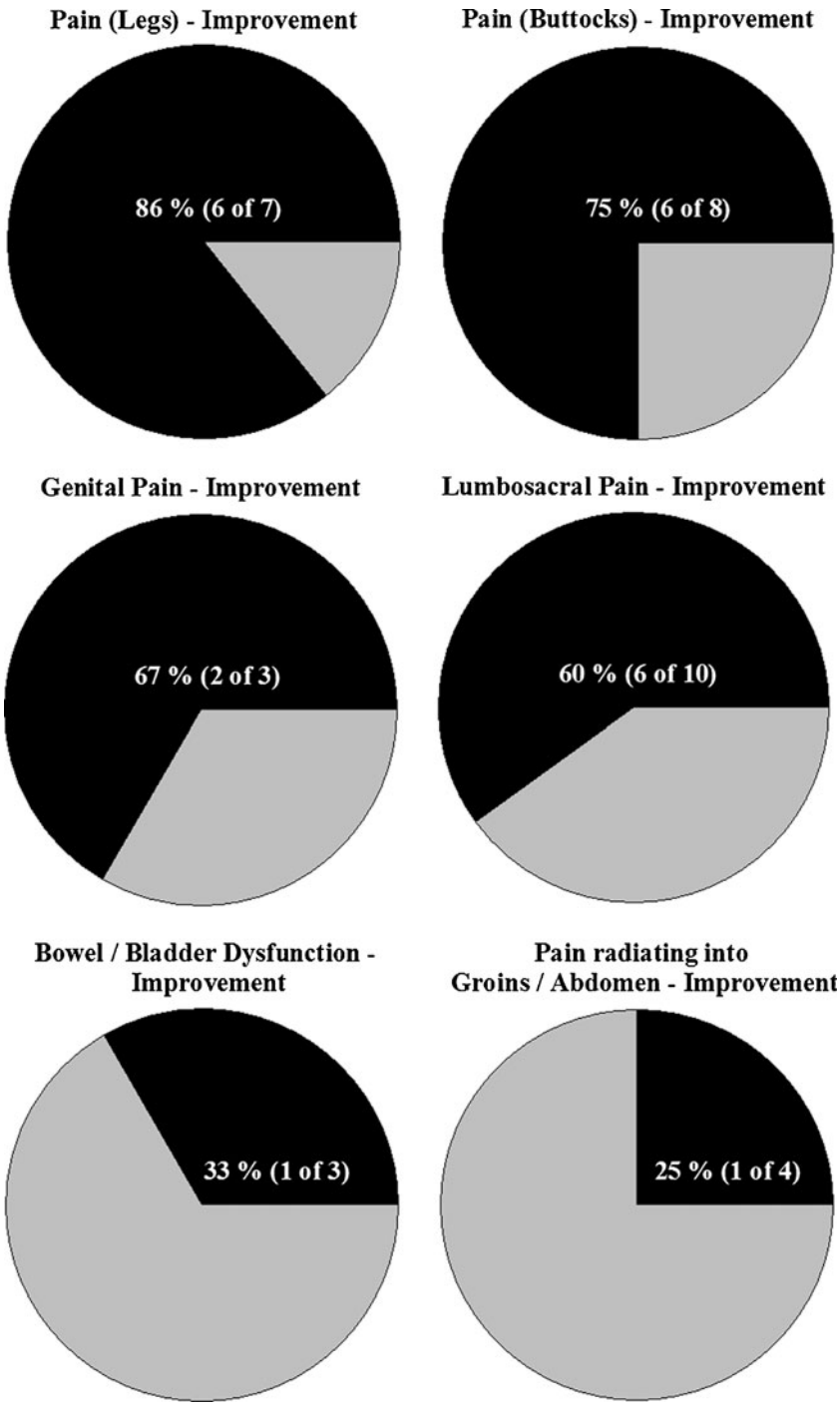

Fig. 4 Patient improvement rate for different symptoms (Fig. 3)

or from direct impairment of the affected nerve root itself. Further explanations for symptoms are (2) bone erosion and compression of periostal pain fibers, which may result in sacral pain, and (3) pseudoradicular radiation of pain into the buttocks, legs and groin. Our results imply that symptoms that can be attributed to bone erosion and pseudoradicular radiation are more likely to benefit from surgery than radicular symptoms (Fig. 4). The latter may be influenced by permanent impairment of the nerve itself because of structural changes of the nervous tissue as a consequence of compression or stretching by the expanding cyst, which may result in chronic deafferentiation pain.

Different surgical approaches have been used to treat perineural cysts. Most approaches are based on resection or fenestration of the cyst wall into the epidural space [2, 10, 11], which may be followed by closure of the defect with muscle flap, gel foam or fibrin glue [1, 5], or neck ligation

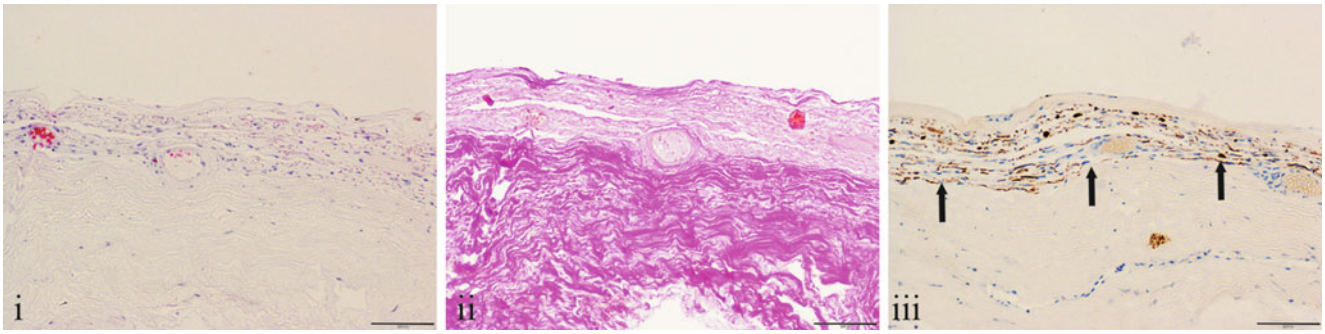

Fig. 5 Histology revealed membranous connective tissue: (i) HE staining and (ii) Elastica van Gieson stain. Nerve fibres were superficially embedded within the connective tissue [marked by arrows in (iii), anti-NF antibody]. Original magnification (OM): ×100. Scale bar: 500 μm

after cyst wall resection [7]. The authors of the latter study used image-guided percutaneous aspiration of cyst contents, which induced a collapse of the cyst and hence reduced symptoms, as a diagnostic tool prior to surgery [7]. One study reports a case of cyst fenestration and intraoperative drainage of fluid [3]; furthermore, shunting of the sacral cyst to the peritoneum has been proposed [4]. In contrast, our approach aims to establish free CSF communication between the thecal sac and cyst in order to eliminate the valve mechanism rather than resection or disruption of the cyst wall. To the best of our knowledge, this is the first study reporting a patient series using this approach despite the fact that this microsurgical approach is also used by other neurosurgical centers.

In 8 of 13 patients symptoms improved significantly, while 5 patients did not benefit from the procedure. Careful review of imaging and clinical data revealed that in our collective, patients with small cysts (<1 cm) did not benefit from surgery. This finding corresponds to the results of Voyadzis and co-workers who observed a correlation between cyst size and clinical outcome [11]. Therefore, we suggest that cysts of a <1 cm diametershould be approached with caution even in the presence of delayed contrast filling on postmyelographic CTs. Further, we observed that in our collective all patients who did not benefit from surgery had multiple cysts, and in four of these patients small or promptly contrast-enhancing cysts remained untreated. In contrast, only three of the eight patients who improved after surgery had multiple cysts, of which, however, like in the no-benefit group, small and not promptly contrast-enhancing cysts were not treated surgically. The other five patients who benefited from surgery had either large single cysts or multiple cysts of similar size, which were all treated surgically.

Therefore, we propose that:

1. In cases with multiple delayed filling cysts of similar size, all cysts should be treated surgically. We did not observe any difference in clinical outcome for patients with single or multiple large (>1 cm) cysts with documented delayed contrast filling on postmyelographic CT scans, if all cysts were treated surgically.
2. If multiple cysts are present, of which one or several cysts have a diameter of <1 cm or one or several cysts show prompt postmyelographic contrast filling, patients should be carefully and critically informed about the risk of residual symptoms, because in our collective five of eight patients with multiple cysts of this type did not significantly benefit from surgery.

Finally, these data have to be interpreted with caution because of the relatively small size of our patient collective and the heterogenic nature of single or multiple cysts of various sizes, which may have prognostic significance as suggested by our study. Furthermore, this study is a retrospective case collection with its inherent limitations. However, all other reported series of this rarely treated entity are small and have reported various treatment strategies, which makes final recommendations on surgical strategies difficult. A prospective study will be needed to further investigate the treatment approach suggested by the present study.

Conclusion

Microsurgical fenestration between perineural cysts and the thecal sac is a safe surgical approach in the treatment of symptomatic cysts yielding results comparable to patient series with other surgical strategies [5, 11]. Major complications are rare: 1 case of CSF leakage that was treated successfully by a lumbar drain for 7 days in a series of 13 patients. Our data suggest that patients with single or multiple perineural cysts of >1 cm in diameter and delayed contrast filling on postmyelographic CTs benefit from surgery, but all of these lesions have to be treated surgically. Patients with cysts <1 cm in diameter did not significantly benefit from surgery. If multiple lesions were present, of

which some were smaller than 1 cm or promptly filling with contrast on postmyelographic CTs, patients had a significant risk of remaining symptomatic.

Conflicts of interest None.

References

1. Acosta FL Jr, Quinones-Hinojosa A, Schmidt MH, Weinstein PR (2003) Diagnosis and management of sacral Tarlov cysts. Case report and review of the literature. Neurosurg Focus 15:E15
2. Caspar W, Papavero L, Nabhan A, Loew C, Ahlhelm F (2003) Microsurgical excision of symptomatic sacral perineurial cysts: a study of 15 cases. Surg Neurol 59:101–105
3. Chaiyabud P, Suwanpratheep K (2006) Symptomatic Tarlov cyst: report and review. J Med Assoc Thai 89:1047–1050
4. Guest JD, Silbert L, Casas CE (2005) Use of percutaneous endoscopy to place syringopleural or cystoperitoneal cerebrospinal fluid shunts: technical note. J Neurosurg Spine 2:498–504
5. Guo D, Shu K, Chen R, Ke C, Zhu Y, Lei T (2007) Microsurgical treatment of symptomatic sacral perineurial cysts. Neurosurgery 60:1059–1065
6. Langdown AJ, Grundy JR, Birch NC (2005) The clinical relevance of Tarlov cysts. J Spinal Disord Tech 18:29–33
7. Lee JY, Impekoven P, Stenzel W, Löhr M, Ernestus RI, Klug N (2004) CT-guided percutaneous aspiration of Tarlov cyst as a useful diagnostic procedure prior to operative intervention. Acta Neurochir (Wien) 146:667–670
8. Nabors MW, Pait TG, Byrd EB, Karim NO, Davis OD, Kobrine AI, Rizzoli HV (1988) Updated assessment and current classification of spinal meningeal cysts. J Neurosurg 68:366–377
9. Paulsen RD, Call GA, Murtagh FR (1994) Prevalence and percutaneous drainage of cysts of the sacral nerve root sheath (Tarlov cysts). AJNR Am J Neuroradiol 15:293–297
10. Tanaka M, Nakahara S, Ito Y, Nakanishi K, Sugimoto Y, Ikuma H, Ozaki T (2006) Surgical results of sacral perineural (Tarlov) cysts. Acta Med Okayama 60:65–70
11. Voyadzis JM, Bhargava P, Henderson FC (2001) Tarlov cysts: a study of 10 cases with review of the literature. J Neurosurg 95:25–32

Comment

This is an interesting article. It touches on a subject for which a clear decision-making process still eludes us: Which sacral neural cysts are really symptomatic and therefore deserve surgical treatment, and if so, what should the operation consist of ?

In a period of 3 years a total of 13 patients were operated on for 'symptomatic' sacral neural cysts.

As stated by the authors, this number, albeit not very large, from a merely statistical standpoint certainly is clinically considerable. Despite the fact that these cysts are diagnosed with relative frequency, it is often difficult to understand what type of causal relationship if any they have with the patient's complaints.

The authors have carefully imaged these cysts preoperatively, paying close attention to what they think is the main feature contributing to symptoms, that is, the ball and valve communication between the cal sac and the cyst.

The outcome was not great. Five+one patient did not benefit from surgery, which amounts to virtually 50% bad results.

The authors argue that the rest of the patient population clearly benefited in terms of symptom relief, and they are convinced that they have isolated the factors associated with non-response and make their recommendations based on this assumption.

As stated, there are some caveats to the series. In statistical terms it is too small to draw any evidence from it, and even if we did the number of non-respondents to surgery certainly would advise thinking twice before recommending it. The fact that it is retrospective and that it does not have any control population with alternative treatment to match it with is of consideration, especially with this clinical entity where it is so difficult to really get a grip and understand what is causing what in terms of symptoms (as signs are so infrequent). In this sense it is always useful to include some form of patient self-assessment asking how they rated their pre- and postoperative condition and whether they would go back for the procedure once more knowing that these were the expected results.

The authors are encouraged to pursue their clinical investigation in a prospective manner and to come back to us hopefully in the near future with more patients for whom they have applied their final recommendations.

Manuel Cunha e Sa
Almada, Portugal

Acta Neurochir (2011) 153:1435–1442
DOI 10.1007/s00701-011-0952-2

EXPERIMENTAL RESEARCH

Lumbosacral intrathecal nerve roots: an anatomical study

Mehmet Arslan · Ayhan Cömert · Halil İbrahim Açar · Mevci Özdemir · Alaittin Elhan · İbrahim Tekdemir · Shane R. Tubbs · Ayhan Attar · Hasan Çağlar Uğur

Received: 17 July 2010 / Accepted: 19 January 2011 / Published online: 25 March 2011

Abstract
Background The lumbosacral intrathecal anatomy is complex because of the density of nerve roots in the cauda equina. Space-occupying lesions, including disc herniation, trauma and tumor, within the spinal canal may compromise the nerve roots, causing severe clinical syndromes. The goal of this study is to provide spinal surgeons with a detailed anatomical description of the intrathecal nerve roots and to emphasize their clinical importance.
Method Ten formalin-fixed male cadavers were studied. They were dissected with the aid of a surgical microscope, and measurements were performed.
Results The number of dorsal and ventral roots ranged from one to three. The average diameter of roots increased from L1 to S1 (0.80 mm for L1 and 4.16 for S1), respectively. Then their diameter decreased from S1 to S5 (4.16 mm for S1, 0.46 mm for S5). The largest diameter was found at S1 and the smallest at S5. The average number of rootlets per nerve root increased from L1 to S1, then decreased (3.25 for L1, 12.6 for S1, and 1.2 for S5), respectively. The greatest rootlet number was seen at S1, and the fewest were observed at S5. The average diameter of the lateral recess gradually decreased from L1 to L4 (9.1 mm for L1; 5.96 mm for L4) and then increased at L5 level (6.06 mm); however, the diameter of the nerve root increased from L1 to L5. The midpoint of distance between the superior and inferior edge of the intradural exit nerve root was 3.47 mm below the inferior edge of the superior articular process at the L1 level, while the origin of the L5 exit root was 5.75 mm above the inferior edge. The root origin gradually ascended from L1 to L5.
Conclusions The findings of this study may be valuable for understanding lesions compressing intradural nerve roots and may be useful for intradural spinal procedures.

Keywords Anatomy · Cadaver · Cauda equina · Intrathecal nerve root · Lateral recess

M. Arslan
Department of Neurosurgery, Yuzuncu Yıl University,
Faculty of Medicine,
Van, Turkey

A. Cömert (✉) · H. İ. Açar · A. Elhan · İ. Tekdemir
Department of Anatomy, Ankara University, Faculty of Medicine,
Ankara, Turkey
e-mail: comertayhan@yahoo.com

M. Özdemir
Neurosurgery Clinic, Ergani State Hospital,
Diyarbakir, Turkey

S. R. Tubbs
Pediatric Neurosurgery, Children's Hospital,
Birmingham, AL, USA

A. Attar · H. Ç. Uğur
Department of Neurosurgery, Ankara Üniversitesi Tıp Fakültesi,
İbni Sina Hastanesi Beyin Cerrahisi,
06100 Sıhhıye Ankara, Turkey

H. Ç. Uğur
e-mail: ugurhc@yahoo.com

Introduction

The lumbosacral intrathecal anatomy is complex because of the density of nerve roots and is of special interest clinically because of the high frequency of injury to this region [7]. The organization of the intrathecal nerve roots and their cross-sectional anatomy in the cauda equina at each intervertebral disc level has been well described anatomically using in situ fixation techniques and embedding to stabilize the nerve roots and radiologically [4, 5, 8, 12, 13,

15, 18, 24, 25]. Previously studies have provided information regarding positions of the nerve roots in the cauda equina. However, detailed information regarding this anatomy is lacking in the literature. This study aimed to characterize the exiting nerve roots (just before leaving the thecal sac) at the anterolateral region of thecal sac. Such data may be important for resection of intrathecal tumors and for the diagnosis of lumbosacral radiculopathy, and may aid our understanding of nerve root injuries from other various intrathecal pathological processes.

Materials and methods

Ten male formalin-fixed cadavers (21 to 72 years of age at death) from the Department of Anatomy were used to analyze the intrathecal lumbosacral nerve roots. Specimens with gross deformities, with facet hypertrophy, with disc disease and with prior spinal surgery were excluded from this study. Cadavers were placed in the prone position, and complete removal of all soft tissue from the vertebrae was performed. Next, laminectomies were performed with medial facet removal from T8 to the sacrum. In order to expose the neural elements in the thecal sac, the dura and arachnoid mater were opened carefully in the lumbosacral region. All cauda equina roots were exposed. Microdissection was performed under a surgical microscope (Zeiss OPMI 9-FC). The anteroposterior diameter of the osseous lateral recess was measured, and the relationship of the exiting nerve root (just before leaving the thecal sac) to the superior articular process was identified. In order to expose the exit of the nerve root located medially to the pedicle, the facets were removed. In the ventrolateral area of the cauda equina, the layered ventral and dorsal nerve roots were identified for each segment at each lumbar intervertebral disc level. Also the nerve roots were followed from the distal (dural sleeve) to proximal (origin at the conus medullaris) regions to determine anastomoses between nerve roots. Symmetric structures were measured bilaterally. Measurements were made using a digital caliper accurate to 0.01 mm. Statistical analysis was used to determine the average, standard deviation (SD) and minimum and maximum values. Wilcoxon signed ranks tests were used in order to detect differences between the right and left sides ($p<0.05$ was set for statistical significance). The following measurements were obtained:

1. The number of dorsal and ventral roots forming the spinal nerves
2. The diameter of dorsal and ventral roots
3. The number of dorsal and ventral rootlets per nerve root
4. Anteroposterior diameter of the osseous lateral recess
5. The distance between the midpoint of the distance between the superior edge and inferior edge of the intrathecal exit nerve root (x) and the inferior edge of the superior articular process (y). The x point is at the level of the origin of the root sheath (just before the nerve leaves the thecal sac).

Results

In the cauda equina, it was observed that the nerve roots were densely situated (Fig. 1). Dissections revealed that the exiting ventral root was directly over the disc space, although the sensory bundle was always located away from the intervertebral disc and coursed in close proximity to the pedicles (Fig. 2).

A total of 200 ventral and 257 dorsal roots were found bilaterally in 10 specimens. In this study, with an increasing dorsal root number from L1 to L5, one ventral root was always found for each segment on each side; for L1 roots, there was a single dorsal root in 12 specimens, two roots in 7 specimens and three in 1 specimen; for L2, one in 12 specimens and two in 8 specimens; for L3, one in 8 specimens and two in 12 specimens; for L4, one in 7 specimens, two in 12 specimens and three in 1 specimen; and for L5, one in 5 specimens and two in 15 specimens

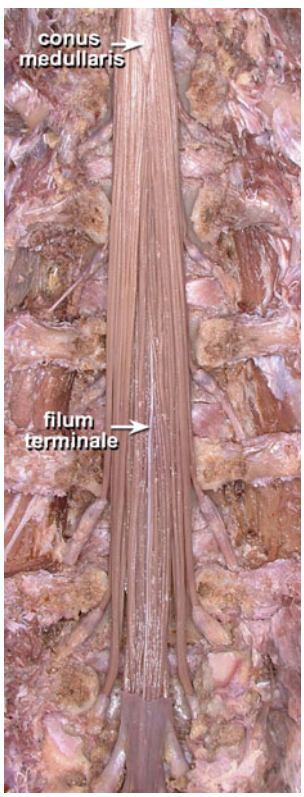

Fig. 1 Posterior view of the cauda equina

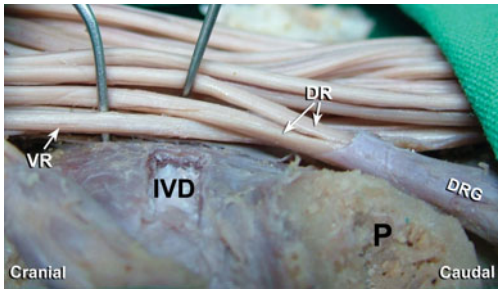

Fig. 2 Picture showing the relationship among the intervertebral disc, pedicle and roots. The motor root has a very close relationship with the intervertebral disc; the dorsal root is situated in close proximity to the pedicle. DRG: dorsal root ganglion, DR: dorsal root, VR: ventral root, IVD: intervertebral disc, P: pedicle

(Fig. 3). There was one ventral root and one dorsal root for each segment on each side in the sacral region; there were significant differences between the right and left sides for the dorsal roots of L5 ($p<0.05$) (Table 1).

The diameter of the roots increased from L1 to S1 because of an increasing number of rootlets (0.80, 1.17, 1.68, 3.15, 3.42, 4.16 mm for L1, L2, L3, L4, L5, S1 nerve roots, respectively) and then decreased toward S5. The average diameter of the dorsal and ventral roots was smallest at S5 (0.34, 0.12 mm) and was largest at S1 (2.67, 1.49). Meaningful differences between sides were observed for dorsal roots at L2, L5, S2 and S5, and ventral roots of L5 and S3 ($p<0.05$) (Table 1).

The number of rootlets per nerve root increased in a rostrocaudal direction (from L1 to S1) then decreased toward S5 (Fig. 4); dorsal and ventral roots having the smallest average number of rootlets were at S5 (0.70, 0.50) and the greatest at S1 (8.60, 4.0). In all, the number of dorsal rootlets was greater compared to ventral rootlets. Significant differences were observed for dorsal L2 and ventral L4 and L5 between the right and left sides ($p<0.05$), respectively (Table 1).

Several interneural connections were identified. The ratio of interconnections was not documented because they were rarely present between the lumbar nerve roots in our specimens. However, interconnections were found more frequently between the sacral roots around the conus medullaris (Fig. 5 and 6).

The lateral recess contained the nerve root, covered by dura mater and bathed in CSF (Fig. 7). In all specimens, the average diameter of the osseous lateral recess gradually decreased from L1 to L4 (9.1, 7.61, 7.3, 5.96 mm for L1, L2, L3, L4 levels, respectively), then increased at L5 (6.06 mm) (Table 2). However, the diameter of the intradural exit nerve root increased from L1 to L5 (0.80, 1.17, 1.68, 3.15, 3.42 mm for L1, L2, L3, L4, L5 nerve roots, respectively).

The actual origin of the root sleeve started at the site where the nerve root leaves the intrathecal region. The midpoint of the distance between the superior edge and inferior edge of the intradural exit nerve root (just before leaving the thecal sac) (Fig. 8) was 3.47 mm below the inferior edge of the superior articular process at the L1 level, while the midpoint of the intradural L5 exit root was 5.75 mm above the inferior edge of the lateral facet (Table 2). The root origin gradually increased from the L1 to L5 level. L1, L2 and L3 roots originated below the inferior edge of the corresponding lateral facet; the origins of the L4 and L5 roots were above the inferior edge of the lateral facet. There were significant differences between the right and left sides for the L5 level ($P<0.05$)

Discussion

The lumbosacral nerve roots innervate muscles that provide movement and allow for the sensation of portions of the lower extremities as well as regulation of bladder function.

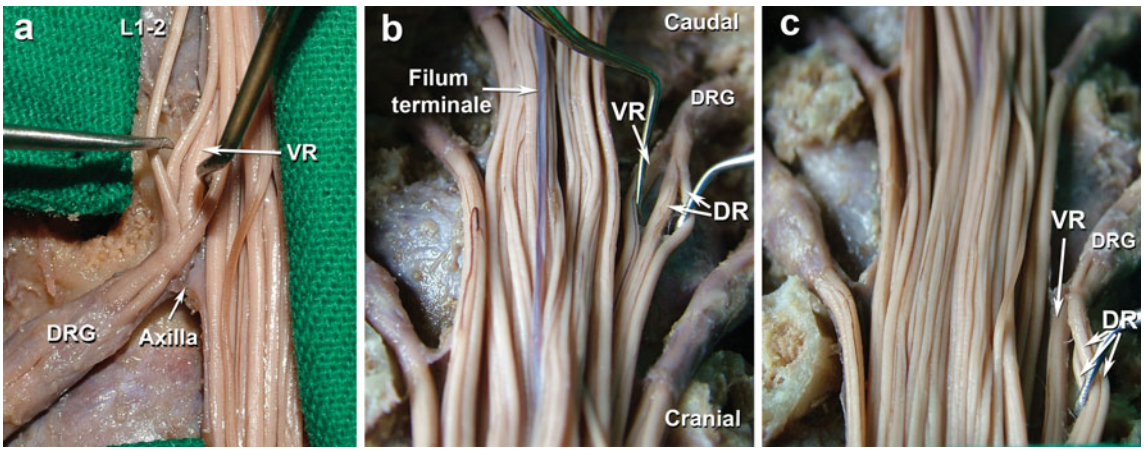

Fig. 3 A view showing the intradural exiting roots forming a spinal nerve. **a** One ventral and three dorsal roots; **b** one ventral and two dorsal roots; **c** one ventral and three dorsal roots. DRG: dorsal root ganglion, DR: dorsal root, VR: ventral root

Table 1 Data derived from the current study

		Number of dorsal roots		Number of ventral roots		Diameter of dorsal roots		Diameter of ventral roots		Rootlet number of dorsal roots		Rootlet number of ventral roots	
Level	Side	Mean ± SD	Range	Mean ± SD	Range	Mean ± SD	Range	Mean ± SD	Range	Mean ± SD	Range	Mean ± SD	Range
L1 Root	Right	1.40±0.52	1.0–2.0	1.0±0	1.0–1.0	0.47±0.23	0.19–0.88	0.34±0.18	0.12–0.59	1.90±0.88	1.0–3.0	1.50±0.53	1.0–2.0
	Left	1.50±0.71	1.0–3.0	1.0±0	1.0–1.0	0.47±0.20	0.23–0.73	0.34±0.18	0.13–0.59	1.70±0.67	1.0–3.0	1.40±0.52	1.0–2.0
	Mean	1.45±0.17	1.0–3.0	1.0±0	1.0–1.0	0.47±0.21	0.19–0.88	0.33±0.59	0.12–0.59	1.80±0.76	1.0–3.0	1.45±0.51	1.0–2.0
L2 Root	Right	1.40±0.52	1.0–2.0	1.0±0	1.0–1.0	0.58±0.39	0.20–1.59	0.34±0.25	0.12–0.95	2.50±1.43	1.0–6.0	1.70±0.95	1.0–4.0
	Left	1.40±0.52	1.0–2.0	1.0±0	1.0–1.0	0.92±0.21	0.63–1.17*	0.51±0.19	0.25–0.77	3.80±0.92	3.0–5.0*	2.10±0.88	1.0–3.0
	Mean	1.40±0.50	1.0–2.0	1.0±0	1.0–1.0	0.75±0.35	0.20–1.59	0.42±0.23	0.12–0.95	3.15±1.34	1.0–6.0	1.19±0.91	1.0–4.0
L3 Root	Right	1.70±0.48	1.0–2.0	1.0±0	1.0–1.0	1.02±0.18	0.78–1.26	0.75±0.15	0.54–0.97	4.00±0.94	3.0–5.0	2.90±0.74	2.0–4.0
	Left	1.50±0.53	1.0–2.0	1.0±0	1.0–1.0	0.96±0.17	0.76–1.27	0.66±0.16	0.45–0.98	3.70±0.82	3.0–5.0	2.60±0.70	2.0–4.0
	Mean	1.60±0.50	1.0–2.0	1.0±0	1.0–1.0	0.98±0.17	0.76–1.27	0.70±0.16	0.45–0.98	3.85±0.87	3.0–5.0	2.75±0.71	2.0–4.0
L4 Root	Right	1.60±0.52	1.0–2.0	1.0±0	1.0–1.0	1.83±0.19	1.55–2.08	1.27±0.27	1.00–1.85	6.90±0.88	6.0–8.0	5.00±1.05	4.0–7.0*
	Left	1.60±0.52	1.0–2.0	1.0±0	1.0–1.0	1.83±0.21	1.57–2.11	1.40±0.20	1.15–1.67	7.20±0.79	6.0–8.0	5.80±0.79	5.0–7.0
	Mean	1.60±0.50	1.0–2.0	1.0±0	1.0–1.0	1.82±0.19	1.55–2.11	1.33±0.23	1.00–1.85	7.05±0.82	6.0–8.0	5.40±0.99	4.0–7.0
L5 Root	Right	2.00±0	2.0–2.0	1.0±0	1.0–1.0	2.09±0.20	1.82–2.35	1.35±0.15	1.15–1.54	8.20±0.79	7.0–9.0	5.40±0.52	5.0–6.0*
	Left	1.60±0.52	1.0–2.0*	1.0±0	1.0–1.0	1.93±0.22	1.68–2.22*	1.47±0.23	1.17–1.82*	7.90±0.88	7.0–9.0	6.10±0.88	5.0–7.0
	Mean	1.80±0.41	1.0–2.0	1.0±0	1.0–1.0	2.01±0.22	1.68–2.35	1.41±0.19	1.15–1.82	8.05±0.82	7.0–9.0	5.75±0.78	5.0–7.0
S1 Root	Right	1.0±0	1.0–1.0	1.0±0	1.0–1.0	2.68±0.33	2.15–3.13	1.49±0.34	1.01–1.95	8.5±1.84	6.0–12	4.0±1.33	2.0–6.0
	Left	1.0±0	1.0–1.0	1.0±0	1.0–1.0	2.65±0.33	2.16–3.12	1.49±0.31	1.05–1.87	8.7±2.11	6.0–13	4.0±0.94	3.0–5.0
	Mean	1.0±0	1.0–1.0	1.0±0	1.0–1.0	2.67±0.32	2.15–3.13	1.49±0.32	1.01–1.95	8.60±1.93	6.0–13	4.0±1.12	2.0–6.0
S2 Root	Right	1.0±0	1.0–1.0	1.0±0	1.0–1.0	1.93±0.37	1.35–2.51 *	1.29±0.36	0.74–1.78	4.4±1.77	2.0–7.0	1.99±0.99	1.0–4.0
	Left	1.0±0	1.0–1.0	1.0±0	1.0–1.0	1.88±0.37	1.18–2.45	1.28±0.34	0.69–1.75	4.3±1.56	2.0–6.0	2.1±0.99	1.0–4.0
	Mean	1.0±0	1.0–1.0	1.0±0	1.0–1.0	1.91±0.36	1.18–2.51	1.29±0.34	0.69–1.78	4.35±1.63	2.0–7.0	2.1±0.96	1.0–4.0
S3 Root	Right	1.0±0	1.0–1.0	1.0±0	1.0–1.0	1.34±0.25	0.99–1.71	0.75±0.22	0.37–1.02*	1.80±0.78	1.0–3.0	1.0±0	1.0–1.0
	Left	1.0±0	1.0–1.0	1.0±0	1.0–1.0	1.35±0.23	1.04–1.72	0.72±0.20	0.35–1.03	1.90±0.73	1.0–3.0	1.0±0	1.0–1.0
	Mean	1.0±0	1.0–1.0	1.0±0	1.0–1.0	1.35±0.24	0.99–1.72	0.74±0.20	0.35–1.03	1.85±0.74	1.0–3.0	1.0±0	1.0–1.0
S4 Root	Right	1.0±0	1.0–1.0	1.0±0	1.0–1.0	0.68±0.17	0.45–0.95	0.33±0.18	0.15–0.74	1.0±0	1.0–1.0	0.60±0.51	0–1.0
	Left	1.0±0	1.0–1.0	1.0±0	1.0–1.0	0.65±0.16	0.43–0.88	0.33±0.18	0.17–0.75	1.0±0	1.0–1.0	0.60±0.51	0–1.0
	Mean	1.0±0	1.0–1.0	1.0±0	1.0–1.0	0.67±0.16	0.43–0.95	0.33±0.18	0.15–0.75	1.0±0	1.0–1.0	0.60±0.50	0–1.0
S5 Root	Right	1.0±0	1.0–1.0	1.0±0	1.0–1.0	0.35±0.06	0.24–0.45*	0.13±0.02	0.1–0.17	0.60±0.51	0–1.0	0.40±0.51	0–1.0
	Left	1.0±0	1.0–1.0	1.0±0	1.0–1.0	0.34±0.06	0.25–0.43	0.12±0.01	0.11–0.16	0.80±0.42	0–1.0	0.60±0.51	0–1.0
	Mean	1.0±0	1.0–1.0	1.0±0	1.0–1.0	0.34±0.06	0.24–0.45	0.12±0.01	0.1–0.17	0.70±0.47	0–1.0	0.50±0.51	0–1.0

*$p < 0.05$; *the diameter of the L2 dorsal root; the rootlet number of L2 dorsal roots, the rootlet number of the L4 ventral root; the number of L5 dorsal roots; the diameter of the L5 dorsal root; the diameter of L5 ventral roots; the rootlet number of L5 ventral roots; the diameter of the S2 dorsal root; the diameter of the S5 dorsal root; the diameter of S3 ventral roots*

The anatomy of the nerve roots within the thecal sac has been well described anatomically and radiologically [4, 7, 8, 18, 24, 25]. We attempted to add to this body of knowledge as pathology in this region is so common. Data of this type may help us understand nerve root injuries due to various pathologies, such as lumbar disc herniation, space-occupying lesions and lumbar trauma. Additionally, interneural interconnections may cloud clinical interpretation of patient presentations [1, 10]. Many authors reported that roots are arranged in pairs [4, 8, 24], whereas in our study, the dorsal roots were composed of several subgroups, and their number varied from one to three. Schallow [18] noted that the diameter of the ventral and dorsal roots was about 2 mm in the L3–S1 lumbar spine. However, the data from Schalow [18] were slightly different compared to our observations. We found that for L1 the mean diameter of the dorsal and ventral root was 0.47 and 0.33 mm and for S1 2.67 and 1.49 mm. In the current study ventrally roots were variably composed of one to seven, which could be separated into independent strands or rootlets; dorsally, there were one to nine. The dorsal and ventral roots had more rootlets with an increasing number of these in a rostral to caudal direction in the lumbar region. However, D' Avellla and Mingrino [5] found more rootlets with as many as 11 rootlets from L4 to S3 (2–6 rootlets on average). Schalow [18] reported that the nerve roots can be easily identified by their rootlets in the cauda equina. However, we do not believe that the nerve roots can be identified by their rootlets because of the several subgroups and variability among the nerve roots found in the present

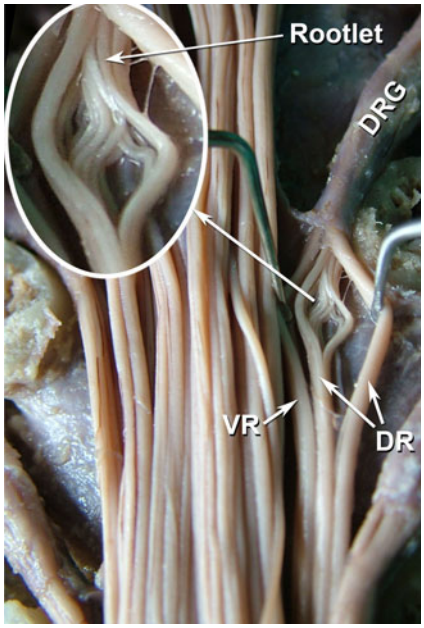

Fig. 4 Magnified view of the rootlets forming the root. The nerve root is organized into small bundles of rootlets covered with an arachnoid membrane

study. In addition, more cranially located root groups were more densely packed and less distinct. However, because most cranially placed roots lie laterally and the lower sacral roots (S2–5) remain in the dorsal midline of the cauda equina, identification of these roots may be difficult. Hauck [7], Hogan [8] and Lang [12] noted that nerve root diameters may affect the degree of blockade after spinal

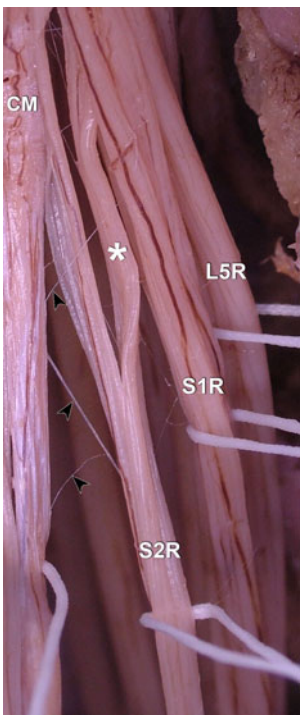

Fig. 5 A view indicating a proximal interconnection between the S1 and S2 roots just below the conus medullaris level. *Anastomosis; CM: conus medullaris; S1R: S1 nerve root; S2 R: S2 nerve root

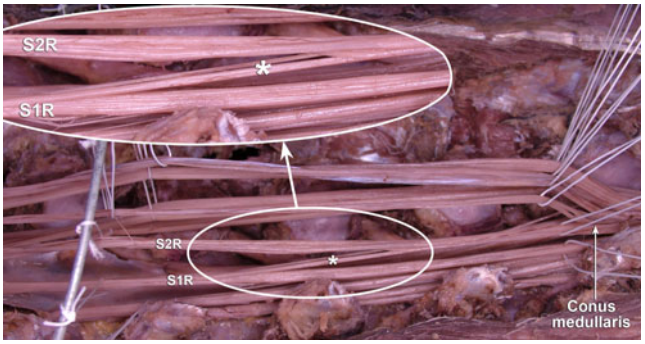

Fig. 6 Interconnection (more distal level) between the S1 and S2 roots and its magnified view was represented. *Anastomosis; S1R: S1 nerve root; S2 R: S2 nerve root

anesthesia. We agree with the authors. The largest root, which was S1 in the current study, had the highest degree of division into root bundles. Therefore, penetration of anesthetic drugs into each rootlet may be reduced. The large size of the roots may resist anesthetic effects, whereas the smaller sizes of roots may facilitate neural blockade and intrathecal neurotoxicity. Based on data from our study, separation of posterior roots into subgroups between one

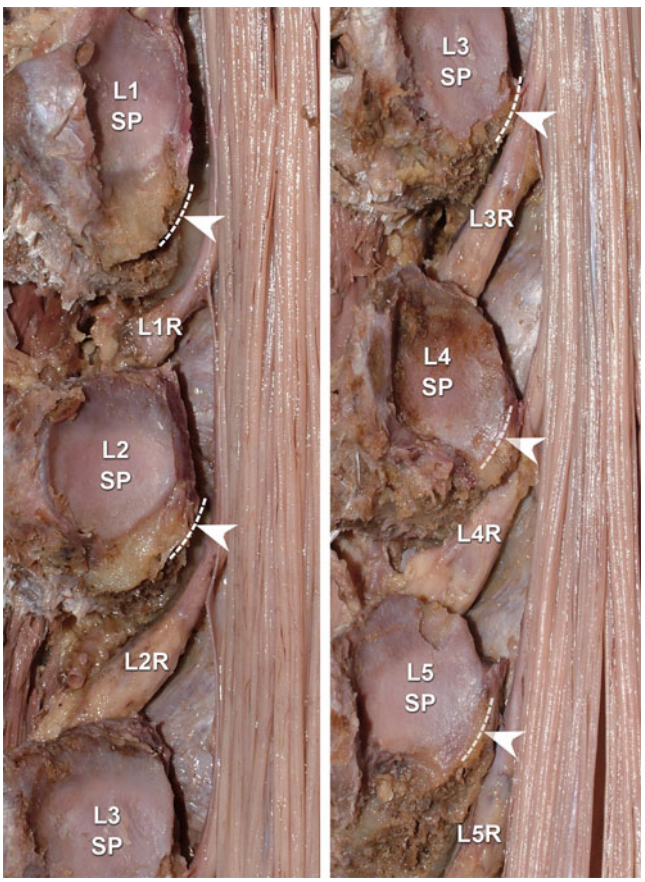

Fig. 7 Posteromedial view of left lumbar nerve roots coursing within the lateral recess. SP: Superior articular process; white arrowhead: lateral recess; dashed line: trace of lateral recess; R: nerve root

Table 2 Diameters of the lateral recess and distance between the origin of the lumbar nerve root and the inferior edge of the superior articular process

		Lateral recess antero-posterior diameter		Nerve root-lateral facet relationship	
Level	Side	Mean ± SD	Range	Mean ± SD	Range
L1	Right	9.27±0.81	8.22–10.4	-3.50±0.63	-2.72–4.31
	Left	8.93±0.80	8.01–10.0	-3.43±0.69	-2.42–4.33
	Mean	9.10±0.80	8.01–10.4	-3.47±0.65	-2.42–4.33
L2	Right	7.65±0.84	6.61–8.87	-2.02±0.43	-1.45–2.75
	Left	7.57±0.87	6.55–8.72	-2.01±0.40	-1.51–2.73
	Mean	7.61±0.83	6.55–8.87	-2.02±0.40	-1.45–2.75
L3	Right	7.33±0.83	6.36–8.35	-0.31±0.09	-0.17–0.45
	Left	7.28±0.86	6.27–8.34	-0.30±0.08	-0.19–0.42
	Mean	7.30±0.82	6.27–8.35	-0.30±0.09	-0.17–0.45
L4	Right	6.02±0.72	4.81–6.95	+1.59±0.55	+1.01–2.35
	Left	5.90±0.66	4.71–6.73	+1.61±0.52	+1.07–2.33
	Mean	5.96±0.67	4.71–6.95	+1.60±0.52	+1.01–2.35
L5	Right	6.09±0.56	5.31–6.71	+5.78±0.65	+4.75–6.80*
	Left	6.05±0.55	5.35–6.72	+5.73±0.61	+4.73–6.71
	Mean	6.06±0.54	5.31–6.72	+5.75±0.61	+4.73–6.80

"-": x points of *L1, L2 and L3 roots originated below the corresponding y points*

"+": x points of *of L4 and L5 roots were above the corresponding y points*

*$p< 0.05$

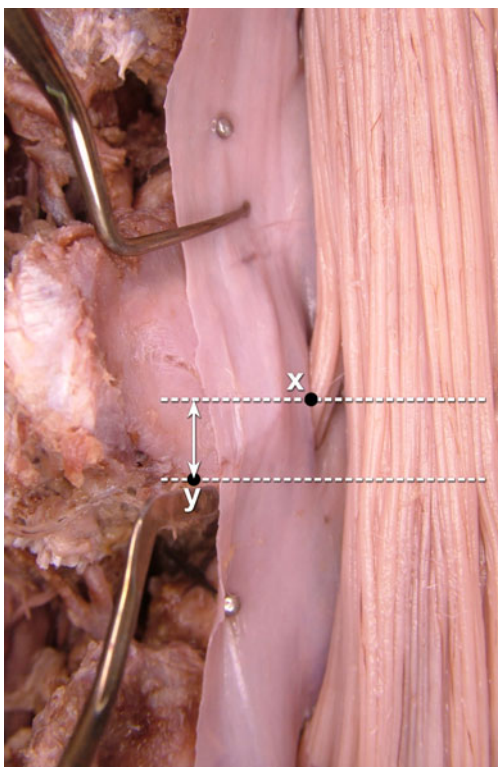

Fig. 8 Picture showing the relationship of the lumbar nerve root to the superior articular process just before the nerve root leaves the thecal sac. Measured vertical distance (x-y) is indicated. (x-y: distance between the midpoint of the distance between the superior edge and inferior edge of the intrathecal exit nerve root and the inferior edge of the superior articular process)

and three may increase the anesthetic effect, because each nerve root is exposed to a greater surface area. Therefore, responses to spinal anesthesia may be different due to the variability of root size for each level among individuals. In addition, within each root layer, the motor roots pass considerably closer to the disc space; therefore, we theorized that ventral cauda equina lesions may more likely affect the motor nerve roots. Preservation of sensation in sacral dermatomes may produce compression syndrome in ventral cauda equina. Numerous studies demonstrated that stretching of intradural nerve roots can damage them [11, 16]. We assumed that stretch-induced nerve root injury may be related to changes in the length of the spinal canal and in the length of the nerve root. The authors stated that the strain effect on the intrathecal nerve root could be reduced because of a shortened nerve root pathway [22, 23, 27]. In our study, the short L1 and L2 roots appeared to become taut more than the others (the most tethered root was L1) and therefore were easily injured by hemilateral anterior compression, such as by a tumor, but they may not be affected by stretch-induced injury due to no crossing of more mobile segments. However, the intrathecal course of the more caudal nerve roots becomes substantially longer as one descends the spine. Because of this, the L4 and L5 roots cross two or more mobile segments; thus, we hypothesize that during normal flexion, movement of the spine may cause exposure to more trauma at degenerative disc levels, such as in the case of excessive disc protrusion. This may expose them to the theoretical risk of stretch-induced injury. The perineurium and endoneurium have considerable mechanical strength and serve to protect neural tissues against mechanical forces. However, the intrathecal nerve roots do not have such a protective sheath

[6]; therefore, the intradural nerve roots are vulnerable to mechanical stretch, including operative maneuvers and trauma. Our study shows that the lumbar nerve roots may be exposed frequently to mechanical trauma at the neck of the nerve root sheath where the nerve root is fixed to surrounding structures. The nerve root may be compressed between the disc margins, facet and ligamentum flavum in the acute angle at the corner of the spinal canal. Disc herniations were associated with root anomalies (abnormal anastomoses between the roots), and bone anomalies (aplastic or hypoplastic lumbar pedicles, transitional vertebrae) were considerably prone to mechanical trauma of the exit root [1]. We assume that the maximum load is positively correlated with the nerve root diameter. There may be a linear relationship existing between increasing strain and injury. Injury is likely to be influenced by the diameter of the nerve root. We postulate that the lithotomy position or excessive flexion of the torso during various surgical procedures may be one of the risk factors for injury to tethered roots in the presence of intrathecal pathologies. It is clearly seen in the current study that the nerve root just before leaving the dural sac is in close proximity to the corresponding disc space. Above the point of emergence of the root from the dural sac, compression will collapse the ventrolateral part of the cauda equina and cause inward kinking of the intrathecal nerve root. Below the point of the origin of the root sheath, at the axillary level, compression will lead to flattening of the emerging root. The lumbar nerve root is fixed to surrounding structures at the neck of the nerve root sheath as it exits the dural sac; during excision of disc herniations above or below the point of the origin of the root sheath, therefore, nerve roots should not be excessively retracted. The nerve root leaving the thecal sac courses very close to the pedicle (especially, dorsal roots), which is a reliable landmark for location of the exiting roots. Improper pedicle screw placement in the lumbar spine may violate the spinal canal with increased risk of injury to dorsal nerve roots. The incidence of interneural interconnections between lumbar nerve roots is 8.5–30% [9, 14, 17]. In the current study, interneural interconnections were rarely found; differently, anastomoses appeared to be more frequent between the dorsal sacral roots at origin from the conus medullaris. The interneural interconnections may cause symptoms at more than one level and may give an incorrect indication of the disc herniation level; therefore, results of decompression may be poor. All spine surgeons should be aware of these nerve root anomalies. The anastomoses existing between dorsal roots may affect the results of surgery in selective dorsal rhizotomy. Identification of specific segmental innervations is important in choosing rootlets to section for rhizotomy for relief of intractable pain. The electromyographic response to stimulation and bony landmarks are used to guide the surgeon. Most authors rely on the electromyographic response to stimulation for rootlet selection [17, 21]; however, Warf and Nelson [26] found inconsistent responses with commonly used methods and stated that such techniques should not be used to select abnormal rootlets for partial dorsal rhizotomy. Based on our dissections, at lower levels of the distal spinal cord, lumbar and sacral roots are so crowded that it is very difficult to identify the limit of the segment of origin of a single root, and also anastomoses may affect the results of the procedure. Therefore, we proposed that sectioning of exiting dorsal rootlets, which are consistent with segments regarding pain in the ventrolateral area of the cauda equina, may be more appropriate for management of intractable pain. As seen in our dissections, dorsal roots and their rootlets can be easily separated from each other in the ventrolateral part of the cauda equina. Disadvantages of this procedure may be the need for additional laminectomy, which exposes the entire cauda equina. In the current study, the number of dorsal rootlets of the L5 and S1 roots was the greatest. This condition should be taken into consideration during microsurgical approaches to the dorsal root entry zone (DREZotomy) for unbearable neuropathic pain.

Lateral spinal stenosis in the lumbar spinal canal is an important clinical problem. Disc margin, facet hypertrophy and ligamentum flavum lead to compression of the root in the lateral recess [3]. Criteria for the diagnosis of lateral recess stenosis are not clearly defined [19]. Several authors have suggested measurement of the lateral recess height on CT as a helpful tool for making decisions regarding management. In a study by Strojnic [19], preoperative measurements of the heights of the lateral recess on CT were performed, and it was concluded that a height of 3.6 mm or less on a CT scan is also indicative of stenosis. Tong et al. [20] reported that the lower limit cutoff should be 3.7 mm at the L1–2 level and 4.3 mm at the L5–S1 level on MRI studies. Ciric et al. [3] evaluated lateral recess stenosis to be less than 2 mm in height. They accepted 5 mm or more as a normal lateral recess. In the work of Binder et al. [2], the anteroposterior diameter of the lateral recess is less than 4 mm in lateral spinal stenosis on CT. A normal anteroposterior diameter of the lateral recess is 3–5 mm and is 1–2 mm in stenotic situations [2]. In our study, in all specimens, the mean diameter of the osseous lateral recess gradually decreased from L1 to L4 (9.10, 7.61, 7.30, 5,96, 6.06 mm for L1, L2, L3, L4, L5 levels, respectively), whereas the diameter of the intrathecal nerve root increased from L1 to L5 (0.80, 1.17, 1.68, 3.15, 3.42 mm for L1, L2, L3, L4, L5 nerve roots, respectively). Based on data from the current study, the anteroposterior diameter of the lateral recess in lateral spinal stenosis should be less than 0.80 mm for the L1 level, 1.17 for L2, 1.68 for L3, 3.15 for L4 and 3.42 for L5. (These values correspond to the intrathecal

nerve root diameter.) The dimension of soft tissue of the lateral lumbar spinal canal should be taken into consideration in the diagnosis of lateral spinal stenosis with possible root compression. The lateral recess stenosis may be more commonly seen at the L4 and L5 levels because of the most narrow lateral recess diameter and the greatest nerve root diameter. The narrowing lateral recess may not contain CSF; therefore, myelography may be the best diagnostic method for lateral recess stenosis [3, 28].

Knowledge of the relationship between the facet and the nerve root may be helpful to predict the location of the origin of the nerve root during disc herniation surgery. In particular, in case of recurrent disc disease, owing to the presence of fibrosis in the operative field, the nerve root may be difficult to identify. Our results indicate that in all cadavers, the origin of the sleeve of the L1, L2 and L3 roots is beneath the inferior edge level of the superior articular process (the L1 root was an average of 3.47 mm below the inferior edge of the lateral facet; L2, 2.02 mm; L3, 0.30 mm). The L4 and the L5 roots originated above the inferior edge level of the lateral facet (L4, 1.60 mm; L5, 5.75 mm). The origin of the root ascended according to the inferior edge level of the corresponding lateral facet in the rostricaudal direction. Also, in lateral spinal stenosis, the relationship between the facet and root origin should be taken into consideration during lateral recess decompression in order to avoid root injury. These results indicate that exploration of the lateral recess at the inferior half of the facet at the L4 and L5 levels will carry a risk of injury to the nerve root.

In conclusion, we believe that the data obtained from anatomical dissection models will be helpful to surgeons with respect to understanding clinical symptomatology by correlating anatomical knowledge with clinical findings, as well as improving the success rate of spinal operations.

Conflicts of interest None

References

1. Artico M, Carloia S, Piacentini M, Ferretti G, Dazzi M, Franchitto S, Bronzetti E (2006) Conjoined lumbosacral nerve roots: Observations on three cases and review of the literature. Neurocirugia (Astur) 17:54–59
2. Binder DK, Schmidt MH, Weinstein PR (2002) Lumbar spinal stenosis. Semin Neurol 22:157–166
3. Ciric I, Mikhael MA, Tarkington JA, Vick NA (1980) The lateral recess syndrome. A variant of spinal stenosis. J Neurosurg 53:433–443
4. Cohen MS, Wall EJ, Kerber CW, Abithol JJ, Garfin SR (1991) The anatomy of the cauda equina on CT scans and MRI. J Bone Joint Surg 73-B:381–384
5. D'Avella D, Mingrino S (1979) Microsurgical anatomy of lumbosacral spinal roots. J Neurosurg 51:819–823
6. Hasue M (1993) Pain and the nerve root. Spine 18:2053–2058
7. Hauck EF, Wittkowski W, Bothe HW (2008) Intradural microanatomy of the nerve roots S1—S5 at their origin from the conus medullaris. J Neurosurg Spine 9:207–212
8. Hogan Q (1996) Size of human lower thoracic and lumbosacral nerve roots. Anesthesiology 85:37–42
9. Kadish LJ, Simmons EH (1984) Anomalies of the lumbosacral nerve roots: An anatomical investigation and myelographic study. J Bone Joint Surg 66-B:411–416
10. Karataş A, Çağlar Ş, Savaş A, Elhan A, Erdoğan A (2005) Microsurgical anatomy of the dorsal cervical rootlets and dorsal root entry zones. Acta Neurochir (Wien) 147:195–199
11. Kitab SA, Miele VJ, Lavelle WF, Benzel EC (2009) Pathoanatomic basis for stretch-induced lumbar nerve root injury with a review of the literature. Neurosurgery 65:161–168
12. Lang J, Geisel U (1983) Lumbosacral part of the dural sac and the topography of its contents. Morphol Med 31:27–46
13. Monajati A, Wayne WS, Rausching W, Ekholm SE (1987) MRI of the cauda equina. AJNR 8:893–900
14. Moriishi J, Otanı K, Tanaka K, Inoue SI (1989) The intersegmental anastomoses between the spinal nerve roots. Anat Rec 224:110–116
15. Naidich TP, King DG, Moran CJ, Sagel SS (1980) Computed tomography of the lumbar thecal sac. J Comput Asist Tomogr 4:37–41
16. Petraco DM, Spivak JM, Cappadona JG, Kummer FJ, Neuwirth MD (1996) An anatomic evaluation of L5 nerve stretch in spondylolisthesis reduction. Spine 21:1133–1139
17. Phillips LH, Park TS (1993) The frequency of intradural conjoined lumbosacral dorsal nerve roots found during selective dorsal rhizotomy. Neurosurgery 33:88–91
18. Schalow G (1985) The problem of cauda equina nerve root identification. Zentralbl Neurochir 46:322–330
19. Strojnic T (2001) Measurement of the lateral recess angle as a possible alternative for evaluation of the lateral recess stenosis on a CT scan. Wien Klin Wochenschr 113:53–58
20. Tong HC, Carson JT, Haig AJ, Quint DJ, Phalke VR, Yamakawa KSJ, Miner JA (2006) Magnetic resonance imaging of the lumbar spine in asymptomatic older adults. J Back Musculoskelet Rehabil 19:67–72
21. Turner RP (2009) Neurophysiologic intraoperative monitoring during selective dorsal rhizotomy. J Clin Neurophysiol 26(2):82–84
22. Ulmer JL, Elster AD, Mathews WP, King JC (1994) Distinction between degenerative and ishmic spondylolisthesis on sagittal MRI images: Importance of increased anteroposterior diameter of the spinal canal " wide canal sign". AJR Am J Roentgenol 163:411–416
23. Wall EJ, Massie JB, Kwan MK, Rydevik BL, Myers RR, Garfin SR (1992) Experimental stretch neuropathy. Changes in nerve conduction under tension. J Bone Joint Surg Br 74B:126–129
24. Wall EJ, Cohen MS, Massie JB, Rydevik B, Garfin SR (1990) Cauda equina anatomy I: Intrathecal nerve root organization. Spine 15:1244–1247
25. Wall EJ, Cohen MS, Abithol JJ, Garfin SR (1990) Organization of intrathecal nerve roots at the level of conus medullaris. J Bone Joint Surg 72:1495–1499
26. Warf BC, Nelson KR (1996) The electromyographic responses to dorsal rootlet stimulation during partial dorsal rhizotomy are inconsistent. Pediatr Neurosurg 25:13–19
27. Weishaupt D, Schmid MR, Zanetti M, Boos N, Romanowski B, Kissling RO, Dvorak J, Hodler J (2000) Positional MRI imaging of the lumbar spine: Does it demonstrate nerve poor compromise not visible at conventional MRI imaging? Radiology 215:247–253
28. Wilmink JT (1989) CT morphology of intrathecal lumbosacral nerve-root compression. AJNR 10:233–248

Acta Neurochir (2011) 153:1443–1445
DOI 10.1007/s00701-011-1019-0

LETTER TO THE EDITOR

Continuous skull traction followed by closed reduction in chronic pediatric atlantoaxial rotatory fixation

Masaaki Chazono · Shigeru Saito · Keisho Liu · Keishi Marumo

Received: 27 January 2011 / Accepted: 4 April 2011 / Published online: 18 April 2011

Dear Editor,

Atlantoaxial rotatory fixation (AARF) is a disorder of childhood commonly encountered in clinical practice. We report a successful case of conservative management with continuous halo-skull traction followed by closed reduction in a patient with chronic pediatric AARF whose parents refuse surgical treatment.

A 7-year-old girl with a history of upper respiratory tract infection developed right-sided neck pain occurring since December 2007. Due to persistent pain whose etiology could not be identified by a pediatrician, she was referred to our department in August of 2008. Three-dimensional computed tomography (3D-CT) clearly showed a lateral inclination of 21 degrees in the AP view (Fig. 1a). Magnetic resonance imaging (MRI) identified a synovial effusion within the anterior atlantoaxial joint space characterized by low signal intensity on T1-weighted images and high signal intensity on T2-weighted images (Fig. 1b). Although spinal cord impingement was observed between the dens and the posterior arch of C1, the patient was neurologically intact. The clinical and radiological findings were considered definitive for chronic AARF. After admission in October of 2008, the patient's head was immobilized with the halo-ring under general anesthesia. An initial attempt at closed reduction was unsuccessful. Therefore, the patient was in bed in "supine" skull traction at night and seated in a wheelchair during daytime hours under "sitting" skull traction from 2.5–6 kg for 2 months. Lateral plain x-rays showed a little change in the atlantoaxial angle. No neurological deficits were identified during skull traction. We recommended surgical intervention to her parents in order to treat the chronic AARF, but they rejected the offer and requested the continuous conservative management. In December of 2008, a second closed reduction maneuver was performed. Holding the halo-ring firmly attached to the patient's head and applying her head with the longitudinal and right-sided rotational force, we successfully elevated the atlas and reduced it with crepitation. A coronal reconstruction image of MPR-CT showed a reduction of C1/C2. The patient was immediately put into a halo-vest for 3 months. Three months after removal of the halo-vest, a coronal reconstruction image of MPR-CT revealed spontaneous bony fusion at the right-sided facet joint of C1/2 (Fig. 1c). In contrast, MRI demonstrated a remarkable shrinkage of the synovial effusion within the anterior atlantoaxial joint space, which was swollen before treatment, resulting in an indirect decompression of the spinal cord (Fig. 1d). At the final follow-up, limited range of rotation on her neck was seen, but the patient had no symptoms such as neck pain or neurologic involvement, no torticollis.

Multiplanar reconstruction CT and 3D-CT studies are valuable for the diagnosis and evaluation of AARF, including determination of the type and degree of articulating facet displacement of the atlantoaxial subluxation. 3D-CT in particular shows the spatial relations of the atlantoaxial joint with particular clarity, thereby aiding in arriving at a correct diagnosis. Ishii et al. demonstrated that both facet joint deformity and lateral inclination of the atlas

M. Chazono (✉)
Department of Orthopaedic Surgery,
NHO Utsunomiya National Hospital,
2160, Shimo-okamoto,
Utsunomiya, Tochigi 329–1193, Japan
e-mail: chazono@pop02.odn.ne.jp

M. Chazono · S. Saito · K. Liu · K. Marumo
Department of Orthopaedic Surgery,
The Jikei University School of Medicine,
Tokyo, Japan

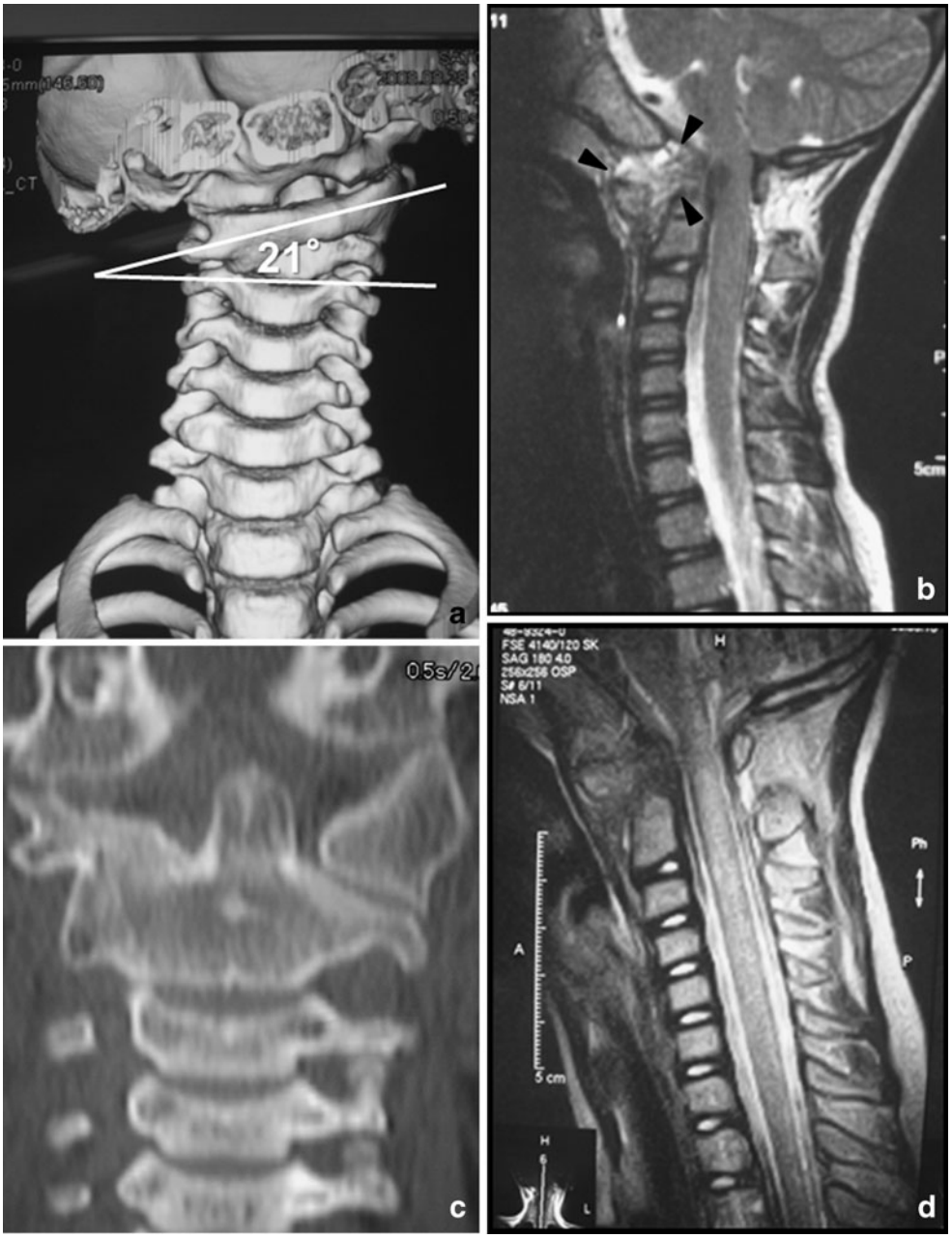

Fig. 1 **a** Three-dimensional computed tomography (3D-CT) clearly shows a lateral inclination of 21 degrees in the AP view. **b** Sagittal T2-weighted MRI demonstrates that synovial effusion within the anterior atlantoaxial joint space is well visualized on the image as an area of high signal intensity (*arrowheads*). **c** Coronal reconstruction image of multi-planar computed tomography reveals spontaneous bony union at the right-sided facet joint of C1/2 at 3 months after halo-ring immobilization. **d** Sagittal T2-weighted MRI demonstrates a remarkable shrinkage of the synovial effusion within the anterior atlantoaxial joint space

observed on 3D-CT could be useful signs to predict the prognosis and the treatment of choice in patients with chronic AARF, and in particular that greater than 20 degrees of lateral inclination of the atlas was a significant indicator of an irreducible subluxation [1]. In addition, Pang and Li reported on a set of AARF cases in which C1/2 facet joint locking due to bone union strongly correlated with delays longer than 3 months [2, 3]. In the present case, despite the presence of a 21-degree lateral inclination of the atlas in a patient with chronic AARF of 10 months' duration, long-term halo-traction followed by closed reduction was successfully able to reduce the subluxation and also may have released the patient's ligamentocapsular contractures. MRI is also a reliable imaging modality for assessing the integrity of the transverse ligament in AARF patients [4]. A unique finding in our patient was the MRI documentation of gradual shrinkage of the synovial effusion within the anterior atlantoaxial joint space after the successful closed reduction and its ultimate disappearance at the last follow-up. This finding indicates that the atlantoaxial stability obtained by closed reduction and subsequent halo-vest immobilization may have promoted the regression of the synovial effusion within the anterior atlantoaxial joint space.

The optimal management of chronic AARF is controversial. Many investigators have advocated operative reduction in patients with chronic AARF, resulting in approximately 30% of such patients requiring cervical

fusion [5]. However, in the present case, because multiplanar reconstruction computed tomography showed no bony union of the atlantoaxial joint at initial presentation and her patient refused the surgical management, we treated this case of chronic AARF conservatively. It was not intended to achieve spontaneous fusion at the right side of lateral mass at the last follow-up.

In conclusion, this case suggests that continuous halo-skull traction followed by closed reduction could be an option of management in some pediatric patients with chronic AARF. However, the maneuvers may cause pediatric patients to be traumatic for both physical and psychological issues.

Acknowledgments The authors gratefully thank the patient and his family for allowing us to present the clinical data reported here.

Conflicts of interest None.

References

1. Ishii K, Chiba K, Maruiwa H, Nakamura M, Matsumoto M, Toyama Y (2006) Pathognomonic radiological signs for predicting prognosis in patients with chronic atlantoaxial rotatory fixation. J Neurosurg Spine 5:385–391
2. Pang D, Li V (2005) Atlantoaxial rotatory fixation: Part 2-New diagnostic paradigm and new classification based on motion analysis using computed tomographic imaging. Neurosurgery 57:941–953
3. Pang D, Li V (2005) Atlantoaxial rotatory fixation: Part 3-A prospective study of the clinical manifestation, diagnosis, management, and outcome of children with atlantoaxial rotatory fixation. Neurosurgery 57:954–972
4. Roche CJ, O'Malley M, Dorgan JC, Carty HM (2001) A pictorial review of atlanto-axial rotatory fixation: key points for the radiologist. Clin Radiol 56:947–958
5. Subach BR, McLaughlin MR, Albright AL, Pollack IF (1998) Current management of pediatric atlantoaxial rotatory subluxation. Spine 23:2174–2179

Acta Neurochir (2011) 153:1447–1448
DOI 10.1007/s00701-011-1027-0

LETTER TO THE EDITOR

Spontaneous disruption of dura mater and fascicular continuity of the L5 nerve root by a calcified disc herniation

Richard Bostelmann · Sven Eicker · Hans-Jakob Steiger · Jan Frederick Cornelius

Received: 21 January 2011 / Accepted: 8 April 2011 / Published online: 27 April 2011

Dear Editor,

We report a "little pearl" in spinal neurosurgery concerning a severe nerve root and dura avulsion caused by a calcified disc.

A 47-year-old male patient with radiculopathy (3/5 motor weakness of ankle and toe extension, numbness in the right lateral lower leg) and disc herniation proven by magnetic resonance imaging (MRI, T1-weighted and T2-weighted) was treated by microsurgical management (no previous surgery). After careful opening of the yellow ligament, a very uncommon situation revealed itself. The dural layer of the nerve root was circumferentially disrupted, resulting in a direct view of the fascicles, which were tightly laid together. The continuity of the two most medially located fascicles was disrupted. No leaking of cerebrospinal fluid was observed. Complete inspection revealed that an almost completely calcified and solid disc herniation was in direct contact with the pathology inside the nerve root, only a few millimeters distal from leaving the thecal sac (Fig. 1). The only reason for the described nerve root lesion that could be seen was the very sharp-edged disc hernia, impinging on the root, causing this serious injury. Resection of the herniation and nucleotomy were performed through the perforation hole. After freeing the nerve root, its continuity was reconstructed and stabilized with fibrin glue. The specimen was examined histopathologically. The largest piece was found to be a grayish-to-white, 30 × 25 × 5-mm piece of cartilaginous filaments. After decalcification, distinct degenerative disc material was demonstrated on light microscope inspection, consisting predominantly of cartilaginous filaments with fibrous and mucin-like degenerative alterations and scattered chronic inflammatory cell infiltration. At 15 weeks after surgery, the patient had no sensory deficit or residual pain. He was completely satisfied and returned to work. Even the paresis of the right foot had ameliorated.

Intradural disc herniation has been reported as a rare and particular type of intervertebral disc herniation. The incidence reported for this special entity ranges from 0.001% to 1% [2, 9]. The incidence of intra*radicular* herniations (type B intradural disc herniations [6]) is assumed to be 5% of intra*dural* disc herniations [4]. Even though intra*radicular* herniation at the same level and same

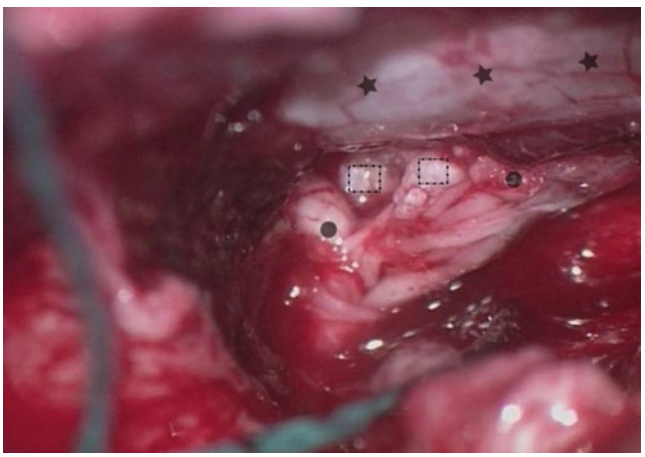

Fig. 1 View through the operating microscope of the L4-5 level after fenestration and flavectomy from the right side. The destructive calcified herniated disc material (*dashed square*), which led to dural and fascicular injury (*black dot*) of the L5 nerve root, is clearly seen. *Black stars* intact thecal sac

R. Bostelmann (✉) · S. Eicker · H.-J. Steiger · J. F. Cornelius
Department of Neurosurgery,
Heinrich-Heine-University of Duesseldorf,
Moorenstrasse 5,
40225 Duesseldorf, Germany
e-mail: richard.bostelmann@med.uni-duesseldorf.de

side without previous surgery has been described elsewhere [1, 4–7, 9], no one has reported severe avulsion of a lumbar nerve root without previous surgery, as in our case. Nowadays, MRI is an adequate diagnostic tool.

There are anatomical data [2, 8–10] supporting the assumption of congenital preconditions that put a nerve root at risk of being injured by a disc herniation, but hereditary factors are probably not sufficient for dural tearing, as we can easily conclude from the incidence rate of epidural disc herniation compared with intradural disc herniation. Acquired cofactors, such as spondylotic changes, chronic inflammation, repeated minor trauma, and previous surgery, therefore seem to be mandatory [3]. Moreover, little attention has been paid to the sequester's nature itself as a cause for tearing, or, as in our case, disrupting the dura and avulsing fascicles of the nerve root. In particular, severe degeneration to the stage of calcification and sharp edges of the disc fragment is presumably one of the cofactors for dural penetration and nerve fiber injury.

Disclosure There are no conflicts of interest. Part of this work was presented as a poster at the annual meeting of the DWG (Deutsche Wirbelsäulengesellschaft), December 2010 in Bremen, Germany.

Reference

1. Barbera J, Gonzalez-Darder J, Garcia-Vazquez F (1984) Intraradicular herniated lumbar disc. Case report. J Neurosurg 60:858–860
2. Bayassi S (1998) Intradural lumbar disk herniation (ILDH). Case report and literature review. Neurol Neurochir Pol 32:1295–1301
3. Epstein NE, Syrquin MS, Epstein JA, Decker RE (1990) Intradural disc herniations in the cervical, thoracic, and lumbar spine: report of three cases and review of the literature. J Spinal Disord 3:396–403
4. Jackson RP, Kornblatt MD (1997) Lumbar intraradicular disk herniation: report of three cases. Orthopedics 20:980–985
5. Mercier P, Hayek G, Ben AH, Tounsi R, Fournier D, Menei P, Ben MH, Guy G (1997) Intradural lumbar disk hernias. Apropos of 6 cases and review of the literature. Neurochirurgie 43:142–147
6. Mut M, Berker M, Palaoglu S (2001) Intraradicular disc herniations in the lumbar spine and a new classification of intradural disc herniations. Spinal Cord 39:545–548
7. Ozdemir N, Yilmaz HS, Acar UD, Tektas S (2004) Intraradicular lumbar disc herniation: report of two cases and review of the literature. Br J Neurosurg 18:637–643
8. Penning L, Wilmink JT (1981) Biomechanics of lumbosacral dural sac. A study of flexion-extension myelography. Spine (Phila Pa 1976) 6:398–408
9. Schisano G, Nina P (1998) Intraradicular lumbar disc herniation: case report and review of the literature. Neurosurgery 43:400
10. Spencer DL, Irwin GS, Miller JA (1983) Anatomy and significance of fixation of the lumbosacral nerve roots in sciatica. Spine (Phila Pa 1976) 8:672–679

Acta Neurochir (2011) 153:1449–1453
DOI 10.1007/s00701-011-1020-7

CASE REPORT

Terminal ventriculostomy as an adjuvant treatment of complex syringomyelia: a case report and review of the literature

David A. Wilson · David J. Fusco · Harold L. Rekate

Received: 10 February 2011 / Accepted: 4 April 2011 / Published online: 27 April 2011

Abstract Complex syringomyelia is multifactorial, and treatment strategies are highly individualized. In refractory cases, sectioning of the filum terminale, also known as terminal ventriculostomy, has been described as a potential adjuvant treatment to alleviate syrinx progression. A 10-year-old boy with a history of arachnoiditis presented with complex syringomyelia, progressive lower extremity motor weakness, and spasticity. Previously, he had failed spinal cord detethering and direct syrinx shunting. Imaging studies demonstrated a holocord syrinx extending to the level of his conus medullaris and into the filum terminale. The patient underwent an uncomplicated lumbar laminectomy and transection of the filum terminale. Operative pathologic specimens demonstrated a dilated central canal within the filum. Postoperative imaging demonstrated significant reduction in the diameter of the syrinx. At follow-up, the patient's motor symptoms had improved. Terminal ventriculostomy may be a useful adjuvant in treating caudally placed syringes refractory to other treatments. This procedure carries low neurological risk and involves no hardware implantation. In select cases, terminal ventriculostomy may help preserve neurological function in the face of otherwise progressive syringomyelia.

This manuscript has not been presented at a conference.

This is not a clinical trial and does not require a registration number.

D. A. Wilson · D. J. Fusco · H. L. Rekate
Division of Neurological Surgery, Barrow Neurological Institute,
St. Joseph's Hospital Medical Center,
Phoenix, AZ, USA

H. L. Rekate (✉)
c/o Neuroscience Publications, Barrow Neurological Institute,
350 West Thomas Road,
Phoenix, AZ 85013, USA
e-mail: neuropub@chw.edu

Introduction

Syringomyelia is an insidious and progressive condition characterized by the accumulation of excess cerebrospinal fluid (CSF) within the spinal cord. Syrinx formation is caused by derangements in CSF dynamics that lead to a build up of intramedullary fluid and subsequent neurological symptoms [15]. Syringomyelia is multifactorial and can be caused by obstructions at any point in the CSF pathways affecting the spinal cord [15, 17]. As such, it is associated with several conditions, most notably Chiari 1 and 2 malformations, spinal cord tumors, infection, and trauma [3, 4, 12]. The appropriate treatment depends on the predominant pathologic mechanism and may include suboccipital decompression, spinal cord detethering, tumor resection, or shunting of the syrinx itself [1, 3, 16]. First described by Gardner in 1977, terminal ventriculostomy, or transection of the filum terminale, is an another technique for treating syringes that extend to the conus medullaris and filum terminale [10]. Although terminal ventriculostomy is seldom used, it can be a useful adjuvant in the management of caudally placed syringes refractory to other treatments.

Clinical presentation

History

A 10-year-old boy with a complex medical history presented with progressive decline in his lower extremity function. He had a history of a rare saprophytic fungal meningitis causing arachnoiditis, spinal cord tethering, and complex syringomyelia. Previously, he had undergone multiple interventions, including two detethering

procedures, placement of a syringosubarachnoid shunt, and a myelotomy for direct drainage of the syrinx. His most recent intervention, a circumferential upper thoracic spinal cord detethering and myelotomy for direct drainage of the syrinx, had occurred 2 months before this presentation. After that surgery, he had temporarily regained the ability to ambulate with assistance. During the month before the current presentation, however, he had experienced a progressive decline in bilateral lower extremity function and urinary incontinence.

Hospital course

At presentation, the patient was nonambulatory. His physical examination demonstrated marked bilateral lower extremity spasticity and no lower extremity movement. Magnetic resonance (MR) imaging of his full spine demonstrated marked progression of a complex syrinx (Fig. 1) that extended from the upper thoracic cord to the conus medullaris, expanding the spinal cord and distending the filum terminale.

Due to the distal extension of the syrinx into the filum terminale, the patient underwent an L1-2 laminectomy for filum transection. A surgical specimen of the filum terminale was sent to pathology and demonstrated an abnormally large central canal remnant lined with ependymal cells (Fig. 2). Postoperative MR imaging performed 3 days following surgery demonstrated significant decompression of the syrinx cavity (Fig. 3a).

Follow-up

In the immediate postoperative period, the patient's motor examination remained unchanged. He was discharged to a rehabilitation facility. Three months after surgery, he demonstrated weak spontaneous movement in his hip flexors (graded strength: 2/5). He could walk in a pool and ambulate with maximum assistance with a front-wheel walker. At last follow-up, 16 months following the procedure, his clinical status remained stable, with no new deterioration in neurological function. MRI obtained at that time demonstrated continued decompression of his thoracic and lumbar syrinx (Fig. 3b).

Discussion

This case demonstrates the utility of terminal ventriculostomy as an adjuvant treatment for caudal syringes refractory to other interventions. In this case, a complex syrinx progressed despite a prior radical detethering procedure and previous placement of a syringosubarachnoid shunt. Terminal ventriculostomy was performed to open the caudal aspect of the syrinx cavity into the spinal subarachnoid space at the level of the filum terminale.

An appreciation of the mechanisms of syrinx formation is crucial in evaluating treatment options and understanding the role of terminal ventriculostomy in selected cases. In

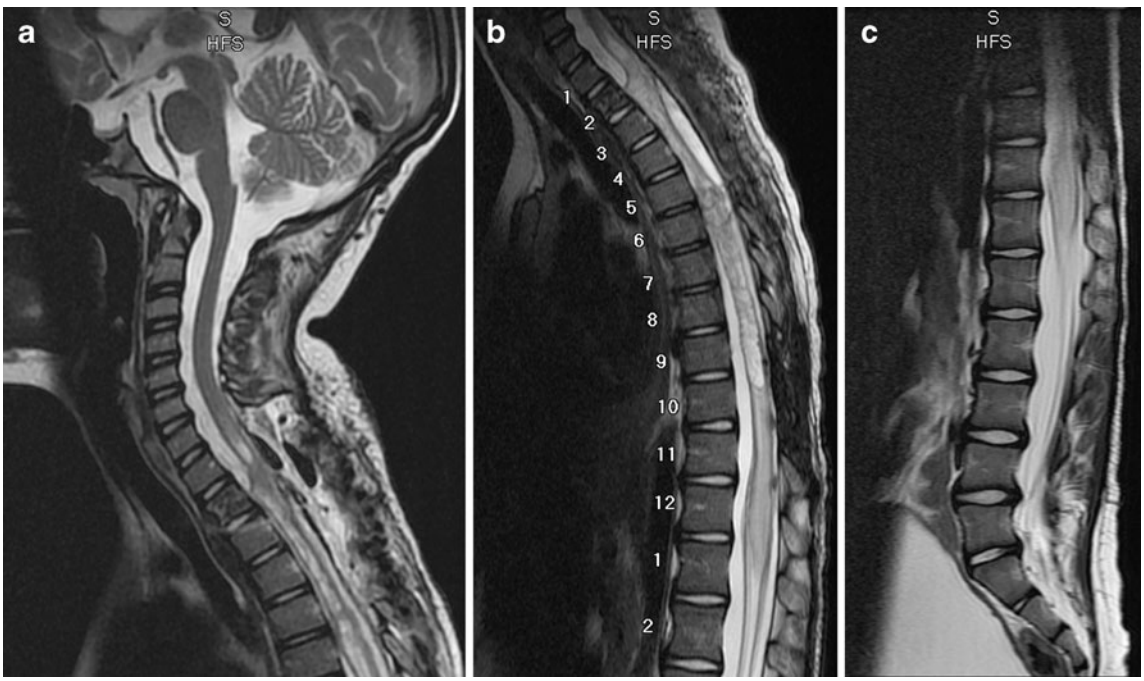

Fig. 1 Preoperative cervical (**a**), thoracic (**b**), and thoracolumbar (**c**) sagittal T2-weighted magnetic resonance (MR) imaging sequences demonstrating a complex syrinx extending from the lower cervical level to the filum terminale. Used with permission from Barrow Neurological Institute

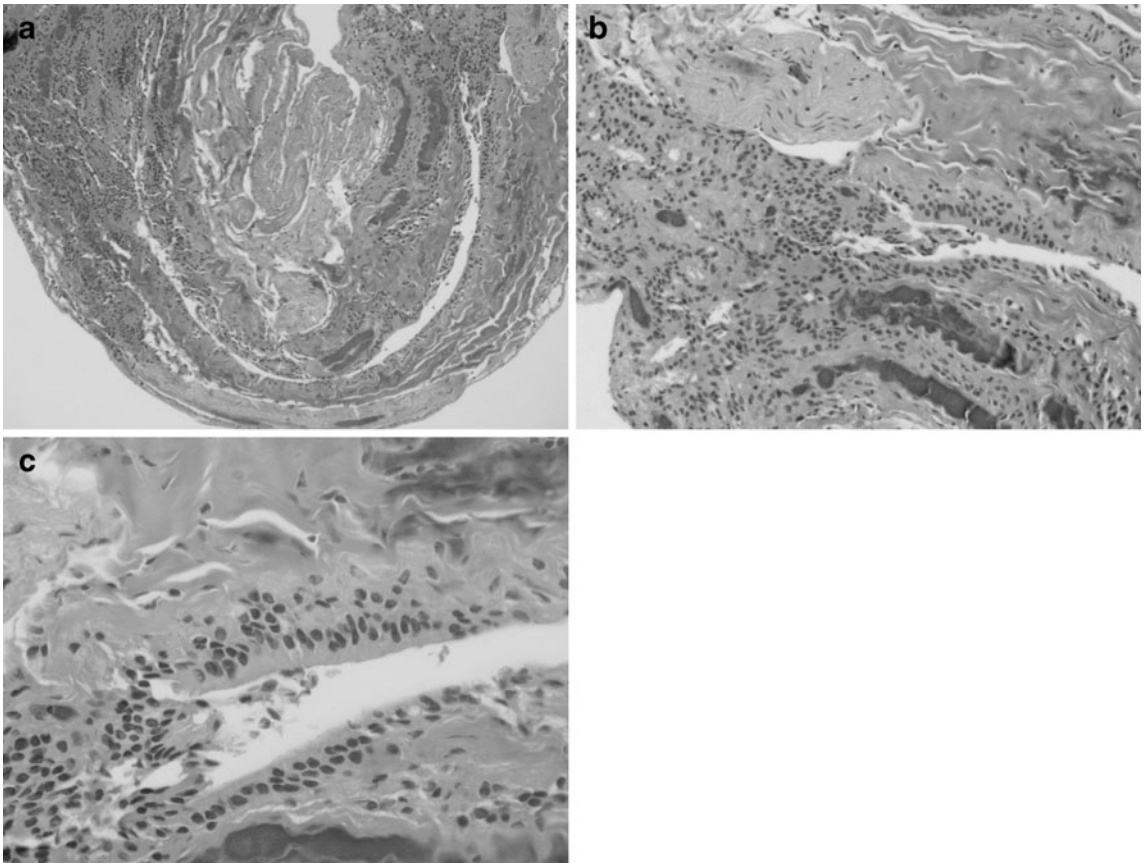

Fig. 2 Low- (**a**), medium- (**b**), and high-power (**c**) microscope views of the surgical specimen demonstrating a persistent ependymal-lined central canal within the filum terminale. Used with permission from Barrow Neurological Institute

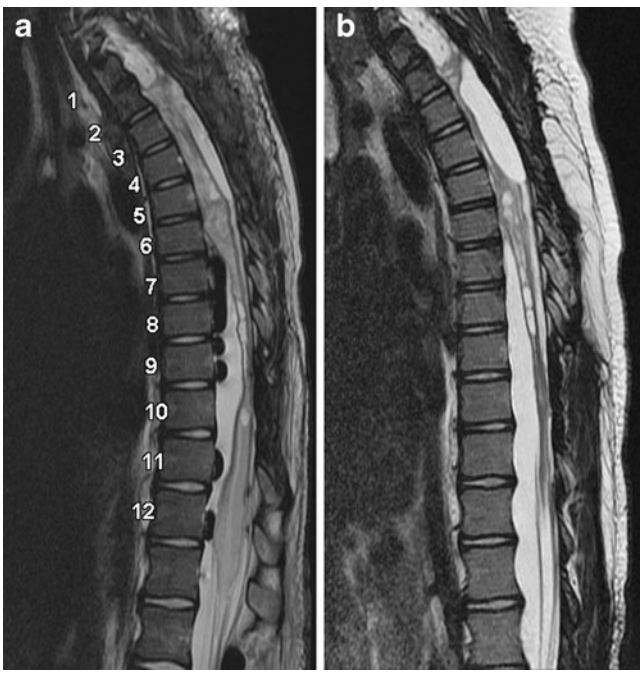

Fig. 3 Postoperative thoracic sagittal T2-weighted MRI sequence demonstrating marked reduction in the size of the syrinx cavity 3 days (**a**) and 16 months (**b**) after surgery. Used with permission from Barrow Neurological Institute

1958, Gardner and Angel proposed the hydrodynamic theory, in which syringomyelia develops from a persistent opening of the central canal at the obex in the setting of fourth ventricular outlet obstruction [9]. In this scenario, CSF pulsations create a "water-hammer" effect, driving fluid into the central canal [8]. Although mechanistically appealing, Gardner's hypothesis fails to explain syrinx formation in the absence of a Chiari malformation. In 1972 Ball and Dayan proposed a more unifying mechanism, the perivascular dissection theory, in which disruptions of the spinal subarachnoid space promote CSF flow across perivascular spaces into the spinal cord parenchyma [2]. Unlike Gardner's hypothesis, this mechanism helps to explain syrinx formation in a variety of settings, including trauma, arachnoiditis, tethered cord, and Chiari malformation. Some evidence also suggests that increases in venous hydrostatic pressure within the epidural space may play a role in the development of a pre-syrinx state that may progress to syringomyelia [7, 13]. Because the veins draining the spinal cord are valveless, venous hypertension caused by an obstruction or mass would be expected to promote interstitial build-up of fluid within the spinal cord.

Although the pathophysiology of syrinx formation is not completely understood, the above theories are all based on the notion that the central canal remains a potential space susceptible to CSF accumulation, particularly in young patients [14]. Embryologically, the central canal, or *ventriculus terminalis*, resembles a ventricle. In this way, syringomyelia is analogous to hydrocephalus, that is, blockage of spinal fluid pathways leads to the accumulation of fluid within the primitive ventricle of the spinal cord. In cases of caudal syringes extending to the conus medullaris, terminal ventriculostomy brings the syrinx cavity into communication with the spinal subarachnoid space, allowing the syrinx to decompress with minimal morbidity [15].

Despite its theoretical appeal, terminal ventriculostomy is seldom described in the literature. Gardner et al. first proposed terminal ventriculostomy for the treatment of caudally located syringomyelia in a series published in 1977 [10]. Of the 12 patients who underwent transection of the tip of the conus medullaris, 11 demonstrated neurological improvement at a follow-up period ranging from 12 to 31 months. All specimens confirmed the presence of a patent central canal extending up to 8 cm into the filum terminale, indicative of dysfunctional CSF flow. Although follow-up is limited, this series suggests that opening a persistent central canal at the tip of the conus medullaris may partially restore physiologic CSF dynamics and alleviate syrinx progression, at least temporarily. In 1983 Williams and Fahy published a "critical appraisal" of terminal ventriculostomy [18]. In their series, 31 patients with syringomyelia underwent filum terminale excision. Although 21 patients initially demonstrated subjective or objective improvements after surgery, the majority continued to deteriorate at follow-up [18]. These findings underscore the notion that while terminal ventriculostomy may provide a temporary reprieve from symptom progression, the underlying course of the disease is unlikely to be affected.

In our case, terminal ventriculostomy was performed in a 10-year-old boy with a complex syrinx that extended into the filum terminale. After surgery, he experienced improvement in his subjective clinical symptoms and objective motor performance that lasted up to his most recent follow-up, 16 months later. His postoperative MR images demonstrated a significant reduction in the size of the syrinx (Fig. 3), and sections of the filum terminale taken during surgery demonstrated a persistent ependymal-lined central canal (Fig. 2). These findings confirm that the procedure effectively opened the syrinx cavity into the subarachnoid space, corroborating the aforementioned rationale. Our case differs significantly from two recent reports that demonstrate syrinx resolution after filum terminale transection in the setting of tethered cord syndrome [6, 11]. In our patient, no radiographic or clinical evidence of tethered cord syndrome was present, and a clear infectious etiology of syringomyelia had already been established. Furthermore, the persistent central canal within the filum terminale suggests that transection of the filum relieved the syrinx by creating a pathway for CSF flow from the spinal cord to the spinal subarachnoid space rather than by acting as a detethering procedure. In cases of spinal arachnoiditis, recent data suggest that increased tensile radial stress in the spinal cord may lead to syrinx formation by transiently lowering pressure in the cord and subsequently drawing in interstitial fluid which may become trapped within the spinal cord [5]. This mechanism makes terminal ventriculostomy an intuitively appealing treatment in cases of arachnoiditis. Analogous to a third ventriculostomy, sectioning of the filum terminale in the setting of a persistently open intramedullary fluid compartment leads to an equilibrium in pressure between the intramedullary and spinal subarachnoid spaces and provides a route of egress for high-pressure intramedullary fluid. Although scarring in the subarachnoid space is a potential cause for failure of the terminal ventriculostomy, this patient's CSF dynamics were normal enough to allow continued long-term patency of the terminal ventriculostomy. Had the arachnoiditis led to terminal ventriculostomy failure, placement of a lumbar-peritoneal shunt may have helped maintain patency of the ventriculostomy. This possibility was discussed but proved to be unnecessary in our patient.

The durability of terminal ventriculostomy over time has been a major concern. The case series published by Williams and Fahy suggests that the beneficial effects of this procedure are often transient [18]. In this case, however, the patient's clinical status remained stable until last follow-up, 16 months after surgery. While his improvement plateaued in the 3 months following surgery, he did not experience any neurological deterioration during the follow-up period that might be expected from the natural course of complex syringomyelia. Furthermore, his MRI obtained 16 months after the terminal ventriculostomy demonstrated continued decompression of his syrinx cavity. Although terminal ventriculostomy was not a definitive cure, it appears to have stabilized this patient's previously progressive syringomyelia, both clinically and radiographically.

This case illustrates the use of terminal ventriculostomy in the management of syringes extending to the conus medullaris when other first-line treatments have failed. Our case suggests that this procedure may be best reserved for patients with radiographic evidence of syrinx extension into the filum terminale. While it is clear that terminal ventriculostomy is not a first-line treatment of syringomyelia, our experience illustrates that the procedure should be kept in the neurosurgeon's armamentarium as a possible adjuvant in cases of complex syringomyelia refractory to standard treatments. Although it does not address the underlying cause of syringomyelia, terminal ventriculostomy, in select cases, may

be a useful adjuvant therapy to slow neurological deterioration and to preserve some lower extremity function in the face of an otherwise progressive disease.

Conflicts of interest None.

References

1. Aghakhani N, Parker F, David P, Morar S, Lacroix C, Benoudiba F, Tadie M (2009) Long-term follow-up of Chiari-related syringomyelia in adults: analysis of 157 surgically treated cases. Neurosurgery 64:308–315
2. Ball MJ, Dayan AD (1972) Pathogenesis of syringomyelia. Lancet 2:799–801
3. Batzdorf U (2000) Primary spinal syringomyelia: a personal perspective. Neurosurg Focus 8:E7
4. Batzdorf U (2005) Primary spinal syringomyelia. J Neurosurg Spine 3:429–435
5. Bertram CD, Bilston LE, Stoodley MA (2008) Tensile radial stress in the spinal cord related to arachnoiditis or tethering: a numerical model 1. Med Biol Eng Comput 46:701–707
6. Caird J, Flynn P, McConnell RS (2008) Significant clinical and radiological resolution of a spinal cord syrinx following the release of a tethered cord in a patient with an anatomically normal conus medullaris. Case report. J Neurosurg Pediatr 1:396–398
7. Fischbein NJ, Dillon WP, Cobbs C, Weinstein PR (2000) The "presyrinx" state: is there a reversible myelopathic condition that may precede syringomyelia? Neurosurg Focus 8:E4
8. Gardner WJ (1977) Syringomyelia. Surg Neurol 7:370
9. Gardner WJ, Angel J (1958) The mechanism of syringomyelia and its surgical correction. Clin Neurosurg 6:131–140
10. Gardner WJ, Bell HS, Poolos PN, Dohn DF, Steinberg M (1977) Terminal ventriculostomy for syringomyelia. J Neurosurg 46:609–617
11. Hsu AR, Hou LC, Veeravagu A, Barnes PD, Huhn SL (2009) Resolution of syringomyelia after release of tethered cord. Surg Neurol 72:657–661
12. Koyanagi I, Iwasaki Y, Hida K, Houkin K (2005) Clinical features and pathomechanisms of syringomyelia associated with spinal arachnoiditis. Surg Neurol 63:350–355
13. Medow J, Sansone J, Iskandar BJ (2008) Syringomyelia and hydromyelia. In: Albright AL, Pollack IF, Adelson PD (eds) Principles and practice of pediatric neurosurgery. Thieme, New York, pp 444–476
14. Milhorat TH, Kotzen RM, Anzil AP (1994) Stenosis of central canal of spinal cord in man: incidence and pathological findings in 232 autopsy cases. J Neurosurg 80:716–722
15. Rekate HL (2002) Syringomyelia in children. In: Batjer HL, Loftus CM (eds) Textbook of neurological surgery: principles and practice. Lippincott Williams & Wilkins, Baltimore, pp 960–966
16. Sgouros S, Williams B (1995) A critical appraisal of drainage in syringomyelia. J Neurosurg 82:1–10
17. Stoodley MA, Jones NR, Yang L, Brown CJ (2000) Mechanisms underlying the formation and enlargement of noncommunicating syringomyelia: experimental studies. Neurosurg Focus 8:E2
18. Williams B, Fahy G (1983) A critical appraisal of "terminal ventriculostomy" for the treatment of syringomyelia. J Neurosurg 58:188–197

Comment

The authors describe the case of a 10-year-old boy with acquired syringomyelia secondary to fungal meningitis. Standard interventions including detethering, syrinx shunt, and open drainage of the syrinx via myelotomy had failed to control the syrinx. Sectioning of the filum at the level of the conus led to both clinical benefit and radiological improvement in the syrinx.

As the authors point out the Gardner hypothesis requires an obstruction at the foramen magnum and patency of the central canal of the spinal cord and so fails to account for many cases of syringomyelia, including their case. They discuss the concept advanced by Ball and Dyan that proposes an ingress of CSF from the spinal subarachnoid compartment along the perivascular spaces into the parenchyma of the spinal cord with subsequent cavitation and syrinx formation. This latter theory does not require that the central canal remain patent or indeed that there be any anatomical communication between the syrinx and the central canal though this would presumably have to be the case here if the cut end of the central canal (terminal ventriculostomy) is indeed the mechanism by which the syrinx has been decompressed.

The suggestion that syringomyelia be thought of as "hydrocephalus of the spinal cord" and that terminal ventriculostomy be analogous to third ventriculostomy is an interesting one. However, by draining the CSF in the syrinx into the very compartment from which it was formed might be considered analogous to performing ETV for "communicating hydrocephalus" and might in part account for the late failure rate of this technique suggested in the published literature.

The report is both interesting and provocative. It highlights a potentially useful technique for those faced with the depressing entity of refractory syringomyelia.

Dominic Thompson
London, UK

Acta Neurochir (2011) 153:1455–1459
DOI 10.1007/s00701-011-1023-4

REVIEW ARTICLE

"Minimally invasive" lumbar spine surgery: a critical review

Michael Payer

Received: 4 April 2011 / Accepted: 5 April 2011 / Published online: 1 May 2011

Abstract
Background Minimal-access technology has evolved rapidly with "tubular" or "percutaneous" approaches for decompression and stabilization in the lumbar spine. Potential benefits (smaller scars, diminished local pain, reduced blood loss, reduced postoperative wound pain, shorter hospital stays) have to be weighed against possible drawbacks (reduced orientation, steep learning curve, increased radiation exposure, dependency on technology, cost). While non-comparative case series are often rather enthusiastic, comparative studies and particularly RCTs are scarce and might convey a more realistic appreciation.
Methods A MEDLINE search via PubMed was performed to find all English-language studies comparing "open" or "traditional" or "conventional" with "minimally invasive" or "percutaneous" or "tubular" approaches in degenerative lumbar spine surgery.
Results Only nine comparative studies could be retrieved altogether. No clear benefit could be found for minimally invasive procedures in lumbar disc herniation, TLIF, or PLIF. There seems to be a slight advantage in terms of hardware safety in open procedures.
Conclusions This review, based solely on the very limited number of available *comparative* studies, shows no relevant benefit from minimally invasive techniques, and a tendency for more safety in open procedures in lumbar disc herniation, TLIF and PLIF.

Keywords Spine surgery · Lumbar spine · Minimally invasive · Percutaneous · Tubular · Review

Abbreviations

VAS	Visual analogue scale
EBL	Estimated blood loss
TLIF	Transforaminal lumbar interbody fusion
PLIF	Posterior lumbar interbody fusion
ODI	Oswestry disability index
LOS	Length of stay
RCT	Randomized controlled trial

Introduction

As for many other surgical subspecialties, minimal-access technology has evolved remarkably over the past two decades for spine surgery. Numerous endoscopic, tubular, and percutaneous approaches have been developed for traditional decompression and stabilization or placement of newly developed implants such as spacers and artificial discs. The trend for these less-invasive techniques is understandable, as smaller access should result in smaller scars, diminished local pain, reduced blood loss, reduced postoperative wound pain, and therefore shorter hospital stays with the potential to carry out certain procedures on an outpatient basis [10]. However, minimally invasive procedures have several challenges [13]:

– Three-dimensional anatomical exposure and therefore orientation is considerably reduced; manipulating instruments through small access channels is particularly

M. Payer (✉)
Department of Neurosurgery, Klinik Hirslanden,
Witellikerstrasse 40,
8032 Zurich, Switzerland
e-mail: mpayer@hotmail.com

M. Payer
Department of Neurosurgery, University Hospital of Geneva,
Geneva, Switzerland

demanding; and complication management may be very difficult and even necessitate conversion to open surgery
- A strong dependency on technical equipment (access instruments, fluoroscopy, navigation) may make minimally invasive procedures more expensive and subject to technical failures
- Placing spinal implants through tubes or "percutaneously" commonly requires high doses of radiation exposure for both the surgeon (team) and the patient
- Technical dependency coupled with increased manual challenges accounts for a very steep (i.e., long and again expensive and often complication-ridden) learning curve.

All of this leads to the fundamental question: Is there a true benefit of so-called "minimally invasive" spinal surgery or is it just a new trend with increased risks?

There are numerous enthusiastic non-comparative case series on minimally invasive spinal surgery, but caution is necessary: in the attempt to celebrate technical advances, both the involved spinal surgeons and their corresponding industry partners may be biased in analyzing "their" new surgical methods.

This critical review is undertaken in an attempt to identify potential advantages or disadvantages of minimally invasive techniques in the most commonly practiced procedures for lumbar degeneration, based exclusively on *comparative* studies.

Materials and methods

A MEDLINE search via PubMed was performed to find all English-language studies comparing "open" or "traditional" or "conventional" with "minimally invasive" or "percutaneous" or "tubular" approaches in degenerative lumbar spine surgery. Title-screening with these search terms included all language publications with the date of last search on July 31, 2010. Endoscopic procedures were not included in this review. If the title did not clearly rule out a positive search result, the abstract was screened, and if the abstract did not clearly rule out a positive search result, the article was read through. The identified articles were grouped together for the most common (and thus lumbar) spinal procedures: lumbar disc herniation (LDH), posterior lumbar interbody fusion (PLIF), and transforaminal lumbar interbody fusion (TLIF).

Results

Only nine comparative studies could be retrieved: two about lumbar disc herniation [1, 6], four about TLIF [3, 12, 14, 16] and three about PLIF [5, 9, 11]. No comparative article could be retrieved about the most common lumbar spine procedure of all, pure lumbar decompression for stenosis.

Lumbar disc herniation

One retrospective and one prospective comparative study were found.

Harrington in his retrospective study compared 35 open with 31 minimally invasive cases (expanding retractor and microscope): While surgical duration, blood loss, complications, and outcome were similar in both groups, pain medication requirements (average dose of hydrocodone 13.4 mg for the minimally invasive group and 20.9 mg for the open group) and hospitalization duration (discharge on the day of surgery in 45% in the minimally invasive group vs. 6% in the open group) were less in the minimally invasive group [6].

Arts in his randomized controlled trial found that conventional microdiscectomy with muscle retractor and microscope or loupe magnification in 159 cases resulted in generally equal outcome with slightly better pain results than microscopic disc herniation removal through a tube in 166 cases. The surgeons were familiar with both techniques and concluded that "patients who underwent tubular diskectomy fared worse with regard to leg and back pain and fewer patients reported complete recovery at 1 year". At the final 1-year follow-up, the mean Roland-Morris Disability Questionnaire score was in favor of the "conventional" group (3.4 vs. 4.7 in the "tubular" group), as was improvement on the visual analogue scale for leg and back pain and self-reported recovery (79% "good" in the conventional vs. 69% in the tubular group) [1].

TLIF

Four retrospective studies and no prospective study were retrieved.

Villavicencio et al., in their retrospective study, compared 63 open with 76 matching minimally invasive cases with a mean follow-up of 37.5 months and found that patients in the open TLIF group had greater VAS improvement and overall satisfaction than the minimally invasive group; mean EBL was less in the minimally invasive group but also low in the open group (367 cc) and hospital stay 1 day shorter in the minimally invasive group. The total rate of neurological deficit was 10.5% in the minimally invasive TLIF group compared to 1.6% in the open group. They concluded that "on the basis of the results of this study, it is safe to say that minimally invasive TLIF technique is not superior compared to the open approach. The potential benefits of less blood loss and a faster

recuperation appear to be offset by a higher rate of neurological complications" [16].

Peng et al. found a similar long-term clinical outcome and fusion rates at 2 years when retrospectively comparing 29 minimally invasive with 29 open TLIF cases; postoperative pain medication was only slightly higher in the open group, mean EBL 150 ml in the minimally invasive and 681 ml in the open group, and surgery time was longer in the minimally invasive group (216 vs. 170 min) [12].

Schizas and colleagues document a shorter hospital stay in their initial experience with 18 cases of minimally invasive compared to 18 open TLIFs; they concluded that "no difference was observed in postoperative pain, initial analgesia consumption, VAS or ODI between the groups. Three pseudarthroses were observed in the minimally invasive TLIF group although this was not statistically significant. A steeper learning effect was observed for the minimally invasive TLIF group" [14].

Dhall and coworkers compared 21 cases of mini-open TLIF with average follow-up of 24 months with 21 cases of open TLIF with mean follow-up of 34 months. While EBL (194 cc vs. 505 cc) and length of stay (3 days vs. 5.5 days) were reduced in the mini-open group, a higher rate of hardware-associated complications was found in the mini-open TLIF (one misplaced screw, one cage migration, one pseudarthrosis) compared to the open technique (one misplaced screw) [3].

PLIF

Two retrospective studies and one prospective cohort study were retrieved.

Ntoukas retrospectively compared 20 minimally invasive with 20 open PLIFs and found ”less blood loss, less postoperative pain, quicker recovery and shorter duration of hospitalization. However, in the long run, one year after surgery, both groups showed no significant difference with regards to clinical and radiographic outcome", and "...on despite these benefits, the minimally invasive group also experienced a longer surgical and radiation time as compared to the 'open' group" [9].

Gepstein retrospectively compared 30 cases of minimally invasive PLIF with average follow-up of 29 months with earlier 30 cases of open PLIF for post-discectomy pain. Mean hospitalization was 2.75 days and blood loss negligible in the minimally invasive group, 5.5 days and 750 cc in the open group. Clinical and radiological results were comparable at the mean follow-up of 29 months in the minimally invasive group and 37 months in the open group [5].

Park prospectively documented 32 minimally invasive and 29 open PLIF cases, whereby minimally invasive procedures were not covered by the country’s insurance and thus were chosen only by financially "healthy" patients. The authors found no significant difference between the two groups in clinical and radiographic results with 1-year minimum follow-up. The minimally invasive group had less EBL of 433 cc on average compared to 738 cc in the open group and a shorter hospital stay of 5.3 days compared to 10.8 days in the open group. Whether the financial background played a role in leaving the hospital earlier to return to professional activity earlier must remain open. The minimally invasive group needed longer surgical time with 192 min vs. 149 min in the open group and showed two cases of technical complications in the form of misplaced pedicle screw and cage migration [11].

Discussion

"Minimally invasive" spinal procedures have been (and in many spinal centers still are) in the focus of both the medical technology industry and the involved developing surgeons. Some undebatable advantages may exist in creating reduced access morbidity, but making a compromise on exposure and depending on "heavy" technological equipment may come at a high price in terms of patient safety and finance.

In this review, "traditional" and "minimally invasive" approaches in the most common posterior lumbar procedures were analyzed from available *comparative* articles. In lumbar disc herniation, no relevant benefit was found in minimally invasive procedures [1, 6]. Though LOS and perioperative pain medication were reduced in the minimally invasive group in one study, such a retrospective evaluation can be biased as incentives for discharge might have been different for the groups; furthermore, perioperative pain medication differed only so little that there are no relevant consequences in daily practice (average dose of hydrocodone 13.4 mg for the minimally invasive group and 20.9 mg for the open group) [6]. In the single more meaningful prospective study a slight superiority in clinical 1-year outcome could be shown for the "open" procedure [1].

No convincing benefit was found for minimally invasive TLIF compared to open TLIF [3, 12, 14, 16]. The report of higher rates of neurological complications [16], a "steep learning curve" [14], and higher rate of hardware-associated complications [3] for the minimally invasive techniques convey little enthusiasm. The only potential advantage in the minimally invasive TLIF was a reduced EBL in one series [12], which in a retrospective series has limited meaning as more attention on hemostasis is likely to be spent on the "new" minimally invasive technique.

For PLIF, slightly reduced initial postoperative LOS or EBL could be reported for minimally invasive techniques, whereas long-term outcome was not different between open and minimally invasive procedures [5, 9, 11], However,

decreased EBL and shorter LOS in the "new minimally invasive" technique again is a weak argument, as the new technique has been compared retrospectively with a historical "open" control group [5]. In the only prospective study, misplaced pedicle screws and cage migration, though rare, were found only in the minimally invasive group [11].

Although this review, based solely on comparative studies, is far from giving answers as to which approach is best for which spinal procedure, it clearly shows not only no relevant benefit from minimally invasive procedures, but even a tendency for safer open surgery.

The current literature review finding is in accordance with Epstein's remarkable comment on minimally invasive cervical laminoforaminotomy: Many neurosurgical operations are already very difficult even with maximal exposure; optimal exposure facilitates maneuvering the microscope and surgical instruments, avoids the movement restrictions of minimally invasive approaches, and helps to limit complications by adequate exposure of neural and vascular structures. He further argues that the true complication rate, on or off the learning curve, might not be available, and that informal colleague discussions reveal disillusion and reverting back to open procedures; the overall aim of spinal surgery is to perform safe and cost-effective procedures [4].

Compared to transthoracic, transabdominal, or arthroscopic procedures, where increased use of minimally invasive surgery is facilitated by anatomically pre-existing cavities, minimally invasive spinal procedures from a posterior approach lack such "key-hole" anatomy and can only be performed by either making compromise on exposure or increasing the use of technological help such as navigation and computer assistance in hardware placement. However, there are several practical concerns with both of these "compensatory" strategies:

- Learning curves are a particular challenge in all surgical specialties, as optimal surgical management requires many years of experience. Investing more time in minimally invasive procedures either prolongs the entire surgical training duration or requires cutting back on traditional techniques, which in turn hurts intraoperative crisis management and decision-making [2]. These deficiencies deserve educational effort at a higher priority than accorded so far.
- Radiation exposure during minimally invasive procedures has not been clearly evaluated so far and may be a concern; though systematic comparative studies are not available, one prospective controlled trial found that minimally invasive lumbar microdiscectomy exposed the surgeon to significantly more radiation than open microdiscectomy [8]. On the other hand, navigation-assisted fluoroscopy has also been shown to decrease radiation exposure during minimally invasive spine surgery in the case of TLIF; however, as this was a cadaver study, interpretation is limited [7].
- The recent explosion of innovative technology in minimally invasive spine surgery, coupled with navigation, creates new cost. Assessment of cost-effectiveness, e.g., in quality-adjusted life years is always a future undertaking and not directly available [15]. However, as the cost-effectiveness must remain open, it is at least clear that additional technological use primarily increases cost and may or may not be "redeemed" in the future.

Shortcomings of this review are the limited number of available comparative studies with an extreme paucity of RCTs, and the lack of comparable financial analyses for the reported open and minimally invasive procedures. Altogether, the role of so-called minimally invasive spinal surgery is far from being defined and Sibylline oracles such as "With education, training, and further research, more of our traditional open surgical management will be augmented or replaced by these technologies and approaches in the future" [10] may possibly turn into a disillusion.

Conclusions

This review, based solely on the very limited number of available *comparative* studies, shows no relevant benefit from minimally invasive techniques, and a tendency for more safety in open procedures in lumbar disc herniation, TLIF, and PLIF.

Conflicts of interest None.

References

1. Arts MP, Brand R, van den Akker ME, Koes BW, Bartels RH, Peul WC, Leiden-The Hague Spine Intervention Prognostic Study Group (SIPS) (2009) Tubular diskectomy vs. conventional microdiskectomy for sciatica: a randomized controlled trial. JAMA 302 (2):149–158
2. Chung RS, Ahmed N (2010) The impact of minimally invasive surgery on residents' open operative experience: analysis of two decades of national data. Ann Surg 251(2):205–212
3. Dhall SS, Wang MY, Mummaneni PV (2008) Clinical and radiographic comparison of mini-open transforaminal lumbar interbody fusion with open transforaminal lumbar interbody fusion in 42 patients with long-term follow-up. J Neurosurg Spine 9(6):560–565
4. Epstein NE (2009) Minimally invasive/endoscopic vs. "open" posterior cervical laminoforaminotomy: do the risks outweigh the benefits? Surg Neurol 71(3):330–331
5. Gepstein R, Shabat S, Reichel M, Pikarsky I, Folman Y (2008) Treatment of postdiscectomy low back pain by percutaneous

posterior lumbar interbody fusion versus open posterior lumbar fusion with pedicle screws. Spine J 8(5):741–746
6. Harrington JF, French P (2008) Open versus minimally invasive lumbar microdiscectomy: comparison of operative times, length of hospital stay, narcotic use and complications. Minim Invasive Neurosurg 51(1):30–35
7. Kim CW, Lee YP, Taylor W, Oygar A, Kim WK (2007) Use of navigation-assisted fluoroscopy to decrease radiation exposure during minimally invasive spine surgery. Spine J 8(4):584–590
8. Mariscalco MW, Yamashita T, Steinmetz MP, Krishnaney AA, Lieberman IH, Mroz TE (2010) Radiation exposure to the surgeon during open lumbar microdiscectomy and minimally invasive microdiscectomy: a prospective, controlled trial. Spine 36(3):255–260
9. Ntoukas V, Müller A (2010) Minimally invasive approach versus traditional open approach for one level posterior lumbar interbody fusion. Minim Invasive Neurosurg 53(1):21–24
10. Oppenheimer JH, DeCastro I, McDonnell DE (2009) Minimally invasive spine technology and minimally invasive spine surgery: a historical review. Neurosurg Focus 27(3):E9
11. Park Y, Ha JW (2007) Comparison of one-level posterior lumbar interbody fusion performed with a minimally invasive approach or a traditional open approach. Spine 32(5):537–543
12. Peng CW, Yue WM, Poh SY, Yeo W, Tan SB (2009) Clinical and radiological outcomes of minimally invasive versus open transforaminal lumbar interbody fusion. Spine 34(13):1385–1389
13. Perez-Cruet MJ, Fessler RG, Perin NI (2002) Review: complications of minimally invasive spinal surgery. Neurosurgery 51(5 Suppl):S26–S36
14. Schizas C, Tzinieris N, Tsiridis E, Kosmopoulos V (2009) Minimally invasive versus open transforaminal lumbar interbody fusion: evaluating initial experience. Int Orthop 33(6):1683–1688
15. Smith HE, Rihn JA, Brodke DS, Guyer R, Coric D, Lonner B, Shelokov AP, Currier BL, Riley L, Phillips FM, Albert TJ (2009) Spine care: evaluation of the efficacy and cost of emerging technology. Am J Med Qual 24(6 Suppl):25S–31S
16. Villavicencio AT, Burneikiene S, Roeca CM, Nelson EL, Mason A (2010) Minimally invasive versus open transforaminal lumbar interbody fusion. Surg Neurol Int 1:12

Acta Neurochir (2011) 153:1461–1468
DOI 10.1007/s00701-011-1003-8

CLINICAL ARTICLE

Cooled radiofrequency application for treatment of sacroiliac joint pain

Haktan Karaman · Gönül Ölmez Kavak · Adnan Tüfek · Feyzi Çelik · Zeynep Baysal Yıldırım · Mehmet Salim Akdemir · Orhan Tokgöz

Received: 7 January 2011 / Accepted: 17 March 2011 / Published online: 10 April 2011

Abstract
Background The unavailability of an effective and long-lasting treatment for sacroiliac-based pain has led researchers to study the efficacy of radiofrequency in denervation. In this study, we aimed to investigate the efficacy and safety of novel cooled radiofrequency application for sacral lateral-branch denervation.
Methods Patients experiencing chronic sacroiliac pain were selected for our observational study. Fluoroscopy guidance cooled radiofrequency denervation was applied on the L5 dorsal ramus and the S1-3 lateral branches on patients who had twice undergone consecutive joint blockages to confirm the diagnosis and obtained at least 75% pain relief. At the 1st, 3rd and 6th month postoperatively, the patients' pain was evaluated using a visual analog scale (VAS), and their physical function was evaluated with the Oswestry Disability Index (ODI).
Results Cooled radiofrequency was applied on a total of 15 patients. Prior to the procedures, the median VAS score (interquartile range) was 8 (7–9), but at the 1st, 3rd and 6th month, this had fallen to 3 (1–4), 2 (1–3) and 3 (2–4). The baseline median ODI score (interquartile range) was 36 (32–38), while at the 1st, 3rd and 6th month, it was 16 (8–20), 12 (9–18) and 14 (10–20), respectively. At the final control, while 80% of the patients reported at least a 50% decline in pain scores, 86.7% of those reported at least a ten-point reduction in ODI scores.
Conclusion It was seen that the cooled radiofrequency used for sacroiliac denervation was an effective and safe method in the short to intermediate term.

Keywords Cooled radiofrequency · Sacroiliac joint · Pain · Denervation · Radiofrequency

H. Karaman (✉)
Pain Management Center, Department of Anesthesiology,
Dicle University,
21280 Diyarbakir, Turkey
e-mail: haktan72@yahoo.com

G. Ö. Kavak · A. Tüfek · F. Çelik · Z. B. Yıldırım ·
M. S. Akdemir · O. Tokgöz
Department of Anesthesiology, Dicle University,
21280 Diyarbakir, Turkey

Introduction

Although there are many reasons for chronic low-back pain, an important source of labor loss in society, perhaps the most puzzling is pain resulting from sacroiliac joints. Research has shown that at least 15–30% of chronic low-back pain is of sacroiliac origin [4, 9, 25]. However, it does not manifest itself in a typically unique clinical pattern (most axial low-back pains resemble one another). In addition, there are no sufficient criteria for diagnosis. Therefore, it is difficult to treat [9].

The sacroiliac joint is a complex structure made up of intra-articular and extra-articular components. This joint, which has the largest joint surface in the body, is no different from other joints in that it becomes a source of pain as it undergoes the degeneration that accompanies aging. However, the pain generated by the sacroiliac joint is not simply the result of degeneration. Many other factors—such as infection, inflammatory diseases affecting the sacroiliac joint (e.g., ankylosing spondylitis and Reiter's syndrome), malignancy, pregnancy, lumbar spinal fusion, accidents, falls, torsional strain and repetitive trauma, trauma and idiopathic reasons—are the most frequently encountered [2, 4, 11, 15].

The most complex aspect of the sacroiliac joint is the feature related to its innervations. The innervations of the anterior and posterior parts of the joint are different from one another [1]. While it is thought that the sensorial branches of the posterior part stem mostly from the L4-S3 dorsal rami, some authors believe that the L3 and S4 are also responsible for innervations [4]. In fact, the most important peculiarity creating this complexity is the absence of a single-type innervation in the sacroiliac joint. Just as innervations can vary from person to person and from level to level, even in the same person there may be differences between the right and left sides [1, 4, 6, 25].

One of the most difficult aspects of chronic sacroiliac pain is the difficulty in reaching a diagnosis. This is because clinical presentation is mostly non-specific and the specificity of the stress maneuver and Patrick's and Gaenlen's tests, frequently used in physical examination, have low specificity [12]. Similarly, such imaging methods as plain radiography, computed tomography (CT), magnetic resonance imaging (MRI), photon emission CT (SPECT) and bone scans also have low sensitivity and specificity [20]. Perhaps it is also for this reason that the only reliable diagnostic method used is local anesthetic applied to the sacroiliac joint, along with imaging methods [1, 4, 18, 22].

The treatment of sacroiliac low-back pain begins with empirically non-invasive conservative treatment methods. These include NSAIDs, physical therapy, massage and chiropractic manipulation [1, 7]. In chronic, persistent and serious cases, steroid injections into the sacroiliac joint are also used [20]. However, unfortunately, this is not effective long-term [13]. It has been argued that fusion, one of the surgical methods, is also not sufficiently effective [5].

The unavailability of an effective and long-lasting treatment for sacroiliac-based pain has led researchers to study the efficacy of radiofrequency (RF) in denervation. In recent years, denervation of the lateral branches, which invervate the sacroiliac joint, with RF has begun to attract great interest [1, 6, 14, 25]. Nevertheless, unfortunately, with conventional RF, only small lesions are formed; and consequently, the chance of successfully finding and denerving nerves which have already complex and variable localizations are lowered [17].

Cooled RF (CRF), used as an alternative to conventional RF, is a method with a closed water circuit. Because of this property, the electrodes can create a wider heat lesion without charring of tissues in the proximity of the probe tip. Compared with conventional RF, the chance of getting hold of the nerves increases [6, 16]. Nevertheless, there are still insufficient studies on the efficacy of this method.

In this study, we investigated the 6-month effectiveness and safety of denervation of the sacral lateral branches observationally in chronic pain originating in the sacroiliac joint.

Methods

Study design and setting

After obtaining approval from the institutional review board, this study was conducted in the pain management unit of a university hospital using a observational, non-randomized and non-controlled method. Patient enrollment began in December 2009 and ended in June 2010. After providing written and oral information related to the study and the treatment to all the patients, written consent that they accepted the treatment was obtained from all of them.

Follow-up period The patients were interviewed before and 1, 3 and 6 months after the procedure independently by a physician who was not part of the study.

Participants

The following criteria for including patients in the study were used: (1) axial low-back pain observed below the L5 vertebra for 6 months; (2) greater than 75% pain relief from two separate intra-articular blocks with no more than 2 ml local anesthetic injected per block; (3) failure to obtain adequate response to previous conservative treatments conducted for at least 3 months; (4) being older than 18 years of age.

The following criteria for exclusion from the study were used: (1) findings of lumbar disc herniation with associated radiculopathy; (2) the finding of spinal canal stenosis confirmed by MRI or CT; (3) having had previous spinal surgery for whatever reason (regardless of whether it was in the region where the procedure is to be performed); (4) the presence of psychiatric disorder; (5) pregnancy; (6) presence of general contraindications to invasive procedures (e.g., hemorrhagic diathesis, systemic infection or local infection where the procedure is to be applied, and a known history of allergies to substances that are to be used).

Procedures

Diagnostic sacroiliac joint blockage

To confirm that the chronic pain was coming from the sacroiliac joint, all patients were subject twice, at 1-week intervals, to image-guided controlled comparative anesthetic blocs to the sacroiliac joint prior to CRF. The patients were placed in the prone position on the C-arm table for the procedure. Under anterior-posterior (AP) view, a 21-G spinal needle was inserted in the lower third of the sacroiliac joint. After confirming the intraarticular en-

trance with 0.5 ml conrast material, 2 ml local anesthetic was injected. In the first procedure, a 2% lidocaine was used, while in the second, a 0.5% bipuvacaine was injected. Patients, who were discharged immediately after the procedure, were asked to carry on with their normal routine and record their pain in a pain diary on a visual analog scale (VAS). One week after each procedure, the patients were reevaluated. Denervation of the sacroiliac branches was only planned for patients who had shown at least a 75% reduction in their pain scores compared with the initial value.

CRF procedures

All procedures were C-arm fluoroscopy-guided and performed under local anesthesia. Two hours before the procedure, the patients who were to undergo the procedure were given antibiotics intravenously and taken into the operating room. After undergoing routine monitoring (e.g., pulsoximetry, TA and ECG), they were placed in the prone position on the fluoroscopy table. The area where the procedure was to be performed was cleaned with an iodine antiseptic solution and draped to maintain a sterile environment. So as not to mask potential complications, in general, sedation was not preferred. However, when necessary, for light sedation, 1–3 mg midazolam and/or 50–100 μg fentanyl were given intravenously. Local anesthetic was applied subcutaneously with a 1% lidocaine infiltration.

For L5 dorsal ramus denervation, technique has been extensively explained in previous literature [17]. In short, the target location is the notch between the ala of the sacrum and the superior articular process of the sacrum. This corresponds to the known running course of the L5 dorsal ramus. A 17-G introducer with stylet was inserted onto this target location. The tip of the stylet's location and depth was checked with the oblique and lateral images. After satisfactory positioning, to prevent procedure-related pain, the stylet was removed and 0.5 ml lidocaine was injected through the introducer. Then, the SInergy probe (Baylis Medical, Montreal, Canada) was put into place and denervation (set temperature=60°C, ramp rate=80°C/min, time=2:30 min) was performed. At this stage, a single lesion was formed in all patients.

Denervation of the S1-3 lateral branches was performed in a way similar to that found in the literature [16]. Briefly, the pelvises of the patients, who were lying in a prone position, were viewed using AP imaging. Once the locations of the sacral foramina were located, denervation was performed beginning with the S1 level and moving in succession. To facilitate the procedure, a 27-G spinal needle was inserted in every foramina to act as a guide. With the help of the Epsilon Ruler (Baylis Medical, Montreal, Canada), the sacral foramina, approximately 1 cm away, were reached by the introducer with stylet (Fig. 1). After the end of the stylet touched the bone, the depth of the needle was checked with a lateral image (Fig. 2). What is most crucial at this stage is making sure that the needle does not mistakenly enter the foramina. Once the needle is satisfactorily positioned, the SInergy (Baylis Medical, Montreal, Canada) CRF probe is inserted and a lesion was formed (set temperature=60°, ramp rate=80°C/min, time=2:30 min). This procedure was repeated for all target locations at each level. At the S1 and S2 levels, three lesions were created on the right, according to the position of the hands on a clock, at 2:30, 4:00 and 5:30 and on the left at 9:30, 8:00 and 6:30. At the S3 level, a total of two lesions were made on the right, at 2:30 and 4:00, and on the left, at 8:00 and 9:30. A total of nine lesions were made unilaterally for each patient.

After the procedure, the patients were transferred to recovery rooms, where they would stay for 4 h. Here, the patients were interviewed by the clinical nurse to identify early complications and then were discharged with their instructions. Post-operatively, the patients were told that, for a few days, they should avoid excessive activity, lifting, or other forms of increased physical activity.

Outcome measurements

Pain was evaluated on a ten-point VAS score. On this scale, a score of "0" represents no pain, while "10" is defined as the most possible pain imaginable. Physical function was assessed by the 50-point Oswestry Disability Index (ODI). Patient satisfaction was evaluated on a four-point scale: 1=bad, 2=fair, 3=good and 4=excellent.

In addition, the data on the variable patients' age, sex, duration of symptom, symptom's side and complications to the procedure were collected for statistical analysis.

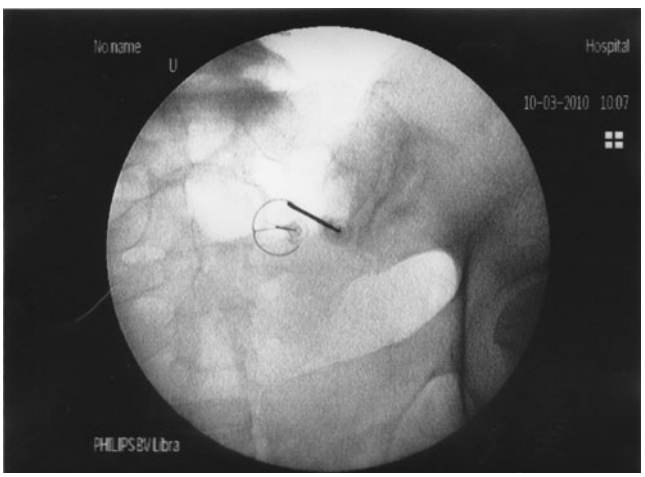

Fig. 1 In the AP image, a picture of the positions of the CRF probe, taking the Epsilon Ruler and spinal needle as a reference. In this picture, the probe is placed at the 2:30 level

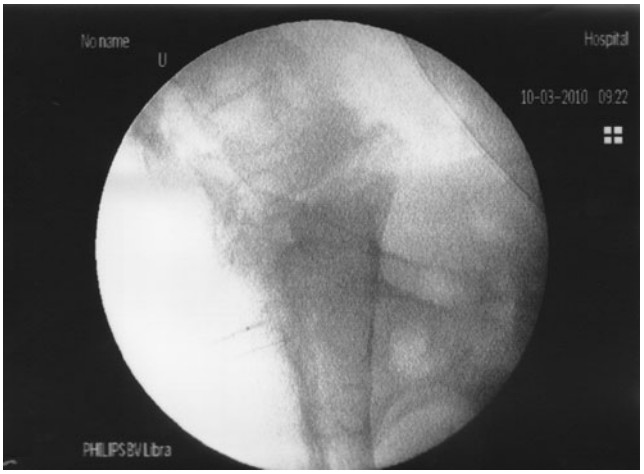

Fig. 2 In the lateral image, a picture showing the depth of the CRF probe. What should be focused on here is checking whether the tip of the probe has entered the sacral foramen

The criteria for successful treatment were established as a reduction of pain by at least 50% in the VAS score and an improvement in the ODI score of at least 10 points.

Statistical methods

All data were analyzed using the statistical package SPSS version 15.0 for Windows and Medcalc version 10.3.0.0 for Windows. Repeated measurements ANOVA parametric test for repeated measurements was used to evaluate the improvements in VAS and ODI scores both before and after the procedure. When the repeated measurements ANOVA test showed a statistical difference, we used a paired samples *t*-test with Bonferonni's correction to perform pairwise comparisons. Also, we used the Spearman correlation coefficients to study the effects of various factors on the outcomes. $P<0.05$ was considered statistically significant in all analyses.

Results

Demographic characteristics and descriptive data

A total of 21 patients were included in the study. Six patients, because they did not obtain ≥75% pain relief either in the first diagnostic block (four patients) or the second confirmatory diagnostic block (two patients), were excluded from the denervation procedure. Thus, a total of 15 patients underwent denervation. The mean age of patients receiving a sacral lateral branch neurotomy (±SD) was 47.1±16.2 years; of these patients, 80% were women. While the mean period for symptoms (±SD) was 41.6±43.6 months, the procedure was performed unilaterally on all the patients (Table 1).

Outcome data

Pain relief While the median VAS score (interquartile range) was 8 (7–9) prior to the procedure, by the 1st month, it had decreased to 3 (1–4); the values for the 3rd and 6th months were 2 (1–3) and 3 (2–4), respectively (Fig. 3). Compared with the baseline, while all follow-ups showed a statistically significant decline in VAS score, when the follow-up periods were compared with one another, there was no statistically significant difference (Table 2). At the final follow up, 80% of the patients reported a decrease in pain of at least 50%. All of the patients participating in the study reported a decline in pain scores of at least 2 points.

Physical improvement The average ODI score (interquartile range) prior to the neurotomy was 36 (32–38), while by the 1st month it had improved to 16 (8–20). The values for the 3rd and 6th months were 12 (9–18) and 14 (10–20), respectively (Fig. 4). Compared with the baseline, a statistically significant decline in ODI scores was seen at all follow-up periods. However, when compared with each other, there was no statistically significant difference between follow-up periods (Table 2). In the 6th month, 86.7% of the patients reported improvement of at least 10 points on their ODI scores.

Moreover, taking the 6th month as the base, the influence of various factors such as age, sex and duration of symptom on ODI and VAS scores were researched. No statistically significant impact of these factors was found (Table 3). However, a positive correlation between the reduction in the VAS and ODI scores in the 6th month was found (Table 4).

Patient satisfaction Evaluating patient satisfaction using the four-point patient satisfaction scale, (1=the least satisfaction and 4=the greatest satisfaction), the percent of

Table 1 Demographic characteristics

Age (year)	Mean±SD	47.1±16.2
	Range	29–76
Gender	Women *n* (%)	12 (80)
	Men *n* (%)	3 (20)
Duration of symptom (month)	Mean±SD	41.6±43.6
	Range	8–120
Side	Right *n*	9
	Left *n*	6

SD standard deviation

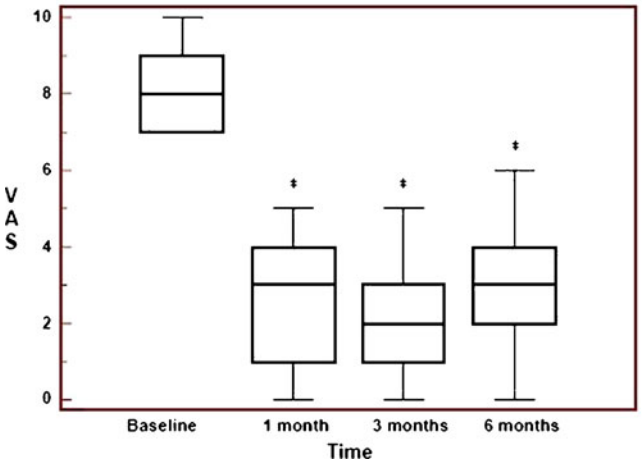

Fig. 3 Changes in VAS values at follow-ups. Compared with the baseline, a statistically significant difference is seen between the scores of all follow-up periods. *$P<0.05$

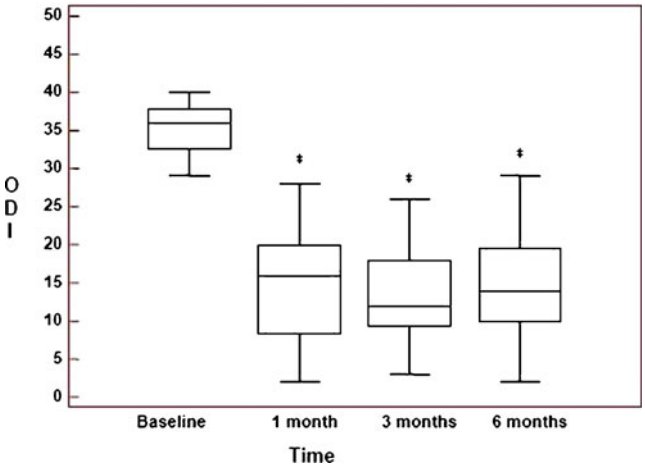

Fig. 4 Change of ODI scores over time. When compared with the baseline, a statistically significant difference was seen between all follow-up periods. *$P<0.05$

those stating "good and excellent" was 80% (12 persons) on the last follow-up.

Safety

No major complications, such as neuritis, motor neuron damage, infection, hemorrhagia or hematoma, were encountered either during or after the procedure. The hip pain that was seen in nearly all of the patients and lasted about 5 days dissipated without any intervention other than simple analgesics.

Discussion

This observational study on the efficacy of CRF denervation in patients with sacroiliac-based chronic pain had highly successful results. While a ≥50% decrease in VAS scores compared with the baseline was seen in 80% of our patients, ODI scores increased by 10 points in 86.7% of them. The basic reason for our obtaining such a degree of success may be our strict inclusion criteria. We performed two consecutive sacroiliac diagnostic blocks with two different local anesthetics on our patients who we believed had clinically sacroiliac-based pains to confirm such a diagnosis. That at least 75% pain relief was obtained for at least 3 h after each of these blocks was our most important criterion. Thus, we believe that we reduced the false-positive rate to a meaningful level.

There are many treatment modalities to treat sacroiliac joint pain. One of them is conservative management. The conservative treatment of sacroiliac joint pain primarily involves medical management, with little benefit from physical therapy. Indeed, the conservative treatments primarily should address the underlying cause. For example, while in postural and gait disturbances, exercise therapy and manipulation may reduce pain and improve mobility; in patients with true or apparent leg length

Table 2 Pair-wise comparisons of all-time VAS and ODI scores

			Mean difference	Standard error	P [a]	95% CI [a]
$VAS_{baseline}$	–	$VAS_{1\ month}$	5.7	0.4	<0.0001	4.5–6.9
	–	$VAS_{3\ months}$	6.0	0.4	<0.0001	4.7–7.3
	–	$VAS_{6\ months}$	5.5	0.4	<0.0001	4.2–6.8
$VAS_{1\ month}$	–	$VAS_{3\ months}$	0.3	0.2	1.0000	-0.5–1.0
	–	$VAS_{6\ months}$	-0.3	0.3	1.0000	-1.2–0.7
$VAS_{3\ months}$	–	$VAS_{6\ months}$	-0.5	0.2	0.2434	-1.3–0.2
$ODI_{baseline}$	–	$ODI_{1\ month}$	19.9	1.7	<0.0001	14.6–25.1
	–	$ODI_{3\ months}$	21.1	1.6	<0.0001	16.2–26.0
	–	$ODI_{6\ months}$	20.1	1.7	<0.0001	14.9–25.3
$ODI_{1\ month}$	–	$ODI_{3\ months}$	1.3	1.4	1.0000	-3.0–5.5
	–	$ODI_{6\ months}$	0.3	1.6	1.0000	-4.6–5.2
$ODI_{3\ months}$	–	$ODI_{6\ months}$	-1.0	0.8	1.0000	-3.5–1.5

VAS Visual Analog Scale, *ODI* Oswestry Disability Index

[a] Bonferroni corrected

Table 3 Effects of various factors on outcome at 6 months after treatment

			Decrease in VAS	Decrease in ODI
Spearman rank correlation coefficient	Duration of symptom	Correlation coefficient	0.000	0.066
		Significance level *P*	1.000	0.806
		n	15	15
	Gender	Correlation coefficient	-0.299	-0.279
		Significance level *P*	0.263	0.296
		n	15	15
	Age	Correlation coefficient	0.472	0.419
		Significance level *P*	0.077	0.117
		n	15	15

discrepancy, the use of shoe inserts to more equitably distribute the load borne by the sacroiliac joints may be useful. Yet, there is no controlled study evaluating patients with injection-confirmed sacroiliac joint pain [4, 24]. Also, one of the treatments that can be applied is intra-articular injection. Many investigators suggest that fluoroscopically guided sacroiliac joint injections with local anesthetic and steroids can provide good to excellent pain relief lasting up to 1 year [4]. However, these injections have been performed into the sacroiliac joint for decades, though evidence of their long-term benefit is mixed [8]. Latterly, RF lesioning of the sacroiliac joint's dorsal innervations has been introduced to prolong the duration pain relief and to avoid the side effects of steroids [8]. There are five different types of RF technique used. One of these techniques is the conventional monopolar RF method. With this method, an RF lesion is created on sacral nerves at 80–90°C. The efficacy of conventional monopolar RF treatment of the sacroiliac joint is illustrated by several studies [3, 12, 25]. Although the patients' selection criteria, RF parameters and success definition have varied widely between studies, the biggest problem is that only smaller lesions can be created by this method [17]. Because of variable and extensive innervations of the dorsal sacroiliac joint, it may miss some nerve branches without exhaustive search and concomitant tissue trauma [8]. To circumvent anatomical variations in innervations, conventional bipolar RF has been used to ablate either the SI joint itself, or the sacral lateral branches by other researchers [1, 10]. With this method, it is aimed to ablate the locations of multiple nerves at once, creating larger lesions. Since there are only two studies assessing the effectiveness of conventional bipolar RF, it cannot be said that this method is an effective and reliable treatment option. Another method for the RF lesioning of the sacroiliac joint is pulsed RF applications. Like the conventional RF technique, this method also use electrical stimulation to guide electrode placement near individual lateral branches of the dorsal sacral rami [8], but there is only one study, in which the patients underwent pulsed RF application of the medial branch of L4, posterior primary rami of L5, and lateral branches S1 and S2, in this method [23]. More recently, a new treatment method for sacroiliac joint pain—namely, bipolar palisade treatment of sacroiliac joint pain—has been introduced by Cosman and Gonzales [8]. This bipolar "palisade" (a defensive fence) creates a continuous lesion spanning the region through which multiple sacral lateral branch nerves travel along irregular, branching paths to reach the sacroiliac joint [8]. However, there is no clinical trial assessing the efficacy of this method, so it is too early to say something about the efficacy of this method. As a new treatment option introduced recently, CRF may be superior to all of them because obviously bigger lesions can be created by CRF, minimizing the effect of tissue charring to limit lesion expansion. Thus, to create a large lesion with this method increases the likelihood of the sacral nerve ablation because multiple sacral lateral branch nerves travel along irregular, branching paths to reach the sacroiliac joint.

Table 4 Correlations between the post-procedure changes in VAS and ODI scores

			ODI
Spearman's rho	VAS	Correlation Coefficient	0.755[a]
		Sig. (two-tailed)	0.001
		n	15

[a] Correlation is significant at the 0.01 level (two-tailed)

In a controlled study on the efficacy of CRF, Cohen et al. [6] found that 57% of the patients had ≥50% pain 6 months after the procedure. There are two possible reasons for a success lower than ours. First, in this study, a single diagnostic block was performed on the patients. As the authors themselves emphasize, single sacroiliac blocks can produce up to 20% false positives [12, 13]. Therefore, false positives may have directly led to a negative conclusion. Second, in this study, different from ours, conventional RF was used at the L4 and L5 levels. Because conventional RF

creates a lesion in a more limited area, the chance of reaching the nerves targeted for denervation may be lower [7]. Regardless of the extent of speculation concerning innervation by the L4 dorsal ramus of the sacroiliac joint, the contribution of the L5 dorsal ramus has generally been confirmed [7, 17]. Hence, omitting the L5 dorsal ramus could be a reason for the negative or low success of denervation. Moreover, when positioning a conventional electrode, it is common practice to align the long axis of the active tip with the running course of the nerve. This maximizes the length of nerve coagulation, but requires precise electrode trajectory. However, because the lesion created by CRF is spherical, the different electrode trajectory may not affect the lesion orientation [17]. In other words, forming maximal coagulation through CRF depends more on proximity to the target than on the electrode trajectory. Therefore, performing CRF on the L5 nerve theoretically improves the chance of success.

In a retrospective case series researching the effectiveness of CRF, Kapural et al. [16] performed 47 procedures (unilaterally and bilaterally) on 27 patients. They emphasized that 50% of the patients reported a 50% decrease in VAS scores and a similar improvement in other physical parameters. The reason for the relatively lower success they obtained compared with our study may be their condition of a 50% or higher relief of pain with the diagnostic block. Our condition that such pain relief be at least 75% may have helped us achieve a patient group that would respond better to the denervation procedure. Furthermore, compared with our patient group, the higher average age (61 years) of the patients in this group and the longer symptom period (6.2 years) may also have led to a relatively less successful outcome.

The most important problem for denervation procedures is the short clinical effect due to nerve ending regeneration. For example, the pain relief after facet joint RF typically begins to diminish at about 6 months after the procedure, and most patients experience full pain recurrence by about 1 year after the procedure [21]. However, the duration of the effect of sacroiliac joint RF is unknown yet.

The RF application has some complications restricting its use. RF ablation, by generating heat in neural tissue and producing coagulation, carries potential risks of neuritis [19]. As to minor complications, temporary numbness [6, 7, 17], temporary increase in pain [7, 17] and infection [7] were also reported. In our study, we did not encounter any complications other than temporary and limited complaints of pain. All of these data show that the CRF procedure is a safe method. However, to demonstrate that it is completely safe, extensive long-term studies are needed.

The major limitation of this study was the small number of cases with short follow-up period. In addition, there was no control group undergoing conservative treatment only or sham treatment. Without a control group and a clearcut image-based diagnosis, it may be impossible to know whether or not the technique was effective. Hence, to rule out the potential placebo effect, randomised controlled studies with longer follow-up period are needed. Nevertheless, we believe our study is significant in that it provides important clues for the use of CRF, a new way of treating sacroiliac joint pain.

In conclusion, this report demonstrates that in the short to intermediate term, CRF is an effective and safe method for the treatment of sacroiliac joint pain.

Conflicts of interest None.

References

1. Burnham RS, Yasui Y (2007) An alternate method of radiofrequency neurotomy of the sacroiliac joint: a pilot study of the effect on pain, function, and satisfaction. Reg Anesth Pain Med 32:3–6
2. Chou LH, Slipman CW, Bhagia SM, Tsaur L, Bhat AL, Isaac Z, Gilchrist R, El Abd OH, Lenrow DA (2004) Inciting events initiating injection-proven sacroiliac joint syndrome. Pain Med 5:26–32
3. Cohen SP, Abdi S (2003) Lateral branch blocks as a treatment for sacroiliac joint pain: a pilot study. Reg Anesth Pain Med 28:113–119
4. Cohen SP (2005) Sacroiliac joint pain: a comprehensive review of anatomy, diagnosis, and treatment. Anesth Analg 101:1440–1453
5. Cohen S, Hurley RW (2007) The ability of diagnostic spinal injections to predict surgical outcome. Anesth Analg 105:1756–1775
6. Cohen SP, Hurley RW, Buckenmaier CC 3rd, Kurihara C, Morlando B, Dragovich A (2008) Randomized placebo-controlled study evaluating lateral branch radiofrequency denervation for sacroiliac joint pain. Anesthesiology 109:279–288
7. Cohen SP, Strassels SA, Kurihara C, Crooks MT, Erdek MA, Forsythe A, Marcuson M (2009) Outcome predictors for sacroiliac joint (lateral branch) radiofrequency denervation. Reg Anesth Pain Med 34:206–214
8. Cosman ER Jr, Gonzalez CD (2011) Bipolar radiofrequency lesion geometry: implications for palisade treatment of sacroiliac joint pain. Pain Pract 11:3–22
9. Dreyfuss P, Dreyer S, Cole A, Mayo K (2004) Sacroiliac joint pain. J Am Acad Orthop Surg 12:255–265
10. Ferrante FM, King LF, Roche EA, Kim PS, Aranda M, Delaney LR, Mardini IA, Mannes AJ (2001) Radiofrequency sacroiliac joint denervation for sacroiliac syndrome. Reg Anesth Pain Med 26:137–142
11. Fortin JD (1993) Sacroiliac joint dysfunction. A new perspective. J Back Musculoskelet Rehabil 3:31–43
12. Gevargez A, Groenemeyer D, Schirp S, Braun M (2002) CT guided percutaneous radiofrequency denervation of the sacroiliac joint. Eur Radiol 12:1360–1365
13. Hansen HC, McKenzie-Brown AM, Cohen S, Swicegood JR, Colson JD, Manchikanti L (2007) Sacroiliac joint interventions: a systematic review. Pain Physician 10:165–184
14. Kim HJ, Shin DG, Kim HI, Shin DA (2005) Selective neurotomy of sacral lateral branches for pain of sacroiliac joint dysfunction. J Korean Neurosurg S 38:338–343

15. Humphrey SM, Inman RD (1995) Metastatic adenocarcinoma mimicking unilateral sacroiliitis. J Rheumatol 22:970–972
16. Kapural L, Nageeb F, Kapural M, Cata JP, Narouze S, Mekhail N (2008) Cooled radiofrequency system for the treatment of chronic pain from sacroiliitis: the first case-series. Pain Pract 8:348–354
17. Kapural L, Stojanovic M, Bensitel T, Zovkic P (2010) Cooled radiofrequency (RF) of L5 dorsal ramus for RF denervation of the sacroiliac joint: technical report. Pain Med 11:53–57
18. Maigne JY, Aivaliklis A, Pfefer F (1996) Results of sacroiliac joint double blocks and value of sacroiliac pain provocation test in 54 patients with low back pain. Spine 21:1889–1892
19. Mikeladze G, Espinal R, Finnegan R, Routon J, Martin D (2003) Pulsed radiofrequency application in treatment of chronic zygapophyseal joint pain. Spine J 3:360–362
20. Muhlner SB (2009) Review article: radiofrequency neurotomy for the treatment of sacroiliac joint syndrome. Curr Rev Musculoskelet Med 2:10–14
21. Niemisto L, Kalso E, Malmivaara A, Seitsalo S, Hurri H (2003) Radiofrequency denervation for neck and back pain. A systematic review of randomized controlled trials. Cochrane Database Syst Rev 1:CD004058
22. Slipman C, Sterenfeld E, Chou L, Herzog R, Vresilovic E (1998) The predictive value of provocative sacroiliac joint stress maneuvers in the diagnosis of sacroiliac joint syndrome. Arch Phys Med Rehabil 79:288–292
23. Vallejo R, Benyamin RM, Kramer J, Stanton G, Joseph NJ (2006) Pulsed radiofrequency denervation for the treatment of sacroiliac joint syndrome. Pain Med 7:429–434
24. Vanelderen P, Szadek K, Cohen SP, De Witte J, Lataster A, Patijn J, Mekhail N, van Kleef M, Van Zundert J (2010) 13. Sacroiliac joint pain. Pain Pract 10:470–478
25. Yin W, Willard F, Carreiro J, Dreyfuss P (2003) Sensory stimulation-guided sacroiliac joint radiofrequency neurotomy: technique based on neuroanatomy of the dorsal sacral plexus. Spine 28:2419–2425

Acta Neurochir (2011) 153:1469–1475
DOI 10.1007/s00701-011-1007-4

CLINICAL ARTICLE

Surgical management of intracranial subependymomas

Julia Annabel Kandenwein · Azize Bostroem · Mareike Feuss · Torsten Pietsch · Matthias Simon

Received: 30 January 2011 / Accepted: 24 March 2011 / Published online: 16 April 2011

Abstract
Background Intracranial subependymomas are rare, slow-growing and usually non-invasive tumors. The aim of this study was to analyze our experience with the surgical treatment of intracranial subependymomas.
Methods Between 1991 and 2007, 11 patients with intracranial subependymomas had surgery in our institution. Mean age of the patients was 54.4 years (ranging from 40 to 85 years).
Results Tumors were located in the fourth ventricle in seven patients and in the lateral ventricle in four patients. Most patients presented with symptoms related to intracranial hypertension and/or cerebellar signs and symptoms (headache: eight patients; dizziness: six patients; nausea: six patients; gait ataxia: four patients), one patient with cognitive decline and flattened affect, and one patient with a hemiparesis. Six patients presented with hydrocephalus, but only one needed a permanent cerebrospinal fluid (CSF) shunt. Complete removal of the tumor was possible in eight cases. Following surgery, only one patient experienced a permanent drop of his Karnofsky Performance Index (from 70 to 60). Median follow-up was 37 months. There were no true recurrences during follow-up. A second surgery was required 7 years after the first operation for progression of an incompletely resected tumor.
Conclusions Removal of symptomatic subependymomas can be performed safely. Prognosis is excellent after a complete resection. The potential for a surgical cure, low surgical complication rates and the risk of undertreatment of a more aggressive tumor together may justify surgery for asymptomatic lesions

Keywords Intracranial subependymoma · Surgery · Ventricular tumors

J. A. Kandenwein (✉) · A. Bostroem · M. Feuss · T. Pietsch · M. Simon
Neurochirurgische Klinik, Universitätskliniken Bonn,
Sigmund-Freud-Straße 25,
53105 Bonn, Germany
e-mail: julia.kandenwein@hotmail.de

Introduction

Intracranial subependymomas are rare, slow-growing and usually non-invasive tumors. They often remain asymptomatic during the patient's life, and are diagnosed only at autopsy. Matsumura and co-workers identified four incidental cases in a series of 1,000 necropsies, and seven symptomatic tumors among 1,000 serial surgeries for brain tumors [18]. Symptomatic subependymomas often present with symptoms and signs of hydrocephalus. Males are more often affected than females [6–9, 17, 19, 21]. Overall, approximately two-thirds of subependymomas arise in the fourth ventricle and one-third arise in the lateral or third ventricles [16, 19, 21, 22, 24]. Rarely, subependymomas may grow in the spinal cord [12, 27]. The differential diagnosis includes ependymomas, but also central neurocytomas, oligodendrogliomas, giant cell astrocytomas, and sometimes meningiomas. Magnetic resonance imaging (MRI) findings are often not diagnostic [2].

A few familial cases of subependymoma have been reported [1, 5]. Otherwise, the causation and pathogenesis of these neoplasms remains unclear. Cytogenetic studies have been performed in a few tumors. Abnormal chromosomal copy numbers were identified in a significant proportion of cases. Interestingly, these findings were quite distinct from the results of similar analyses of ependymomas [10].

Subependymomas are assigned to the WHO grade I. Histologically anaplastic tumors have not been described,

but recurrence, subependymal spread and central nervous system (CNS) metastasis have been observed in a few cases [3, 9, 21, 26]. No consistent histological predictors of an aggressive clinical course have been identified [18, 20, 21]. Rapid growth of a formerly asymptomatic subependymoma has been reported [11]. Subependymomas (similar to other benign ventricular pathologies such as colloid cysts) may cause sudden death most likely resulting from acute obstructive hydrocephalus [23, 25]. In summary, even some patients with asymptomatic tumors may not fare as well as suggested by the histology.

Patients with symptomatic subependymomas require surgical treatment. Observation may be an option for incidental growths. As outlined above, a sizable proportion of these tumors may never become symptomatic [9, 17, 21]. For the present paper we have analyzed our institutional experience with $n=11$ of these rare tumors. Treatment recommendations are based on only a few small series reported in the literature. We present short-term and long-term surgical results. Our series includes only intracranial growths, and a relatively high number of tumors located in the fourth ventricle. We also give a short review of the relevant literature.

Patients and methods

Between August 1991 and April 2007, 11 patients (three females, eight males) underwent surgery for an intracranial subependymoma at the Department of Neurosurgery in Bonn (see Table 1). The patients' age at the time of surgery ranged from 39 to 74 years (mean: 54.4 years). Relevant clinical (including follow-up) data were collected through a chart review and telephone interviews as necessary. Median follow-up was 37 months (mean 52.4 months; range: 6–115 months). We also analyzed all available neuroimaging studies and radiological reports.

For this paper, all histological diagnoses were reviewed at the Department of Neuropathology/German Brain Tumor Reference Center at the University of Bonn using the 2007 WHO classification of tumors of the Central Nervous System [22]. Histological examinations included hematoxylin/eosin (HE) staining and immunohistochemistry with antibodies against glial fibrillary acidic protein (GFAP), epithelial membrane antigen (EMA) and Ki-67 (MIB-1).

Results

Clinical presentation

All patients harbored symptomatic tumors. The mean duration of clinical symptoms at the time of diagnosis was 6.5 months,

Table 1 Clinical features of 11 subependymomas

Patient no.	Age	Sex	Max. diameter	Location	Hydrocephalus	Symptoms	Duration of symptoms (months)	Preop. KPI	Degree of Resection	KPI (at last follow-up)	Recurrent tumor (follow-up in months)
1	50	M	3	Right lateral ventricle (anterior horn)	No	Headache	0.5	80	Total	90	No (85)
2	74	M	4	Right lateral ventricle (anterior horn)	Transient	Headache, personality change	0.5	60	Total	80	No (32)
3	63	M	3	(Caudal) 4th ventricle	No	Dizziness nausea	9	80	Subtotal	80	Yes (second surgery after 86 months)
4	55	M	2.5	(Caudal) 4th ventricle	Yes	Headache, ataxia	6	80	Total	90	No (9)
5	39	M	4	(Caudal) 4th ventricle	Transient	Dizziness, nausea	24	90	Subtotal	90	No (6)
6	60	F	3.5	(Caudal) 4th ventricle	No	Headache, dizziness	3	90	Total	90	No (29)
7	49	F	2	(Caudal) 4th ventricle	Transient	Headache, dizziness, nausea, ataxia	2	80	Total	90	No (36)
8	54	F	11	Left lateral ventricle (cella media, trigonum & inferior horn)	No	Headache, nausea, hemianopsia	1	80	Total	90	No (87)
9	49	M	8	Right lateral ventricle (cella media & anterior horn)	Transient	Headache, nausea, hemiparesis	2	80	Total	70	No (37)
10	57	M	3	(Caudal) 4th ventricle	No	Dizziness, ataxia	12	90	Subtotal	100	No (54)
11	48	M	6.5	4th ventricle & right cerebellopontine angle	Transient	Headache, dizziness, nausea, ataxia, cranial nerve palsies	12	60	Total	60	No (115)

KPI Kamofsky Performance Index, *M* male, *F* female

ranging from 2 weeks to 24 months. Eight cases presented with headache, six cases with dizziness, six cases with nausea, four cases with ataxia, one patient showed personality changes and one presented with a hemiparesis (Table 1).

Radiological findings

Preoperative CCT (cranial computer tomography) and MRI findings could be analyzed in all cases (Fig. 1). Seven tumors were localized in the fourth ventricle and four in the lateral ventricles. The maximum tumor diameter varied between 2 and 11 cm (median 3 cm). MRI studies revealed infiltrative growth into the surrounding brain in one tumor of the left lateral ventricle (confirmed at surgery). All other tumors were well-circumscribed. The tumors were usually inhomogenous and hypointense to isointense on T1-weighted images. T2-weighted imaging showed a hyperintense signal in all cases. The majority of tumors showed enhancement after application of gadolinium-diethylene triamine pentaacetic acid (DTPA). Moderate enhancement was seen in seven tumors, and two cases showed only slight contrast enhancement. Calcifications were detected in only two tumors.

Histopathology

Tumors consisted of clusters of glial cells with round to oval nuclei with granular chromatin embedded in a fibrillary glial matrix. Hyalinized vessels and cystic changes were frequent. The tumors showed low to moderate cellularity. There was no significant mitotic activity. The tumor cells were found to express glial fibrillary acidic protein (GFAP). In three cases, a dot-like reactivity with antibodies against epithelial membrane antigen (EMA) was present. The MIB Index (Ki-67) was <3% in all cases. All cases were assigned to WHO grade I (Fig. 2).

Surgical management

Patients with tumors in the fourth ventricle were operated upon in the sitting (five patients) or prone position (two patients) with mild flexion of the head. Surgery was performed through a median suboccipital approach with partial resection of the posterior arch of the atlas in four cases. Tumors located in the lateral ventricle were accessed via a frontal transcortical (three patients) or via an anterior transcallosal route (one patient). One patient was operated on via a parietal transcortical approach for a tumor located in the cella media, the trigonum and the inferior horn of the lateral ventricle.

Tumors were generally firm and often well-demarcated. However, all tumors adhered strongly to adjacent structures. In three cases infiltrative growth involving the floor of the fourth ventricle was noted. Small portions of the respective tumors near the obex and in the inferior part of the rhomboid fossa were intentionally left behind in order to avoid a postoperative neurological deficit. A complete tumor removal was achieved in the other eight cases including a case with a giant 11-cm tumor of the left lateral ventricle with infiltrative growth (73%).

Preoperative hydrocephalus was present in six patients (55%). Three patients were treated with transient external cerebrospinal fluid (CSF) drainage, and one patient underwent placement of a permanent ventriculo-peritoneal shunt 14 days before the actual tumor surgery. After the operation, the patient became shunt-free. One patient developed a postinfectious hydrocephalus following an episode of postoperative meningitis which required treatment with a ventriculo-peritoneal shunt. Other perioperative complications included a CSF fistula and an epidural hematoma requiring surgical evacuation. In the latter case, aggravation of the patient's preoperative hemiparesis due to a lacunar infarction in the internal capsule was seen.

Functional outcomes and follow-up

Functional outcomes after surgery were good in most cases. The median KPI at last follow-up was 90 (range: 60–100). Only two patients had a KPI of <80 at last follow-up (see Table 1). Permanent (albeit very minor) functional worsening following surgery was seen in only one case (a drop in the KPI from 70 to 60).

During follow-up there were no recurrences following a complete tumor resection. One patient with residual tumor in the region of the obex was diagnosed with tumor progression 6 years after the first surgery, and underwent a second operation for a 25-mm tumor without complications 7 years and 3 months after the first surgery. The other two patients with residual tumors were serially followed with MRI for 6 and 54 months, respectively, without evidence of tumor progression.

Discussion

Subependymomas are rare tumors. Only a few patient series have been published. Table 2 summarizes the more recent (after 1990) case series published in English. Almost all cohorts reported are small and detail retrospective data only [6–9, 14, 17, 19, 21, 29]. Rushing and co-workers collected 83 cases, but these authors provide limited clinical data, and rather focus on histopathological findings [22]. Ragel et al. [21] reported 16 cases, but only eight cases were treated at their own institution, and clinical data from the remaining eight patients were not provided. Our series adds 11 patients, i.e., a significant number of patients, to the existing literature. Similar to other cohorts, the tumors

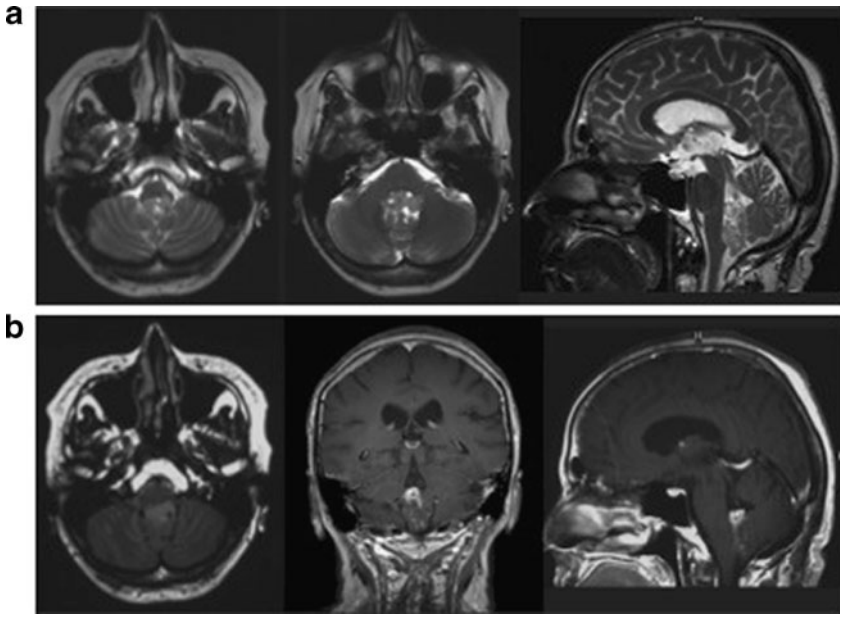

Fig. 1 **a**, **b** MRI appearance of a subependymoma. This tumor was diagnosed in a 60-year-old female patient (see Table 1, patient no. 6) following a 3-month history of headache and dizziness. The tumor could be completely resected and the patient recovered without deficits. There was no recurrence after a follow-up of 3 years. **a** T2-weighted images nicely show a sharply demarcated growth in the caudal fourth ventricle. The tumor parenchyma appears inhomogenous on T2-weighted images. **b** FLAIR imaging depicts a hyperintense lesion (*left*). There is patchy and inhomogenous contrast enhancement (*middle and right* contrast enhanced T1-weighted scans)

from the present series were typically diagnosed in middle-aged patients, males were more frequently affected than females and most tumors were localized in the posterior fossa [6–9, 17, 19, 21].

The principal goal of surgery in symptomatic cases is a maximum safe tumor resection. Gross total resection rates in most series were >70%. Collectively, our data and the data reported in the literature clearly show that subependymomas are cured by a total resection. Recurrent tumors were only diagnosed in patients who had a subtotal resection [6–9, 14, 17, 19, 21, 29].

While a total resection should be the surgical goal, this must be weighted carefully against the morbidity of aggressive surgery in cases with a high risk of incurring a relevant neurological deficit through the surgery. Hence, it should be noted that mortality and morbidity rates after resection of supratentorial subependymomas are satisfying in all published series [6–9, 14, 17, 19, 21, 29]. The perioperative mortality in the present series was 0%, and only one patient (9%) experienced a permanent (albeit very minor) drop of his KPI (from 70 to 60) after surgery. Three of our patients harbored rather large tumors, measuring

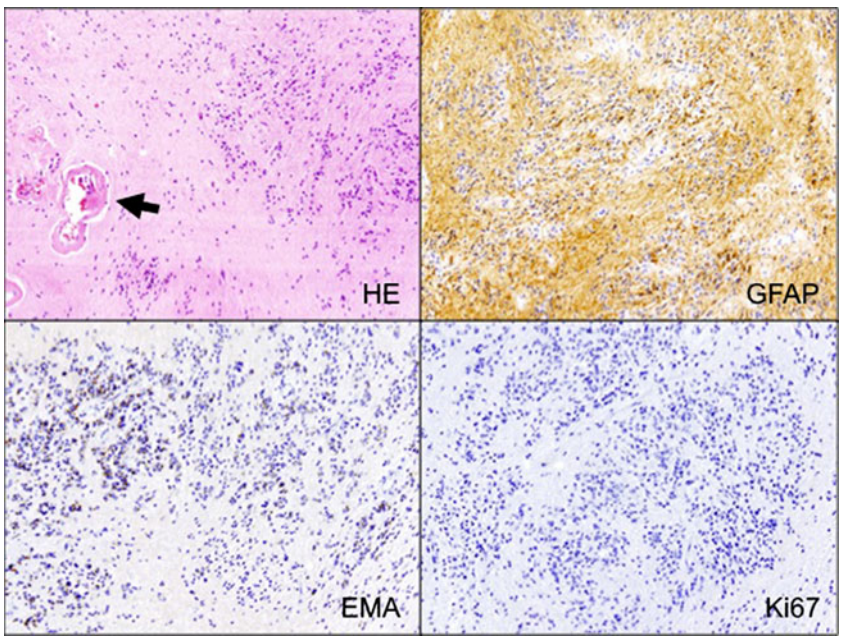

Fig. 2 Typical histological appearance of a subependymoma (*HE* hematoxylin/eosin). Tumors are composed of glial (glial fibrillary acidic protein/GFAP positive) neoplastic cells embedded in a fibrillary matrix. Hyalinized vessels are frequently observed (*arrow*). Tumors show a low to moderate cellularity, and mitoses are usually not seen. Only occasional cells stain positive for the proliferation marker Ki-67 (MIB-1). A dot-like immunoreactivity may occur after staining for the EMA

Table 2 Clinical features of subependymomas—a tabular summary of the literature 1994–2011

Author	Patient no.	Mean age	Location	Surgical approach	Percent hydrocephalus postop	Complete resections	Mortality & morbidity	Mean follow-up (years)	Recurrence
Ildan et al. 1994 [6]	5	39	Lateral ventricle (2) 4th ventricle (3)	Transcallosal	0%	80%	20% 0%	2.0	0
Maiuri et al. 1997 [17]	8	33.6	Lateral ventricle	n.m.	0%	75%	12.5% 12.5%	3.8	0d
Nishio et al. 2000 [19]	4	48.3	Lateral ventricle.	Transcallosal (2), transsortical (2)	0%	75%	0% 0%	8.8	0
Im et al. 2003 [7]	7	45	Lateral ventricle (6) 3rd ventricle (1)	Transcallosal (4) Transcortical (3)	14%	71%	0%b 14.3%	3.5	29%
Mallik et al. 2003 [30]	5	5	3rd ventricle (1) 4th ventricle (4)	n.m.	n.m.	n.m.	20% n.m.	n.m.	50%
Ragel et al. 2006 [21]	8[a]	48.6	Lateral ventricle (2) 4th ventricle (3) Supratent lobar (2) Spinal cord (1)	n.m.	0%	100%	0% 12.5%	2.2	0
Rushing et al. 2007 [22]	34%	n.m.	Lateral ventricle (17) 4th ventricle (15) Others n.m.	n.m.	n.m.	53%	18% n.m.	4	n.m.
Limaiem et al. 2008 [13]	6	35.8	Lateral ventricle (5) 4th ventricle (1)	n.m.	0%	83.3%	0%c 0%c	range: 2 months to 10 years	0c
Fujisawa et al. 2010 [4]	5	53.2	Lateral ventricle (5)	Transcallosal (2) transsortical (3)	20%	100%)	0% n.m.	9	0
Kandenwein et al. 2011 [this study]	11	54.4	Lateral ventricle (4) 4th ventricle (7)	Transcallosal (1) Transcortical (3)	9%	73%	0% 18.2%	4.3	9%

n.m. not mentioned

[a] Only patients with surgical and follow-up data are shown

[b] One patient died after repeat surgery

[c] Follow-up/clinical data were provided for only 5/6 patients

[d] Follow-up were provided for only 5/8 patients

from 6.5 to 11 cm. Also, our series includes many tumors located in the fourth ventricle (64%). Surgery in this location carries significant risks due to the proximity of eloquent structures such as the brainstem, the posterior inferior cerebellar artery and the lower cranial nerves. Specifically, subependymomas often seem to arise or involve the obex. Damage to the obex may result in sleep apnea and chronic aspiration [28]. Surgery of lateral ventricular tumors also entails relevant risks, e.g., damage to the fornices in cases with tumors of the anterior horn.

Surgery for subependymomas also aims at the restoration of normal CSF pathways. Hydrocephalus is a major cause of morbidity in patients with subependymomas. Four (36%) of our patients presented with symptoms and signs of hydrocephalus. Patients with subependymomas may die from acute obstruction of the CSF pathways similarly to patients with colloid cysts and other intraventricular pathologies [11, 23]. In our experience, almost all patients have normal CSF pathways after resection of their tumor. Only one of our patients required a permanent ventriculo-peritoneal-shunt, and this patient became CSF drainage dependent only following a postoperative meningitis. Similarly, the series of Im and co-workers include one patient who needed a CSF shunt 3 weeks after tumor surgery [7].

Confirmation of the tumor histology is another important goal of surgery for a presumed subependymoma. MRI findings are usually not diagnostic. The differential diagnosis includes ependymoma (younger patients, sometimes infiltrative growth), central neurocytoma (more vascularized), meningioma (stronger contrast enhancement), oligodendroglioma and giant cell astrocytoma. A 'wait and see strategy' will therefore entail a relevant risk of undertreatment if a more aggressive tumor is mistaken for a subependymoma. Approximately half of all ependymomas are assigned to the WHO grade III (anaplastic ependymomas), and these tumors require radiotherapy following surgery [3].

Patients with symptomatic tumors will have surgery. Surgical indications for asymptomatic growths are less well defined. Probably less than half of all subependymomas will eventually become symptomatic [9, 17]. On the other hand, postponing surgery for a resectable and presumably benign tumor of the fourth ventricle may result in a subtotal operation for a much larger tumor with a significantly higher risk for neurological deterioration later on. One case of a rapid expansion of a previously asymptomatic subependymoma has been reported [11]. Several cases of sudden death caused by intracerebral subependymomas have been described in the literature [23, 25]. This and the potential of a surgical cure, the relatively low operative risks, and in particular the risk to overlook a more aggressive pathology may argue for surgery also in cases with asymptomatic tumors.

The role of radiotherapy for subependymomas is probably limited. Follow-up imaging studies of seven patients who underwent radiotherapy after a subtotal tumor resection showed that these tumors can be radioresponsive, particularly with doses of 5,000 cGy or greater [15]. A subependymoma recurring after multiple subtotal resections has been successfully managed with stereotactic radiosurgery [3]. In contrast, tumor progression after primary gamma knife treatment was seen in a pediatric case [9] and there is also a case report of subependymal seeding after surgery and radiosurgery [26]. We do not have experience with radiotherapy for subependymomas. The relatively low recurrence rate in patients with residual tumors would suggest that there is no indication for radiotherapy as part of the primary treatment of subependymomas.

Conclusion

Subependymomas are benign tumors, which can be operated upon with relatively low complication and recurrence rates. The differential diagnosis includes various more aggressive neoplasms (e.g., gliomas and ependymomas).

Conflict of interest None

References

1. Cheng TM, Coffey RJ, Gelber BR, Scheithauer BW (1993) Simultaneous presentation of symptomatic subependymomas in siblings: case reports and review. Neurosurgery 33:145–150
2. Duong H, Sarazin L, Bourgouin P, Vézina JL (1995) Magnetic resonance imaging of lateral ventricular tumours. Can Assoc Radiol J 46:434–442
3. Ecker RD, Pollock BE (2004) Recurrent subependymoma treated with radiosurgery. Stereotact Funct Neurosurg 82:58–60
4. Fujisawa H, Hasegawa M, Ueno M (2010) Clinical features and management of five patients with supratentorial subependymoma. J Clin Neurosci 17:201–204
5. Honan WP, Anderson M, Carey MP, Williams B (1987) Familial subependymomas. Br J Neurosurg 1:317–321
6. Ildan F, Cetinalp E, Bagdatoglu H, Tunah N, Gönlüşen G, Karadayi A (1994) Surgical treatment of symptomatic subependymoma of the nervous system. Report of five cases. Neurosurg Rev 17:145–150
7. Im SH, Paek SH, Choi YL, Chi JG, Kim DG, Jung HW, Cho BK (2003) Clinicopathological study of seven cases of symptomatic supratentorial subependymoma. J Neurooncol 61:57–67
8. Katayama S, Fujita K, Takeda N, Hashimoto K, Tamaki N, Asada M (1998) Subependymoma in the lateral ventricle incidentally detected by routine brain examination—case report. Neurol Med Chir (Tokyo) 38:47–50
9. Kim HC, Kim IO, Kim CJ, Cho BK, Kim WS, Yeon KM (2004) Subependymoma in the third ventricle in a child. Clin Imaging 28:381–384
10. Kurian KM, Jones DT, Marsden F, Openshaw SW, Pearson DM, Ichimura K, Collins VP (2008) Genome-wide analysis of subependymomas shows underlying chromosomal copy number

changes involving chromosomes 6, 7, 8 and 14 in a proportion of cases. Brain Pathol 18:469–473
11. Laxton AW, Shannon P, Nag S, Farb RI, Bernstein M (2005) Rapid expansion of a previously asymptomatic subependymoma. Case report. J Neurosurg 103:1084–1087
12. Lee KS, Angelo JN, McWhorter JM, Davis CH Jr (1987) Symptomatic subependymoma of the cervical spinal cord. Report of two cases. J Neurosurg 67:128–131
13. Limaiem F, Bellil SB, Bellil K, Chelly I, Jemel H, Haouet S, Khalai M, Zitouna M, Kahir N (2008) Subependymomas: a clinicopathological study of 6 symptomatic cases. Pathologica 100:401–404
14. Lobato RD, Sarabia M, Castro S, Esparza J, Cordobés F, Portillo JM, Rivas JJ (1986) Symptomatic subependymoma: report of four new cases studied with computed tomography and review of the literature. Neurosurgery 19:594–598
15. Lombardi D, Scheithauer BW, Meyer FB, Forbes GS, Shaw EG, Gibney DJ, Katzmann JA (1991) Symptomatic subependymoma: a clinicopathological and flow cytometric study. J Neurosurg 75:583–588
16. Louis DN, Ohgaki H, Wiestler OD, Cavenee WK, Burger PC, Jouvet A, Scheithauer BW, Kleihues P (2007) The 2007 WHO Classification of Tumours of the Central Nervous System. Acta Neuropathol 114:97–109
17. Maiuri F, Gangemi M, Iaconetta G, Signorelli F, Del Basso De Caro M (1997) Symptomatic subependymomas of the lateral ventricles. Report of eight cases. Clin Neurol Neurosurg 99:17–22
18. Matsumura A, Ahyai A, Hori A, Schaake T (1989) Intracerebral subependymomas. Clinical and neuropathological analyses with special reference to the possible existence of a less benign variant. Acta Neurochir (Wein) 96:15-25
19. Nishio S, Morioka T, Mihara F, Fukui M (2000) Subependymoma of the lateral ventricles. Neurosurg Rev 23:98–103
20. Prayson RA, Suh JH (1999) Subependymomas: clinicopathologic study of 14 tumors, including comparative MIB-1 immunohistochemical analysis with other ependymal neoplasms. Arch Pathol Lab Med 123:306–309
21. Ragel BT, Osborn AG, Whang K, Townsend JJ, Jensen RL, Couldwell WT (2006) Subependymomas: an analysis of clinical and imaging features. Neurosurgery 58:881–890
22. Rushing EJ, Cooper PB, Quezado M, Begnami M, Crespo A, Smirniotopoulos JG, Ecklund J, Olsen C, Santi M (2007) Subependymoma revisited: clinicopathological evaluation of 83 cases. J Neurooncol 85:297–305
23. Ryder JW, Kleinschmidt-DeMasters BK, Keller TS (1986) Sudden deterioration and death in patients with benign tumors of the third ventricle area. J Neurosurg 64:216–23
24. Scheithauer BW (1978) Symptomatic subependymoma. Report of 21 cases with review of the literature. J Neurosurg 49:689–696
25. Schwarz KO, Perper JA, Rozin L (1987) Sudden, unexpected death due to fourth ventricular subependymoma. Am J Forensic Med Pathol 8:153–157
26. Seol HJ, Hwang SK, Choi YL, Chi JG, Jung HW (2003) A case of recurrent subependymoma with subependymal seeding: case report. J Neurooncol 62:315–320
27. Shimada S, Ishizawa K, Horiguchi H, Shimada T, Hirose T (2003) Subependymoma of the spinal cord and review of the literature. Pathol Int 53:169–173
28. Sutton L, Goldwein J, Schwartz D (1999) Ependymomas. In: Albright L, Pollack I, Adelson D (eds) Principles and practice of pediatric neurosurgery. Thieme, New York, pp 609–628
29. Yu T, Zeng C, Zhao JZ (2010) [Intracranial subependymoma: clinical features and surgical management of 22 cases]. Zhonghua Yi Xue Za Zhi 90:756–759
30. Mallik MK, Babu N, Kakkar N, Khosla VK, Banerjee AK, Vasishta RK (2003) Subependymomas in children: a report of five cases including two with osseous metaplasia. Neurol India 51:98-99

Acta Neurochir (2011) 153:1477–1485
DOI 10.1007/s00701-011-1028-z

CLINICAL ARTICLE

Primary Ewing's sarcoma of cranial bones: analysis of ten patients

Pravin Shashikant Salunke · Kirti Gupta · Vinod Malik · Narendra Kumar · Lauren E. Henke · Chunyu Cai · Wei-Shen Chen · John D. Pfeifer

Received: 14 November 2010 / Accepted: 8 April 2011 / Published online: 26 April 2011

Abstract
Objective Ewing's sarcomas are the second most common bone tumors in children and primary involvement of the cranium is uncommon. We analyzed retrospectively the data of ten patients with this rare subset of disease, who had been treated at our institute since 2005. Our aim was to assess the outcomes, recurrence rates and the selection of appropriate treatment methods.

Methods The patients were reviewed with respect to their clinical presentations, treatment, and outcomes. Computed tomographic scanning of the brain was performed for all patients. Skeletal surveys with routine radiographs and technetium-99 bone scans to detect extracranial Ewing's sarcomas were performed for all patients. For all ten patients, radical tumor excision was achieved surgically. Chromosomal translocation studies were carried out on paraffin blocks for nine patients, using fluorescence in situ hybridization (FISH) and polymerase chain reaction (PCR). All patients were then subjected to adjuvant multidrug chemotherapy and radiotherapy. The follow-up periods ranged from 2 months to 5 years (mean, 17.6 months).
Results The predominant presenting features were headaches, increased intracranial pressure, scalp swelling and trigeminal nerve involvement. The erosion of dura and intradural extension was noted in eight patients in our series. All nine patients, in whom FSIH and reverse transcriptase PCR (RT-PCR) was done, tested positive for *EWS–FLI1*(t22:12) translocation. All patients underwent radical excision within safe limits, followed by chemoradiation. Three patients had local recurrences, which were detected within 12 months after surgery. All three of them died within weeks of presentation with recurrence. One patient experienced a recurrence after 30 months. This recurrent tumor was completely excised, and additional chemotherapy was administered. There was a local recurrence again after 18 months that was treated with surgery and chemoradiation, and the patient is still surviving 5 years after the primary surgery. One patient had metastasis at presentation and died within 2 months of surgery. The remaining five seem to have good outcomes, though the follow-ups were not very long.
Conclusion The treatment of primary Ewing's sarcoma of the cranium still remains to be radical surgery, aggressive

P. S. Salunke (✉) · V. Malik
Department of Neurosurgery, PGIMER,
Chandigarh, India 160012
e-mail: drpravin_salunke@yahoo.co.uk

V. Malik
e-mail: Vinodmalik72@yahoo.com

K. Gupta
Department of Hispathology, PGIMER,
Chandigarh, India
e-mail: Kirtigupta10@yahoo.co.in

N. Kumar
Department of Radiotherapy, PGIMER,
Chandigarh, India
e-mail: drnarendra74@gmail.com

L. E. Henke · C. Cai · W.-S. Chen · J. D. Pfeifer
Department of Pathology, Washington University,
St. Louis, USA

L. E. Henke
e-mail: henke.lauren@gmail.com

C. Cai
e-mail: CCai@path.wustl.edu

W.-S. Chen
e-mail: WChen@path.wustl.edu

J. D. Pfeifer
e-mail: pfeifer@path.wustl.edu

multidrug chemotherapy, and radiotherapy. Neoadjuvant chemotherapy may not work in patients with large intracranial extension due to raised pressure making decompression imperative. The outcome is usually good if there is no early recurrence. Early recurrence, presence of metastasis and extremes of age probably bears a poor outcome. However, a larger series is required to confirm these findings.

Keywords Ewing's sarcoma · Cranial bones · Outcome

Introduction

Primary Ewing's sarcomas of the cranial bones are uncommon and constitute 1% of all Ewing's sarcomas [7]. Apart from a few case reports, there is only one series of 14 patients [1, 3, 4, 6–8, 11, 13, 15, 19, 21, 22, 24, 25]. The literature suggests that radical resection followed by chemoradiation bears a better outcome, unlike for Ewing's sarcomas occurring elsewhere. Also, recurrences have been found only in a few patients [4, 6, 7, 14, 19, 24, 25]. However, we found certain differences in the outcome of ten patients of our series. The clinico-radiological presentation, treatment given and outcomes of these ten patients have been assessed.

Patients and methods

Patient details and preoperative workup The data for ten patients with primary Ewing's sarcomas of the cranium, who had been surgically treated in our department since 2005, were analyzed retrospectively. All patients were from the northern part of India and were treated at PGIMER, Chandigarh, India. The demographic data, clinical details, radiological features, management and outcome were compiled and analyzed (Table 1). All patients had preoperative plain and contrast computed tomography (CT) scan and magnetic resonance imaging (MRI). The extent of bony involvement was studied on CT scan bone window. MR venogram was done in cases with suspected sinus involvement.

Surgical management All patients underwent tumor excision as radical as possible, within the safe limits. A large skin flap was raised. Dissection was carried out until normal bone on all sides could be exposed. Craniotomy was made through the normal bone. Tumor was excised as much as possible. The infiltrated dura was not opened if it was not breached by the tumor. However, if it was breached, the infiltrated dura was excised radically and repaired using pericranium, temporalis fascia, or fascia lata.

Diagnosis Histopathological examination in all cases showed round cell tumor. Periodic acid Schiff staining was done in all cases. CD99 staining was done to confirm Ewing's sarcoma. Staining for vimentin, synaptophysin, chromogranin and desmin was carried out. Chromosomal translocation (fusion transcription) studies for calvarial Ewing's sarcoma were carried out on paraffin blocks of nine patients using fluorescence in situ hybridization (FISH) and reverse transcriptase polymerase chain reaction (RT-PCR) techniques. The paraffin blocks were sent to Washington University of Medicine, St. Louis, USA, as this facility was not available in India. They were tested for one genetic abnormality, namely, *EWS–FLI1* fusions as a result of the t(11;22) translocation.

Adjuvant therapy Following the radical excision, the patients received induction chemotherapy with two cycles of cyclophosphamide (1,200 mg/m^2) plus vincristine (1.5 mg/m^2) plus adriamycin (75 mg/m^2), alternating with ifophospamide (1,800 mg/m^2) and etoposide (100/m^2) administered at 3 weeks. Eight weeks later, the local area was irradiated with 40–50 Gy. This was followed by eight cycles of chemotherapy, with the same drugs as for induction chemotherapy, at 3-week intervals.

Follow-up

The patients underwent follow-up monitoring, on an outpatient basis, at monthly intervals. To avoid loss at follow-up, the telephone numbers (mobile numbers) and complete addresses of the patients and the relatives were noted. Thus, the information was acquired telephonically, especially in patients who expired.

Ethical considerations

The study was a retrospective one. It did not delay the management or add to the financial burden in any form. The chemoradiation is akin to Ewing's sarcoma elsewhere and radical surgery is as described in the literature. Informed consent was taken from all the patients. Furthermore, clearance was obtained from the institutional ethics committee.

Results

Clinical presentation

The youngest patient was 3 years old and the oldest 62 years. There were two patients in their 1st decade of life, four in the 2nd decade, two in the 3rd decade, and one patient in the 4th decade. Of the ten patients, only two were

Table 1 The clinical presentation, bone involved, presence of metastasis, dural invasion and outcome of ten patients with primary Ewing's sarcoma of the cranial bones

Patient no.	Age (years)/sex	Location	Clinical features	Bone scan	Dural erosion	Treatment	Outcome
1. P	3/male	Temporal squama Petrous	Increased ICP/ataxia	Nil	+ve	S + RT + C	Recurrence 8 months—death
2. L	8/male	Frontoparietal	Large fronto parietal swelling + Increased ICP pressure + right hemiparesis	Nil	+ve	S + RT + C	Alive, 18 months, no recurrence
3. A	11/male	Anterior skull base (ethmoid)	Raised ICP	Nil	+ve	Biopsy + C + S + RT + C	Alive 14 months, no recurrence
4. Ab	12/male	Temporal squama + petrous	Raised ICP	Nil	+ve	S + RT + C	Recurrence at 12 months—death
5. A	15/male	Temporal base + grater wing of sphenoid + lateral wall of orbit	Proptosis + drowsy, raised ICP + hemiparesis	Pelvic mets	+ve	S + RT + C	2 months—neutopenia + septicemia + death
6. K	16/female	Temporo parietal	Seizures + raised ICP	Nil	+ve	S + RT + C	Alive 24 months
7. M	23/male	Greater wing of sphenoid involving the CS	Trigeminal involvement (V1 + V2 + V3) + ophthalmoplegia(CS)	Nil	-ve (only thickening)	S + RT + C	Alive 4 months
8. V	23/female	Greater sphenoid wing involving the CS	Seizures + temporal headache+V1 and V2 + opthalmoplegia(CS)	Nil	-ve (only thickening)	S + RT + C	Alive 24 months
9. D	39/male	Frontal	Frontal swelling with left hemiparesis + raised ICP	Nil	+ve	S + RT + C; reop. 30 months and 48 months	Recurrence twice 30 and 48 months after the primary surgery, alive—60 months
10. K	62/male	Occipital	Occipital swelling + cerebellar signs + raised ICP + blindness	Nil	+ve	S + RT + C	Recurrence + death, 6 months

CS cavernous sinus, *ICP* intracranial pressure, *S* surgery, *RT* radiotherapy, *C* chemotherapy, *reop.* reoperated

The paraffin blocks of nine patients (except patient number 7) were tested for translocation 11:22 using FISH/PCR, and all of them tested positive

females. The duration of presenting symptoms was between 2 and 8 weeks. Raised intracranial pressure was the presenting symptom in eight and was the commonest symptom. Two of these patients had near blindness with secondary optic atrophy. Local swelling was seen in three patients. Cavernous sinus was involved in two patients and they presented with ophthalmoplegia with trigeminal involvement. Two patients had hemiparesis and two ataxia. One patient who had an anterior cranial base lesion, had undergone a endonasal biopsy outside and was given chemoradiation. However, the lesion had assumed a large size, causing drowsiness due to raised intracranial pressure in less than a month and had to be operated on. The differential diagnosis for those with large scalp swellings were: (1) calvarial Koch's, which is common in India; (2) bony lesions like eosinophoilic granulomas, bony hemangiomas, and sarcomas; (3) dural based lesions producing hyperostosis like meningiomas. For lesions of the temporal bone involving the cavernous sinus, fungal lesions were frequent, followed by round cell tumors. In the one involving the anterior cranial fossa mass, fungal mass and esthesioneuroblastoma were the differentials.

Radiology and bone scan

CT scan showed that the temporal bone was the commonest bone to be involved (4/10 patients, 40%). The greater wing of the sphenoid, temporal squama, petrous bone and occipital bone, frontal and parietal bones and ethmoids were the involved bones, in combination or alone. Both the inner and outer tables were involved. There was erosion of the bone and osteoblastic activity (reactive sclerosis) of the bone at places. Rarefaction or bony destruction at places was noted in all cases. (Fig. 1). Lytic lesions were seen on plain radiographs and onion peeling was not seen. MRI showed lobulated lesion well demarcated and enhancing; extending in subgaleal tissue in all cases with vault lesion. (Fig. 2). The dura was eroded in 80% of the cases, with the lesion extending intradurally (Fig. 2). One patient had hemorrhage in the lesion (Fig. 3). Similarly, the one arising from the anterior cranial fossa base (ethmoid sinuses) was masquerading as a fungal infection that is common in India. The cavernous sinus was involved in two patients. In nine patients, skeletal survey with technetium-99 isotope bone scans for extracranial Ewing's sarcoma yielded negative results. In one patient, there was a mild isotope uptake in the left iliac bone, but the pelvic radiographs were normal.

Operative findings

In lesions involving the vault, the galea was not stuck and could be elevated from the tumor capsule (Fig. 4a-c). In all the cases, tumor had eroded the bone completely and had involved the dura with its thickening. In eight patients, the tumor had breached the dura. There was a good plane from the brain parenchyma in all the primary surgeries. The tumor was reddish gray, rubbery in consistency and vascular. Total excision was achieved in five patients. Near total excision in three patients with temporal-petrous involvement, and in two patients with cavernous sinus involvement, subtotal excision was achieved.

Pathology

Histopathological examination of specimens from all patients showed malignant round cell tumors involving bone. The tumor cells were arranged in sheets, and few pseudorosettes were discernible There were foci of hemorrhage but no necrosis. Staining of the tissue with periodic acid-Schiff stain revealed the presence of glycogen granules. Vimentin and CD99 was positive in all the cases (Fig. 5a-c).

Chromosomal study FISH and RT-PCR on all nine paraffin blocks revealed *EWS-FLI1* fusions (Fig. 5d).

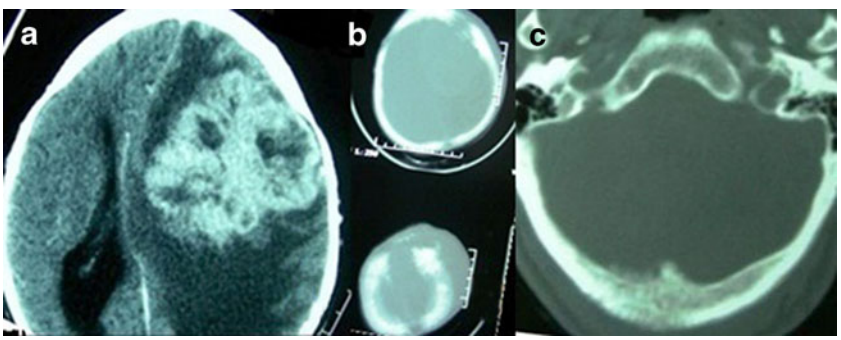

Fig. 1 CT findings in calvarial Ewing's sarcoma. **a** Contrast CT scan showing a lesion with perilesional edema. **b** CT scan bone window showing eroded bone with no sclerosis. Both the tables are involved. **c** CT scan bone window showing rarefaction and expansion with erosion of the occipital bone close to the internal occipital protuberance. Both the inner and outer table are thinned out with adjoining reactive sclerosis (osteoblastic activity)

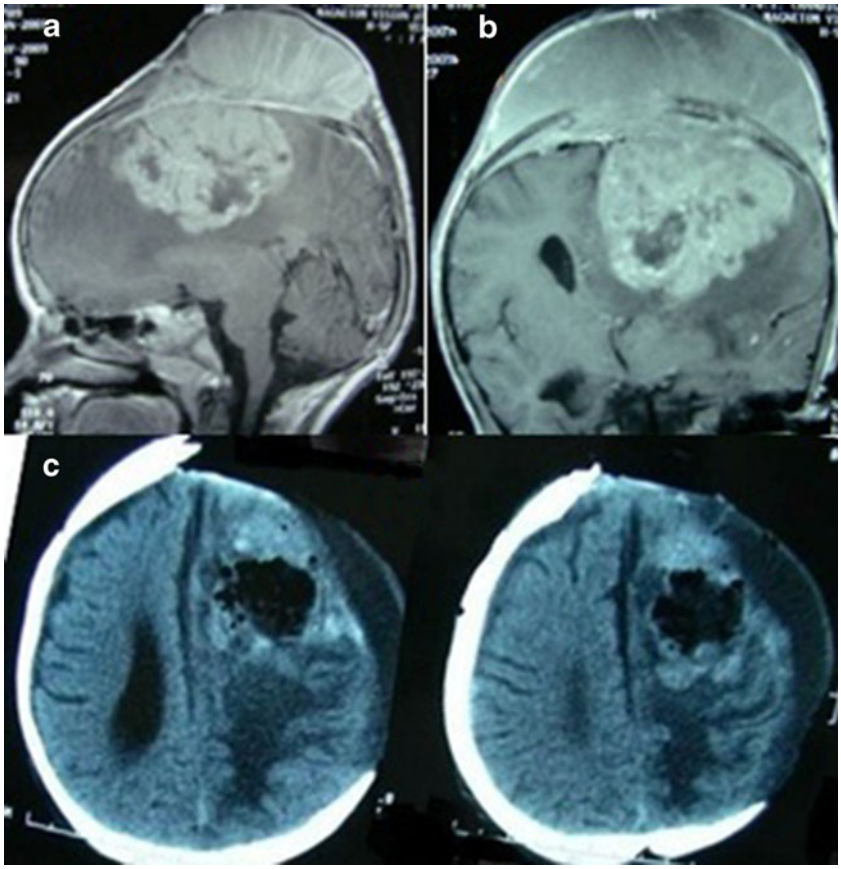

Fig. 2 MRI and postoperative imaging findings in the case of a patient with classical calvarial Ewing's sarcoma. **a** Contrast sagittal MRI showing enhancing lesion involving the fronto-parietal calvaria with subgaleal and intradural extension. **b** Contrast coronal MRI showing midline calvarial lesion with bilateral subgaleal involvement but the intradural extension was on the left side alone. **c** Postoperative axial CT showing gross total excision

Follow-up

The follow-up periods ranged from 2 months to 5 years (mean, 17.6 months) at the time of review. Four patients had recurrence after gross/near total excision. Two of these patients had recurrence in 6–8 months, one at 12 months. The fourth patient had recurrence after 2.5 years. He was operated upon and administered adjuvant chemotherapy. He had recurrence after another year and a half and was reoperated on again, followed by chemotherapy. This patient is still surviving, 5 years after the first surgery. Surgery after chemoradiation was more difficult than primary surgery as the tumor was adhered to the brain parenchyma. The other two patients with recurrence, in

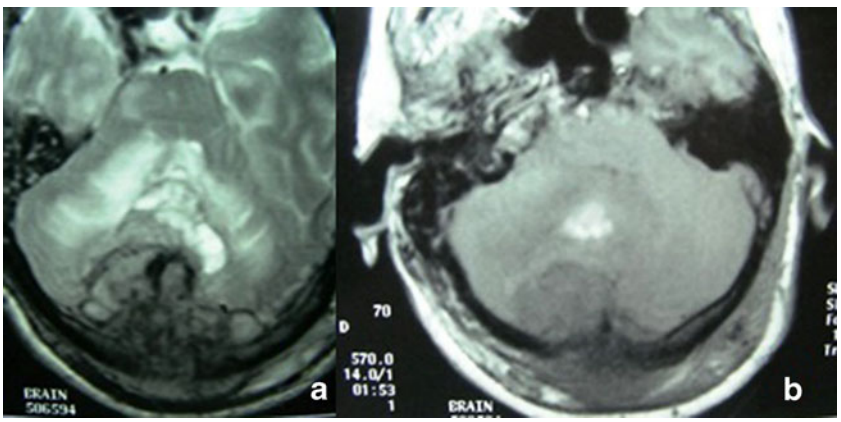

Fig. 3 Variation in MRI findings in a patient with occipital Ewing's sarcoma. **a** T2-weighted axial MRI showing heterogenous, lobulated lesion with anterior hyperintensity, involving the occipital bone and extending into the cerebellar parenchyma and subgaleal tissue. Fourth ventricle is compressed anteriorly. **b** T1-weighted axial MRI showing hyperintensity in the anterior portion of lesion corresponding to the hyperintense signal on T2, thus suggesting intratumoral bleed

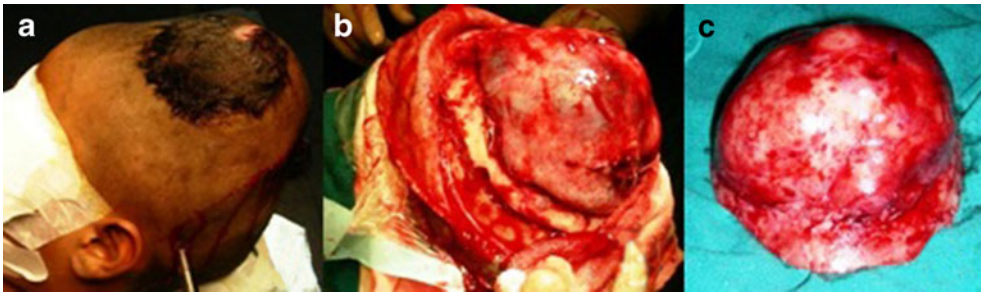

Fig. 4 **a** Intraoperative picture showing large swelling and proposed line of skin incision. **b** Skin flap raised anteriorly. Craniotomy with a margin of normal bone around. **c**) The extradural lesion removed en bloc. Intradural lesion was removed separately

extremes of age were not fit for surgery and both of them expired. The fourth patient, who had a recurrence at 12 months after primary surgery, did not give consent for surgery and finally died within 15 days of presentation.

Overall compliance to chemoradiation was good. Chemotherapy was given with adequate antiemetic covers, so only one patient developed grade III (RTOG grade for acute reaction) nausea vomiting, requiring parentral fluid supplement. One patient developed grade II leucocytopenia, for which chemotherapy was interrupted for 2 weeks, and one patient developed grade III leucocytopenia and died. Grade II anemia was noticed in two patients, requiring blood transfusion.

Three patients had presented with scalp swelling. Postoperatively, all of them had visible calvarial defects. However, one patient died in 6 months and the other had recurrence twice in 5 years, for which he was operated on, and cranioplasty was never offered to him. The third patient has refused cranioplasty as of now.

There were four deaths in our series; three of whom had recurrences in less than 1 year. The fourth patient had an asymptomatic metastastic lesion in the pelvis, and died within 2 months due to septicaemia, secondary to neutropenia following chemotherapy.

Discussion

The classic Ewing's sarcoma, primitive neuroectodermal tumor, Askin's tumor and extraosseous Ewing's sarcoma are all derived from the same primordial bone marrow-derived mesenchymal stem cell [23]. Ewing's sarcomas account for approximately 10% of primary malignant bone tumors. Most of the primary tumors occur in the long bones

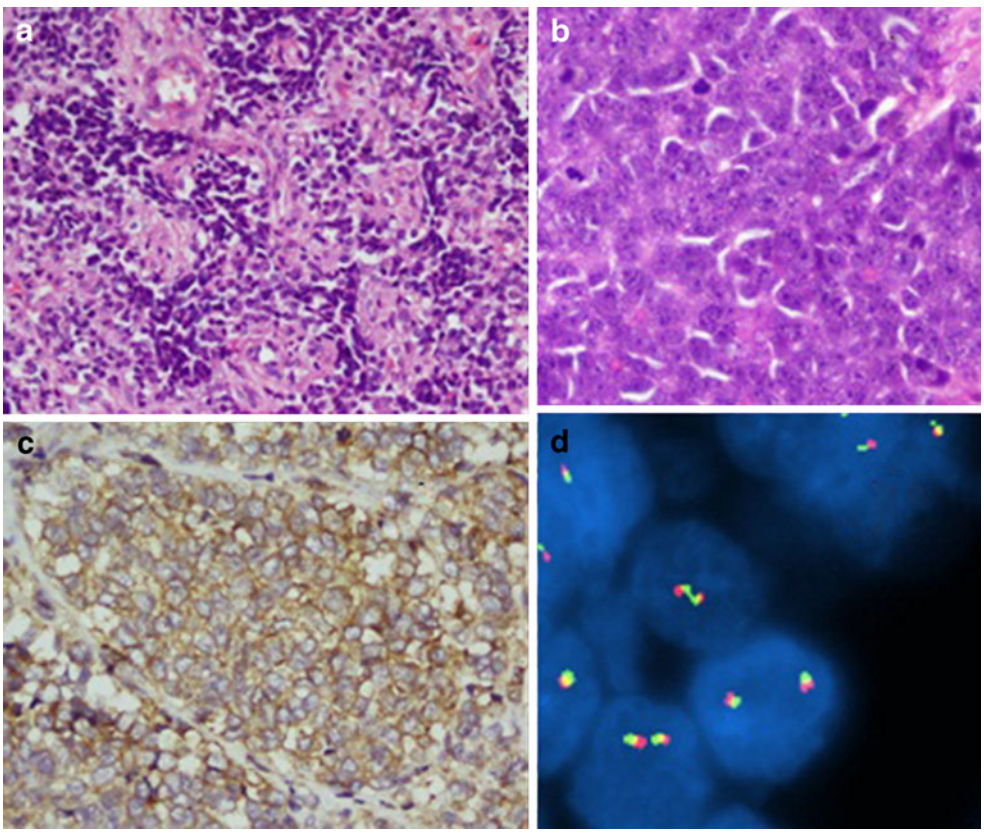

Fig. 5 **a** Small, round-to-oval tumor cells with prominent perivascular arrangement (H & E, ×200). **b** Round-to-oval cells with high N-C ratio with brisk mitotic activity (H & E, ×400). **c**) Neoplastic cells showing strong membraneous staining for Mic-2/CD99 (immunoperoxidase, ×400). **d** Representative image of FISH labeling using *EWS* break-apart probes

(47%), pelvis (19%), or ribs (12%), but only 1-4% of these sarcomas arise in the skull, usually on the frontal or parietal bone [25]. They have also been reported to arise at the skull base in children [7, 25]. In fact, 70% of the tumors arose from the skull base (one from the anterior cranial fossa base and six from the middle cranial fossa base) in our series.

Approximately 90% of cases occur in the first two decades of life, with the peak incidence being between 5 and 13 years of age [7]. However, in our series only 50% of the patients were in the first two decades, though 80% of them were below 26 years of age. Male patients were more frequently affected than female patients, with a reported ratio of 1.6:1 [7, 25]. This ratio was 4:1 in our series. The most frequent neurological signs in patients with intracranial Ewing's sarcomas are headache and papilledema, as was noted in our 80% of our patients.

The behavior of these tumors in the cranium has been found to be somewhat different from that in other areas, in the following respects. (1) The incidence of secondary spread is less. (2) The typical onion-peel appearance may not be found in cranial tumors. In the present study, we did not observe this appearance in any tumor. (3) The prognosis is slightly better. In fact, after total excision and chemoradiation, the 5-year survival rates range from 39% to 65%, especially with the round cell chemotherapy (RCT)-II protocol [7, 25].

Metastasis is present in about 25% of the patients with Ewing's sarcoma in general [9]. This, however, is rarely seen in calvarial Ewing's sarcoma [25]. There was only one patient in our series at presentation, with a possible lesion on bone scan in the pelvis. None of the patients in the present series had metastatic lesions at follow-up.

Radical excision bears better results, and almost all studies on skull bone Ewing's sarcoma suggested radical excsion, but it is technically challenging to perform total resection of cranial tumors in the petrous region, torcular region, and clivus [3, 7]. The method used for some extracranial sarcomas—involving biopsy, followed by adjuvant therapy (for local and systemic control with down staging of tumor), and then tumor excision followed by consolidation chemotherapy and radiotherapy—may work in calvarial Ewing's sarcoma [2, 15]. Resection might be easier and safer, with smaller cranial defects to close, and the long-term outcomes might be as good as or better than those currently achieved with the present treatment protocols. In one of our cases, a nasal biopsy was taken, followed by chemoradiation. However, the tumor had assumed a significant intracranial size giving rise to raised pressure symptoms requiring urgent surgery even before the first cycle of chemotherapy could be completed. Thus, presurgical chemotherapy to downstage the tumor, as for extracranial Ewing's sarcoma, may not be possible in calvarial Ewing's sarcoma, as the majority of the patients who present with rapidly increasing lesion with raised intracranial pressure. This makes excision—or at least decompression—imperative at the earliest. It may be of help in cases who present without raised intracranial pressure.

Patients with apparently localized disease at the diagnosis have occult metastatic disease; multidrug chemotherapy as well as local disease control with surgery and/or radiation is indicated in the treatment of all patients. Current regimens for the treatment of localised bony Ewing's sarcoma achieve a 5-year survival of approx 70% [12]. Vincristine, adriamycin, and cyclophosphamide (VAdriaC), alternating with ifosfamide and etoposide, has been shown to improve the outcome and is now a commonly used chemotherapy [12].

Local control can be achieved by surgery and/or radiation. Surgery is generally the preferred approach if the lesion is resectable [16]. Radiation therapy is appropriate for those with unresectable disease and as adjuvant therapy for those with inadequate margins or residual microscopic disease or who have viable tumor in a resected specimen [16]. In calvarial Ewing's sarcoma it is usually not possible to get margins free of microscopic tumor, so adjuvant radiotherapy of 40–50 Gy is administered to the local area [7]. Also as described previously, radical excision may not be safe in lesions involving the clivus, torcula, cavernous sinus.

Recurrence of Ewing's sarcoma of bone in general (ETB) is most common within 2 years of initial diagnosis (approximately 80%) [17]. Higher rates of local failure are seen in patients older than 14 years who have tumor more than 8 cm in length [10]. The overall prognosis for patients with recurrent Ewing's sarcoma is poor; 5-year survival following recurrence is approximately 10–15%. Time to recurrence is the most important prognostic factor. Patients who recurred greater than 2 years from initial diagnosis had a 5-year survival of 30% versus 7% for patients who recurred within 2 years. Patients with both local recurrence and distant metastases have a worse outcome than patients with either isolated local recurrence or metastatic recurrence alone [17, 20].

We observed certain differences from the reported cases and series of calvarial Ewing's sarcoma. The dura was eroded in 80% of cases. The recurrence rate in our series was higher than previously reported. There were four recurrences, three of which occurred within 12 months (early recurrence) after seemingly gross total excision and chemoradiation, and matches with Ewing's sarcoma at other regions. Besides, the mortality rate in our series, particularly those with early recurrence was high. Three of four patients who had recurrence in less than a year died within a month of detection of recurrence. The fourth patient who died had an asymptomatic pelvic metastasis at

presentation. The high mortality rate for patients with early recurrence matches with Ewing's sarcoma of bone in general. This is contrary to the previously reported cases and series of calvarial Ewing's sarcoma, where recurrences have rarely occurred. The cases reported with recurrences and/or death reported to date have been included in Table 2.

All those with recurrences in our series had large tumor size (>8 cm at least in one dimension) with dural infiltration. Only one patients with a large tumor at presentation did not have recurrence, at least for 2 years.

The answer to why certain patients do better than others may lie at the molecular level [5]. In the case of Ewing's sarcoma, most tumors have a balanced translocation involving chromosomes 11 and 22, which fuse portions of the Ewing's sarcoma gene (*EWS*) on 22q12 with the *FLI1* gene on 11q24, thus creating a novel fusion gene with oncogenic properties. Substitution of the EWS domain with a portion of the FLI1 transcriptional domain results in an *EWS–FLI1* fusion transcript with increased transcriptional activity compared with that of normal *FLI1*. Other *EWS-ETS* gene family rearrangements have been identified in the remaining 15% of tumours, with the t(21;22)(q22;q12) translocation resulting in fusion of *EWS* with the *ERG* gene on 21q22 being the second most common. Studies are being carried out to determine if it has a bearing on the prognosis. Besides, Ewing's sarcoma has overlapping morphologic features with other round cell tumors of childhood and adolescence. For prognosis and appropriate management, it is important to differentiate Ewing's sarcoma from classic neuroblastoma, Wilms' tumor, and rhabdomyosarcoma in particular [5]. Nine patients in our series, in whom chromosomal studies were carried out on paraffin blocks, revealed t(11:22) *EWS-ETS* translocation. However, only one genetic abnormality was tested for.

While using RT-PCR to detect *EWS-ETS* fusion transcripts, several alternative forms of *EWS–FLI1* have been described, reflecting the different breakpoints in *FLI1* and *EWS*. The most common type, designated *EWS–FLI1* type 1, consists of the first seven exons of *EWS* joined to exons 6–9 of *FLI1*, and accounts for approximately 60% of cases.

Table 2 Recurrences, deaths and metastasis found in the literature review and in the present series

Reference no.	Age/sex	Site	Maximum size of the lesion in one dimension (cm)	Dural erosion	Therapy	Follow-up period (months)	Survival
19	10/male	Parieto-occipital			S + R + C	24	Alive, metastasis (+)
6	11/female	Temporal			R + C + BMT	46	Died due to recurrence
14	7/female	Occipital			S + R + C	24	Alive, metastasis (+)
24	11/female	Occipital			S + C	18	Died due to metastasis
13	1/female	Parietal			S + C	9	Died of sepsis, clinically free of tumor
4	15/male	Frontoparietal			S + R + C	26	Alive, intracranial metastasis(+)
7	13/female	Parietal			S + R + C	68	Alive, recurred 2 years after surgery
25	1.5/female	Occipital			S + R + C	78	Recurred thrice and operated every time and finally died of systemic metastasis
Present series	3/male	Temporal squama + petrous	8.5	+ve	S + R + C	8	Recurrence 8 months—death
Present series	12/male	Temporal squama + petrous	8	+ve	S + R + C	12	Recurrence 12 months—death
Present series	15/male	Temporal base + greater wing of sphenoid + lateral wall of orbit	5.5	+ve	S + R + C	2	Had pelvic metastasis at presentation. Neutropenia + septicaemia—death in 2 months
Present series	62/male	Occipital	7.5	+ve	S + R + C	8	Recurrence 8 months—death
Present series	39/male	Frontal	7.5	+ve	S + R + C	60	Recurrences at 30 and 48 months after primary surgery, alive

S surgery, *R* radiotherapy, *C* chemotherapy

The type 2 *EWS–FLI1* fusion also includes *FLI1* exon 5 and is present in a further 25%. The fusion transcript type may determine the prognosis, with the presence of *EWS–FLI1* fusion transcript type 1 being associated with improved outcome compared with that in patients with other fusion transcript types [5]. However, this may be limited to patients with localized disease. The *EWS–FLI1* fusion transcript type 1 appears to encode a less active chimaeric transcription factor and to be associated with a lower proliferation index than that of tumours with other fusion transcript types. Unfortunately, the latest studies show no differences in prognosis with relation to the break point [18].

In conclusion, primary Ewing's sarcoma of the cranium differs from the lesion at other sites radiologically and by the absence of metastasis. The treatment consists of radical surgical excision within safe limits, especially in cases with raised intracranial pressure, followed by chemoradiation. Recurrence is usually local, and is treated with surgical debulking for raised pressure, followed by chemotherapy. Early recurrence and extremes of age are probably associated with poor outcome. A larger series is required to confirm the above findings.

Conflicts of interest None.

References

1. Ahmad FU, Suri A, Mahapatra AK, Ralte A, Sarkar C, Garg A (2004) Giant calvarial Ewing's sarcoma. Pediatr Neurosurg 40 (1):44–46
2. Bacci G, Ferrari S, Longhi A, Donati D, Barbieri E, Forni C, Bertoni F, Manfrini M, Giacomini S, Bacchini P (2004) Role of surgery in local treatment of Ewing's sarcoma of the extremities in patients undergoing adjuvant and neoadjuvant chemotherapy. Oncol Rep 11(1):111–120
3. Balasubramaniam S, Nadkarni T, Menon R, Goel A, Rajashekaran P (2008) Primary Ewing's sarcoma of the petroclival bone. J Clin Neurosci 15(6):712–714
4. Biousse V, Newman NJ, Lee AG, Eggenberger E, Patrinely JR, Kaufman D (1998) Intracranial Ewing's sarcoma. J Neuroophthalmol 18:187–191
5. Burchill SA (2003) Ewing's sarcoma: diagnostic, prognostic, and therapeutic implications of molecular abnormalities. J Clin Pathol 56(2):96–102
6. Davidson MJC (1991) Ewing's sarcoma of the temporal bone: a case report. Oral Surg Oral Med Oral Pathol 72:534–536
7. Desai KI, Nadkarni TD, Goel A, Muzumdar DP, Naresh KN, Nair CN (2000) Primary Ewing's sarcoma of the cranium. Neurosurgery 46(1):62–68, discussion 68–69
8. Erol FS, Ozveren MF, Ozercan IH, Topsakal C, Akdemir I (2001) Primary Ewing's sarcoma of the occipital bone—case report. Neurol Med Chir (Tokyo) 41(4):206–209
9. Esiashvili N, Goodman M, Marcus RB Jr (2008) Changes in incidence and survival of Ewing sarcoma patients over the past 3 decades: Surveillance Epidemiology and End Results data. J Pediatr Hematol Oncol 30(6):425–430
10. Fuchs B, Valenzuela RG, Sim FH (2003) Pathologic fracture as a complication in the treatment of Ewing's sarcoma. Clin Orthop 415:25–30
11. Garg A, Ahmad FU, Suri A, Mahapatra AK, Mehta VS, Atri S, Sharma MC, Garg A (2007) Primary Ewing's sarcoma of the occipital bone presenting as hydrocephalus and blindness. Pediatr Neurosurg 43(2):170–173
12. Grier HE, Krailo MD, Tarbell NJ, Link MP, Fryer CJ, Pritchard DJ, Gebhardt MC, Dickman PS, Perlman EJ, Meyers PA, Donaldson SS, Moore S, Rausen AR, Vietti TJ, Miser JS (2003) Addition of ifosfamide and etoposide to standard chemotherapy for Ewing's sarcoma and primitive neuroectodermal tumor of bone. N Engl J Med 348(8):694–701
13. Hadfield MG, Luo VY, Williams RL, Ward JD, Russo CP (1996) Ewing's sarcoma of the skull in an infant. A case report and review. Pediatr Neurosurg 25:100–104
14. Hollody K, Kardos M, Grexa E, Meszaros I (1992) Ewing's sarcoma in the occipital bone. Case report. Acta Paediatr Hung 32:371–378
15. Kobayashi H, Terasaka S, Yamaguchi S, Kubota K, Iwasaki Y (2008) Primary Ewing's sarcoma: peripheral primitive neuroectodermal tumour of the jugular foramen. Acta Neurochir (Wien) 150(8):817–821
16. Krasin MJ, Davidoff AM, Rodriguez-Galindo C, Billups CA, Fuller CE, Neel MD, Merchant TE (2005) Definitive surgery and multiagent systemic therapy for patients with localized Ewing sarcoma family of tumors: local outcome and prognostic factors. Cancer 104(2):367–373
17. Leavey PJ, Mascarenhas L, Marina N, Chen Z, Krailo M, Miser J, Brown K, Tarbell N, Bernstein ML, Granowetter L, Gebhardt M, Grier HE (2008) Prognostic factors for patients with Ewing sarcoma (EWS) at first recurrence following multi-modality therapy: a report from the Children's Oncology Group. Pediatr Blood Cancer 51(3):334–338
18. Le Deley MC, Delattre O, Schaefer KL, Burchill SA, Koehler G, Hogendoorn PC, Lion T, Poremba C, Marandet J, Ballet S, Pierron G, Brownhill SC, Nesslböck M, Ranft A, Dirksen U, Oberlin O, Lewis IJ, Craft AW, Jürgens H, Kovar H (2010) Impact of EWS-ETS fusion type on disease progression in Ewing's sarcoma/peripheral primitive neuroectodermal tumor: prospective results from the cooperative Euro-E.W.I.N.G. 99 trial. J Clin Oncol 28(12):1982–1988
19. Mohan V, Gupta SK, Goel AK, Mohanty S, Sawhney K, Shukla PK (1981) Primary Ewing's sarcoma of the calvarial bones. Neurol India 29:75–77
20. Rodriguez-Galindo C, Billups CA, Kun LE, Rao BN, Pratt CB, Merchant TE, Santana VM, Pappo A (2002) Survival after recurrence of Ewing tumors: the St Jude Children's Research Hospital experience, 1979–1999. Cancer 94(2):561–569
21. Sharma A, Garg A, Mishra NK, Gaikwad SB, Sharma MC, Gupta V, Suri A (2005) Primary Ewing's sarcoma of the sphenoid bone with unusual imaging features: a case report. Clin Neurol Neurosurg 107(6):528–531
22. Sharma RR, Netalkar A, Lad SD (2000) Primary Ewing's sarcoma of the greater wing of the sphenoid bone. Br J Neurosurg 14 (1):53–56
23. Suvà ML, Riggi N, Stehle JC, Baumer K, Tercier S, Joseph JM, Suvà D, Clément V, Provero P, Cironi L, Osterheld MC, Guillou L, Stamenkovic I (2009) Identification of cancer stem cells in Ewing's sarcoma. Cancer Res 69(5):1776–1781
24. Tournut P, Turjman F, Laharotte JC, Froment JC, Gharbi S, Duquesnel J (1994) Primary Ewing's sarcoma of the skull presenting as an acute surgical emergency. Childs Nerv Syst 10:193–194
25. Yasuda T, Inagaki T, Yamanouchi Y, Kawamoto K, Kohdera U, Kawasaki H, Nakano T (2003) A case of primary Ewing's sarcoma of the occipital bone presenting with obstructive hydrocephalus. Childs Nerv Syst 19(12):792–799

Acta Neurochir (2011) 153:1487–1495
DOI 10.1007/s00701-011-1046-x

CLINICAL ARTICLE

Application of intraoperative indocyanine green videoangiography to brain tumor surgery

Eui Hyun Kim · Jin Mo Cho · Jong Hee Chang · Sun Ho Kim · Kyu Sung Lee

Received: 15 February 2011 / Accepted: 3 May 2011 / Published online: 19 May 2011

Abstract
Background Videoangiography using indocyanine green (ICG) has been used in the ophthalmologic field for a long time. It was introduced to the neurosurgical field several years ago but has been limited to vascular surgeries. We applied ICG videoangiography to brain tumor surgery and evaluated the usefulness.
Methods Twenty-three patients with a brain tumor who underwent microsurgical resection were analyzed. The pathological diagnosis was meningioma in 15 patients, metastasis in three, glioma in three, and hemangioblastoma in two. A microscope with a special filter and infrared excitation light to illuminate the operating field was used in this study. The intravascular fluorescence was imaged with a video camera attached to the microscope. ICG was injected intravenously with the dose of 5–25 mg, and overall, ICG was injected intraoperatively 32 times.
Results ICG videoangiography allowed for an excellent evaluation of blood flow in the tumoral and peri-tumoral vessels both before and after the resection in all cases.
Conclusions ICG videoangiography is a useful method for monitoring blood flow in the exposed vessels during microsurgery for a brain tumor. This noninvasive method is simple, safe, cost-effective, and easily repeatable. Before resection, it provides information on the tumoral and peri-tumoral circulation including sequential visualization of vessels or direction of the blood flow. After resection, it checks the patency of the peri-tumoral vessels and is especially useful for the vein. This ICG videoangiography can be an alternative tool to intraoperative angiography or Doppler ultrasonography in selective cases.

Keywords Brain tumor · Indocyanine green · Surgical microscope · Videoangiography

E. H. Kim · J. M. Cho · J. H. Chang (✉) · S. H. Kim · K. S. Lee
Department of Neurosurgery, Neuro-Oncology Clinic and Brain Research Institute, Yonsei University College of Medicine,
134 Shinchon-dong, Seodaemoon-gu,
Seoul 120–752, Korea (R.O.K.)
e-mail: changjh@yuhs.ac

Introduction

Manipulation of tumor-related and normal brain vessels is always important in all brain tumor surgeries. When a tumor has many feeding arteries and draining veins, all vessels should be identified and coagulated in order to ensure a clean operative field and reduce blood loss. It is more important not to injure all normal vessels near the tumor mass. Generally, vessels can be evaluated intraoperatively by microvascular Doppler sonography (MDS) and digital subtraction angiography (DSA). MDS has many advantages: low cost, noninvasiveness, and short time to results. However, this is not very useful for the evaluation of venous blood flow and not reliable for small vessels. DSA is the standard method for the assessment of cerebral vessels, but it is an invasive procedure. It is also expensive and requires additional time, intraoperative equipment, and human resources. Moreover, due to its low spatial resolution, this method cannot be applied to small vessels [8, 11]. Indocyanine green (ICG) has been used for the visualization of vessels mainly in the ophthalmologic field. Even though fluorescence angiography was first started in the neurosurgical field in 1967, it has not been practically used. However, there have been an increasing number of reports indicating that this technique is very useful in neurovascular surgery [2, 4, 6–9, 12]. Recently, some authors started using ICG videoangiography for the surgery of brain tumors [3, 10]. We also applied ICG videoangiography to a

brain tumor surgery and found it very useful when it was used in selective cases.

Methods

Patient population

Between June of 2009 and May of 2010, ICG videoangiography was used intraoperatively in 23 patients with a brain tumor. There were nine male and 14 female patients, with ages ranging from 33 to 85 years (mean, 54.3 years). The pathological diagnosis was meningioma in 15 patients, metastasis in three, glioma in three, and hemangioblastoma in two. All patients were interviewed regarding a history of iodine allergy, pregnancy, or previous anaphylactic reactions to contrast media injections before the operation. The ICG videoangiography was performed before and/or after tumor resection.

Techniques of ICG videoangiography

ICG is a near-infrared fluorescent dye of which absorption and emission peaks are 805 nm and 835 nm, respectively. These peaks lie within the optical window in which near-infrared light can penetrate to depths of several millimeters to a few centimeters. After the intravenous injection, ICG binds to plasma proteins very tightly within 1–2 s so that it remains exclusively intravascular and cannot be excreted in the kidney. ICG is not metabolized in the body and is excreted by the liver. Its plasma half-life is 3–4 min. In this study, a surgical microscope (Carl Zeiss Co., Oberkochen, Germany) was used in which a near-infrared excitation light source, an optical filter, and a video camera are altogether integrated. The infrared 800 (IR 800) fluorescence mode is designed for excitation in the wavelength range of 700–780 nm, and for fluorescence visualization in the wavelength range of 820–900 nm.

After we cleaned the surgical field with hemostasis, the area of our interest was targeted with a microscope. The tracking camera of the Stealth navigation system (Medtronic Navigation, Louisville, CO, USA) was put away from the surgical field as the camera beam for tracking interferes with the excitation light for ICG videoangiography. One vial of ICG (25 mg) was dissolved in 5 ml of normal saline, and then 0.3 mg/kg of ICG was injected as a bolus. The total dose of ICG never exceeded 5 mg/kg. ICG videoangiography was performed before and/or after tumor resection. ICG injection was repeated with 10 min of interval between each injection. ICG was given through a peripheral intravenous line and arterial phase began about 20–30 s after the injection. The images were immediately replayed on the external screen of a microscope, and then interpreted.

Results

A total of 32 times of ICG videoangiography were performed in 23 patients. The characteristics of these patients are summarized in Table 1. From ICG injection until interpretation, it took less than 5 min in all cases. There was no hardware failure or user failure. No side-effects were observed after intravenous injection of the ICG dye. With high image quality and spatial resolution, ICG videoangiography visualized blood vessels with very useful information about the patency and direction of blood flow in veins and even small perforating arteries.

Pre-resection ICG videoangiography was performed in seven patients and its main purpose was the localization of blood vessels. ICG videoangiography was performed before dural opening in four patients with meningiomas and hemangioblastomas, all cortical blood vessels emitted strong fluorescence penetrating semi-transparent dura mater. Especially, in two patients with hemangioblastomas, ICG videoangiography showed not only feeding arteries and blood vessels but also a hyper-vascularized tumor mass itself with sequential visualization. On the other hand, checking the patency of arteries and veins was the main purpose of ICG videoangiography after tumor removal. In 11 of 12 patients with meningiomas near cerebral cortex convexity, ICG videoangiography was performed after tumor resection, which showed strong fluorescence from all superficial cortical arteries and veins. In three meningiomas on an anterior clinoid process or a tuberculum sellae, we needed to increase sensitivity of fluorescence detection in order to visualize small deep-seated vessels properly. In two glial tumors near the insular cortex, we performed videoangiography before and after tumor removal so that we could detect vasospasm on the M3 middle cerebral arterial branches. In one of them, significant vasospasm developed and papaverine was applied to the M3 branches.

Illustrative cases

Case 1 (Patient 3)

A 45-year-old female patient with a left parasagittal meningioma underwent tumor removal surgery. The tumor mass was friable, but the tumor capsule was very thin and adhesive to the surrounding normal brain cortex. Although the tumor capsule was successfully dissected from the brain cortex and large cortical veins with great care, we were not sure if the cortical veins were patent as they had been manipulated a lot during the dissection. MDS did not demonstrate any meaningful signal on the cortical veins. ICG videoangiography was performed, which showed intact flow of all cortical veins running over the tumor bed (Fig. 1).

Table 1 Characteristics of patients studied with ICG videoangiography

Patient no.	Age/sex	Diagnosis	Location	No. of ICG injections		Investigations with ICG videoangiography	Benefit from ICG videoangiography
				Before TR	After TR		
1	F/80	Meningioma	F convexity	–	1	Patency of cortical veins	–
2	F/53	Meningioma	Sphenoid ridge	–	1	Patency of cortical veins	–
3	F/45	Meningioma	P parasagittal	–	1	Patency of cortical veins	–
4	M/49	Meningioma	F convexity	1	–	localization of cortical veins before dural opening	Safe dural incision
5	F/41	Meningioma	P parasagittal	1	1	localization of cortical veins before dural opening Patency of cortical veins	Safe dural incision
6	F/64	Meningioma	F parasagittal	–	1	Patency of cortical veins	–
7	F/51	Meningioma	F parasagittal	–	1	Patency of cortical veins	–
8	F/69	Meningioma	F, P parasagittal	–	1	Patency of cortical veins	–
9	M/57	Meningioma	ACP	–	1	Patency of deep-seated large arteries and perforators	–
10	F/69	Meningioma	ACP	–	1	Patency of deep-seated large arteries and perforators	–
11	F/45	Meningioma	Tuberculum sellae	–	1	Patency of deep-seated large arteries and perforators	–
12	F/80	Meningioma	F parasagittal	–	1	Patency of cortical veins	Further tumor resection
13	F/62	Atypical meningioma	F, T convexity	–	1	Patency of cortical veins	–
14	M/37	Atypical meningioma	P parasagittal	–	1	Patency of cortical veins	Further tumor resection
15	M/64	Atypical meningioma	P parasagittal	–	2	Blood flow direction of cortical veins Patency of cortical veins	Fistula localization
16	F/49	Metastatic brain tumor (melanoma)	F	–	1	Patency of cortical veins	–
17	M/49	Metastatic brain tumor (lung cancer)	T, O	1	2	Patency of cortical veins and anastomotic vein	–
18	M/68	Metastatic brain tumor (lung cancer)	T, O	–	1	Patency of cortical veins and anastomotic vein	Further tumor resection
19	F/33	Glioblastoma	Insular	1	2	Patency of M3 branches of MCA	–
20	M/63	Giant cell glioblastoma	P	–	1	Patency of cortical veins	–
21	M/44	Anaplastic astrocytoma	Insular	1	2	Patency of M3 branches of MCA	Papaverine treatment Hypervolemic therapy
22	M/37	Hemangioblastoma	Cerebellum	1	–	Localization of a tumor, a feeding artery, and a draining vein	Safe dural incision Safe tumor dissection
23	F/41	Hemangioblastoma	Cerebellum	2	–	Localization of a tumor, a feeding artery, and a draining vein	Safe dural incision Safe tumor dissection

ACP anterior clinoid process; *F* frontal; *ICG* indocyanine green; *MCA* middle cerebral artery; *O* occipital; *P* parietal; *T* temporal; *TR* tumor removal

Case 2 (Patient 5)

A 41-year-old female patient presented with a parasagittal meningioma on the right parietal lobe. Before we opened the dura mater, the superior sagittal sinus and cortical drainage veins were localized by ICG videoangiography (Fig. 2). Based on this finding, a precise dural incision was made, avoiding the injury on the cortical veins underneath the dura mater. The tumor mass was resected totally without injury to the cortical drainage veins.

Case 3 (Patient 21)

A 44-year-old man with a brain tumor on the left-side insular area underwent an awake surgery for the tumor removal. After the dissection of the Sylvian fissure, the tumor was exposed

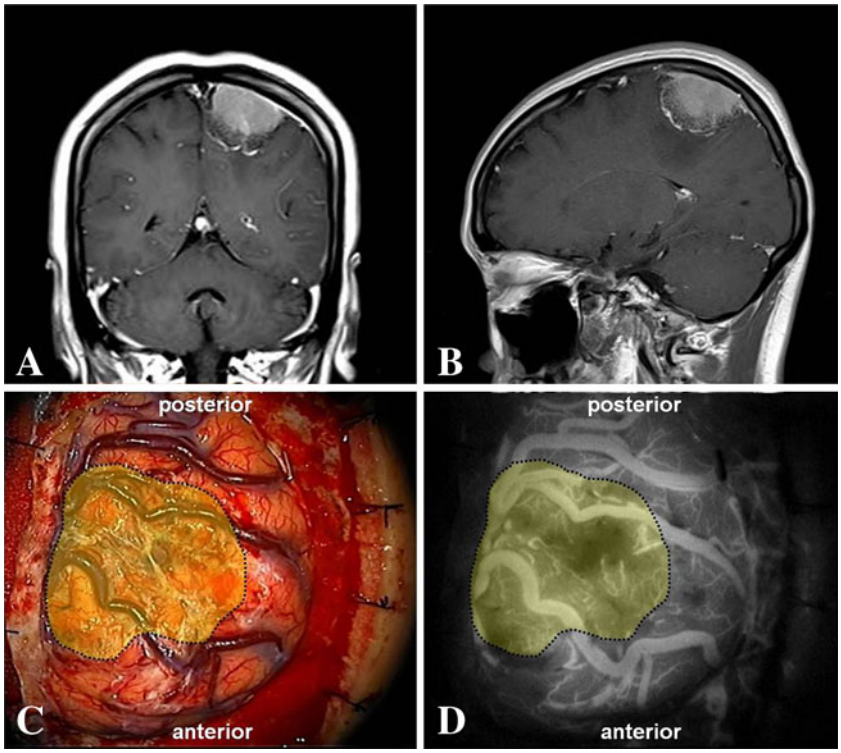

Fig. 1 Preoperative magnetic resonance imaging shows a meningioma on the left parietal lobe (**a**, **b**). Indocyanine green videoangiography shows intact flow of all cortical veins running over the tumor bed (*yellow zone bordered by dotted line*) (**c**, **d**)

together with M3 branches of the left MCA. Before starting tumor resection, we performed ICG videoangiography in order to figure out the anatomical relationship between the tumor and MCA branches. After the tumor was removed and dissected from the surrounding vessels, ICG videoangiography was performed again, which showed intact blood flow of all MCA branches (Fig. 3). Pathological examination revealed that the tumor was an anaplastic astrocytoma.

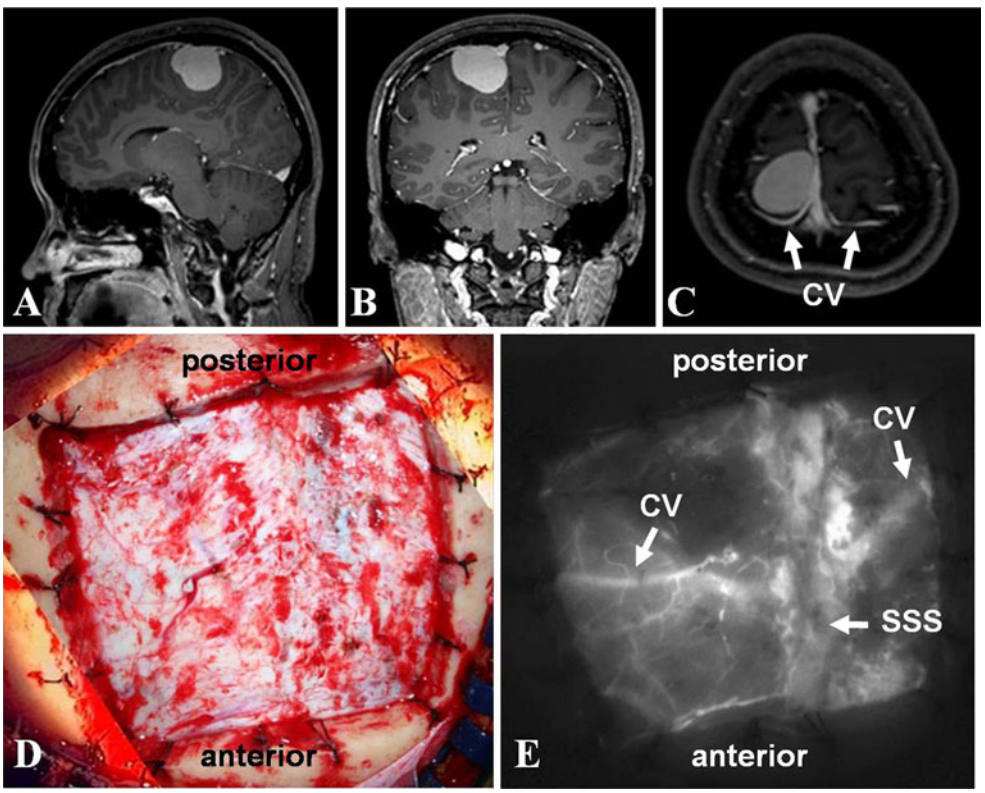

Fig. 2 A parasagittal meningioma is seen with two cortical veins (CV) on the right parietal lobe (**a**–**c**). Before the opening of the dura mater, the superior sagittal sinus (SSS) and cortical veins are localized by indocyanine green videoangiography (**d**, **e**). With this result, a dural incision is made avoiding the injury on the cortical veins underneath the dura mater

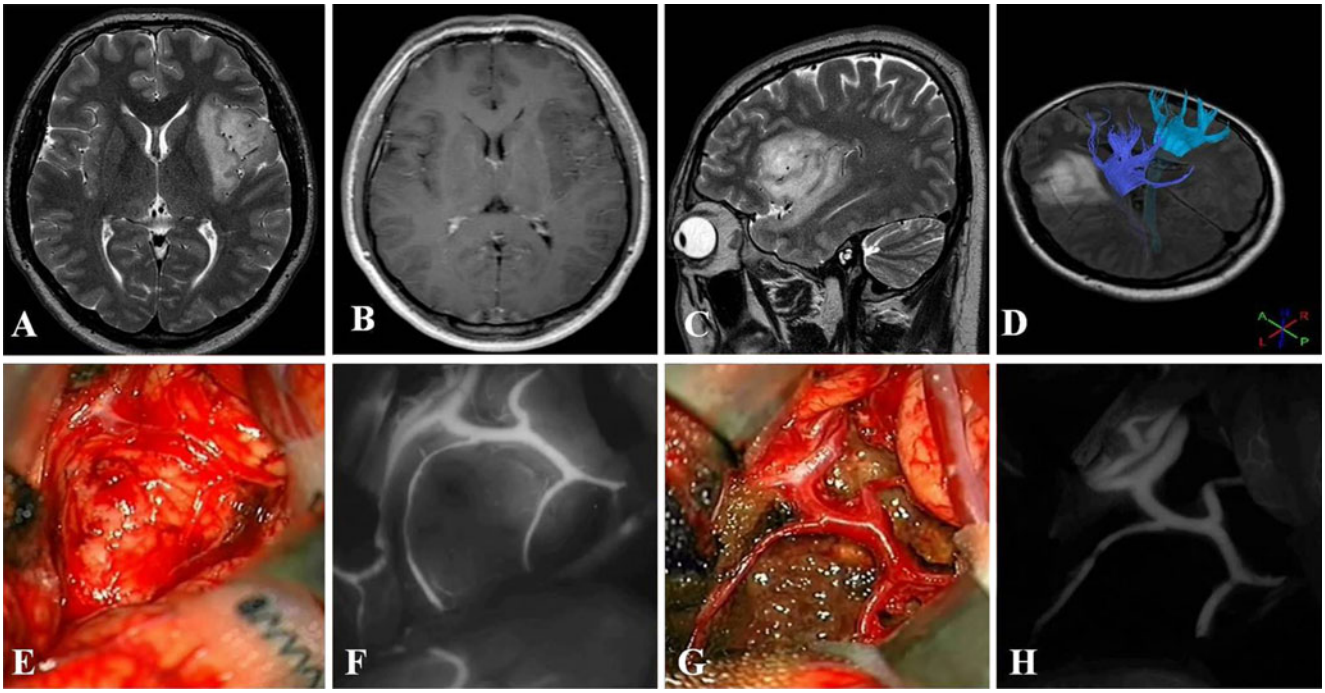

Fig. 3 A brain tumor on the left-side insular area is identified on the preoperative magnetic resonance imaging, which is hyperintense on T2-weighted images and is poorly enhanced by gadolinium on T1-weighted images (**a**–**d**). After dissection of the Sylvian fissure, a pre-resection photograph (**e**) and indocyanine green (ICG) videoangiography (**f**) show the anatomical relationship between middle cerebral artery (MCA) branches and the underlying tumor. After the tumor resection, all M3 branches are thought to be preserved (**g**) and an ICG videoangiography confirms that the blood flow of all MCA branches is intact (**h**)

Case 4 (patient 14)

A 37-year-old man with a parasagittal meningioma on the right parietal lobe underwent tumor resection. The tumor originated from the wall of the superior sagittal sinus, where a large draining vein entered the superior sagittal sinus. As we tried not to sacrifice this large draining vein, a small portion of the tumor was left around the vein. When we stopped removing the tumor, the vein was thought to be patent. However, ICG videoangiography revealed that this vein did not have any venous flow in it (Fig. 4). We continued to remove all the remnant tumor with coagulation of the large vein, and achieved total removal of the tumor. Fortunately, the patient did not have any postoperative problems.

Case 5 (Patient 23)

A 41-year-old female patient presented with a tumor on the left cerebellar hemisphere. A preoperative MRI revealed the tumor had a solid portion as well as cystic portion, which was very consistent with a hemangioblastoma. The solid portion of the tumor was strongly enhanced with gadolinium on T1-weighted images of MRI. DSA showed a highly vascularized tumor. Feeding arteries and draining veins were localized preoperatively based on radiological findings. Intraopera-

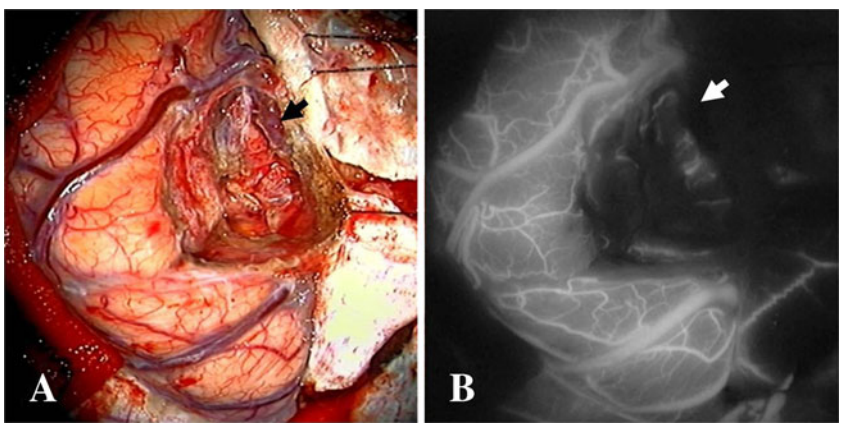

Fig. 4 After removal of a parasagittal meningioma on the parietal lobe, the photograph shows a small residual portion of tumor adhered to a large draining vein (*black arrow*) into the superior sagittal sinus (**a**). However, indocyanine green videoangiography reveals that there is no blood flow in it (*white arrow*) (**b**)

tively, after the exposure of the dura mater, ICG videoangiography was performed in order to localize the tumor mass before we opened the dura mater. It elaborately visualized the feeding arteries, draining veins, and the tumor (Fig. 5). Based on the results of the ICG videoangiography, a dural incision was made and the tumor was safely approached. All feeding arteries were identified and coagulated first, and lastly, the draining vein into the left transverse sinus was identified and coagulated. We achieved total removal of the tumor with minimal blood loss. By pathological examination, the tumor turned out to be a hemangioblastoma.

Discussion

The anatomical and hemodynamic relationship between a tumor and a vascular system is very essential in brain tumor surgery. Brain tumors often alter the surrounding brain circulation. DSA and magnetic resonance angiography and computed tomography angiography are useful tools for preoperative evaluation of a vascular system. However, when a procedure-related change in a vascular system is expected during a surgery, intraoperative imaging is very valuable and could be extremely effective in decreasing the operative morbidity and unexpected deterioration. Even though MDS and DSA have been major intraoperative vascular imaging tools so far, they have their own limitations and disadvantages [8, 11]. MDS has been most widely used as it is noninvasive, very simple, and can be performed in a minute. In most cases, MDS is very useful in the evaluation of a large artery. However, for the evaluation of a vein that has low blood flow in it, or a small perforating artery of which the diameter is less than 0.5 mm, the usefulness of MDS is questionable. As for DSA, it is the standard method for the assessment of a vascular system. However, it is an invasive procedure and, even though it is regarded as a safe imaging tool, it potentially increases operative morbidity. It is also very expensive, as it requires additional personnel and equipment. The time for setup is much longer than in other methods because it is technically demanding. The results of DSA need to be interpreted as the images are not integrated into the operative view. In addition, the spatial resolution of the intraoperative DSA is very limited, so visualization of small perforators is almost impossible.

ICG videoangiography is very simple and inexpensive. It is also very quick, as the time to result is less than 5 min. This technique is noninvasive and can be easily repeated

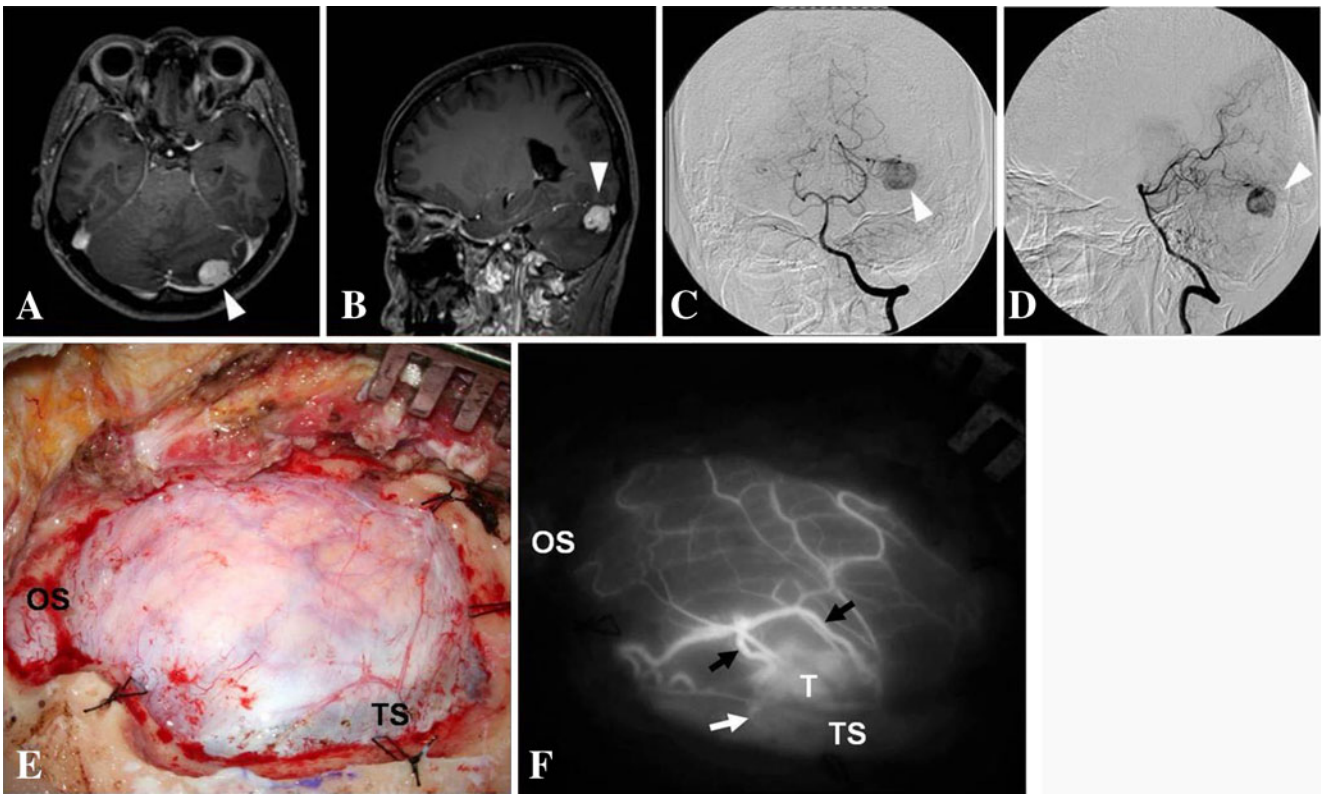

Fig. 5 All preoperative radiological findings are consistent with a hemangioblastoma (*white arrow heads*) lying on the left cerebellar hemisphere (**a**–**d**). After unilateral suboccipital craniotomy, a left transverse sinus and an occipital sinus are exposed (**e**). Indocyanine green videoangiography before dural opening shows feeding arteries (*black arrows*) and a draining vein (*white arrow*) (**f**). *OS* occipital sinus; *T* tumor; and *TS* transverse sinus

with an interval of 5–10 min. It provides real-time information on the patency of the arterial and venous vessels of all relevant diameters even though the information is not quantitative. As all images are integrated into the operative view, it is so much easier to have a comprehensive anatomical orientation that the surgical procedure can be much safer. ICG is a very safe compound with frequencies of 0.05-0.2% of side-effects; serious side-effects include hypotension, arrhythmia, or anaphylactic shock and mild side-effects include nausea, itching sense, or skin eruptions [1, 5]. However, ICG videoangiography has the limitation that it is available only for what is visible in the operative field. In order to visualize blood vessels, they should be exposed first and not covered by a blood clot. Therefore, when a deep-seated tumor is approached through a long, narrow corridor, it is not easy to clearly visualize normal and tumor-related vessels with ICG videoangiography and consequently may not be very useful [8]. The best candidate for ICG videoangiography is a tumor located superficially, which can be exposed widely with surrounding blood vessels. Another limitation of ICG videoangiography has been the absence of integration with the surgical microscope. This technique originally requires stopping the surgical procedure, moving the microscope away from the surgical field, and bringing the near-infrared light source and a camera into the surgical field. Not to mention that it prolongs the operation time, and the surgical corridor is sometimes too narrow to make the excitation light reach the tumor and, at the same time, to aim the video camera at the tumor. Raabe et al. [11] noted this problem in their experiences and emphasized the importance of the integration of all the components in ICG videoangiography. In this study, we used an OPMI Pentero microscope in which a near-infrared excitation light source, an optical filter, and a video camera were integrated. The FL800 module of the Leica microscope (Leica Co., Wetzlar, Germany) also has a special attachment for the ICG videoangiography. Due to this integration, the utilization of ICG videoangiography has been enhanced. In our series, the procedure was easily performed and the time to the results never took longer than 5 min.

We applied this method to brain tumor surgery and found it very useful both before and after tumor resection. In seven patients, ICG videoangiography was performed eight times before starting tumor removal. The main goal of pre-resection ICG videoangiography was localizing blood vessels in relation to the tumor. It visualized the tumor-feeding arteries, draining veins, and passing-by normal vessels. The spatial resolution was good enough to reveal if a vessel was a tumor-related or a normal passing-by vessel. It was also available for deep-seated vessels through a deep and narrow surgical corridor, even though its signal was not as strong as in superficial tumors. Interestingly, as ICG fluorescence can penetrate dura mater with an adequate dose of ICG and detection sensitivity, pre-resection evaluation of cortical vessels was available before the opening of the dura mater. We were able to localize the sinuses and unexposed cortical veins underneath the dura mater before opening it (Fig. 2). In case 5, which involved a hemangioblastoma (patient 23), besides localizing the tumor-feeding arteries and draining veins before the dural opening, the hypervascular tumor mass was also visualized underneath the dura mater on ICG videoangiography. After the dural opening, the brain swelling was so severe that we could not perform ICG videoangiography. Even though the tumor-feeding arteries and draining veins were preoperatively localized with cerebral angiography, we found it was much easier to have a comprehensive anatomical orientation with ICG video-angiography as all images were integrated into the operative view. In addition to the localization of blood vessels, ICG videoangiography provides information on the direction of blood flow, which is a very distinguished advantage that MDS does not have. In case that we cannot expose the whole course of blood vessels from the origins to the destinations, ICG videoangiography revealed the direction the arteries or veins are heading. In one case (patient 15), involving a meningioma that invaded and filled a superior sagittal sinus on the preoperative MRI, we thought the blood in the cortical veins would flow from a superior sagittal sinus to the hemisphere cortex. Preoperative angiography showed very poor filling of a superior sagittal sinus so that parasagittal cortical veins were hardly seen. However, with excellent visualization on ICG videoangiography, the blood flow direction of the cortical veins was figured out, which was the opposite to the normal as we expected. This patient also had an arterio-venous fistula that was previously seen on preoperative DSA. We found ICG videoangiography very convenient as it precisely localized the fistulous point of the tumor in the operative field.

After tumor resection, ICG videoangiography was performed 24 times in 20 patients. It allowed an immediate check of the patency of blood vessels around a tumor, which would be the biggest advantage of ICG video-angiography. The gross appearance of blood vessels was not always reliable. We experienced three cases (patients 12, 14, and 18) in which the peri-tumoral normal veins looked intact after tumor removal; however, post-resection ICG videoangiography revealed that they had no blood flow in them (Fig. 4). Including these three cases, in 15 patients whose veins were evaluated with MDS and ICG videoangiography concomitantly after tumor resection, MDS failed to show consistent and reliable results in all of them. Therefore, we think ICG videoangiography is very valuable especially in the evaluation of venous blood flow. On the contrary, in the evaluation of arterial blood flow in the other five patients, the results of MDS were always

compatible with that of ICG videoangiography. When ICG videoangiography showed poor blood flow in an artery after violent manipulation during tumor removal, papaverine was applied on the injured artery so that the blood flow could be restored. Even though both ICG videoangiography and MDS were useful and reliable in the evaluation of arterial blood flow, when it comes to a small perforating artery, ICG videoangiography was superior to MDS.

Conclusions

Microscope-integrated ICG videoangiography has many advantages compared to other intraoperative vascular imaging modalities such as MDS and DSA. Before tumor resection, ICG videoangiography was found to be very useful for (1) the localization of the blood vessels and dural sinuses and sometimes even a tumor mass, (2) the detection of blood flow direction, and (3) the localization of the fistula. Owing to this imaging technique, it was very convenient to distinguish tumor-related vessels from normal ones in superficially located meningiomas and hemangioblastomas as well as to see the direction of blood flow in drainage veins in parasagittal meningiomas with obstruction of a superior sagittal sinus. After resection, it immediately showed the patency of the peritumoral vessels, which often led to a change of the surgical plan, further resection of a remaining tumor, sacrifice of a cortical draining vein, and papaverine treatment on a vessel with vasospasm. When the patency of a vessel was of concern on ICG videoangiography, medical treatment, like as hypervolemic therapy, was started immediately even during the surgery. Even though this technique is exclusively available for an exposed blood vessel, it can be an alternative of MDS and a complementary diagnostic tool for DSA in selective cases.

Acknowledgments This work was supported by the Mid-career Researcher Program through a National Research Foundation grant funded by the Korean Ministry of Education, Science, and Technology (No. R01-2008-000-20545-0), and a faculty research grant of Yonsei University College of Medicine for 2008 (6-2008-0174) to Jong Hee Chang.

Conflicts of interest None.

References

1. Cochran ST, Bomyea K, Sayre JW (2001) Trends in adverse events after IV administration of contrast media. Am J Roentgenol 176:1385–1388
2. de Oliveira JG, Beck J, Seifert V, Teixeira MJ, Raabe A (2008) Assessment of flow in perforating arteries during intracranial aneurysm surgery using intraoperative near-infrared indocyanine green videoangiography. Neurosurgery 62:1300–1310
3. Ferroli P, Acerbi F, Albanese E, Tringali G, Broggi M (2011) Application of intraoperative indocyanine green angiography for CNS tumors: results on the first 100 cases. Acta Neurochir Suppl 109:251–257
4. Hänggi D, Etminan N, Steiger HJ (2010) The impact of microscope-integrated intraoperative near-infrared indocyanine green videoangiography on surgery of arteriovenous malformations and Dural arteriovenous fistulae. Neurosurgery 67:1094–1104
5. Hope-Ross M, Yannuzzi LA, Gragoudas ES, Guyer DR, Slakter JS, Sorenson JA, Krupsky S, Orlock DA, Puliafito CA (1994) Adverse reactions due to indocyanine green. Ophthalmology 101:529–533
6. Imizu S, Kato Y, Sangli A, Oguri D, Sano H (2008) Assessment of incomplete clipping of aneurysms intraoperatively by a near-infrared indocyanine green-video angiography (Niicg-Va) integrated microscope. Minim Invasive Neurosurg 51:199–203
7. Jing Z, Ou S, Ban Y, Tong Z, Wang Y (2010) Intraoperative assessment of anterior circulation aneurysms using the indocyanine green video angiography technique. J Clin Neurosci 17: 26–28
8. Killory BD, Nakaji P, Gonzales LF, Ponce FA, Wait SD, Spetzler RF (2009) Prospective evaluation of surgical microscope-integrated intraoperative near-infrared indocyanine green angiography during cerebral arteriovenous malformation surgery. Neurosurgery 65:456–462
9. Ma C-Y, Shi J-X, Wang H-D, Hang C-H, Cheng H-L, Wu W (2009) Intraoperative indocyanine green angiography in intracranial aneurysm surgery: Microsurgical clipping and revascularization. Clin Neurol Neurosurg 111:840–846
10. Murai Y, Adachi K, Matano F, Tateyama K, Teramoto A (2011) Indocyanin green videoangiography study of hemangioblastomas. Can J Neurol Sci 38:41–47
11. Raabe A, Beck J, Gerlach R, Zimmermann M, Seifert V (2003) Near-infrared indocyanine green video angiography: a new method for intraoperative assessment of vascular flow. Neurosurgery 52:132–139
12. Woitzik J, Horn P, Vajkoczy P, Schmiedek P (2005) Intraoperative control of extracranial-intracranial bypass patency by near-infrared indocyanine green videoangiography. J Neurosurg 102:692–698

Comment

The authors present their experience on brain tumor surgery assisted by the intra-operative use of indocyanine green videoangiography (ICG). In this series, ICG emerges as a simple, inexpensive, rapid, non-invasive, and reliable implementation for vascular management in the neuro-oncological setting. The authors report advantages and limits of the technique by means of an effectively illustrated surgical series. For educational purposes, we can synthesize that ICG might be functional to selected surgical scenarios. For example, when the tumor is located close to major vessels that could be potentially injured by surgery (i.e., Sylvian fissure tumors), when approaching high vascularized tumors (i.e., hemangioblastomas or some meningiomas), or when the direction of the blood flow of peri-tumoral vasculature must be recognized in a pre-resection stage in order to plan a correct removal strategy (i.e., cortical veins in parasagittal meningioma surgery).

We agree with the authors that brain tumor surgery can, in selected cases, take advantage of the intra-operative use of ICG. Further studies on a large series of patients are needed to define the real clinical impact of ICG on a patient's outcome.

Domenico d'Avella
Alessandro Della Puppa
Padova, Italy

Comment

Intraoperative indocyanine green (ICG) angiography is an established method to support the microsurgical therapy of intracranial aneurysms and AVMs. The authors performed ICG angios during the removal of 15 meningiomas, three metastases, three gliomas, and two hemangioblastomas, which allowed them to make several useful findings at different phases of surgeries, including:

* localization of the sinus and cortical veins before opening the dura.

* visualization of feeding arteries, draining veins, and mass of a hemangioblastoma before opening the dura.

* relationship between an insular anaplastic astrocytoma and branches of the MCA.

* cortical vein patency in the tumor bed after removal of a meningioma.

* a vein thought to be open was not and could be sacrificed for a total removal.

The authors are to be congratulated for a timely addition to the growing list of instances during CNS tumor surgery in which ICG angio may reveal important aspects.

Juha E Jääskeläinen
Kuopio, Finland

Acta Neurochir (2011) 153:1497–1499
DOI 10.1007/s00701-011-0991-8

LETTER TO THE EDITOR

Paradoxical fluorescence after administration of 5-aminolevulinic acid for resection of a cerebral melanoma metastasis

Philippe Schucht · Jürgen Beck · Istvan Vajtai · Andreas Raabe

Received: 16 February 2011 / Accepted: 2 March 2011 / Published online: 24 May 2011

Sir,

Five-aminolevulinic acid (5-ALA) is increasingly used for resection of high-grade glioma; however, little is known of its fluorescent behavior in other cerebral tumors. In this letter, we report our findings of a paradoxical fluorescent pattern after administration of 5-ALA in a metastatic melanoma.

A 69-year-old man was admitted for apraxia and disorientation after a skiing accident. The patient's previous medical history included the excision of malignant melanomas 9 years earlier, with no known metastatic spread. Magnetic resonance imaging (MRI) showed a brightly enhancing, centrally necrotic, solitary right frontal tumor mass, indicating a glioblastoma or metastasis.

A solution of 1.5 g ALA was orally administered 4 h preoperatively. A craniotomy guided by neuronavigation was performed, followed by durotomy. Using a surgical microscope and light source at 5-ALA excitation wavelength (OPMI Neuro/NC4 system-fluorescence kit, Carl Zeiss, Oberkochen, Germany), neither bright nor vague fluorescence was emitted by the tumor mass. The surrounding tissue, however, exhibited solid red fluorescence up to a distance of 5 mm from the solid tumor core. The intraoperative navigation system (Brainlab, Feldkirchen, Germany) confirmed that the peritumoral "5-ALA-positive" fluorescent tissue was outside the strongly enhancing tumor (MRI). Intraoperative cryosection analysis revealed no infiltrating tumor cells in the "5-ALA-positive" tissue; however, the non-fluorescent "5-ALA-negative" solid tumor mass showed metastatic malignant melanoma. The postoperative MRI showed a gross total resection of the tumor.

The gross surgical specimens were histologically examined. This included a nodule (3 × 2 × 2 cm) and six largely intact mapping biopsy samples each measuring approximately 0.3-0.4 cm in diameter. Samples were processed according to standard histopathological techniques (fixation in 4% buffered formalin; 3-μm thick sections; hematoxylin/eosin stain). Light microscopy confirmed that the tumor nodule contained amelanotic malignant melanoma (Fig. 1a). Conversely, all mapping biopsies taken from the peritumoral fluorescent tissue showed edematous cortical and subcortical brain parenchyma with reactive gliosis that was devoid of tumor infiltration (Fig. 1b-d).

To the best of our knowledge, this is the first reported case of a resection procedure for cerebral melanoma metastasis assisted by 5-ALA fluoroscopy. One study has shown that the use of 5-ALA resulted in a significantly improved rate of gross total resection that translated into prolonged progression-free survival [2]. However, the behavior of 5-ALA in cerebral lesions other than malignant glioma, and its value for resection and impact on survival remain undetermined. By analogy to malignant glioma, the

P. Schucht (✉) · J. Beck · A. Raabe
Department of Neurosurgery, Bern University Hospital, Inselspital,
3010 Bern, Switzerland
e-mail: philippe.schucht@insel.ch

I. Vajtai
Department of Neuropathology, Bern University Hospital, Inselspital,
Bern, Switzerland

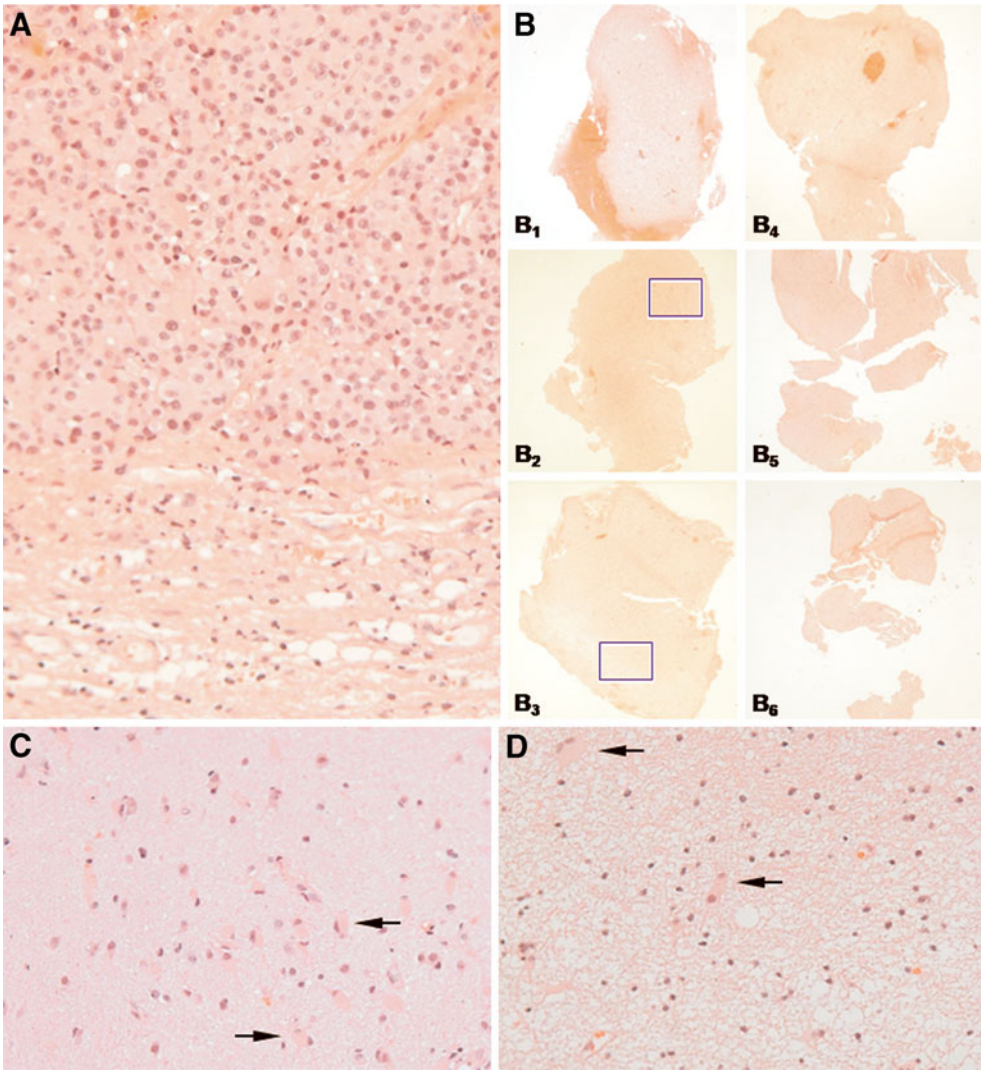

Fig. 1 **a** Solid tumor mass (*upper two-thirds*) composed of plump epithelioid melanocytes largely devoid of pigment granula (magnification ×150); relatively sharp circumscription toward peritumoral brain parenchyma (*lower third*) is observed. **b_1-b_6** (×5) *Boxes* in **b_2** and **b_3** indicate areas depicted at high magnification (×200) in **c** and **d**, respectively. **c** Detailed view of peritumoral cortex shows reactive astrogliosis with gemistocytic morphology (*arrows*) (×200). **d** Detailed view of peritumoral white substance reveals spongy to vacuolated aspect due to edema. Reactive astrocytes are highlighted by *arrows*. All microphotographs represent slides stained with hematoxylin and eosin

potential benefits—such as a higher rate of complete resections and prolonged local disease control—should be considered for cerebral melanoma metastasis.

An absence of 5-ALA-induced fluorescence has been described in some forms of metastatic deposits [4]. Utsuki et al. [4] reported on a series of peritumoral tissue samples from glioma and cerebral metastasis that had shown vague fluorescence despite the lack of unambiguous infiltration by tumor cells on histology. It has also been suggested that some of the protoporphyrin IX produced in tumor cells may spill outside the tumor boundaries and accumulate in the surrounding tissue [3]. This is an unlikely explanation in our case, since the tumor did not show protoporphyrin accumulation. A vague fluorescence, despite the lack of neoplastic cells, has been attributed to an inflammatory reaction in surgeries for recurrent disease [1]. The peculiarity of the present case is the observation of an undescribed constellation of bright fluorescence in the uninvolved perilesional tissue—as opposed to the lack of signal within the tumor itself.

Although the distribution of fluorescence radically departed from an expected pattern, it nevertheless proved of great help in visualizing the tumor-brain interface. It is likely that 5-ALA might evolve into a useful ancillary tool for brain metastasis surgery, provided that consistent fluorescence patterns will have emerged from current and future research.

Acknowledgements The final version of the manuscript was edited by Susan Wieting, Inselspital, Department of Neurosurgery, Publications Office, Bern, Switzerland.

Conflicts of interest None.

References

1. Filbeck T, Roessler W, Knuechel R, Straub M, Kiel HJ, Wieland WF (1999) 5-aminolevulinic acid-induced fluorescence endoscopy applied at secondary transurethral resection after conventional resection of primary superficial bladder tumors. Urology 53:77–81
2. Stummer W, Pichlmeier U, Meinel T, Wiestler OD, Zanella F, H-Jr R (2006) Fluorescence-guided surgery with 5-aminolevulinic acid for resection of malignant glioma: a randomised controlled multicentre phase III trial. Lancet Oncol 7:392–401
3. Utsuki S, Miyoshi N, Oka H, Miyajima Y, Shimizu S, Suzuki S, Fujii K (2007) Fluorescence-guided resection of metastatic brain tumors using a 5-aminolevulinic acid-induced protoporphyrin IX: pathological study. Brain Tumor Pathol 24:53–55
4. Utsuki S, Oka H, Sato S, Shimizu S, Suzuki S, Tanizaki Y, Kondo K, Miyajima Y, Fujii K (2007) Histological examination of false positive tissue resection using 5-aminolevulinic acid-induced fluorescence guidance. Neurol Med Chir 47:210–214

Acta Neurochir (2011) 153:1501–1508
DOI 10.1007/s00701-011-1034-1

CLINICAL ARTICLE

The Geriatric Scoring System (GSS) in meningioma patients—validation

Or Cohen-Inbar · Gil E. Sviri · Jean F. Soustiel · Menashe Zaaroor

Received: 21 January 2011 / Accepted: 14 April 2011 / Published online: 12 May 2011

Abstract
Background Meningiomas are the most common primary brain tumor, the incidence of which rises with age. The Geriatric Scoring System (GSS) was constructed in an attempt to answer which elderly subpopulation will benefit from a surgical intervention in terms of their overall physical and functional state of health. The GSS incorporates different prognostic indicators, both clinical and radiological, for risk stratification.
Objective The purpose of the study was to validate the previously defined GSS for the evaluation and risk stratification of elderly patients suffering from intracranial meningioma.
Methods One hundred and twenty patients aged over 65 years admitted to the RAMBAM Medical Center with meningiomas during the years 2005–2010 were characterized, forming an independent cohort. We report the presenting symptoms, chronic illness and radiological features, as well as perioperative and long-term follow-up results up to 5 years after the surgery.
Results Nine outcome parameters were tested against the GSS score on admission. Survival, Barthel Index, Karnofsky Performance Scale (KPS), consciousness expressed by the Glasgow Coma Scale (GCS) [14] score 5 years after surgery, recurrence within and beyond 12 months of surgery, the length of hospitalization both overall and in a neurosurgical intensive care unit. A GSS score higher than 16 was associated with a significantly more favorable outcome.
Conclusion The present results suggest that common experience-based considerations may be optimized and implemented into a simple scoring system that in turn may allow for outcome prediction and evidence-based decision making.

Keywords Elderly · Evidence based medicine · GSS score · Meningioma · Prognosis

O. Cohen-Inbar · G. E. Sviri · J. F. Soustiel · M. Zaaroor
Department of Neurosurgery,
Rambam Maimondes Health Care Campus,
Haifa, Israel

O. Cohen-Inbar · G. E. Sviri · J. F. Soustiel · M. Zaaroor
Faculty of Medicine, Technion Israel Institute of Technology,
Haifa, Israel

O. Cohen-Inbar
Neurosurgical Department, Rambam Health Care Campus,
P.O.Box 9602, Haifa 31096, Israel

O. Cohen-Inbar (✉)
Molecular Immunology Laboratory,
Technion Institute of Technology,
Haifa, Israel
e-mail: orcoheninbar@gmail.com

Introduction

Meningiomas are thought to originate from arachnoid cap cells, which form the outer layer of the arachnoid mater and the arachnoid villi [20]. Meningioma is the most common primary brain tumor, accounting for 33.8% of all primary brain and central nervous system tumors reported in the United States between the years 2002 and 2006 [33]. The prevalence of pathologically confirmed meningioma is approximately 97.5/100,000 in the United States [1]. Since a proportion of meningiomas are not surgically managed, these are probably underestimations. In addition, autopsy and imaging studies have estimated subclinical meningioma rates of up to 2.8% in women [17, 32]. Established risk factors for meningioma development are few. Among these, ionizing radiation is the primary environmental risk factor at present, with a sixfold to tenfold risk [12, 24, 26, 29]. An

association between hormones and meningioma risk has been suggested by a number of findings, including the increased incidence of post-pubertal disease in women versus men (2:1), with the highest ratio of 3.15:1 during the peak reproductive years [3, 31]. The etiologic link between cell phone usage and meningioma development is one of great interest to the general public. At least ten studies have examined the association between cell phone use and tumors of the brain [13, 15, 21].

The elderly patient poses a medical challenge in all aspects of medicine and for any surgical intervention. Nevertheless, accumulating evidence supports the notion that although the clinical presentation of patients with meningioma is commonly diverse, these tumors seem to present as a distinct clinical entity in the elderly patient. It seems that a thorough understanding of the clinical behavior of meningioma in the elderly patient is lacking. Accordingly, the criteria in choosing among treatment options, such as lifestyle and survival improvement versus side effects, complications and neurological deficits, are not evidence based. Different clinical studies have been conducted in an attempt to set treatment guidelines, but their conclusions are inconsistent or even contradictory.

Previous work done by our group reported the presenting symptoms, chronic illnesses and their impact, and the perioperative and long-term follow-up results of 250 patients admitted to our institute during a 10-year period (1995–2005) [4]. The aim of this retrospective study was to gain a better understanding of this tumor's behavior in the elderly, trying to define and identify prognostic indicators within this population group. Based on univariant and multivariate analysis, significant prognostic indicators were identified and were implemented into a new Geriatric Scoring System (GSS) (Table 1). The GSS incorporates essential independent considerations and patient factors on admission, including tumor size and location, peritumoral edema, neurological deficits, Karnofsky score [2, 5], and associated diabetes, hypertension or lung disease. Seven outcome parameters were retrospectively tested using the scoring system; namely, mortality, Barthel Index score [19], Karnofsky score and consciousness expressed by the Glasgow Coma Scale (GCS) score [14] 5 years after surgery, as well as recurrence within and beyond 12 months. Age proved to inversely correlate with outcome. Morbidity and mortality were significantly lower in women. The extent of surgical resection had no influence on functional outcome, although radical resection was associated with significantly lower mortality. Generally, a GSS score higher than 16 was found to be associated with a significantly more favorable outcome. These results suggested that common experience-based considerations may be optimized and implemented into this simple scoring system that in turn may allow for outcome prediction and evidence-based decision making. In this study, we aimed to validate this scoring system, independently from the previous cohort, by reviewing all patients operated on at our institute between the years 2005 and 2010.

Patients and methods

Inclusion criteria

A retrospective chart review of all patients aged over 65 years admitted to and operated on at the Department of Neurosurgery at Rambam Medical Center for intracranial meningiomas during the period 01/2005–10/2010 was conducted. A comprehensive demographic database was constructed (Table 2). Seventy-seven women and 43 men ranging in age between 65 and 88 years old (mean age, 73±5.8 years) were included.

Exclusion criteria

Patients not operated on at the study period for any reason were excluded. Additionally, any patients with a histopath-

Table 1 The Rambam Geriatric Scoring System (GSS)

Admission parameter	1 point	2 points	3 points
Size	>5 cm	3–5 cm	<3 cm
Neurological deficit	Progressive	Stable severe	None, minor
Karnofsky Performance Scale	<50	60–80	90–100
Tumor location	Falcine, parasagittal, foramen magnum	Tentorial, posterior fossa, jugular foramen	Convexity, intraventricular, sphenoid wing, tuberculum sellae, cavernous sinus, optic nerve
Peritumoral edema	Severe	Mild	None
Diabetes mellitus	Not controlled	Medically controlled	None
Hypertension	Not controlled	Medically controlled	None
Pulmonary disease	Severe	Mild	None

Table 2 Demographic data

Age groups	65-69	70-74	75-79	80-	Total
Patient numbers	44	27	31	18	120
Patient %	36.66	22.5	25.83	15	100

ological diagnosis different than meningioma, regardless of the preoperative suspicion were excluded.

Clinical presentation

Board-certified neurosurgeons logged onto patient hospital charts the presenting symptoms, their severity, past medical history, chronic illnesses and treatment (Table 3). The different factors comprising the GSS scoring system were logged, including functional and performance state expressed using the internationally accepted Karnofsky Performance Scale (KPS) [2, 5] as well as findings on neurological examination (Table 3).

Imaging studies

Experienced neuroradiologists, blinded to the clinical data, characterized preoperative imaging studies according to tumor location, defined according to accepted nomenclature, size and number of lesions, and presence of peritumoral edema (Table 3). A severe edema was defined when brain structures were shown to be displaced (herniated), while a mild edema refers to a clearly visible peritumoral edema, not overtly displacing brain structures. Postoperative image studies, taken at several time points after the surgical intervention, namely perioperatively (within 48 h of surgery), during the initial 12 months after the operation, 12 months and 5 years after the surgical intervention, were reviewed accordingly (Table 4).

Outcome

Outcome data were collected at several time points after the surgical intervention: perioperatively, during the initial 12 months after the operation, 12 months and 5 years after surgery (Table 4). Outcome parameters were assessed by two independent observers blinded to patient data. Patient's charts were used for the immediate outcome parameters, whereas the out-patient clinic charts and medical records from further hospitalizations were used for long-term follow-up. Functional and performance state was recorded using internationally accepted scoring systems, namely, the KPS [2, 5], Barthel Index score [19], and consciousness expressed by the GCS score [14] (Table 4).

A univariant analysis of the GSS score on admission against nine different outcome parameters was performed, in an attempt to further validate and support reported initial findings, performed on an independent cohort [4].

Statistical analysis

Statistical tests were performed using SPSS version 17 software (SPSS, Chicago, IL). For univariant analysis, Pearson's correlation, chi-square test and Fisher's exact test were used for comparison of non-parametric data. Comparison of quantitative parameters such as age or length of hospitalization in different outcome groups was performed using a *t*-test, ANOVA with post-hoc Scheffe test in case of a normal distribution and Mann-Whitney *U*-test in a non-normal distribution. For statistical purposes, the Karnofsky index was further simplified into three categories: poor (≤50), fair (50–70) and good (≥80).

Table 3 Admission parameters data (presented as percent of the cohort)

Sex	35.8 males, 64.2 females
Blood type	1.7 (A-), 30.8 (A+), 5 (B-), 16 (B+), 0.8 (AB-), 10.9 (AB+), 1.7 (O-), 32.5 (O+)
Tumor location	49.2 convexity, 20.8 parasagittal, 7.5 falcine, 0.8 olfactory groove, 10 sphenoid wing/clinoidal, 5 tuberculum sellae, 5.8 posterior fossa, 0.8 foramen magnum
Histology	92.5 typical (grade 1), 6.7 atypical (grade 2), 0.8 anaplastic (grade 3)
	Grade 1 subtypes 2.4 microcystic, 3.5 angiomatous, 7.1 psammomatous, 47.1 transitional, 11.8 fibrous/fibroblastic, 28.2 meningothelial
Size	13.3 were <3 cm, 48.3 were 3–5 cm, 34.2 were 5–7 cm, 4.2 were >7 cm
Peritumoral edema	48.3 severe, 37.5 mild, 14.2 none/negligible
KPS admission	41.7 had a score <50, 43.3 had a score 60–80, 15 had a score >80
Neurological deficit	6.7 had no deficit, 20 mild, 41.7 stable severe, 31.7 progressive deficit
Hypertension (HTN)	20.8 no, 30.8 medically controlled, 25 partially controlled, 23.3 uncontrolled
Diabetes mellitus	72.5 no, 9.2 medically controlled, 12.5 partially controlled, 5.8 uncontrolled
Respiratory disease	91.7 no, 5.8 mild chronic, 0.8 severe chronic, 1.7 end stage lung disease

Table 4 Outcome parameters data (presented as percent of the cohort)

(Data presented as percent of the cohort)	
nICU admission	Range 0–60 days, mean 5.48±6.9 days, median 3 days
Overall admission	Range 4–65 days, mean 13.66±9.7 days, median 11 days
Recurrence in 1 year	11.5 yes, 88.5 no
Overall recurrence	24.1 yes, 75.9 no
KPS after 5 years	19.8 had a score <50, 26.7 had a score 60–80, 53.5 had a score >80
Barthel Index after 5 years	Score range 15–105, mean score 76.49±22.1, median 85
GCS after 5 years	Score range 3–15, mean score 13.63±1.79, median 14
Survival 3 months	5.8 did not survive, 94.2 survived
Overall survival	8.3 survived less than 1 year, 6.7 survived 1–3 years, 4.2 survived 3–5 years, 11.7 survived >5 years, 69.2 are alive as to date (different time frames after surgery)

Results

Cohort overview

Admission parameters

Reviewing all patients operated on at our institute during the years 2005–2010 over the age of 65, a cohort of 120 patients was analyzed (Table 2). This is an independent cohort with regards to previous work done at our institute on the matter, unrelated to the population onto which the GSS score was constructed after univariant and multivariant analysis. The mean age was 73±5.8 years, the median was 73 years. Males composed 35.8% of the population. The frequency of the A+blood type is substantially lower in the cohort with regards to the distribution in the Israeli population, amounting to 30.8%, compared with a frequency of 38% in the Israeli population. Of the lesions, 49.2% were classified as convexity, 20.8% parasagittal, 10% sphenoid wing or clinoid meningiomas. The vast majority of the patients (92.5%) had a typical type grade 1 meningioma, of which the transitional type was the most common (47.1%), along with meningothelial (28.2%), and fibrous/fibroblastic (11.8%). An atypical grade 3 meningioma was found in 6.7% and only 0.8% had an anaplastic type grade 3 meningioma. The sizes of the lesions that were operated on were 3–5 cm in 48.3% of cases, while 38.3% of the lesions were larger than 5 cm, and 13.3% were smaller than 3 cm. A severe peritumoral edema on admission was noted in 48.3% of the cases, a mild edema was noted in 37.5%. Functional status (KPS) was severely disabled in 41.7%. A neurological deficit was present in 93.3% of the patients to some degree. With regards to chronic illnesses and overall health, 79.2% had hypertension (HTN), 27.5% of the patients had diabetes mellitus (DM), 8.3% of patients suffered from a respiratory disease. The mean GSS score on admission was 16.6±2.9, range 10–23, with a median of 16.0. For frequency distribution of the different admission parameters refer to Table 3.

Outcome parameters

The mean admission time at the neurosurgical intensive care unit (nICU) was 5.48±6.9 days, the mean overall hospital admission time was 13.6±9.7 days. Recurrence within 12 months was registered in 11.5%; overall recurrence after surgery was noted in 24.1%. KPS in 5 years of surgery was low (severely disabled, lower than 50) in 19.8%, partially debilitated (KPS between 60 and 80) in 26.7%, and not debilitated in 53.5%. The mean Barthel ADL Index for patient independence 5 years after surgery was 76.49±22. The mean GCS score 5 years after surgery was 13.6±1.79. Survival in the immediate 3 months after surgery was 94.2%. Overall, 8.3% of patients survived less than 1 year after surgery, 11.7% survived beyond 5 years after surgery; 69.2% are still alive as to date. For frequency distribution of the different outcome parameters refer to Table 4.

Univariant analysis

Admission GSS score was analyzed against different outcome parameters. Results of univariant analysis are summarized in Table 5.

Recurrence Those patients suffering a recurrence within 12 months of surgery, as well as a later recurrence, had a significantly lower GSS score on admission.

Performance 5 years after surgery Those patients presenting with a higher GSS score had a significantly higher performance level and functioning 5 years after the surgery, as measured in the KPS [2, 5], Barthel [19] and GCS [14] indices.

Hospitalization A very strong negative correlation is shown between the GSS scores on admission and the time spent in the nICU and overall hospitalization time. This is further emphasized when comparing the GSS<16 patient group versus the GSS>16 patient group hospitalization time.

Table 5 Univariant analysis of the GSS score versus different outcome parameters

Outcome parameter examined		Mean GSS	*p*
Recurrence within 12 months of surgery	A linear relationship between the risk of recurrence and GSS on admission		
	Yes	14.85	0.007
	No	17.1	
Recurrence beyond 12 months of surgery	A linear relationship between the risk of recurrence and GSS on admission		
	Yes	15.58	0.008
	No	17.29	
KPS 5 years after the surgery	A linear relationship between the functional state 5 years after surgery and the GSS score on admission		
	<50	13.45	<0.0001
	60–80	15.96	<0.0001
	>80	18.78	<0.0001
Barthel Index 5 years after the surgery	A very strong linear correlation between GSS scores on admission and Barthel Index 5 years after the surgery		
	Pearson correlation 0.775		
GCS score 5 years after the surgery	A very strong linear correlation between GSS scores on admission and GCS score 5 years after the surgery		
	Pearson correlation 0.627		
nICU admission	A very strong negative correlation between GSS scores on admission and nICU admission in days. Pearson correlation −0.352		<0.0001
	GSS <16	Mean 9.05 days, median 6.5 days	
	GSS >16	Mean 3.55 days, median 2 days	
Overall admission	A very strong negative correlation between GSS scores on admission and nICU admission in days. Pearson correlation −0.336		0.001
	GSS <16	Mean 17.1 days, median 15.0 days	
	GSS >16	Mean 11.81 days, median 9 days	
Survival 3 months after surgery	Yes	16.84	<0.0001
	No	12.71	
Survival	<1 year after surgery	13.7	0.003
	1–3 years after surgery	14.88	
	3–5 years after surgery	16.20	
	Alive as of 09/2010, <5 years after surgery	16.98	
	>5 years after surgery	17.57	

Survival A very strong correlation is shown between the GSS score on admission and overall survival, grouped into several time frames after the surgical intervention (3 months, up to 12 months, 1–3 years, 3–5 years, beyond 5 years).

Discussion

The advances made in medicine and the increase in life expectancy combined with new advances in radiology and diagnosing skills have led to an increase in the incidental finding of meningiomas. Meningiomas comprise approximately 21% of all primary intracranial tumors, and when data from autopsies are included, this figure rises to above 40%, thus showing that many remain clinically silent, never coming to clinical attention [6, 7, 18, 30]. A question arises concerning the benefit of surgery for those elderly patients for whom surgical resection is possible; namely, when there is no technical limitation to surgery. What elderly subpopulation will benefit from surgical intervention in terms of their overall physical and functional states of health?

Different clinical studies have been conducted over the years in an attempt to set treatment guidelines, but their conclusions are inconsistent and at times contradictory [8–11, 16, 22, 23, 25, 27, 28, 30]. Several scoring systems have been proposed, but their components are very subjective in definition and cannot be adequately compared due to both inter-examiner and intra-examiner variability [16, 28].

Godfrey and Caird [11], viewing 111 elderly patients with intracranial meningiomas, found that the clinical

presentation of progressing neurological deficits and cognitive impairment is similar to that of younger patients, and operative management led to improvement in most cases with low accompanying morbidity and mortality. In a review by Brigham Women's Hospital Clinical Services [9], no difference between age groups was found in survival after resection of a meningioma. Roser and co-workers [27, 30] defined meningioma in the elderly patient as a separate clinical entity in comparison with that in the young, since cellular proliferation, vascularity and intra-tumoral hormonal profiles change with age. Patil et al. [22] examined all patients who underwent a craniotomy for resection of intracranial meningioma between the years 1997 and 2006 at 123 VA hospitals. The elderly cohort comprised 21.2% (n=258) of the total study population. After carefully controlling for various patient characteristics, ASA class and functional status, elderly patients were found to have a poorer outcome after surgical resection of intracranial meningioma than younger subjects.

Lee and Sade [16] suggested an algorithm based on balancing the risks and benefits of surgery, termed as the "CLASS" algorithm. Risk factors included comorbidities (C), defined by the American Society of Anesthesiology (ASA) score I–III, location (L) defined as low/moderate/high risk based on the experience of the senior author and age (A). These were assigned a score of −2 to 0. Beneficial factors were defined as size (S), in which the greater the tumor size is, the higher the score, ranging from 0 to 2, and signs and symptoms (S), which were also increasing in score with severity. According to this system, the patients were grouped into three groups by scores, the operative intervention was decided by the senior author blinded to the patients' scores, and a correlation between the initial score and outcome was shown. This system has several disadvantages. First, comorbidities are defined by a general non-specific scale, which does not offer a registry for improving a patient's score by better controlling a chronic illness. Additionally, location is defined subjectively, and age is an independent unchangeable parameter. Thus, in the risk factors group, there is no real opportunity for risk stratification and risk improvement for the patient. For the beneficial factors, a strange conclusion rises from the algorithm, in which the bigger the tumor and the worse clinically the patient presents, the better the score is. This would suggest that a stable patient with a resectable tumor not burdening the brain is a less attractive surgical candidate.

Sacko et al. [28] assessed the surgical outcome of 74 elderly patients aged 80 years or more that were operated on for intracranial meningiomas during the years 1990–2005. A retrospective analysis of the factors influencing the surgical outcome culminated in the formation of a scoring system, termed as the "SKALE" grading system. This stands for sex (S), in which females received 2 points while males received 0 points, KPS (K), ASA (A), location (L) defined as critical in the cranial base, eloquent area and near the large vessels, and peritumoral edema (E). Patients with a SKALE score of more than 8 were found to have an excellent outcome. The authors report in inverse correlation between the extent of surgical resection and outcome, stating that "Mortality was higher in patients with total excision than in patients with partial excision," and "The radical tumor removal showed a higher risk of morbidity, but not mortality." Although bearing some resemblance to the GSS system, the SKALE grading system and the data it is based on raises several questions. The use of the ASA system for comorbidities suffers the same criticism as for the CLASS system, as does the scoring of the sex, an unchangeable factor. The definition of critical regions is highly subjective and not reproducible and the possibilities for risk improvement and restratification do not exist.

We report the presenting symptoms, chronic illnesses and their impact, perioperative and long-term follow-up results of 120 patients admitted to our institute during a 5-year period, forming an independent group to the initially largest patient group having a detailed comprehensive database and time-corrected long-term follow-up.

With regards to the different blood group distribution within the cohort, the frequency distribution of blood type in the ABO and Rh groups paralleled the distribution in the Israeli population with one exception, stable in both this cohort and previous work (separate cohort) done at our institute analyzing the elderly patients with meningiomas operated on during the years 1995–2005 [4]. In both populations, the frequency of the A+blood type is substantially lower with regards to the distribution

Table 6 Blood group distribution in the Israeli population and patient groups

Population	A+	B+	AB+	O+	A-	B-	AB-	O-
Israeli population	38%	16%	6%	30%	4%	2%	1%	3%
Elderly meningioma patients, 2005-2010	30.8%	16%	10.9%	32.5%	1.7%	5%	0.8%	1.7%

Data regarding the blood group distribution in the Israeli population was received from the blood bank at Rambam Health Care Campus

in the Israeli population, similar between the cohort, with 28% in previous papers and 30.8% in this current cohort, compared with a frequency of 38% in the Israeli population (Table 6). This may suggest a protective effect this blood group conveys and requires further investigation and validation.

The GSS score, proposed previously by our group, constructed after a thorough analysis of a large cohort from univariant and multivariant analysis, was challenged again in this paper. In this scoring system, eight clinico-radiological patient parameters upon admission are logged: tumor size and location, peritumoral edema, neurological deficits, Karnofsky score, associated diabetes, hypertension or lung disease. Each of the parameters is assigned a score ranging from 1 to 3; thus, the total score ranges from 8 to 24. The GSS was tested in our patient group; the link between the variables and patient presentation was predicted, and the score distribution to patient groups was similar in nature to that accepted in other scales (internal validation). Nine outcome parameters were tested against the GSS score: survival (3 months after surgery and overall), Barthel Index, Karnofsky score and GCS score 5 years after operation, and tumor recurrence (within and beyond 12 months of operation), admission time (both in nICU and overall). It is shown with statistical significance, for all outcome parameters tested, that a patient presenting with a score of 16 or higher may benefit from a surgical intervention and has a favorable prognosis thereafter (Tables 5).

Conclusion

The GSS score is appealing due to its simplicity and reproducibility, on the one hand, and its use as a follow-up clinical aid for the preoperative assessment of the elderly patient suffering from a meningioma.

We believe that the use of the GSS score in the preoperative patient evaluation will help in identifying those patients most likely to benefit from a surgical intervention. The GSS score provides a comprehensive assessment tool, approaching the patient and the tumor as two completing pieces of the question, both contributing to operative decisions. The use of the GSS score allows for outcome prediction and evidence-based decision making, taking the same experience-based considerations practiced by experienced neurosurgeons and adding to it a statistically proven basis. The GSS scoring system is undergoing further evaluation at our department, being used prospectively for all patients presenting with primary brain tumors. Future applications for all age groups and different neoplastic lesions are being pursued.

Conflicts of interest None.

References

1. CBTRUS (Central Brain Tumor Registry of the United States) Statistical Report (2009–2010). Primary (malignant and non-malignant) brain and CNS tumor age-specific incidence rates by major histology groupings, histology and age at diagnosis, CBTRUS 2002–2006. http://www.cbtrus.org
2. Clancey JK (1995) Karnofsky performance scale. J Neurosci Nurs 27:220
3. Claus EB, Black PM, Bondy ML, Calvocoressi L, Schildkraut JM, Wiemels JL, Wrensch M (2007) Exogenous hormone use and meningioma risk: what do we tell our patients? Cancer 110:471–476
4. Cohen-Inbar O, Soustiel JF, Zaaroor M (2010) Meningiomas in the elderly, the surgical benefit and a new scoring system. Acta Neurochir (Wien) 87:87–97
5. Crooks V, Waller S, Smith T, Hahn TJ (1991) The use of the Karnofsky Performance Scale in determining outcomes and risk in geriatric outpatients. J Gerontol 46:M139–M144
6. Cushing H (1922) The meningiomas (dural endotheliomas): their source and favoured sets of origin. Brain 45:282–306
7. Cushing H Eisenhardt H (1938) Meningiomas: their classification, regional behavior, life history and surgical end results. Charles C. Thomas, Springfield
8. D'Andrea G, Roperto R, Caroli E, Crispo F, Ferrante L (2005) Thirty-seven cases of intracranial meningiomas in the ninth decade of life: our experience and review of the literature. Neurosurgery 56:956–961
9. Drummond KJ, Zhu JJ, Black PM (2004) Meningiomas: updating basic science, management, and outcome. Neurologist 10:113–130
10. Hadded GF, OA-MSIA (2009) Extrinsic tumors, meningiomas. In: Youmans JR (ed) Youmans neurological surgery. Saunders, Philedelphia
11. Godfrey JB, Caird FI (1984) Intracranial tumours in the elderly: diagnosis and treatment. Age Ageing 13:152–158
12. Hijiya N, Hudson MM, Lensing S, Zacher M, Onciu M, Behm FG, Razzouk BI, Ribeiro RC, Rubnitz JE, Sandlund JT, Rivera GK, Evans WE, Relling MV, Pui CH (2007) Cumulative incidence of secondary neoplasms as a first event after childhood acute lymphoblastic leukemia. JAMA 297:1207–1215
13. Inskip PD, Tarone RE, Hatch EE, Wilcosky TC, Shapiro WR, Selker RG, Fine HA, Black PM, Loeffler JS, Linet MS (2001) Cellular-telephone use and brain tumors. N Engl J Med 344:79–86
14. Jennett B, Bond M (1975) Assessment of outcome after severe brain damage. Lancet 1:480–484
15. Johansen C, Boice J Jr, McLaughlin J, Olsen J (2001) Cellular telephones and cancer–a nationwide cohort study in Denmark. J Natl Cancer Inst 93:203–207
16. Lee JH, Sade B (2009) The novel "CLASS" algorithmic scale for patient selection in meningioma surgery. In: Lee JH (ed) Meningiomas: diagnosis, treatment, and outcome. Springer, London, pp 217–223
17. Krampla W, Newrkla S, Pfisterer W, Jungwirth S, Fischer P, Leitha T, Hruby W, Tragl KH (2004) Frequency and risk factors for meningioma in clinically healthy 75-year-old patients: results of the Transdanube Ageing Study (VITA). Cancer 100:1208–1212
18. Kurland LT, Schoenberg BS, Annegers JF, Okazaki H, Molgaard CA (1935–1977) The incidence of primary intracranial neoplasms in Rochester, Minnesota. Ann N Y Acad Sci 381:6–16
19. Mahoney FI, Barthel DW (1965) Functional evaluation: the barthel index. Md State Med J 14:61–65
20. Mawrin C, Perry A (2010) Pathological classification and molecular genetics of meningiomas. J Neurooncol 99:379–391

21. Muscat JE, Malkin MG, Thompson S, Shore RE, Stellman SD, McRee D, Neugut AI, Wynder EL (2000) Handheld cellular telephone use and risk of brain cancer. JAMA 284:3001–3007
22. Patil CG, Veeravagu A, Lad SP, Boakye M (2010) Craniotomy for resection of meningioma in the elderly: a multicentre, prospective analysis from the National Surgical Quality Improvement Program. J Neurol Neurosurg Psychiatry 81:502–505
23. Pompili A, Cacciani L, Cattani F, Caroli F, Crecco M, Mastrostefano R, Mazzitelli MR, Raus L (1997) Intracranial meningiomas in the elderly. Minerva Med 88:229–236
24. Preston DL, Ron E, Yonehara S, Kobuke T, Fujii H, Kishikawa M, Tokunaga M, Tokuoka S, Mabuchi K (2002) Tumors of the nervous system and pituitary gland associated with atomic bomb radiation exposure. J Natl Cancer Inst 94:1555–1563
25. Rengachary SS, Suskind DL (1991) Meningiomas in the elderly and asymptomatic meningiomas. In: Al-Mefty O (ed) Meningiomas. Raven Press, New-York, pp 153–159
26. Ron E, Modan B, Boice JD Jr, Alfandary E, Stovall M, Chetrit A, Katz L (1988) Tumors of the brain and nervous system after radiotherapy in childhood. N Engl J Med 319:1033–1039
27. Roser F, Ebner FH, Ritz R, Samii M, Tatagiba MS, Nakamura M (2007) Management of skull based meningiomas in the elderly patient. J Clin Neurosci 14:224–228
28. Sacko O, Sesay M, Roux FE, Riem T, Grenier B, Liguoro D, Loiseau H (2007) Intracranial meningioma surgery in the ninth decade of life. Neurosurgery 61:950–954
29. Sadetzki S, Flint-Richter P, Starinsky S, Novikov I, Lerman Y, Goldman B, Friedman E (2005) Genotyping of patients with sporadic and radiation-associated meningiomas. Cancer Epidemiol Biomark Prev 14:969–976
30. Sutherland GR, Florell R, Louw D, Choi NW, Sima AA (1987) Epidemiology of primary intracranial neoplasms in Manitoba, Canada. Can J Neurol Sci 14:586–592
31. Vadivelu S, Sharer L, Schulder M (2010) Regression of multiple intracranial meningiomas after cessation of long-term progesterone agonist therapy. J Neurosurg 112:920–924
32. Vernooij MW, Ikram MA, Tanghe HL, Vincent AJ, Hofman A, Krestin GP, Niessen WJ, Breteler MM, van der Lugt A (2007) Incidental findings on brain MRI in the general population. N Engl J Med 357:1821–1828
33. Wiemels J, Wrensch M, Claus EB (2010) Epidemiology and etiology of meningioma. J Neurooncol 99:307–314

Comment

The paper by Or Cohen-Inbar and colleagues deals with the dilemma of whether to operate or not on elderly patients (age>65 years) affected by intracranial meningiomas. With the aging of the population and because of the age distribution of this tumor, this clinical issue is progressively increasing in importance. As others did before, the authors try to define a score in order to give a scientific answer to the initial question.

The major weakness of this study is inherent to its retrospective design. There are similar prospective investigations [5] and we agree with the authors that the significance of the proposed GSS score remains to be judged in the future.

Domenico d'Avella, Padova, Italy
Marco Locatelli, Milano, Italy

Acta Neurochir (2011) 153:1509–1510
DOI 10.1007/s00701-011-0969-6

LETTER TO THE EDITOR

Clival meningioma presenting with respiratory arrest

Joana Silva · Clara Chamadoira · António Cerejo · Rui Vaz

Received: 29 January 2011 / Accepted: 7 February 2011 / Published online: 24 February 2011

Dear Editor

We present the case of a 42-year-old female patient, previously healthy, who was found unconscious at home. Intubated and ventilated at home, she was transported to hospital. On admission, her eyes were open and she was following verbal orders. The cause for the situation was not clear. After respiratory assistance, the patient was extubated, being fully conscious, without signs of cranial nerve paralysis or motor weakness. Magnetic resonance imaging (MRI) of the brain revealed a clivus meningioma (Fig. 1 - upper images).

After 24 h in the Neurocritical Care Unit, with cardiac and respiratory monitoring, she suffered a new episode of respiratory palsy, without any predisposing factor or disturbances of blood pressure and cardiac rhythm. She was obeying orders, trying to communicate by movements and, again, with no other neurological signs. After 1 min, respiratory help was provided, with oro-tracheal intubation and ventilation.

The patient was operated on 48 h later by a right retrosigmoid approach in the semi-sitting position, with complete removal of the tumor (Fig. 1 - lower images). Pathology confirmed a transitional meningioma.

After surgery, there were palsies of the cranial nerves on the right side, from third nerve to lower cranial nerves. The patient was extubated 2 days after surgery, without respiratory problems. The cranial nerve did recover in the following months, and after 1 year there are no neurological deficits except hearing loss on the right side.

Clival meningiomas generally present with insidious symptoms related to cranial nerve involvement, cerebellar or brain stem compression and increased intracranial pressure [5, 6]. Presentation of a clival meningioma with sudden respiratory arrest as the initial event has not been previously described.

Respiratory dysfunction is a possible manifestation of brainstem compression, which may affect nuclei and pathways involved in respiratory control [3] and may be combined with elevated intracranial pressure due to intratumoral bleeding or obstruction of cerebrospinal fluid flow [2]. In the present case, however, there were no signs of bleeding or hydrocephalus in MRI.

The treatment for clival meningioma presenting with respiratory arrest is surgical removal, with brainstem decompression. Complete removal is possible using a retrosigmoid approach [1, 4]. In the present case, there was an immediate recovery of respiratory function and a very good result 1 year after surgery. In this critical situation, surgery should be performed as soon as possible, avoiding serious and permanent morbidity and, eventually, death.

J. Silva (✉) · C. Chamadoira · A. Cerejo · R. Vaz
Department of Neurosurgery, Hospital São João,
University of Porto,
4200–319 Porto, Portugal
e-mail: joana.msilva@ymail.com

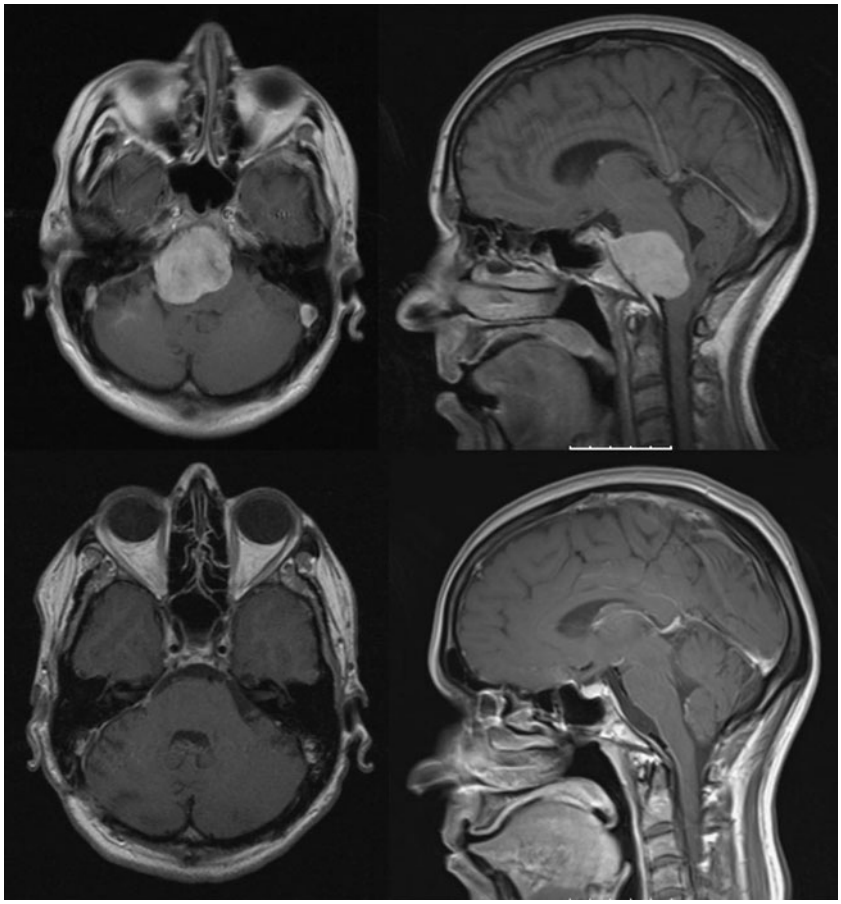

Fig. 1 MRI scan. Pre-operative (*upper images*), and post-operative (*lower images*) showing complete removal of the tumor

Conflicts of interest None.

References

1. Bambakidis NC, Kakarla UK, Kim LJ, Nakaji P, Porter RW, Daspit CP, Spetzler RF (2008) Evolution of surgical approaches in the treatment of petroclival meningiomas: a retrospective review. Neurosurgery 62(6 Suppl 3):1182–1191
2. Moss IR (2005) Canadian association of neuroscience review: respiratory control and behavior in humans: lessons from imaging and experiments of nature. Can J Neurol Sci 32 (3):287–297
3. Nogués MA, Benarroch E (2008) Abnormalities of respiratory control and the respiratory motor unit. Neurologist 14(5):273–288
4. Samii M, Tatagiba M, Carvalho GA (1999) Resection of large petroclival meningiomas by the simple retrosigmoid route. J Clin Neurosci 6(1):27–30
5. Seifert V (2010) Clinical management of petroclival meningiomas and the eternal quest for preservation of quality of life: personal experiences over a period of 20 years. Acta Neurochir 152(7):1099–1116
6. Van Havenbergh T, Carvalho G, Tatagiba M, Plets C, Samii M (2003) Natural history of petroclival meningiomas. Neurosurgery 52(1):55–64

Acta Neurochir (2011) 153:1511–1517
DOI 10.1007/s00701-011-1040-3

CASE REPORT

Atypical adult medulloblastoma

Maziar Behbahani · Edward Jerome St. George · Laurance T. Dunn · Donald M. Hadley · William Stewart

Received: 24 November 2010 / Accepted: 20 April 2011 / Published online: 9 May 2011

Abstract Medulloblastomas are malignant primitive neuro-ectodermal neoplasms of childhood. In adults, clinical manifestations, imaging and prognosis can be different from that observed in children. Three adult patients with confirmed diagnoses of medulloblastoma are discussed in this report. They presented with unusually prolonged clinical courses and with imaging more suggestive of L'hermitte-Duclos disease. Medulloblastoma should be considered in all adults with posterior fossa masses despite having clinical and radiological features suggestive of a low-grade tumour. Definitive diagnosis requires histological confirmation in all cases.

Keywords Medulloblastoma · L'hermitte-Duclos disease · Adult · MRI characteristics

Introduction

Medulloblastomas are malignant primitive neuro-ectodermal tumours (PNET) most commonly found in children. Although these lesions comprise 25% of childhood brain tumours, they are only found in 1% of adults diagnosed with CNS malignancies [4, 6, 10, 11]. Commonly, tumours in adults may display both an atypical clinical course and imaging characteristics [6, 11].

Three cases of adult medulloblastoma with indolent clinical courses and initial imaging suggestive of L'hermitte-Duclos disease (LDD) are discussed. We argue the importance of inclusion of medulloblastoma in the differential diagnosis of any posterior fossa tumour in an adult despite apparently benign clinical and radiological findings.

This article was presented as a poster in the British Neurooncology Society conference held in Hull in June 2009.

M. Behbahani (✉) · E. J. St. George · L. T. Dunn
Department of Neurosurgery, Institute of Neurological Sciences, Southern General Hospital,
Glasgow G51 4TF, UK
e-mail: mbehbahani@me.com

D. M. Hadley
Department of Neuroradiology, Institute of Neurological Sciences, Southern General Hospital,
Glasgow G51 4TF, UK

W. Stewart
Department of Neuropathology, Institute of Neurological Sciences, Southern General Hospital,
Glasgow G51 4TF, UK

Case report

Patient 1

A 47-year-old female presented with a 1-year history of progressive cough impulse headache and upper cervical pain. Examination revealed right-sided cerebellar signs, horizontal nystagmus and normal optic discs. MRI showed bilateral extensive non-enhancing lesions in the cerebellar hemispheres with mild compression of the fourth ventricle. The abnormalities demonstrated a striated pattern, consistent with LDD (Fig. 1). SPECT scan of the brain was inconclusive. Investigations for Cowden's syndrome and satellite lesions in the neuroaxis were negative. Due to the progressive nature of the symptoms, the patient underwent posterior fossa decompression and biopsy. Histopathological examination showed poorly differentiated tumour cells with a high proliferative index (Ki67) (Fig. 2). Immunostaining of the tumour confirmed a meduloblastoma WHO grade 4 (Table 1).

The patient received cranio-spinal radiotherapy thereafter with good response. The residual posterior fossa tumour remains unchanged 3 years after treatment.

Patient 2

A 44-year-old female presented with a 4-year history of visual disturbance, vertigo and disordered balance. Clinical

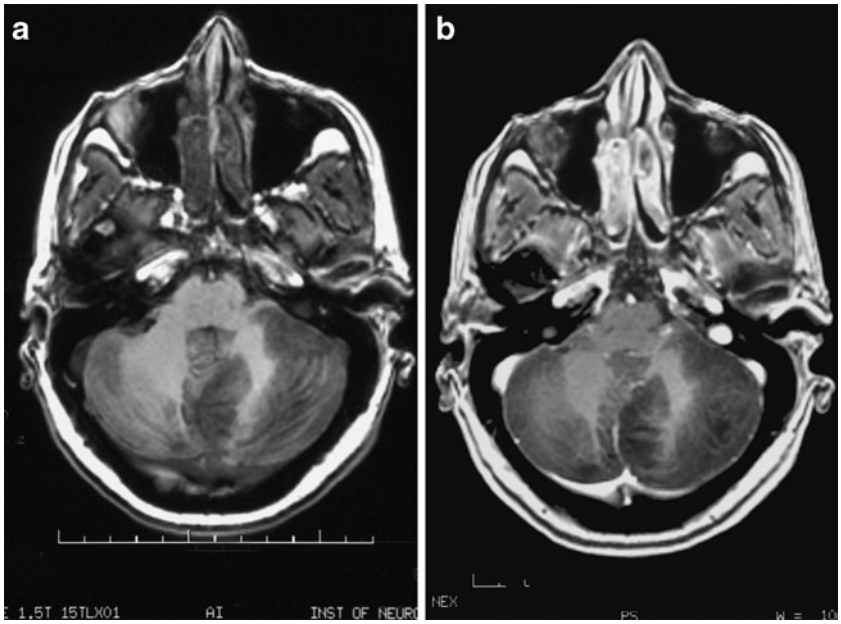

Fig. 1 MRI brain, axial views of the cerebellum. T1-weighted image (T1WI) with and without contrast demonstrating an extensive bilateral hemispheric lesion with involvement of the vermis. The striated pattern of the thickened folia is more notable in the left hemisphere. There is no enhancement with gadolinium (right)

findings were limited to lateral gaze nystagmus and an impaired tandem gait.

Brain MRI revealed a diffuse non-enhancing abnormality of the vermis and right inferior cerebellar peduncle. The cerebellar folia were thickened with hyperintense signal on T2-weighted images. In addition a high signal lesion causing mild rotation of the medulla was noted and thought to represent either an arachnoid or epidermoid cyst. There was also a suggestion of slight enhancement within the medulla, inferior to the fourth ventricle. The radiological findings were interpreted as LDD (Fig. 3). Due to the indolent nature of the presentation, an observational strategy, with 6 monthly interval imaging, was adopted. Despite minimal symptoms, gradual radiological progression was observed over a 3-year period culminating in tonsillar herniation and hydrocephalus.

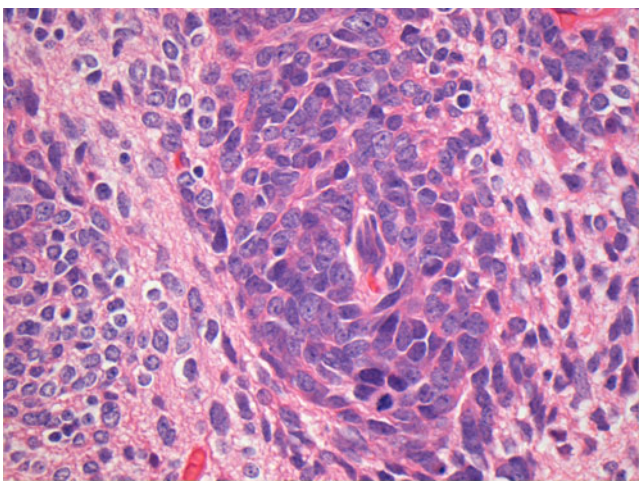

Fig. 2 Haematoxylin and eosin stain of tissue specimen obtained from patient 1 demonstrating poorly differentiated tumour cells

A posterior fossa decompression and biopsy were therefore performed. Histopathology showed increased cellularity, with no anaplasia, and the appearances were considered to be reactive and non-diagnostic. The patient remained stable for another 4 years when signs of increased intracranial pressure recurred. Clinical assessment revealed the pre-existing nystagmus, cerebellar signs and a right pronator drift. Imaging demonstrated hydrocephalus with marked enhancement of the diffuse lesion involving the cerebellum and inferior cerebellar peduncle (Fig. 4).

Stereotactic biopsy of the cerebellar lesion and insertion of a ventriculo-peritoneal shunt were undertaken. Histopathological examination, on this occasion, showed nodules of poorly differentiated pleomorphic tumour cells (Fig. 5). Immunohistochemistry was positive for synaptophysin, S100 and N-CAM, consistent with a diagnosis of medulloblastomas WHO grade 4(Table 1).

Postoperatively the hydrocephalus resolved, but there was no improvement in cerebellar function. As the lesion was deemed unresectable, the patient received cranio-spinal radiotherapy with stabilization of the disease for a further 18 months. Subsequent radiological progression was managed with chemotherapy; however, the patient was eventually referred for terminal care some 3 years after histological diagnosis.

Patient 3

A 30-year-old female presented with 4 months of dizziness, headaches and diplopia. Examination revealed enlargement of the physiological blind spots, papilloedema, bilateral 6th nerve palsies and impairment of tandem gait. Brain MRI demonstrated a mass lesion in the right cerebello-pontine (CP) angle with an intra- and extradural component associated with a small area of

Table 1 Detailed immunohistochemistry profile of the three patients

	N-CAM	Chromogranin	Synaptophysin	GFAP	S100	LCA	CAM 5.2	CK	MNF	CD99
P1	+	+	Faintly +	+/−	NA	–	–	–	–	–
P2	+	–	+	–	+	–	–	–	–	
P3	+	+	–	+/−	NA	–	–	–	–	–

+: positive for antigen, – : negetive for antigen, +/−: weakly positive for surface antigen, NA: not available

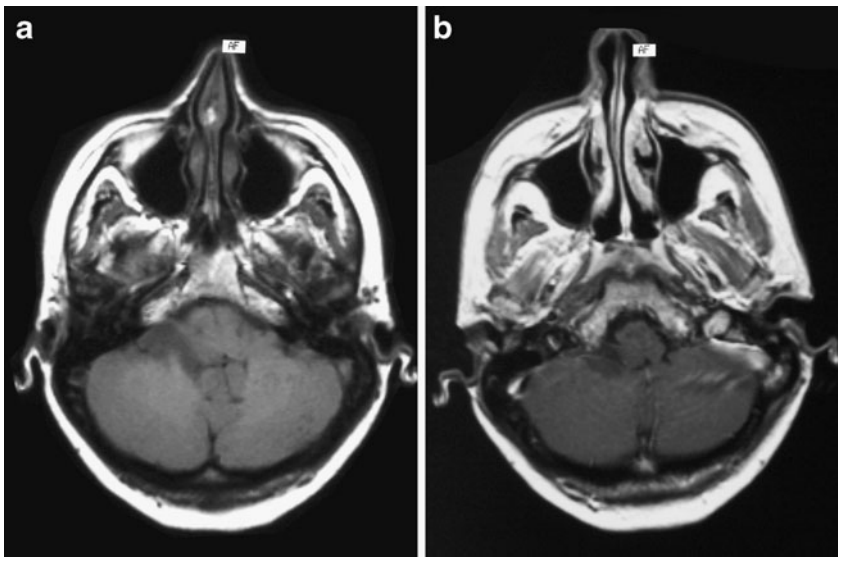

Fig. 3 MRI brain, axial views of the cerebellum. T1WI reveals the abnormality in the vermis and right inferior cerebellar peduncle. The right CP angle lesion, causing rotation of the brain stem, is demonstrated. Early T1WI with contrast did not show any enhancement

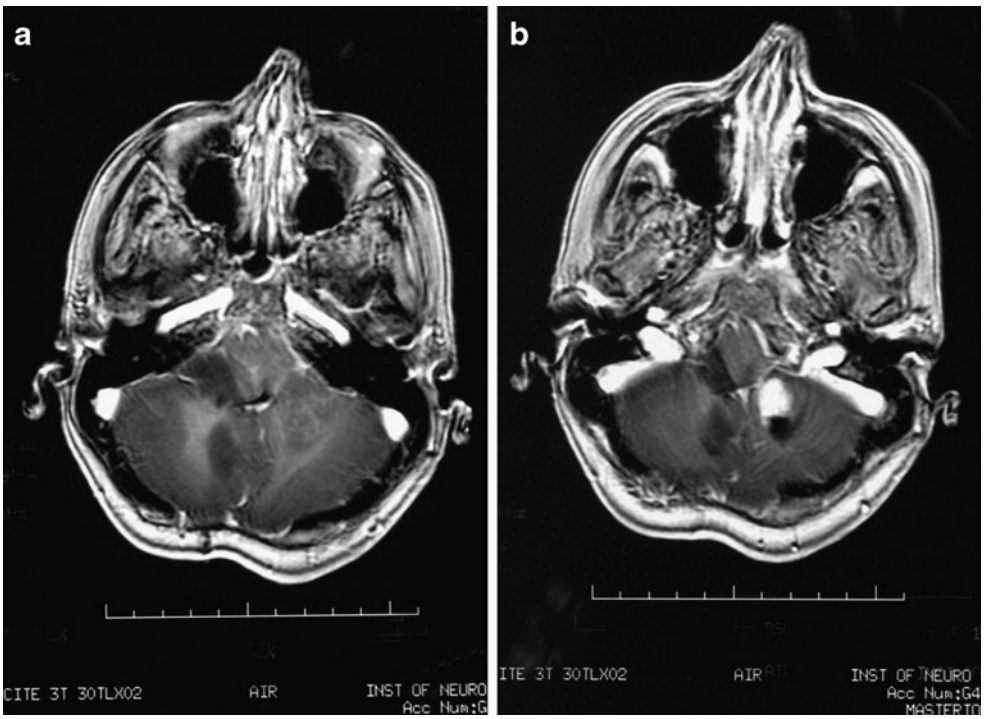

Fig. 4 Progression of disease. On T1WI axial contrast-enhanced views of the cerebellum, extensive involvement of both cerebellar hemispheres is now apparent with avid enhancement of the mass in the left medial-inferior cerebellar hemisphere. The mass effect is more marked

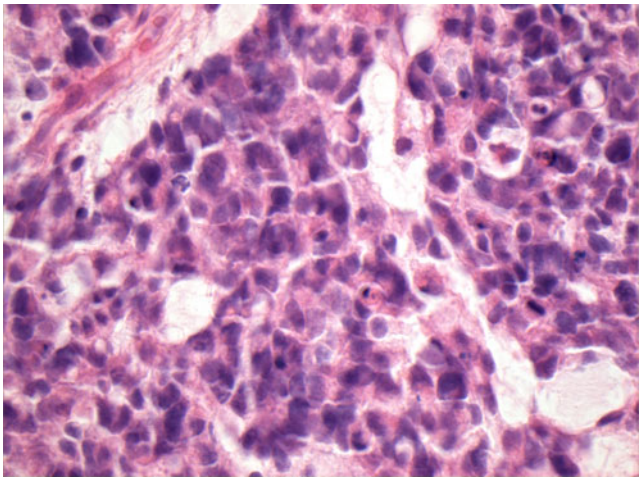

Fig. 5 H&E stain of tissue specimen obtained from patient 2 demonstrating poorly differentiated pleomorphic tumour cells

enhancement. Delayed scanning showed further enhancement of the lesion, adjacent dura, both sylvian fissures as well as the inferio-medial right occipital lobe. The appearances were suggestive of a hamartomatous neoplasm such as gangliocytoma; however, the delayed enhancement was considered atypical (Fig. 6). CT venography also revealed left transverse sinus thrombosis.

The patient underwent insertion of a ventriculo-peritoneal shunt for the control of intracranial hypertension and was later anticoagulated. Due to the benign appearance of the CP angle lesion, interval imaging was proposed. However, 2 months post surgery the patient reported recurrent headaches and a transient paraparesis. Repeat MRI showed progression of the CP angle lesion in addition to a thoracic intradural extramedullary enhancing mass (Fig. 7). MR spectroscopy (MRS) of the posterior fossa lesion revealed a marked increase in the choline (Cho) peak, a reduction in the N-acetyl aspartate (NAA) and creatine (Cr) peaks with the presence of small amounts of lactate, indicating increased cell turnover as is commonly observed in malignant tumours. A thoracic laminectomy and biopsy of the spinal lesion were performed. Histopathological examination showed small to medium sized tumour cells with rounded nuclei and minimal cytoplasm (Fig. 8). These were positive for N-CAM and chromogrannin. The proliferative index was moderate (25% Ki67 positive). The findings were most consistent with a medulloblastomas WHO grade 4 (Table 1). The patient received radiotherapy and adjuvant chemotherapy with complete response of the cranial and spinal disease observed on imaging. However, 18 months after treatment, extensive disease recurrence was demonstrated and deemed untreatable. The patient died 4 months later.

Discussion

Adult medulloblastoma are uncommon lesions and comprise only 1% of adult central nervous system tumours [6, 11]. The majority of medulloblastomas occur within the first decade of life, and these tumours usually manifest with signs and symptoms of increased intracranial pressure [4, 10, 11]. The mean interval between the onset of symptoms and diagnosis is about 6 months in both adult and paediatric cohorts [3, 11]. The tumours arise from primitive neuroectodermal cells, which are originally present in the roof of the fourth ventricle, and subsequently migrate rostrally and laterally

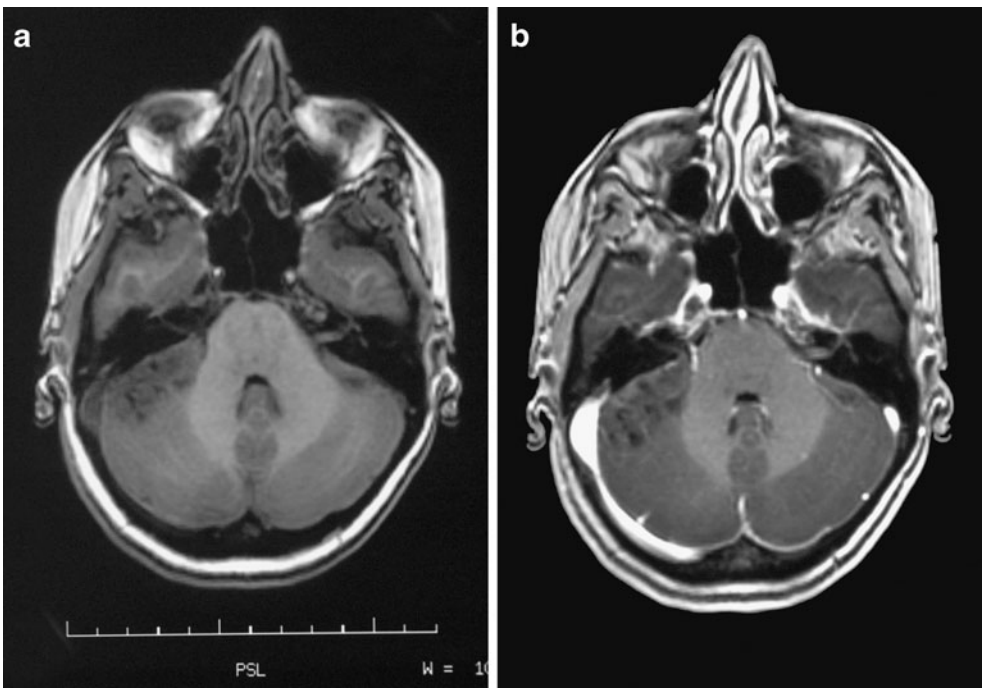

Fig. 6 MRI brain, axial views of the cerebellum. T1WI demonstrates the heterogeneous right CP angle tumour. T1WI with contrast (right) shows slight enhancement at the periphery

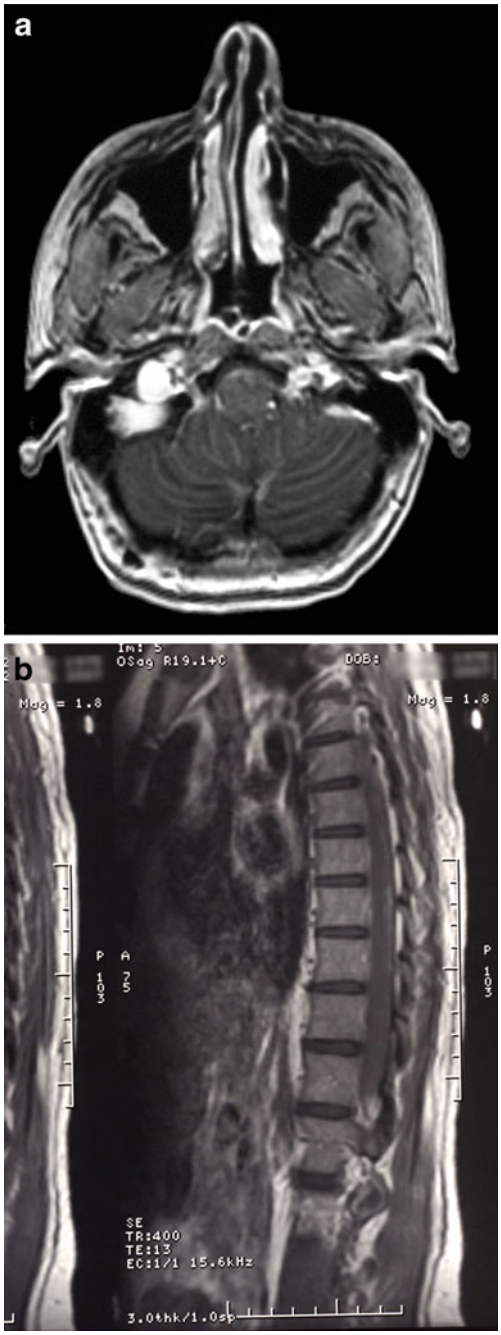

Fig. 7 MRI brain T1WI with contrast axial view demonstrating the enhancing right CP angle lesion with mass effect and effacement of the 4th ventricle. MRI thoracic spine (T1WI with contrast sagittal view) demonstrates irregular enhancement of the meninges posterior to the cord

[6]. With increasing age lateral migration predominates, and this may explain the hemispheric location of these tumours in adults [6]. Radiologically, medulloblastomas have been characterized as solid, homogeneously enhancing, midline masses of the posterior fossa, usually arising from the fastigium [3, 6]. They appear isointense on T2WI because of their hypercellularity [1, 6]. Furthermore, these tumours

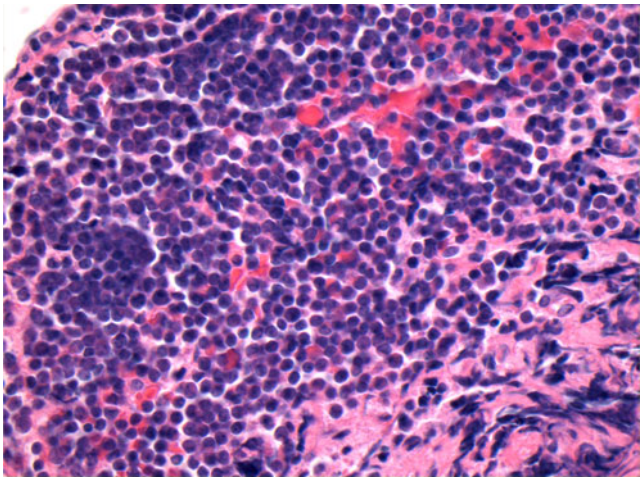

Fig. 8 H&E stain of specimen obtained from patient 3 demonstrating small to medium sized tumour cells with rounded nuclei and minimal cytoplasm

show restriction on diffusion images (DWI) because of reduced extracellular water. On MRS, an increase in the Cho/Cr and Cho/NAA ratios is seen [6]. In children the prognosis is directly influenced by age and extent of the disease at diagnosis, and currently the best treatment available comprises surgery and radiotherapy followed by chemotherapy, which can offer up to 70% 3-year disease-free survival [10].

However, the clinical and radiological features may differ in the adult and paediatric cohorts [5, 11]. Overall atypical imaging features are commoner in adults and include cyst formation, irregular enhancement, extension through fourth ventricle foramina and presentation as a CP angle mass [5, 11]. There are also reports suggesting that adults may have a better outcome; however, the prognostic factors and best treatment options, in this patient group, remain unclear [5].

L'hermitte-Duclos disease (LDD, dysplastic gangliocytoma) is a rare cerebellar lesion of uncertain aetiology. The debate as to whether it constitutes a neoplastic, malformative or hamartomatous lesion remains unresolved [1, 3, 6–9, 12–14]. This abnormality usually presents in the 3rd and 4th decade, with symptoms of slowly progressive raised intracranial pressure. The lesions may occur sporadically or in association with Cowden's (multiple hamaratomas neoplasia) syndrome [1, 3, 9, 12, 14]. Radiologically there is thickening of the cerebellar folia, producing a typical hyperintense striated pattern on T2-weighted images and a hypointense signal on T1WI [1, 6, 12, 14] (Fig. 9). Usually there is an absence of enhancement following gadolinium administration and increased signal on DWI [6, 13]. On MR spectroscopy there is a reduction of the NAA/Cr ratio, but the Cho/Cr ratio is unchanged [6, 7, 14]. The majority of patients undergo either surgical biopsy for tissue diagnosis or decompression for the relief of symptoms [3, 9, 12, 13].

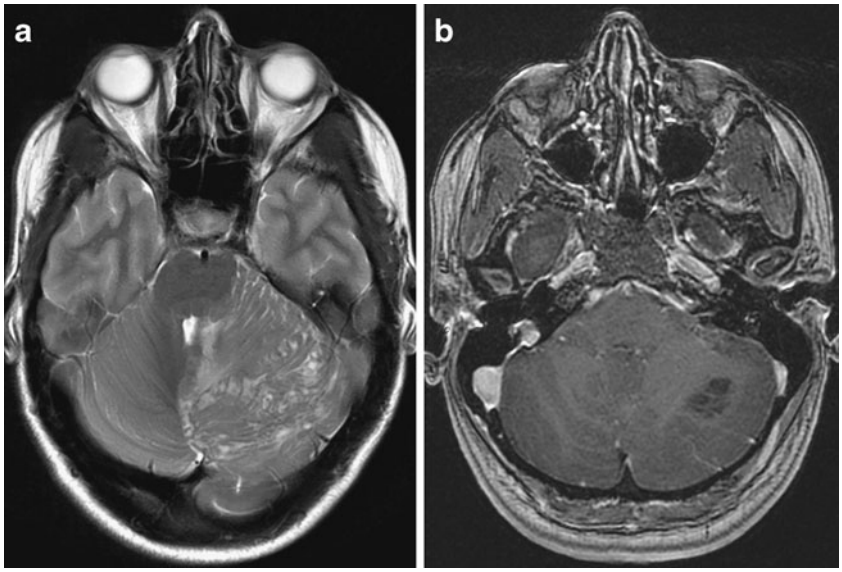

Fig. 9 MRI brain T2WI and T1WI with contrast of histologically confirmed L'hermitte-Duclos disease. Characteristic thickened folia with a striated pattern, hypointense signal and lack of enhancement are demonstrated

Histologically the lesions are represented by an overgrowth of bizarre large ganglion cells, replacing the Purkinje and granular cells, and in addition there is excessive myelination of the molecular layer [1, 3, 9, 12, 14]. Malignant transformation of LDD is very unlikely; however, there have been case reports documenting the subsequent development of malignant astrocytoma following an initial diagnosis of dysplastic gangliocytoma [2].

The three adult patients discussed, presented in an atypically indolent fashion. Patients 1 and 2 were symptomatic for 12 and 48 months, respectively, which is unusually long for medulloblastoma, commonly associated with a short prodrome [3, 11]. The third patient presented after a shorter period of 4 months; however, the disease progression in all three was slower than one observes in the paediatric group.

Patients 1 and 2 were found to have extensive, mass-producing, non-enhancing abnormalities of both the cerebellar hemispheres and vermis. This diffuse and infiltrative pattern was unusual for medulloblastoma, which typically presents as a solid mass. The thickened, striated cerebellar folia seen on imaging would be consistent with a radiological diagnosis of LDD. The third patient's imaging revealed a right CP angle tumour with both extra- and intra-axial components. Small foci of enhancement were seen within the lesion on delayed scanning, but hamartoma or gangliocytoma remained the main differential radiological diagnoses.

In patient 1 and 2 the bilateral and diffuse nature of the lesions made surgical excision inappropriate, and therefore only procedures to decompress the posterior fossa and relieve hydrocephalus were undertaken. In the third patient, as the intracranial pressure was already well controlled by a previously inserted VP shunt, there was no immediate clinical indication for excision of the CP angle lesion, and to establish the diagnosis, the thoracic lesion appeared more readily accessible for biopsy.

All three patients were finally diagnosed with medulloblastoma, but interestingly none of the patients were found to have the desmoplastic variant of the disease more commonly found in adults [10]. Malignant transformation of LDD in these patients remains a remote possibility on radiological but not histological grounds, and previous case repoprts have only documented the development of astrocytoma in such cases [2]. Although all three patients were female, this is likely to be entirely coincidental as there is proven male preponderance [10, 11].

In conclusion, these three patients with medulloblastoma presented with atypical clinical and imaging features consistent with a benign or low-grade neoplasm. Medulloblastoma should therefore be considered in all adults with posterior fossa masses despite having clinical and radiological features suggestive of a low-grade tumour. Definitive diagnosis requires histological confirmation in all cases.

Conflicts of interest None.

References

1. Chen KS, Hung PC, Wang HS, Jung SM, Ng SH (2002) Medulloblastoma or cerebellar dysplastic gangliocytoma (Lhermitte-Duclos disease)? Pediatr Neurol 27:404–406
2. Domingo Z, Fisher-Jeffes ND, De Villiers JC (1996) Malignant occipital astrocytoma in a patient with Lhermitte-Duclos disease (cerebellar dysplastic gangliocytoma) British. J Neurosurg 10:99–102
3. Douglas-Akinwande AC, Payner TD, Hattab EM (2009) Medulloblastoma mimicking Lhermitte-Duclos disease on MRI and CT. Clin Neurol Neurosurg 111:536–539
4. Hyman AD, Lanzieri CF, Solodnik P, Sacher M, Rabinowitz JG (1986) Cystic adult medulloblastomas. J Comput Tomogr 10:139–143

5. Malheiros SM, Franco CM, Stávale JN, Santos AJ, Borges LR, Pelaez MP, Ferraz FA, Gabbai AA (2002) Medulloblastoma in adults: a series from Brazil. J Neurooncol 60:247–253
6. Mittal P, Gupta K, Saggar K, Kaur S (2009) Adult medulloblastoma mimicking Lhermitte-Duclos disease: can diffusion weighted imaging help? Neurol India 57:203–205
7. Nagaraja S, Powell T, Griffiths PD, Wilkinson ID (2004) MR imaging and spectroscopy in Lhermitte-Duclos disease. Neuroradiology 46:355–358
8. Nakagawa T, Maeda M, Kato M, Terada N, Shimizu S, Morooka Y, Nakano H, Takeda K (2007) A case of Lhermitte-Duclos disease presenting high FDG uptake on FDG-PET/CT. J Neurooncol 84:185–188
9. Nowak DA, Trost HA (2002) Lhermitte-Duclos disease (dysplastic cerebellar gangliocytoma): a malformation, hamartoma or neoplasm? Acta Neurol Scand 105:137–145
10. Pizer B, Clifford S (2008) Medulloblastoma: new insights into biology and treatment. Arch Dis Child Educ Pract Ed 93:137–144
11. Sarkar C, Pramanik P, Karak AK, Mukhopadhyay P, Sharma MC, Singh VP, Mehta VS (2002) Are childhood and adult medulloblastomas different? A comparative study of clinicopathological features, proliferation index and apoptotic index. J Neurooncol 59:49–61
12. Tan TC, Ho LC (2007) Lhermitte-Duclos disease associated with Cowden syndrome. J Clin Neurosci 14:801–805
13. Thomas B, Krishnamoorthy T, Radhakrishnan VV, Kesavadas C (2007) Advanced MR imaging in Lhermitte-Duclos disease: moving closer to pathology and pathophysiology. Neuroradiology 49:733–738
14. Wu CH, Chai JW, Lee CH, Chen WH, Lee T, Chen CC (2006) Assessment with magnetic resonance imaging and spectroscopy in Lhermitte-Duclos disease. J Chin Med Assoc 69:338–342

Comment

The paper by Behbahani et al. describes three adult patients affected by a posterior fossa PNET who had in common a prolonged indolent course (at least in two) and, at the initial brain MRI, images suggestive of L'hermitte-Duclos disease. This is a small series of quite unusual clinical cases of adult posterior fossa PNET, which expands the clinical spectrum of presenting features of these rare tumors for the adult population.

Domenico d'Avella
Giorgio Perilongo
Padova, Italy

Acta Neurochir (2011) 153:1519–1525
DOI 10.1007/s00701-011-1041-2

CASE REPORT

Neurenteric cyst of the anterior cranial fossa: case report and literature review

Mark W. Little · Mathew R. Guilfoyle · Diederik O. Bulters · Daniel J. Scoffings · Dominic G. O'Donovan · Peter J. Kirkpatrick

Received: 30 March 2011 / Accepted: 26 April 2011 / Published online: 13 May 2011

Abstract Intracranial neurenteric cysts are rare congenital lesions that typically occur in the posterior fossa. We report a case of a 70-year-old gentleman presenting with gait disturbance, found to have a neurenteric cyst primarily arising from and expanding the sella turcica. A review of the literature revealed 27 reports of supratentorial neurenteric cysts. Clinical presentation, radiological characteristics, treatment, prognosis and embryological origin are discussed. Intracranial neurenteric cysts should be included in the differential with any well-demarcated cystic lesion without enhancement on magnetic resonance imaging (MRI). Complete surgical excision is the treatment of choice, with good prognosis.

Case report

A 70-year-old man presented with a 2-year history of progressive gait disturbance. Past medical history was notable for essential hypertension. On examination, visual acuities were 6/9 bilaterally, visual fields were preserved and fundoscopy was normal. The remaining cranial nerves were intact but there was mild increase in tone in the upper limbs and a hesitant gait.

Computed tomography (CT) imaging of the brain demonstrated an extra-axial, homogenously hyperattenuating, 3.5×4×3.5-cm mass expanding the sella turcica and extending superiorly over the tuberculum sellae along the anterior fossa floor, causing some mass effect on the inferior frontal lobes but without significant vasogenic oedema (Fig. 1). There was no discernible contrast enhancement of the lesion or dura and no evidence of bony erosion. Cranial magnetic resonance imaging (MRI) confirmed the lesion was solitary, projected laterally in the suprasellar cistern but did not invade the cavernous sinuses, and was distinct from the normally enhancing pituitary, which was displaced inferiorly (Fig. 2c). On T1-weighted imaging the lesion was slightly hyperintense with respect to CSF, and it was of high signal on T2-weighted imaging (Fig. 2a, b). The lesion did not show restricted diffusion on diffusion-weighted imaging (Fig. 2d) and there was no appreciable enhancement of the cyst wall or its contents after intravenous gadolinium. Apart from scattered, small, white matter T2 hyperintensities, the brain was otherwise of normal appearance. The preoperative radiological differential was a cyst with proteinaceous contents of uncertain aetiology, an atypical non-enhancing meningioma, or a craniopharyngioma. Pituitary function screen and synacthen test were normal.

The patient consented to surgery. Via a right frontotemporal craniotomy and lateral subfrontal approach, the mass was revealed to be a thin-walled, grey-white cyst. The membrane was punctured and gelatinous fluid evacuated. The wall was easily peeled from the dura inferiorly and away from the overlying frontal lobes; there was no macroscopic evidence of brain invasion. Similarly, the optic nerves were displaced laterally but not involved, and

M. W. Little (✉) · M. R. Guilfoyle · D. O. Bulters · P. J. Kirkpatrick
Department of Neurosurgery, Addenbrooke's Hospital, Hills Road, Box 167, Cambridge CB2 0QQ, UK
e-mail: m.little@doctors.org.uk

D. J. Scoffings
Department of Radiology, Addenbrooke's Hospital, Hills Road, Box 167, Cambridge CB2 0QQ, UK

D. G. O'Donovan
Department of Pathology, Addenbrooke's Hospital, Hills Road, Box 167, Cambridge CB2 0QQ, UK

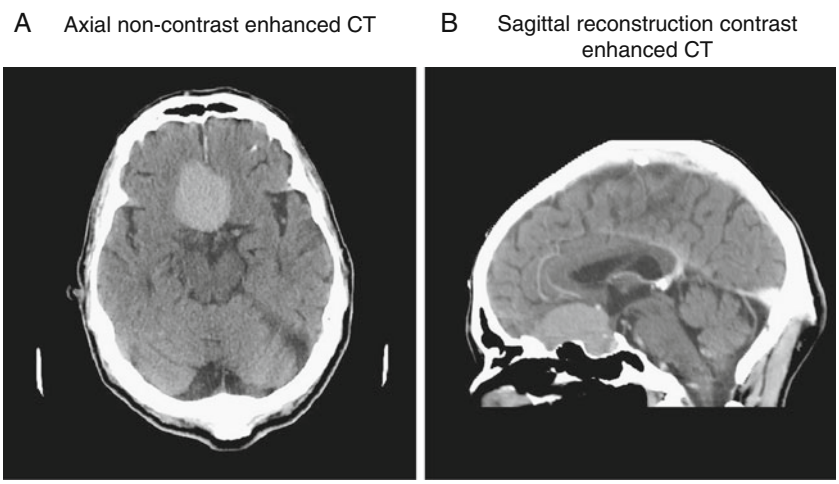

Fig. 1 Pre-operative CT. **a** Axial non-contrast-enhanced CT. **b** Sagittal reconstruction contrast-enhanced CT

the sellar component was easily removed without manipulating the pituitary gland or stalk. The cyst wall over the right anterior clinoid process contained a single red solid nodule which was excised, completing a total macroscopic resection. The evening following surgery, the patient had a witnessed self-limiting tonic-clonic seizure; an urgent CT of the head showed no adverse features. The patient was commenced on phenytoin, which was discontinued on discharge, and has had no further seizures. Two days post-operatively, the patient developed a transient syndrome

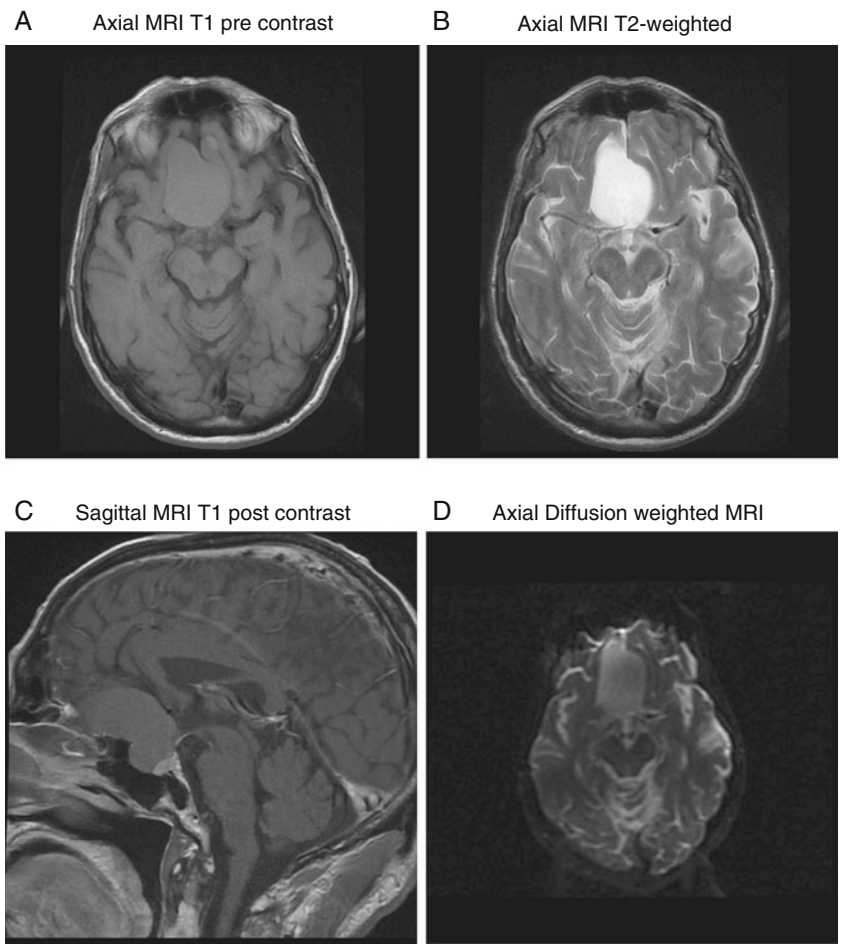

Fig. 2 Pre-operative MRI. **a** Axial MRI T1 pre contrast. **b** Axial MRI T2-weighted. **c** Sagittal MRI T1 post contrast. **d** Axial diffusion-weighted MRI

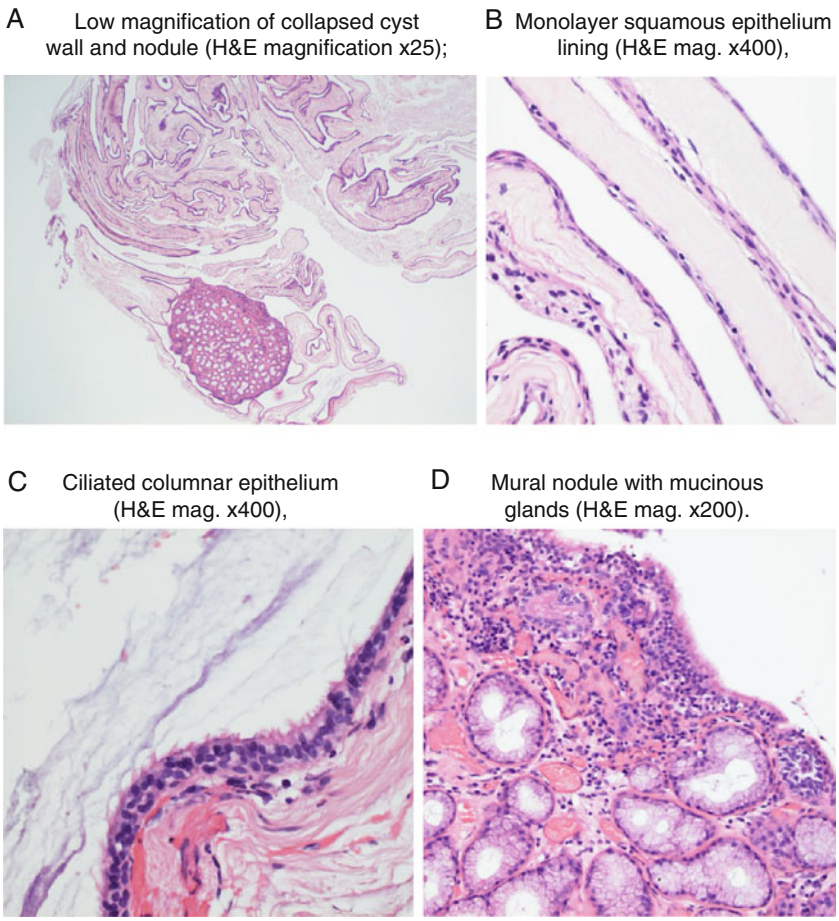

Fig. 3 Histology. **a** Low magnification of collapsed cyst wall and nodule (H & E, magnification ×25). **b** Monolayer squamous epithelium lining (H & E, ×400). **c** Ciliated columnar epithelium (H & E, ×400). **d** Mural nodule with mucinous glands (H & E, ×200)

of inappropriate anti-diuretic hormone secretion (nadir serum sodium 129 mmol/l), which responded to fluid restriction. At 3-month follow-up, the patient remained well with a degree of improvement in his gait.

Microscopy of hematoxylin and eosin stained (H & E) sections revealed a collapsed cyst wall (Fig. 3a), composed of collagen lined by a single layer of squamous epithelium (Fig. 3b) and ciliated columnar epithelium lacking goblet cells (Fig. 3c). A mural nodule composed of mucinous glands was present, covered by ciliated columnar epithelium (Fig. 3d). There was no evidence of squamous metaplasia, neoplasia, or meningioma. Xanthogranulomatous reaction, stellate reticulum, mineralisation, and cholesterol clefts indicative of craniopharyngioma were also absent. Histologically, the appearance was of a benign neurenteric (endodermal) cyst.

Discussion

Neurenteric cysts can occur anywhere throughout the neuraxis and have various synonyms, including endodermal, enteric, enterogenous, respiratory, gastroenterogenous, and archenteric cysts, and have also been labelled gastrocytomas or intestinomas [3, 6, 9, 14, 31]. They most commonly occur in the spinal canal. Intracranially, they are typically located in the posterior fossa [3, 23], usually anterior to the brainstem [23]. Supratentorial neurenteric cysts are extremely rare. To our knowledge, we report the first case of a neurenteric cyst primarily arising from and expanding the sella turcica.

There is a wide differential diagnosis for intracranial neurenteric cysts, depending on their imaging appearance and location, and includes epidermoid, dermoid, arachnoid, parasitic, neoplastic, Rathke's cleft, and colloid cysts [5, 27]. A review of the English language literature revealed 28 reports of supratentorial neurenteric cysts, including the present case [1, 2, 4, 6–8, 11, 13, 15–26, 28–30] (Table 1). Amongst the 15 reports detailing CT findings, six cysts were hyperattenuating, seven were hypoattenuating, and one was isoattenuating and one iso-hypoattenuating. There are no reports of homogeneous enhancement with iodinated contrast agents. Of the 21 cases imaged by MRI with T1-weighted imaging, ten were hyperintense with respect to cerebrospinal fluid (CSF), and ten were isointense with one case of iso-hypointense signal characteristics. Sixteen out of 18 cysts showed hyperintense signal on T2-weighted MRI

Table 1 Literature review of supratentorial neurenteric cysts

Case	Author	Sex	Age	Location	Radiological appearance						Presentation	Treatment	Outcome
					NC CT	T1WI (compared with CSF)	T2WI (compared with brain)	FLAIR (compared with CSF)	T1WI CE	DWI			
1	Basheer et al.	M	54	Right parieto-occipital, extra-axial	Isoattenuating-Hypoattenuating	Hyperintense	–	–	No	–	Headaches	Parieto-occipital craniotomy	Excellent
2	Bavetta et al.	M	28	Right frontal, extra-axial	Hypoattenuating	–	–	–	–	–	Generalised seizures	Craniotomy and complete excision	Excellent
3	Campbell and Verma	F	33	Right frontoparietal	Hypoattenuating	–	–	–	No	–	Focal seizures	Craniotomy, incomplete excision	Good
4	Cheng et al.	M	49	Right frontal, extra-axial	–	Isointense	Hyperintense	Hyperintense	No	–	Memory impairment	Craniotomy, complete excision	Excellent
5	Christov et al.	F	31	Right Frontoparietal		Isointense	Hyperintense	Hyperintense	No	–	Raised intracranial pressure	Craniotomy, complete excision	Good
6	Dunham et al.	F	58	Right parietal, intra-axial	–	Isointense	Hyperintense	–	Minor peripheral enhancement	–	Headache, memory problems.	Craniotomy, complete excision	Excellent
7	Ho et al.	F	45	Right parietal, extra-axial	–	–	Hyperintense	Hyperintense	Multilobulated solid component enhancement	–	Partial seizures, parasthesia	1. Craniotomy, complete excision 2. Cyst fenestration	Good
8	Kachur et al.	F	35	Right frontal, intra-axial	–	Isointense	–	–	No	–	Partial seizures, headache	Craniotomy, complete excision	Good
9	Leventer et al.	F	23	Orbital apex/ superior orbital fissure	Hyperattenuating	–	–	–	–	–	Visual loss, opthalmaplegia in left eye	1. Fluid drainage, incomplete excision, 2. Complete excision	Good
10	List and Williams	F	40	Interhemispheric fissure, extra-axial	–	–	–	–	–	–	Motor deficit, parasthesia, partial seizures	1. Craniotomy, incomplete excision, 2/3. Fluid drainage	Good
11	Marchionni et al.	F	20	Left temporal, peri-insula and cerebellopontine region	–	Hyperintense	–	–	–	–	Headache, hemiparesis, left deafness and blurred vision	Double craniotomy, complete excision	Good
12	Mishra et al.	F	19	Septum pellucidum	Hyperattenuating	Hyperintense	Hyperintense	–	Central enhancement	–	Hydrocephalus	Craniotomy, complete excision	Excellent
13	Mittal et al.	F	76	Right frontoparietal, extra-axial	Hypoattenuating	Isointense	Isointense, with Hyperintense signal at posterolateral margin	–	No	–	Partial seizures, motor deficit	Craniotomy, complete excision	Excellent

14	Miyagi and Katayama	M	63	Right parietal, extra-axial	–	Isointense	Hyperintense	Intermediate intensity between brain and CSF with hyperintense lesion along posterior border of cyst	No	–	Headache and dizziness	Craniotomy, partial excision	Good
15	Morgan et al.	F	30	Oculomotor nerve	–	Isointense	Hyperintense	–	Rim enhancement	–	Right oculomotor nerve paresis	Craniotomy, biopsy, fluid drainage	Good
16	Neckrysh et al.	F	72	Frontal lobe, extra-axial	–	Hyperintense	Hyperintense	–	No	–	Personality change, anosmia	Craniotomy, complete excision	Excellent
17	Preece et al.	F	72	Left frontal, intra-axial	Hypoattenuating	Hyperintense	Hyperintense	Hyperintense	No	–	behavioural change leading to psychosis	Craniotomy	Unknown
18	Preece et al.	M	34	Left frontal, extra-axial	Hypoattenuating	Isointense	Hyperintense	–	No	–	New onset seizures	Craniotomy	Unknown
19	Preece et al.	F	78	Right frontal, extra-axial	Isoattenuating	Iso-hypointense	Hyperintense	–	No	–	Acute onset seizure	Craniotomy	Unknown
20	Preece et al.	M	48	Left intra/ periventricular	Hyperattenuating	Hyperintense	Hyperintense	–	Thin marginal	–	Tremor, numbness right arm, facial droop	Craniotomy	Unknown
21	Preece et al.	M	78	Frontal lobe, extra-axial	Hypoattenuating	Hyperintense	Hyperintense	–	No	–	New onset seizures	Craniotomy	Unknown
22	Reddy et al.	M	20	Axial Left posterior fossa with extension into the temporal region across the tentorium	Hyperattenuating	Hyperintense	Hyperintense	Hyperintense	Peripheral rim enhancement of posterior aspect of lesion	No restriction	Headaches and reduced visual acuity	Craniectomy, subtotal excision	Good
23	Sampath et al.	M	27	Parasellar	–	Hyperintense	Iso/ Hyperintense	–	–	–	Recurrent headaches, vomiting, left sided ptosis	Left frontotemporal craniotomy, cyst resected	Good
24	Scaravilli et al.	M	36	Left optic nerve	Hyperattenuating	–	–	–	–	–	Reduced visual acuity	Orbito-cranial exploration, complete excision	Good
25	Stubenvoll	M	25	Right frontal lobe, extra-axial	–	Isointense	–	Inhomogeneous	–	–	Single generalised seizure	Right anterior craniotomy, cyst fenestration	Good
26	Takumi et al.	M	32	Left frontal convexity	–	Isointense	Hyperintense	–	No	–	Headache, Status epilepticus	Craniotomy, complete excision	Excellent

Table 1 (continued)

Case	Author	Sex	Age	Location	Radiological appearance						Presentation	Treatment	Outcome
					NC CT	T1WI (compared with CSF)	T2WI (compared with brain)	FLAIR (compared with CSF)	T1WI CE	DWI			
27	Tan et al.	F	68	Left frontal, extra-axial	Hypoattenuating	–	–	–	–	–	Hemiparesis, generalised seizures	Craniotomy, complete excision	Excellent
28	Little et al.	M	70	Frontal lobe, extra-axial	Hyperattenuating	Hyperintense	Hyperintense	–	No	No restriction	Gait disturbance	Craniotomy, complete excision	Excellent

M male, *F* female, *FLAIR* fluid attenuation inversion recovery pulse sequence, *T1WI* T1-weighted imaging, *T2WI* T2-weighted imaging, *DWI* diffusion-weighted imaging, *CT* computed tomography, *NC* non contrast, *CE* contrast enhancement

with respect to brain parenchyma, whilst two cases revealed mixed hyper/isointense. Six of seven cases using FLAIR pulse sequences displayed hyperintense signal characteristics with respect to CSF. There are no reports of neurenteric cysts enhancing with gadolinium contrast. These findings highlight the variability in imaging characteristics displayed by neurenteric cysts, probably a reflection of the range in protein level of the cyst contents. Nonetheless, MRI remains the modality of choice given its superior soft tissue contrast and ability to delineate the cyst from surrounding structures, aiding presurgical planning. Specific differential diagnoses can be excluded on the basis of MRI appearance; for instance, there are no reports of isointense signal characteristics relative to CSF on all pulse sequences, allowing discrimination of neurenteric and arachnoid cysts. Furthermore, diffusion weighted imaging can identify epidermoid or dermoid lesions, which show moderate-to-striking diffusion restriction [12].

Neurenteric cysts behave as space occupying lesions and clinical presentation is, therefore, mainly influenced by location. In the literature, the most common presentation is seizure, occurring in 12 cases, all of which involved the cortex [2, 4, 11, 13, 16, 19, 23, 28–30]. Treatment should aim for complete surgical excision of the cyst and contents. Recurrent neurenteric cysts have been reported, and this risk is principally dependent on extent of resection that is achievable [4, 15].

The aetiology of supratentorial neurenteric cysts remains unclear and several hypotheses have been advanced regarding their embryological derivation. A widely held theory of the origin of infratentorial neurenteric cysts is aberrant separation of the notochord during gastrulation, resulting in ectopic endoderm within the ectoderm layer [6, 13]. This notion is lent some support by the association of intraspinal neurenteric cysts with spinal dysraphic syndromes—for example, hemivertebrae, anterior and posterior spina bifida and segmentation abnormalities. Supratentorial neurenteric cysts are somewhat more difficult to explain within this scheme as the closure of the notochord at the cranial end by mesenchyme occurs at the level of the clivus. Graziani et al. [10] contend that supratentorial neurenteric cysts, Rathke's cleft cysts, and colloid cysts all arise from migrating remnants of Seessel's pocket, an endodermal diverticulum that develops from the cranial end of the foregut. The final location of the Seessel's pouch remnant determines the type of cyst: Rathke's cleft cysts result from an intrasellar remnant, colloid cysts reflect remnants in the third ventricle, and cysts formed in the presellar or retrosellar location are neurenteric cysts. Whilst plausible for midline cysts, this theory fails to fully account for paramedian supratentorial neurenteric cysts. One theory proposed by Mittal et al. [19] is that neurenteric cysts are a product of anomalous endodermal cell migration dorsally through the primitive neurenteric canal into the ectoderm.

This theory plausibly explains why lateral supratentorial neurenteric cysts are so rare, as ectopic endodermal cells must travel the furthest distance away from their entry into the neuroectodermal layer.

Conclusions

Supratentorial neurenteric cysts involving the sellar region are rare. Radiological diagnosis is challenging as a result of the variability of imaging characteristics. Intracranial neurenteric cysts should be included in the differential with any well-demarcated cystic lesion without enhancement on MRI. The treatment of choice remains complete surgical excision, and prognosis is good. Further work is needed to validate the embryological origins of supratentorial neurenteric cysts.

Conflicts of interest None.

References

1. Basheer N, Kasliwal MK, Suri A, Sharma MC, Arora A, Sharma BS (2010) Lareal extradural, supratentorial neurenteric cyst. J Clin Neurosci 17:639–641
2. Bavetta S, El-shunnar K, Hamlyn PJ (1996) Neurenteric cyst of the anterior cranial fossa. Br J Neurosurg 10(2):225–227
3. Bejjani GK, Wright DC, Schessel D, Sekhar LN (1998) Endodermal cysts of the posterior fossa, report of three cases and review of the literature. J Neurosurg 89(2):326–335
4. Campbell DA, Varma TR (1991) An extraventricular colloid cyst: case report. Br J Neurosurg 5(5):519–522
5. Chaynes P, Thorn-Kany M, Sol JC, Arué P, Lagarrigue J, Manelfe C (1998) Imaging in neurenteric cysts of the posterior cranial fossa. Neuroradiology 40:374–376
6. Cheng JS, Cusick JF, Ho KC, Ulmer JL (2002) Lateral supratentorial endodermal cyst: case report and review of literature. Neurosurgery 51(2):493–499
7. Christov C, Chretien F, Brugieres P, Djindjian M (2004) Giant supratentorial enterogenous cyst: report of a case, literature review, and discussion of pathogenesis. Neurosurgery 54(3):759–763
8. Dunham CP, Curry B, Hamilton M (2009) Malignant transformation of an intraaxial supratentorial neurenteric cyst-case report and review of literature. Clin Neuropathol 28(6):460–466
9. Giombini S, Lodrini S, Migliavacca F (1981) Intracranial enterogenous cyst. Surg Neurol 16:271–273
10. Graziani N, Dufour H, Figarella-Branger D, Donnet A, Bouillot P, Grisoli F (1995) Do the suprasellar neurenteric cyst, the Rathke cleft cyst and the colloid cyst constitute the same entity? Acta Neurochir (Wien) 133(3–4):174–180
11. Ho LC, Olivi A, Cho CH, Burger PC, Simeone F, Tihan T (1998) Well-differentiated papillary adenocarcinoma arising in a supratentorial enterogenous cyst: case report. Neurosurgery 43(6):1474–1477
12. Inoue T, Kawahara N, Shibahara J, Masumoto T, Usami K, Kirino T (2004) Extradural neurenteric cyst of the cerebellopontine angle: case report. J Neurosurg 100:1091–1093
13. Kachur E, Ang LC, Megyesi JF (2004) Intraparenchymal supratentorial neurenteric cyst. Can J Neurol Sci 31(3):412–416
14. Knight G, Griffiths T, Williams I (1955) Gastrocystoma of the spinal cord. Br J Surg 42(176):635–638
15. Leventer DB, Merriam JC, Defendini R, Behrens MM, Housepian EM, LeQuerica S, Blitzer A (1994) Enterogenous cyst of the orbital apex and superior orbital fissure. Ophthalmology 101 (9):1614–1621
16. List CF, Williams JR (1961) Subdural epithelial cyst in the interhemispheral fissure. Report of a case, with some remarks concerning the classification of intracranial and thelial cysts. J Neurosurg 18:690–693
17. Marchionni M, Smith C, Eljamel MS (2008) Intracranial enterogenous cyst extending into both supratentorial and infratentorial compartments: case report and review of the literature. Skull Base 18:213–216
18. Mishra GP, Sharma RR, Musa MM, Pawar SJ (2000) Endodermal cyst of septum pellucidum and pregnancy: a case report. Surg Neurol 53(6):583–585
19. Mittal S, Petrecca K, Sabbagh AJ, Rayes M, Melançon D, Guiot MC, Olivier A (2010) Supratentorial neurenteric cysts-A fascinating entity of uncertain embryopathogenesis. Clin Neurol Neurosurg 112(2):89–97
20. Miyagi A, Katayama Y (2007) Neurenteric cyst arising in the high convexity parietal lesion: case report. Neurosurgery 60(1):203–204
21. Morgan MA, Enterline DS, Fukushima T, McLendon RE, Cummings TJ (2001) Endodermal cyst of the oculomotor nerve. Neuroradiology 43:1063–1066
22. Neckrysh S, Valyi-Nagy T, Charbel FT (2006) Neuroenteric cyst of the anterior cranial fossa: case report and review of the literature. Surg Neurol 65(2):174–177
23. Preece MT, Osborn AG, Chin SS, Smirniotopoulos JG (2006) Intracranial neurenteric cysts: imaging and pathology spectrum. AJNR Am J Neuroradiol 27:1211–1216
24. Reddy RS, Vijayasaradhi M, Uppin MS, Challa S (2010) A rare case of extradural neurenteric cyst with supratentorial and infratentorial extension. Acta Neurochir (Wien) 152(11):1957–1959
25. Sampath S, Yasha TC, Shetty S, Chandramouli BA (1999) Parasellar neurenteric cyst: unusual site and histology: case report. Neurosurgery 44(6):1335–1337
26. Scaravilli F, Lidov H, Spalton DJ, Symon L (1992) Neuroenteric cyst of the optic nerve: case report with immunohistochemical study. J Neurol Neurosurg Psychiatry 55(12):1197–1199
27. Simon JA, Olan WJ, Santi M (1997) Intracranial neurenteric cysts: a differential diagnosis and review. Radiographics 17:1587–1593
28. Stubenvoll F, Beschorner R, Danz S, Freudenstein D (2006) Fronto-laterally located supratentorial bronchogenic cyst: case report and review of the literature. Clin Neuropathol 25(3):123–127
29. Takumi I, Mori O, Mizutani N, Akimoto M, Kobayashi S, Teramoto A (2008) Expansile neurenteric cyst arising in the frontal lobe associated with status epilepticus: report of a case and discussion of epileptogenesis. Brain Tumor Pathol 25(2):97–101
30. Tan GS, Hortobagyi T, Al-Sarraj S, Connor SE (2004) Intracranial laterally based supratentorial neurenteric cyst. Br J Radiol 77 (923):963–965
31. Tubbs RS, Salter EG, Oakes WJ (2006) Neurenteric cyst: case report and a review of the potential dysembryology. Clin Anat 19 (7):669–672

Acta Neurochir (2011) 153:1527–1528
DOI 10.1007/s00701-011-1015-4

LETTER TO THE EDITOR

Functional? Paraganglioma of the cerebellum

Pravin Shashikant Salunke · Kirti Gupta · Rakshith Srinivasa · Sukumar Sura

Received: 29 March 2011 / Accepted: 1 April 2011 / Published online: 15 April 2011

Dear editor,

Paragangliomas (PGs) are neoplasms originating from the extradrenal paraganglionic system and rarely secrete acetylcholine, cathecholamine or serotonin [2, 4]. They are uncommon in the central nervous system, and the intracerebral location is rare. PGs have been reported in the sella, cerebellopontine angle, pineal body, frontal skull base, petrous ridge, sylvian fissure and cerebellum [4]. So far, only four intracerebellar cases have been reported, including ours [2–4]. This is the first case ever reported of possibly functional intracerebellar PG.

A 35-year-old female presented with holocranial headache with vomiting for 10 months associated with episodes of anxiety and palpitations. Her blood pressure recordings were high and were attributed to raised intracranial pressure. Nervous system examination revealed bilateral papilloedema and subtle left cerebellar signs. Brain MRI showed a left cerebellar mass of 4 × 3 × 4 cm, with multiple flow voids and homogenously enhancing on contrast, with moderate hydrocephalus (Fig. 1a-d). The patient underwent suboccipital craniotomy with gross total excision of the tumour. The tumour was reddish to gray in appearance, vascular and soft to firm, located on the left lateral cerebellar surface extending within. Blood loss was minimised by dissecting all around the tumour without entering it. Gross total excision was achieved. Histopathology revealed diffuse sheets of polygonal cells arranged predominantly in alveolar, pseudopapillary and nesting patterns (zellballen). These nests were surrounded by fine fibrovascular septa with spindle-shaped cells (Fig. 1e,f). The cells had abundant eosinophilic cytoplasm, round centrally placed vesicular nuclei with conspicuous nucleoli and no foci of necrosis. The Ki-67 labelling index was 3–4%. The cells tested positive to S-100, neuron-specific enolase and synaptophysin, and negative to CK, chromogranin, GFAP and EMA (Fig. 1 g-j). The features suggested a paraganglioma.

Postoperatively her headache subsided, her anxiety episodes did not recur, and she became normotensive. Retrospective evaluation of anesthesia notes showed no gross variation in blood pressure intraoperatively. Postoperative urinary vanillylmandelic acid levels and the MIBG scan were normal. She is on a regular follow-up schedule and had no recurrence at 7 months. She did not receive adjuvant radiotherapy.

Extra-adrenal PGs account for 0.06% of all PGs [4]. Sympathetic PGs develop from the truncus sympaticus and are intraabdominal. The parasympathetic PGs arise from intercarotidian tissue, tympanojugular or vagal nerves [2]. They are uncommon in the central nervous system and appear as tumours in the cauda equina region. Only 13 cases of intracerebral PGs have been reported [2, 4]. Intracranial involvement most commonly represents extension from jugulotympanic tumours [4]. However, its

P. S. Salunke (✉) · R. Srinivasa · S. Sura
Department of Neurosurgery, Postgraduate Institute of Medical Education and Research (PGIMER), 160012, Chandigarh, India
e-mail: drpravin_salunke@yahoo.co.uk

R. Srinivasa
e-mail: rakshithsrinivas@yahoo.co.in

S. Sura
e-mail: drskumars@yahoo.com

K. Gupta
Histopathology, PGIMER, Chandigarh, India
e-mail: Kirtigupta10@yahoo.co.in

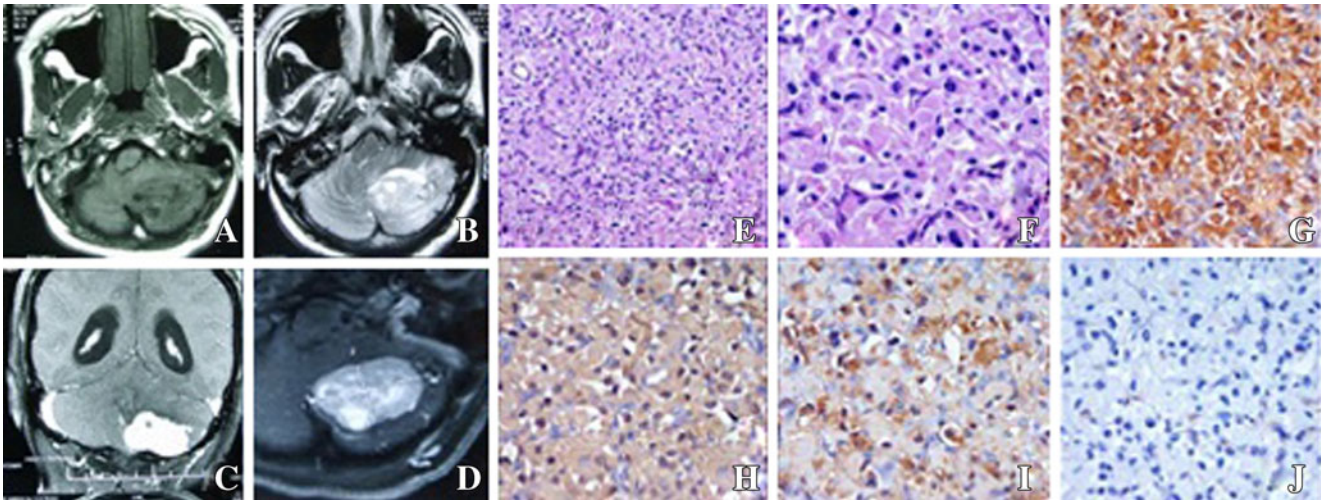

Fig. 1 **a** T1-weighted axial image showing intracerebellar isointense lesion with hypointensities within (flow voids). **b** Lesion appears hyperintense on T2-weighted image with flow voids giving rise to a speckled (salt and pepper) appearance. **c** Coronal contrast MRI showing brilliant enhancement and its extent up to the surface. **d** Axial contrast MRI showing the extent of the lesion. **e**,**f** Neoplastic cells arranged in nests with surrounding fibrovascular septa lined by spindle-shaped cells [H&E ×200 (**a**), ×400 (**b**)]. **g** Neoplastic cells with strong positivity for neuron-specific enolase (immunoperoxidase ×400). **h** Spindle-shaped cells positive to S-100 (×400). **i** Tumor cells positive to synaptophysin (×400). **j** Cells negative with cytokeratin and GFAP (×400)

origin in locations remote from the jugular foramen is debatable, and is possibly from migration of paraganglionic cells or inhibition of the foetal migration from the neural crest leaving some vestigial cell rests in adult CNS or metastatic lesions from extra-adrenal parangliomas/pheochromocytomas [1]. These tumours demomstrate histopathological, immunohistochemical and ultrastructural features similar to their extra-adrenal counterparts. The diagnosis is never made preoperatively. None of them have been reported with symptoms suggestive of a functional tumour except in our case [4].

Typical PGs show a hyperintense signal with a salt and pepper appearance on T2-weighted images and distinct contrast enhancement on T1-weighted images with multiple serpentine and punctuate signal voids [1]. Optimal treatment of cerebellar PG remains unclear. In analogy with head and neck PGs, it seems that gross total resection appears to be curative. Postoperative radiotherapy has been shown to be effective following partial resection [2, 4].

Conflicts of interest None

References

1. Naggara O, Varlet P, Page P, Oppenheim C, Meder JF (2005) Suprasellar paraganglioma: a case report and review of the literature. Neurorad 47:307–12
2. Nitsche M, Prinz M, Hermann RM, Christiansen H, Weiss E (2005) Paraganglioma of the cerebellum: case report and review of the literature. Int J Clin Oncol 10(6):447–452
3. Prayson RA, Chahlavi A, Luciano M (2004) Cerebellar paraganglioma. Ann Diagn Pathol 8(4):219–223
4. Xhumari A, Couvelard A, Redondo A, Kalamarides M (2007) Long-term follow-up of an infratentorial primary paraganglioma: a case report. Br J Neurosurg 21(5):531–535

Acta Neurochir (2011) 153:1529–1533
DOI 10.1007/s00701-011-0994-5

TECHNICAL NOTE

Integration of a 3D ultrasound probe into neuronavigation

Andrea Müns · Jürgen Meixensberger · Sven Arnold · Arno Schmitgen · Felix Arlt · Claire Chalopin · Dirk Lindner

Received: 4 February 2011 / Accepted: 8 March 2011 / Published online: 3 April 2011

Abstract
Background Intraoperative ultrasound (iUS) allows the generation of real-time data sets during surgical interventions. The recent innovation of 3D ultrasound probes permits the acquisition of 3D data sets without the need to reconstruct the volume by 2D slices. This article describes the integration of a tracked 3D ultrasound probe into a neuronavigation.
Methods An ultrasound device, provided with both a 2D sector probe and a 3D endocavity transducer, was integrated in a navigation system with an optical tracking device. Navigation was performed by fusion of preoperatively acquired MRI data and intraoperatively acquired ultrasound data throughout an open biopsy. Data sets with both probes were acquired transdurally and compared.
Results The acquisition with the 3D probe, processing and visualization of the volume only took about 2 min in total. The volume data set acquired by the 3D probe appears more homogeneous and offers better image quality in comparison with the image data acquired by the 2D probe.
Conclusions The integration of a 3D probe into neuronavigation is possible and has certain advantages compared with a 2D probe. The risk of injury can be reduced, and the application can be recommended for certain cases, particularly for small craniotomies.

Keywords Neuronavigation · Intraoperative ultrasound · Tumor resection · 3D probe

A. Müns (✉) · J. Meixensberger · F. Arlt · D. Lindner
Department of Neurosurgery, University Hospital Leipzig,
Liebigstraße 20,
04103 Leipzig, Germany
e-mail: andrea.muens@medizin.uni-leipzig.de

S. Arnold · A. Schmitgen
LOCALITE GmbH,
53757 Sankt Augustin, Germany

J. Meixensberger · C. Chalopin
ICCAS, University of Leipzig,
Leipzig, Germany

Introduction

Two-dimensional ultrasound imaging relies on the skills of the clinician and a trial-and-error approach to obtain good images [13]. In comparison, 3D ultrasound imaging has the potential advantage of being more accurate and repeatable [6]. Early applications of 3D ultrasound imaging have been focused more on cardiac, obstetric and gynecological applications. However, the field of application continues to expand throughout the clinical arena.

Classical neuronavigation is usually based on preoperatively acquired imaging data and is thus not able to reflect the brain shift that occurs during brain surgery [8]. Therefore, intraoperative ultrasound represents an efficient extension for intraoperative imaging and surgical guidance. Tracked ultrasound has gained importance because of the feasibility of applying it for the validation of preoperative planning, the identification of changes such as brain shift or tissue movement, the correction of the operational path and finally resection control in tumor surgery [9].

Meanwhile, iUS has become a well-established imaging modality in different neurosurgical procedures. Because of its low costs, real-time application and the absence of radiation, ultrasound is the modality of choice for many situations.

Usually the fusion of MRI and iUS data is done by volume rendering of tracked 2D slices. To the best of our knowledge, so far 3D probes have not been established or

evaluated for neurosurgery. Therefore, the aim of our study is to integrate a tracked 3D probe in an existing navigation system for the evaluation of its suitability for neurosurgical interventions.

Material and methods

A navigation system (SonoNavigator, LOCALITE, St. Augustin, Germany) containing a video grabber card in combination with an optical tracking system (NDI Polaris, Northern Digital Inc., Waterloo, Canada) and an ultrasound device (Siemens Acuson Antares, Siemens Medical Solutions, Issaquah, WA) were employed. The ultrasound device was provided with both a 2D sector probe (P10-4, Frequency Bandwith 4–10 MHz, aperture 19×12 mm) and a 3D curvilinear mechanical wobbler endocavity transducer (EV9F4, Frequency Bandwith 4–9 MHz, aperture 31× 6 mm). The probes were tracked by mounting passive trackers, each consisting of three spherical markers. As reference a passive tracker was placed on a Mayfield clamp (Ohio Medical Instruments, Cincinnati, OH). Hence, navigation could be performed by fusion of preoperatively acquired MRI data and intraoperatively acquired ultrasound data.

Preoperative planning with the navigation system comprised trajectory planning as well as the definition of various anatomical landmarks in the MR data for the subsequent patient registration in the operating room. The registration based on this set of anatomical landmarks could be improved by a subsequent surface registration [1]. The craniotomy was planned using image guidance based on the MR data.

Pipeline 2D acquisition

A single-cross-wire phantom equipped with a cross of two strings of fishing line in a water bath was employed for the calibration of the 2D ultrasound probe.

About 20 ultrasound images of the calibration point were acquired while varying the direction and angle of the probe. The resulting crosses in the image data were pointed manually and represented the base for obtaining the transformation matrix by a least square estimation. The recalculated positions of the calibration point showed a root mean square (RMS) of 0.8 mm [9]. Performing analog capture of the video signal via the S-Video output device is a possibility for transferring the image data of the 2D ultrasound probe in real-time. At the acquisition time the surgeon swept the probe across the region of interest. Then the image data were converted by the video grabber card so that volume data could be constructed by mapping the video images into the corresponding voxel plane of the volume. Multiple pixel information for one voxel was averaged [9]. For the volume construction, the calibration of the probe needs to be known first.

Pipeline 3D acquisition

For the calibration of the 3D probe a cross-wire phantom with three crosses placed in different depths was used. In comparison to 2D probes, determination of the geometry is simplified by acquisition of the whole volume instead of single slices that first need to be compounded. As the first step, a volume was acquired in which the three different crosses were clearly definable. After transmitting the DICOM volume data to the navigation system, the crosses in the ultrasound volume were assigned manually to the known geometrical positions in the phantom coordinate system. The transformation matrix was achieved by applying a simple point-to-point registration based on [11]. The recalculated positions of the calibration points showed a root mean square (RMS) of 1.4 mm.

The 3D probe contains an ultrasound transducer that is mechanically swept by a motor. The integration of the image data of the 3D probe into the navigation system requires the transmission of the raw 3D data stored in the ultrasound device in DICOM format. These data can be digitally transferred via an ethernet device without any loss of quality. Since image data and tracking information need to be synchronized, the acquisition of the correct tracking information posed a challenge. A solution could be found in close collaboration with the manufacturer Siemens, which enables the user to initiate the acquisition from the navigation system (SonoNavigator, LOCALITE) instead of the ultrasound device.

Once the probe was correctly placed on the area of interest, the user could start the acquisition process from the navigation system. The tracking position was recorded once at the beginning of the acquisition process while the probe remained motionless across the surface. After transferring the raw data to the navigation system, the only processing step that needed to be performed was the generation of the volume of this raw data. Based on the acquired volume, related tracking data and calibration of the 3D probe, image fusion with preoperative image data could be carried out.

Case illustration

A 78-year-old patient with suspicion of lymphoma in the frontotemporal region with basal ganglia involvement was operated on using a navigation system (SonoNavigator, LOCALITE) based on preoperative images (MRI) and intraoperative images (iUS). To confirm the suspicion of lymphoma, an open biopsy was performed. Preoperatively we acquired MRI data with a 1.5-T scanner [Achieva Phillips, T1-weighted spin echo (T1WSE), 48 slices with

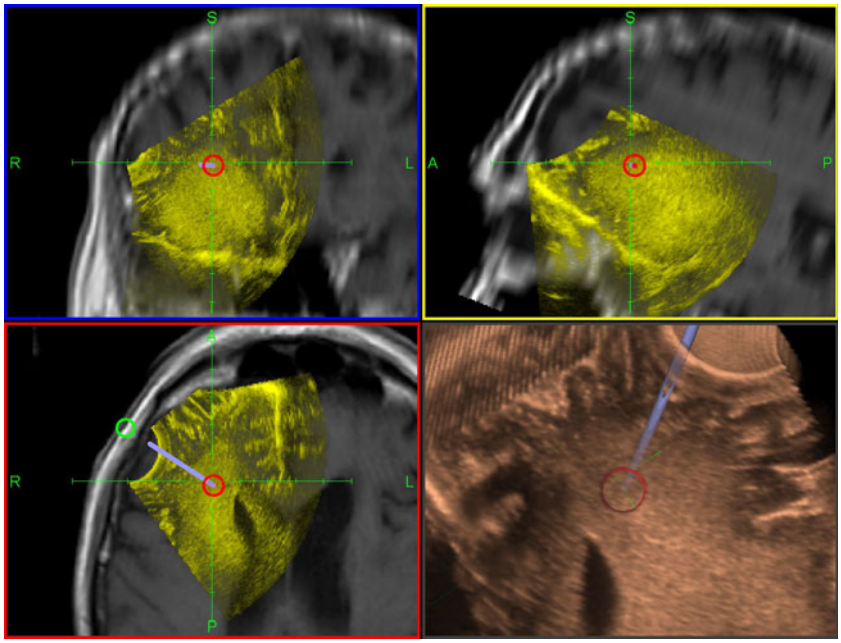

Fig. 1 Three orthogonal MR slices with overlaid 3D ultrasound. The image (bottom right) illustrates the acquired volume

5 mm thickness]. The MRI was arranged 10 days before the operation took place and while the patient underwent dexamethason therapy, which was tapered before the operation.

Based on the MRI data, the optimal surgical trajectory to the brain tumor was planned. Preoperative planning comprised also the definition of seven anatomical landmarks for the subsequent patient registration. After additional surface registration, a registration error (root mean square) of 1.9 mm was measured.

Data sets with both probes were acquired after craniotomy but before dura opening (transdural) and fusioned with the preoperative MRI (Fig. 2). The ultrasound data revealed a significant tumor progression in comparison to the MRI data. Tapering the dexamethason therapy and also the time difference between MRI and US acquisition could account for this progression.

The biopsy confirmed the suspicion of lymphoma, and the treatment was started.

Results

In the presented case, image acquisition and visualization were successfully performed with both probes (EV9F4 and P10-4).

After storing the volumes in the navigation system axial, sagittal and coronal slices from MRI und iUS data were generated and displayed for image guidance throughout the operation.

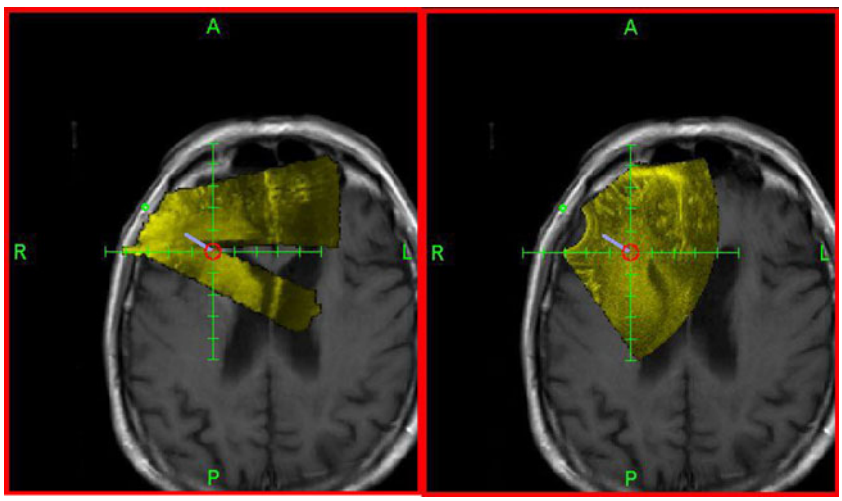

Fig. 2 The same axial slice: (left) with resliced data from the volume acquired by the 2D probe and (right) resliced from the volume acquired by the 3D probe

No volume reconstruction needs to be done in the case of a 3D probe in which the volume data set appears homogeneous and no holes occur (Fig. 1). In comparison to the planes generated from the reconstructed volume of the image data acquired by the 2D probe, the image quality was better (Fig. 2).

Discussion

In neurosurgery, the brain shift, mainly caused by the loss of cerebrospinal fluid and tumor tissue removal, reduces navigation accuracy [4, 10]. Intraoperative imaging such as ultrasound facilitates intraoperative orientation, detection of brain shift and resection control [2, 5, 12] because of the possibility to update the information about the surgical process [5]. Usually fusion of MRI and iUS data is done by volume rendering of tracked 2D ultrasound slices. The majority of the ultrasound devices are provided with an analog S-Video output interface for analog transfer of the video signal. The analog data transfer and the following conversion to digital data mean a loss of quality of the signal. Furthermore, holes can appear in the volume if the sweep cannot be performed in an uninterrupted way, for example, because of a small craniotomy or the size of the probe. If the surface is highly vulnerable as well, placing and sweeping the probe could be associated with a risk of injury.

Using a 3D probe for navigation can help to avoid the mentioned drawbacks. Transmission of the raw data by an ethernet cable ensures high data quality. In comparison to the conventional method with the 2D probe, it is not necessary to reslice the data in the ultrasound device and to downgrade the resolution for analog transmission. If the volume is acquired by the 3D probe, which remains motionless during the acquisition, holes cannot appear in the volume, and since voxels do not need to be summarized in case of multiple values, the data set is more homogenous. Another advantage is that the risk of injury can be reduced with the application of 3D probes because there is no more need to move the probe across the surface. If the craniotomy is small, it is also recommendable to use the 3D probe because the space required to perform the scan is only limited by the size of the probe. The acquisition of the volume by the 3D probe takes less time in comparison to the acquisition by the 2D probe, though the processing for visualization in the navigation system takes a bit more time. The acquisition with the 3D probe, processing and visualization of the volume only took about 2 min in total.

The synchronization between tracking and image data represents a challenge that in our case could be solved in cooperation with the manufacturer. The volume size of the data set is limited by the field of view of the probe. However, Ji et al. [3] have already demonstrated a method to combine multiple true 3D ultrasound data sets.

Conventional 2D ultrasound demands mental compounding of the slices to obtain an impression of the patient's anatomy. This can be time-consuming and requires experience in the interpretation of the slices. For users accustomed to 2D images, getting used to the handling and interpretation of 3D volume images may take time. Identified clinical benefits are the ability to obtain views not possible with 2D imaging and the better understanding of complex structures [7].

Conclusions

This study has shown that the integration of a 3D probe into neuronavigation is possible and has certain advantages compared with a 2D probe.

In conclusion, it can be asserted that the application and integration of a 3D probe in neuronavigation can be recommended for certain cases, particularly for small craniotomies.

Further investigation will also focus on matrix transducers. While mechanical and freehand scanning methods move the transducer crystal to produce 2D images, the matrix transducer arrays are built of a fixed 2D array transducer that generates a real-time 3D pyramidal scan. The application of these probes can also be meaningful in combination with bolus perfusion harmonic imaging (BHI).

Conflicts of interest None.

References

1. Besl PJ, McKay HD (1992) A method for registration of 3-D shapes. Anal Machine Intell 14(2):239–256
2. Bonsanto MM, Staubert A, Wirtz CR, Tronnier V, Kunze S (2001) Initial experience with an ultrasound-integrated single-rack neuronavigation system. Acta Neurochir Wien 143 (11):1127–1132
3. Ji S, Roberts DW, Hartov A, Paulsen KD (2009) Combining multiple true 3D ultrasound image volumes through re-registration and rasterization. Med Image Comput Comput Assist Interv 12(Pt 1):795–802
4. Letteboer MMJ, Willems PWA, Viergever MA, Niessen WJ (2005) Brain shift estimation in image-guided neurosurgery using 3-D ultrasound. IEEE Trans Biomed Eng 52(2):268–276
5. Lindner D, Trantakis C, Arnold S, Schmitgen A, Schneider J, Meixensberger J (2005) Neuronavigation based on intraoperative 3D-ultrasound during tumor resection. Proceedings of computer assisted radiology and surgery (CARS): 815–820
6. Pagoulatos N, Edwards WS, Haynor DR, Kim Y (1998) Calibration and validation of free-hand 3D ultrasound systems based on DC magnetic tracking. In Proc SPIE 3335:59–71
7. Nelson TR, Elvins TT (1993) Visualization of 3D ultrasound data. IEEE Comput Graph Appl 13(6):50–57

8. Roth J, Biyani N, Beni-Adani L, Constantini S (2007) Real-time neuronavigation with high-quality 3D ultrasound sonowand in pediatric neurosurgery. Pediatr Neurosurg 43(3):185–191
9. Trantakis C, Meixensberger J, Lindner D, Strauss G, Grunst G, Schmidtgen A, Arnold S (2002) Iterative neuronavigation using 3D ultrasound. A feasibility study. Neurol Res 24(7):666–670
10. Trantakis C, Tittgemeyer M, Schneider JP, Lindner D, Winkler D, Strauss G, Meixensberger J (2003) Investigation of time-dependency of intracranial brain shift and its relation to the extent of tumor removal using intra-operative MRI. Neurol Res 25(1):9–12
11. Umeyama S (1991) Least-squares estimation of transformation parameters between two point patterns. IEEE Trans Pattern Anal Mach Intell 13(4):376–380
12. Unsgaard G, Ommedal S, Muller T, Gronningsaeter A, Nagelhus Hernes TA (2002) Neuronavigation by intraoperative three-dimensional ultrasound: initial experience during brain tumor resection. Neurosurgery 50(4):804–812, discussion 812
13. York G, Kim Y (1999) Ultrasound processing and computing: Review and future directions. Annu Rev Biomed Eng 1:559–588

Acta Neurochir (2011) 153:1535
DOI 10.1007/s00701-011-1032-3

LETTER TO THE EDITOR

Can stereotactic sample biopsies accurately diagnose mixed germ cell tumors?

Satoru Takeuchi · Yoshio Takasato

Received: 15 March 2011 / Accepted: 12 April 2011 / Published online: 4 May 2011

We read with great interest the article entitled "Are stereotactic sample biopsies still of value in the modern management of pineal region tumours? Lessons from a single-department, retrospective series" by Lefranc et al. [2]. The authors retrospectively analyzed a series of 88 consecutive patients who underwent stereotactic biopsies for pineal region tumors. They reported that accurate tissue diagnoses were obtained in all but one case, and that the pathological diagnoses included 21 germ cell tumors as well as 32 pineal parenchymal tumors, 15 glial tumors, and 20 other tumors. They concluded that stereotactic biopsies for pineal region tumors could provide accurate pathological diagnoses with safety. We wish to provide further comments, especially regarding the issue of accurately diagnosing germ cell tumors. The authors performed staged biopsies to obtain as much tissue as possible and to optimize the sample collection. Furthermore, when the tumor was too small, they performed rosette biopsies by rotating the side-cut needle. The limited amount of tissue sampling in stereotactic biopsies could result in failure to make an accurate diagnosis, especially when dealing with tumors with mixed components, as mentioned by Lefranc et al. We agree with the authors' device for avoiding sampling errors. On the other hand, we consider that it is necessary to provide additional information on whether mixed germ cell tumors can be accurately diagnosed in the authors' series, since the authors did not mention these tumors. Matsutani et al. [3] reported that 32% of intracranial germ cell tumors had coexistence of more than two germ cell tumor components. Depending on the kinds of components present, the treatment strategies can vary, and the outcomes can differ significantly [1, 3]. If mixed germ cell tumors were not diagnosed, we consider that it is too early to reach conclusions on the accuracy of pathological diagnosis with stereotactic biopsies.

Conflicts of interest None.

References

1. Fujimaki T (2009) Central nervous system germ cell tumors: classification, clinical features, and treatment with a historical overview. J Child Neurol 24:1439–1445
2. Lefranc M, Touzet G, Caron S, Maurage CA, Assaker R, Blond S (2011) Are stereotactic sample biopsies still of value in the modern management of pineal region tumours? Lessons from a single-department, retrospective series. Acta Neurochir (Wien). doi:10.1007/s00701-010-0936-7, Epub ahead of print
3. Matsutani M, Sano K, Takakura K, Fujimaki T, Nakamura O, Funata N, Seto T (1997) Primary intracranial germ cell tumors: a clinical analysis of 153 histologically verified cases. J Neurosurg 86:446–455

S. Takeuchi (✉)
Department of Neurosurgery, National Defense Medical College,
3-2 Namiki,
Tokorozawa, Saitama 359-8513, Japan
e-mail: s.takeuchi@room.ocn.ne.jp

Y. Takasato
Department of Neurosurgery, National Hospital Organization
Disaster Medical Center,
Tokyo, Japan

Acta Neurochir (2011) 153:1537–1538
DOI 10.1007/s00701-011-1033-2

LETTER TO THE EDITOR

Can stereotactic sample biopsies accurately diagnose mixed germ cell tumors?

Lefranc Michel · Blond Serge

Received: 9 April 2011 / Accepted: 12 April 2011 / Published online: 4 May 2011

Although stereotactic biopsies are a well-recognized surgical procedure for obtaining a pathological diagnosis with limited surgical risks [3], how this procedure can lead to an accurate diagnosis in heterogeneous tumors is still being discussed. A key element in the management of tumors is access to accurate histological data. Stereotactic biopsies are limited by the fact that they give the pathologist a sample of the tumor. The risk is then to under-grade glial tumors [7] or to miss part of the tumor cell characterization [1]. Mixed germ cell tumors are essentially heterogeneous, and, obviously, the question "Can stereotactic sample biopsies accurately diagnose mixed germ cell tumors?" is really of value.

In our opinion, this question must be answered in three steps:

(1) *Surgical technique*: It is important to limit the risk of sampling error during stereotactic biopsies. In order to avoid sampling errors, we attempt to extract as much tumor tissue as possible: although we initially try to perform staged biopsies, we move to "rosette" biopsies when the tumor volume is too low. MRI analysis is important in order to obtain a trajectory that will explore the different parts of the lesion. As evidenced by our recently published results and when following a rigorous stereotactic methodology, having access to enough tissue without increasing the morbidity rate is possible [6]. In our recently published series, stereotactic biopsies allowed the diagnosis of eight nongerminomatous germ cell tumors. In six cases we found mixed germ cell tumors (immature and mature teratoma in three cases, mature teratoma with embryological carcinoma in one case, germinoma and mature teratoma in one case, and in the last case more than three different tissues) [6].

(2) *Neuro-oncological practice*: Mixed germ cell tumors are mainly pineal region tumors. The management, prognosis, and treatment of tumors in this region are extremely dependent on accurate tissue diagnosis. The only exceptions to this rule are tumors positive for non-germinoma germ cell markers: ßhCG is secreted by choriocarcinomas and germinomas, and alphaFP is secreted by yolk sack tumors and germinomas [2]. A "certain" diagnosis is obtained when serum or CSF assays are positive (ßhCG >50 iu/ml for choriocarcinomas and alfaFP >25 ng/ml for yolk sack tumors). For nongerminatous cell tumors, when the diagnosis is performed according to LCS and blood markers, the treatment is carried out without biopsies [2]. Radiation plus chemotherapy is performed, and surgery is done only in case of a residue. This strategy is widely accepted now. Obviously, in these cases, an important part of these lesions is mixed germ cell tumors. In these cases, even if accurate histological diagnosis is not obtained, it does not impact on oncological management.

(3) *Balance between advantages and limits:* In our opinion, the main goal of stereotactic biopsies is to allow the correct neuro-oncological management of

L. Michel (✉)
Service de Neurochirurgie,
Centre Hospitalier Universitaire (CHU) Amiens,
5 place Victor Pauchet,
80054 Amiens Cedex, France
e-mail: lefrancm@me.com

B. Serge
Service de Neurochirurgie Stéréotactique et Fonctionnelle,
Clinique de Neurochirurgie, Hôpital Roger Salengro,
CHRU Lille,
Lille Cedex, France

theses lesions. In our series, stereotactic biopsies always allow pathological diagnosis and appropriate therapies. Our patients' follow-up data were unsurprising. Surgical risks are very limited during stereotactic biopsies: It was shown that the procedure was accurate, with very few adverse effects and almost no mortality risk [4, 5, 8]. In our series, transient morbidity was only 5.9% [6]. There was neither mortality nor permanent morbidity related to the stereotactic biopsies. Actually, if the goal is to obtain an accurate histological diagnosis, there is no reason to perform open surgical procedures, even if the sample error risk is lower, because stereotactic biopsies allow appropriate management and present a much lower surgical risk.

In conclusion, in our opinion, stereotactic biopsies even for mixed germ cell tumors are the best tool in order to provide a pathological diagnosis because of its high histological accuracy and its very limited surgical risks. However, it must be done following a strict methodology in order to limit the sample error risk.

Conflicts of interest None.

References

1. Bruce JN, Ogden AT (2004) Surgical strategies for treating patients with pineal region tumors. J Neurooncol 69(1–3):221–236
2. Choi JU, Kim DS, Chung SS, Kim TS (1998) Treatment of germ cell tumors in the pineal region. Childs Nerv Syst 14(1–2):41–48
3. Dammers R, Haitsma IK, Schouten JW, Kros JM, Avezaat CJJ, Vincent AJPE (2008) Safety and efficacy of frameless and frame-based intracranial biopsy techniques. Acta Neurochirurgica 150(1):23–29
4. Dempsey PK, Kondziolka D, Lunsford LD (1992) Stereotactic diagnosis and treatment of pineal region tumours and vascular malformations. Acta Neurochir (Wien) 116(1):14–22
5. Kreth FW, Schätz CR, Pagenstecher A, Faist M, Volk B, Ostertag CB (1996) Stereotactic management of lesions of the pineal region. Neurosurgery 39(2):280–289, discussion 289–291
6. Lefranc M, Touzet G, Caron S, Maurage CA, Assaker R, Blond S (2011) Are stereotactic sample biopsies still of value in the modern management of pineal region tumours? Lessons from a single-department, retrospective series. Acta Neurochir (Wien). doi:10.1007/s00701-010-0936-7
7. Maia ACM, Malheiros SMF, da Rocha AJ, Borges LR, Santos AJ, da Silva CJ, de Melo JG, Lanzoni OP, Gabbai AA, Ferraz FA (2004) Stereotactic biopsy guidance in adults with supratentorial nonenhancing gliomas: role of perfusion-weighted magnetic resonance imaging. Journal of Neurosurgery 101(6):970–976
8. Regis J, Bouillot P, Rouby-Volot F, Figarella-Branger D, Dufour H, Peragut JC (1996) Pineal region tumors and the role of stereotactic biopsy: review of the mortality, morbidity, and diagnostic rates in 370 cases. Neurosurgery 39(5):907–912, discussion 912–914

Acta Neurochir (2011) 153:1539–1540
DOI 10.1007/s00701-011-1038-x

LETTER TO THE EDITOR

Surgical management of spheno-orbital meningiomas

Peerooz Saeed

Received: 15 April 2011 / Accepted: 19 April 2011 / Published online: 7 May 2011

Dear Editor,

Dr. Nagatani and colleagues, in their comments on our study of natural history of sphenoid-orbital meningiomas (SOM) [8], have recommended not resecting the portion of SOM involving cavernous sinus (CS) and superior orbital fissure (SOF) in order to avoid the risk of permanent cranial nerve dysfunction.

As indeed pointed out, the resection of SOMs is associated with a range of complications.

The reported numbers of postoperative neurological complications after resections of SOMs (primarily cranial nerve palsies) range up to 100% for trigeminal hypesthesias [3, 9], 13% for oculomotor palsy [2, 5, 10], and up to 6% mortality have also been reported [2, 5]. Furthermore, a recurrence rate of up to 50% after a surgical resection has been reported [1].

As we have explained in our recent paper on the surgical results of SOM [7], given the limited improvement in prognosis and the complications involved in surgery, the aim of surgical treatment for SOM should be restoration of visual acuity and reduction of proptosis, rather than complete tumor removal.

In our group of 66 patients, surgery arrested visual deterioration or improved visual acuity in 91% of our patients. Furthermore, a substantial reduction in proptosis was achieved in 85% of the patients. Proptosis was reduced by 2.6±2.6 mm; however, we had hoped to achieve a better result and were disappointed by this level of improvement [7].

P. Saeed (✉)
Orbital Center, Academic Medical Center,
University of Amsterdam,
P.O. Box 22660, 1100 DD Amsterdam, The Netherlands
e-mail: p.saeed@amc.uva.nl

To resect SOM, different surgical approaches are used, including transzygomatic, pterional, frontotemporal, combined transcranial-transmalar, and cranio-orbital approaches. All of these approaches allow sufficient access to the orbit and middle fossa base for bony and soft-tissue tumor resection, as well as decompression of the SOF and optic canal [1–3, 5, 7, 9, 10].

The surgical approach can be tailored to the individual case. Decompression of the optic canal can be achieved through a frontotemporal approach combined with orbito-zygomatic (OZ) or a frontotemporal approach alone. We recommend that the frontotemporal approach combined with OZ be reserved for cases that require wide surgical exposure.

Recently, Lund and Rose [4] reported 12 patients with SOM who underwent endoscopic endonasal medial orbital wall decompression and decompression of the optic canal in eight patients with opticopathy and visual deterioration. In these patients, the opticopathy improved and the visual acuity improved by one to four lines on the Snellen chart.

In our view, a craniotomy for debulking is not indicated for patients who have mild proptosis or no visual deterioration. Also, when the major symptom is proptosis without optic canal stenosis, an extended lateral orbitotomy alone can be preformed to avoid the complications of a craniotomy. Extended lateral orbitotomy or total lateral orbitotomy has been used routinely for severe cases of Graves' orbitopathy and tumors in the orbital apex [6, 7].

Because the majority of SOMs are resected sub-totally, radiotherapy should be considered as an adjuvant treatment for SOM, as postoperative radiotherapy might give a better control of tumor growth, with minor side effects.

When there is an extension of SOM to CS, we do not recommend a surgical intervention of that portion of tumor, and radiotherapy should be considered. However, the

hyperostotic bone around SOF can be excised safely, without damaging cranial nerves. In conclusion, like Dr. Nagatani and colleagues, we recommend in the surgical resection of SOM a symptom orientated approach as opposed to a radical resection, as extensive surgical resection can be associated with significant postsurgical morbidity.

Conflicts of interest None.

References

1. Bonnal J, Thibaut A, Brotchi J, Born J (1980) Invading meningiomas of the sphenoid ridge. J Neurosurg 53:587–599
2. Carrizo A, Basso A (1998) Current surgical treatment for sphenoorbital meningiomas. Surg Neuro l50:574–578
3. Honeybul S, Neil-Dwyer G, Lang DA, Evans BT, Ellison DW (2001) Sphenoid wing meningioma en plaque: a clinical review. Acta Neurochir (Wien) 143:749–757
4. Lund VJ, Rose GE (2006) Endoscopic transnasal orbital decompression for visual failure due to sphenoid wing meningioma. Eye (Lond) 20:1213–1219
5. Ringel F, Cedzich C, Schramm J (2007) Microsurgical technique and results of a series of 63 spheno-orbital meningiomas. Neurosurgery 60:214–221
6. Rootman J, Stewart B, Goldberg RA (1995) Orbital surgery: a conceptual approach. Lippincott-Raven, Philadelphia
7. Saeed P, van Furth WR, Tanck M, Freling N, van der Sprenkel JW, Stalpers LJ, van Overbeeke JJ, Mourits MP (2011) Surgical treatment of sphenoorbital meningiomas. Br J Ophthalmol. doi:10.1136/bjo.2010.189050
8. Saeed P, van Furth WR, Tanck M, Kooremans F, Freling N, Streekstra GI, Regensburg NI, van der Sprenkel JW, Peerdeman SM, van Overbeeke JJ, Mourits MP (2011) Natural history of spheno-orbital meningiomas. Acta Neurochir (Wien) 153:395–402
9. Sandalcioglu IE, Gasser T, Mohr C, Stolke D, Wiedemayer H (2005) Spheno-orbital meningiomas: interdisciplinary surgical approach, resectability and long-term results. J Craniomaxillofac Surg 33:260–266
10. Shrivastava RK, Sen C, Costantino PD, Della RR (2005) Sphenoorbital meningiomas: surgical limitations and lessons learned in their long-term management. J Neurosurg 103:491–497

Acta Neurochir (2011) 153:1541
DOI 10.1007/s00701-011-1037-y

Surgical management of spheno-orbital meningiomas

Kimihiro Nagatani · Satoru Takeuchi · Naoki Otani · Hiroshi Nawashiro

Received: 17 March 2011 / Accepted: 19 April 2011 / Published online: 7 May 2011

We read with great interest the article entitled "Natural history of spheno-orbital meningiomas" by Saeed et al. [3]. The authors investigated the natural history and growth rate of spheno-orbital meningiomas (SOMs). They reported that a significant number of SOMs were slow-growing tumors and that the initial volume of the tumor and of the soft tissue component was significantly related to the growth rate. Therefore, they advocated a "wait and see" policy in the absence of risk factors. We wish to provide further comment on the issue of surgical morbidity and mortality, which was anticipated by the authors, in the case of SOMs. Oya et al. [2] reviewed 39 patients who had SOMs and had undergone surgery; they reported that persistent oculomotor palsy occurred in three cases (7.7%). They avoided radical resection of portions of the tumor that extended into the cavernous sinus (CS) and superior orbital fissure (SOF) in order to minimize the risk of permanent oculomotor nerve palsy. Mirone et al. [1] also studied a series of 71 patients who had undergone surgery for SOMs. They reported that persistent oculomotor palsy occurred in three cases (4.2%) and that there were no perioperative deaths related to surgery. In their series, the CS and SOF constituted the surgical limits in order to avoid the risk of permanent cranial nerve deficit. On the basis of these reports, we consider that low morbidity and mortality rates can be achieved with surgery limited by the CS and SOF. Unfortunately, the biological behavior of SOMs varies, and some SOMs grow much faster than others [1, 3, 4]. Therefore, we feel that good tumor control of SOMs without morbidity is essential and that resection should be limited up to the CS and SOF to achieve adequate tumor resection with low morbidity.

Conflicts of interest None.

References

1. Mirone G, Chibbaro S, Schiabello L, Tola S, George B (2009) En plaque sphenoid wing meningiomas: recurrence factors and surgical strategy in a series of 71 patients. Neurosurgery 65:100–108
2. Oya S, Sade B, Lee JH (2010) Sphenoorbital meningioma:surgical technique and outcome. J Neurosurg. doi:10.3171/2011.1.JNS101128a
3. Saeed P, van Furth WR, Tanck M, Kooremans F, Freling N, Streekstra GI, Regensburg NI, van der Sprenkel JW, Peerdeman SM, van Overbeeke JJ, Mourits MP (2011) Natural history of spheno-orbital meningiomas. Acta Neurochir (Wien) 153:395–402
4. Schick U, Bleyen J, Bani A, Hassler W (2006) Management of meningiomas en plaque of the sphenoid wing. J Neurosurg 104:208–214

K. Nagatani (✉) · S. Takeuchi · N. Otani · H. Nawashiro
Department of Neurosurgery, National Defense Medical College,
3-2 Namiki,
Tokorozawa, Saitama 359-8513, Japan
e-mail: naval.kimi@gmail.com

Acta Neurochir (2011) 153:1543–1545
DOI 10.1007/s00701-011-0988-3

TECHNICAL NOTE

Easy slip-knot: a new simple tying technique for deep sutures

Yudo Ishii · Shigeyuki Tahara · Kenichi Oyama · Takayuki Kitamura · Akira Teramoto

Received: 21 December 2010 / Accepted: 22 February 2011 / Published online: 26 March 2011

Abstract
Background Knot-tying in the deep operative field is very complicated because of the narrow working space during endoscopic transsphenoidal surgery. We present a novel technique for tying deep knots called the "easy slip-knot," which was developed from a knot used to tie fishing lines.
Method After threading the dura, an easy slip-knot is made outside the nostril. One end of the string is pulled, the knot then naturally slips, and should reach the operative field without needing a knot-pusher.
Findings This method is not complicated, is easily applied to the operative field by slipping the knot into position, and is able to tie sutures securely.
Conclusions The easy slip-knot should be useful for endoscopic surgery.

Keywords Deep suture · Endoscope · Knot tying · Pituitary

Introduction

The dural suture is regarded as important for the complete closure of the sellar floor during the management of pituitary tumors. However, the deep suturing technique is complicated during endoscopic transsphenoidal surgery because of its narrow working space and two-dimensional view. We previously used the knot-sending method for dural sutures, in which a knot was made outside the nostril and sent with a knot-pusher, and was tightened in the deep operative field with two forceps. However, this method is very complicated because the knots have to be made and sent twice for secure tying. We present a new simple technique for tying knots called the "easy slip-knot," which originated from the "scaffold knot" that is used to tie fishing lines and ropes in sports.

Y. Ishii (✉) · S. Tahara · K. Oyama · T. Kitamura · A. Teramoto
Department of Neurosurgery, Nippon Medical School,
1-1-5, Sendagi, Bunkyo,
Tokyo, Japan 113–8603
e-mail: yudoi@aol.com

Materials and methods

We use 5–0 nylon monofilament sutures (SURGIPRO II; Covidien, MA, USA) and two deep suturing needle holders (8055–02, 8055–03, FUJITA, Tokyo, Japan). After threading both sides of the dura (Fig. 2b), the upper part of one side of the suture filament is held and a loop is made with the other side of the suture filament, between the thumb and forefinger, outside the nostril (Fig. 1a). Two more loops are made over both sides of the suture filament and the end is passed through the first loop that was made with the fingers (Fig. 1b). The knot is loosely tightened and the long end of the suture filament is then pulled, the knot should then easily slip and reach the operative field without needing a knot-pusher (Figs. 1c and 2c). Finally, the knot is tightened with two forceps and the excess suture filament is cut off (Fig. 2d).

Discussion

Complete sellar closure is a very important step to prevent the leakage of cerebrospinal fluid (CSF) during pituitary surgery [1, 2]. Traditionally, fat packing, the insertion of a bone fragment, and spraying fibrin glue have been used for sellar closure [3, 5]. If large dural defects and massive intraoperative CSF leakage are encountered, a more reliable

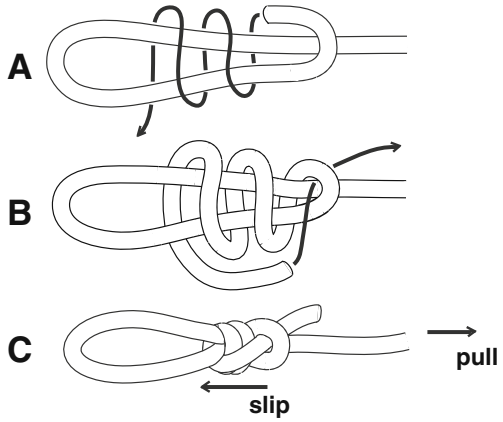

Fig. 1 Easy slip-knot. **a** Make a first loop. **b** Make two more loops over both sides of the suture filament and pass the end through the first loop. **c** Tighten the knot and pull the long end of the suture filament

method for dural closure, such as a dural patch with watertight suture, is needed to prevent postoperative CSF leakage [4, 6]. Recently, we have used the dural suture approach to close the wound [7]. However, as we discuss below, this method for tying was very complicated. After threading both sides of the dura, a surgeon's knot was made outside of the nostril and then pushed into the operative field with a knot-pusher. The knot was tightened with two forceps, and a second simple knot was made and also pushed into the operative field; therefore, this method required that a knot be tied and sent twice. Occasionally, the first knot stuck before reaching its target because of locking.

Our new method, the "easy slip-knot," needs a very simple technique, no repetition of tying, has no stacking, and can be used in other surgical procedures. Furthermore, this knot does not come loose after tightening. Using this technique, sellar closure is markedly easier and the incidence of CSF leakage, a major complication of transsphenoidal surgery, is reduced.

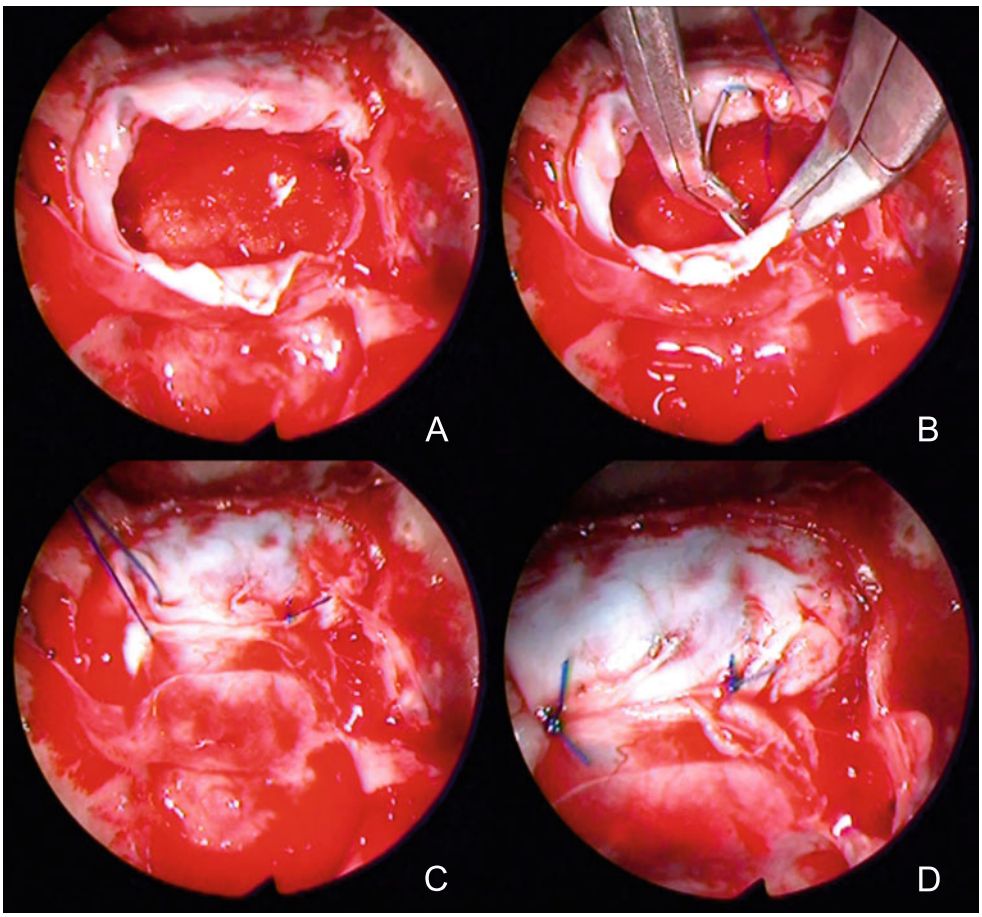

Fig. 2 Intra-operative photos. **a** After removal of a tumor. **b** Threading the dura with a 5–0 nylon suture. **c** Pull the long end of the suture filament and the knot slips until it reaches the operative field. **d** Watertight closure of the dura

Conflict of interest None.

References

1. Black PM, Zervas NT, Candia GL (1987) Incidence and management of complications of transsphenoidal operation for pituitary adenomas. Neurosurgery 20:920–924
2. Ciric I, Ragin A, Baumgartner C, Pierce D (1997) Complications of transsphenoidal surgery: results of a national survey, review of the literature, and personal experience. Neurosurgery 40:225–236
3. Freidberg SR, Hybels RL, Bohigian RK (1994) Closure of cerebrospinal fluid leakage after transsphenoidal surgery: technical note. Neurosurgery 35:159–160
4. Guity A, Young PH (1990) A new technique for closure of the dura following transsphenoidal and transclival operations. Technical note. J Neurosurg 75:168–169
5. Hardy J, McCutcheon IE (1993) Pituitary microadenomas. In: Apuzzo MLJ (ed) Brain surgery: complication avoidance and management. Churchill Livingstone, New York, pp 271–295
6. Kitano M, Taneda M (2004) Subdural patch graft technique for watertight closure of large dural defects in extended transsphenoidal surgery. Neurosurgery 54:653–660
7. Vanaclocha V, Sáiz N, Panta F (1998) Repair of dural defects in awkward areas-technical note. Acta Neurochir 140:615–618

Comment

I liked this friendly, concise report. In the authors' experience, is this technique able to produce better surgical results? It seems to be the case, because they state that "using this technique, sellar closure is markedly easier and the incidence of CSF leakage, a major complication of transsphenoidal surgery, is reduced".

Domenico d'Avella
Padova, Italy

Acta Neurochir (2011) 153:1547
DOI 10.1007/s00701-011-1011-8

BOOK REVIEW

Reuben D. Johnson, DPhil, FRCS; Alexander L. Green, MD, FRCS (eds): Landmark papers in neurosurgery

Oxford University Press, 2010, ISBN 978-0-19-959125-1

Nic de Tribolet

Received: 24 March 2011 / Published online: 7 May 2011

I can't resist stating that this is an excellent book and should be read by every neurosurgeon in training.

The papers the authors have selected as "landmark" are their own choice, and they have avoided publications on surgical techniques.

There are six chapters: neurovascular neurosurgery, neuro-oncology, head injury, spinal neurosurgery, functional and epilepsy neurosurgery, and paediatric neurosurgery.

Each chapter starts with a well-referenced introduction, following which are sections on specific topics all constructed in the same way, like the report of a journal club:

First the details of the study(ies) to be discussed are summarised, then the references of the main study(ies) and related references, which allows putting the main references into perspective. The study design is clearly presented with tables followed by the primary and secondary outcome measures and their results. The above is then summarised in the conclusions. The authors then make a critique based on well-selected references.

This critique reflects the personal opinion of the authors.

Let me take as an example surgery for lumbar disc herniation, very common in practice and an excellent money-making business. The authors conclude from a Norwegian study that "Surgical treatment was better than conservative management at 1-year follow-up, but this difference became less pronounced over a 10-year period"; from a US study that "Patients received benefit from both surgery and conservative management but no conclusions regarding the superiority of either can be made on an intention-to-treat analysis"; finally from a Netherlands study that "Early surgery for sciatica due to lumbar disc prolapse leads to faster recovery and relief of leg pain. However there are no long-term benefits". Rather sobering, isn't it. In the critique however the authors quote another study of the Netherlands examining cost-benefit pointing out that there appears to be a strong economic argument supporting continued surgery for lumbar disc herniation.

What I particularly liked is that the authors are not afraid of discussing controversial topics.

In addition to the precious information provided here, this book will teach young neurosurgeons in training (and the older fully trained ones as well) how to critically read a paper.

N. de Tribolet (✉)
Department of Neurosurgery,
University Hospital of Geneva (HUG),
1211 Geneva, Switzerland
e-mail: Nicolas.detribolet@unige.ch

Conflicts of interest None.

Acta Neurochir (2011) 153:1549
DOI 10.1007/s00701-011-1012-7

BOOK REVIEW

George Samandouras (ed.): The neurosurgeon's handbook

Oxford University Press, 2010, ISBN 978-0-19-857067-7

Nicolas de Tribolet

Received: 24 March 2011 / Published online: 7 May 2011

This book is a comprehensive summary of neurosurgery. It covers almost every topic in a concise text. There are numerous schematic illustrations with drawings in black and red, as well as CT, MRI and plain X-ray images. Each chapter is completed by well-chosen references. Numerous tables facilitate rapid understanding of the topics in a synoptic way. The surgical techniques are briefly described, step by step, although I sometimes missed accompanying illustrations (but of course it is not a book concentrating on surgical techniques).

The middle of the book has a few glossy pages with mainly colour illustrations of the histopathology of brain tumours, but also drawings of some surgical approaches.

The format of this book allows readers to carry it in their pocket. The goal should be to give the reader a quick answer to a particular query. I tried to find "pterional craniotomy" for a description of the most frequently used approach in cranial neurosurgery. In the index I found "pterional approach", which refers to the chapter on patient positioning and common approaches. There I found the description of the supine position and key points of skull topography. But besides the position of the keyhole, there was no step-by-step description with figures of the craniotomy. If I searched the index under "craniotomy", I was referred to one single sentence concerning subdural empyema. I had to go to anterior circulation aneurysms to find a description of the technique. I found the index to be difficult to use sometimes.

Besides this minor critique, I think this is an excellent book for trainees. It is very pleasant to read. Staff members will also find it useful in order to access classification scales quickly.

Conflicts of interest None.

N. de Tribolet (✉)
Department of Neurosurgery,
University Hospital of Geneva (HUG),
1211 Geneva, Switzerland
e-mail: Nicolas.detribolet@unige.ch